



HAL
open science

Striatal and hippocampal dynamics during time categorization

Felipe Rolando

► **To cite this version:**

Felipe Rolando. Striatal and hippocampal dynamics during time categorization. Neuroscience. Université Claude Bernard - Lyon I, 2022. English. NNT : 2022LYO10158 . tel-04837883

HAL Id: tel-04837883

<https://theses.hal.science/tel-04837883v1>

Submitted on 14 Dec 2024

HAL is a multi-disciplinary open access archive for the deposit and dissemination of scientific research documents, whether they are published or not. The documents may come from teaching and research institutions in France or abroad, or from public or private research centers.

L'archive ouverte pluridisciplinaire **HAL**, est destinée au dépôt et à la diffusion de documents scientifiques de niveau recherche, publiés ou non, émanant des établissements d'enseignement et de recherche français ou étrangers, des laboratoires publics ou privés.



THESE de DOCTORAT DE L'UNIVERSITE CLAUDE BERNARD LYON 1

Ecole Doctorale N° ED 476
NEUROSCIENCES ET COGNITION

Discipline : Neurosciences

Soutenue publiquement le 12/12/2022, par :
Felipe Rolando

Striatal and hippocampal dynamics during time categorization

Devant le jury composé de :

Boulinguez, Philippe, Professeur des Universités	Université Lyon 1	Président
Apicella, Paul, Directeur de Recherche	CNRS, Marseille	Rapporteur
Robbe, David, Directeur de Recherche	INSERM, Marseille	Rapporteur
Doyère, Valérie, Directrice de Recherche	CNRS, Paris	Examineur
Girardeau, Gabrielle, Chargée de Recherche	INSERM, Paris	Examineur
Wirth, Sylvia, Directrice de Recherche	CNRS, Lyon	Directrice de thèse

Résumé (Français)

Le temps est une composante de notre environnement que nous ne percevons pas directement. Pourtant, lorsque c'est nécessaire, nous sommes capables d'estimer des durées et de les classer dans le but d'optimiser nos comportements, pour « gagner du temps ». Cette catégorisation temporelle nous permet de distinguer un événement court d'un long, et se produit à différentes échelles temporelles. Le but de ce projet est d'identifier les signatures neurophysiologiques qui permettent de distinguer les durées à l'échelle de quelques secondes. Notre intérêt se porte sur deux structures cérébrales, le striatum et l'hippocampe, qui peuvent être décrites comme étant impliquées dans le temps de l'action et le temps de la mémoire, respectivement. Pour la première fois, nous avons contrasté leur activité dans une tâche de catégorisation temporelle chez le primate non-humain. Nous avons enregistré l'activité de neurones dans ces deux structures chez deux macaques rhésus, pendant qu'ils réalisaient une tâche de catégorisation de durées. Ces durées variaient d'une échelle en dessous de la seconde (0.25s – 0.5s – 1s) à une échelle de plusieurs secondes (2s – 4s – 8s). Après qu'une durée se soit écoulée, le singe doit adapter sa réponse selon que le temps passé soit court, intermédiaire, ou long. L'utilisation de ce modèle animal est justifiée par la proximité neuroanatomique du striatum et de l'hippocampe entre le macaque et l'Homme. De plus, les comportements de catégorisation temporelle sont similaires entre ces deux espèces à l'échelle de la seconde. Pour la première fois, nos résultats montrent des différences importantes entre le striatum et l'hippocampe. Nous montrons que l'activité hippocampique ne porte -quasiment- aucune information sur le temps qui passe. Au contraire, l'activité neuronale dans le striatum reflète le temps écoulé, de 1 seconde à 8 secondes. Nous avons également mis en évidence des codes de temps relatifs, déjà documentés, et l'existence de codes temporels absolus dans le striatum. Les premiers s'adaptent en fonction des durées, et sont liés à l'attente d'un événement futur. Les deuxièmes maintiennent leur activité quelle que soit la durée à estimer. Ils découlent d'un événement passé, et sont probablement sous-tendus par un recrutement séquentiel progressif au sein d'un circuit de neurones. De plus, nous avons mis en évidence que la présence de codes temporels est conditionnée à la demande cognitive de la tâche. Dans l'ensemble, nos résultats suggèrent qu'il est peu probable qu'il existe une « horloge » métronomique qui rythme le temps de façon invariante. Au contraire, le recrutement des circuits striataux est vraisemblablement limité à ses propriétés physiologiques permettant d'inscrire des actions sensori-motrices dans des durées courtes. Nos résultats caractérisent la structure des changements neuronaux dans le striatum et l'hippocampe, et leur adaptation au fil du temps.

Abstract (English)

Time is a component of our environment that we do not perceive directly. However, when necessary, we are able to estimate durations and classify them in order to optimize our behaviours, to "save time". This temporal categorization allows us to distinguish a short event from a long one, and occurs at different temporal scales. The goal of this project is to identify the neurophysiological signatures that allow us to distinguish durations on the scale of a few seconds. We focused on two brain structures, the striatum and the hippocampus, which can be described as involved in time for action and time for memory, respectively. For the first time, we contrasted their activity in a temporal categorization task in non-human primates. We recorded the activity of neurons in these two structures in two rhesus macaques while they performed a time categorization task. These durations varied from a sub-second scale (0.25s - 0.5s - 1s) to a supra-second scale (2s - 4s - 8s). After an interval, the monkey must adapt its response depending on whether the elapsed time was short, intermediate, or long. The use of this animal model is justified by the neuroanatomical proximity of the striatum and the hippocampus between macaque and human. Moreover, temporal categorization behaviours are similar between these two species at the second scale. For the first time, our results support differences between the striatum and the hippocampus. We show that hippocampal activity carries only little information about the passage of time. On the contrary, neuronal activity in the striatum reflects the elapsed time, from 1 second to 8 seconds. We have also highlighted relative time codes, already documented, and the existence of absolute time codes in the striatum. The first ones adapt according to the duration, and are linked to the expectation of a future event. The second ones maintain their activity whatever the duration to be estimated. They arise from a past event, and are probably underpinned by a progressive sequential recruitment within a neuronal circuit. Moreover, we have shown that the presence of temporal codes is conditioned by the cognitive demand of the task. Overall, our results suggest that it is unlikely that there is a metronomic "clock" that invariably paces time. Instead, the recruitment of striatal circuitry is likely limited to physiological properties fitting sensory-motor actions into short durations. Our results characterize the structure of neural changes in the striatum and hippocampus, and their adaptation over time.

Acknowledgements

First, I would like to thank my PhD supervisor, **Sylvia Wirth**, for choosing me to lead this project and for initiating me at the painful but beautiful art of primates' electrophysiology.

I would like to thank the members of the jury for taking the time to read this manuscript: **Gabrielle Girardeau, Philippe Boulinguez** and in particular **Paul Apicella** and **David Robbe** that have kindly accept to evaluate my work.

I want to thank all my co-authors, **Jean-René Duhamel, Valérie Doyère**, also as a jury member, and mainly **Tadeusz Kononowicz**, without whom the level of my analysis would not have reach this level.

I also thank the technical staff to provide the technical support, in particular **Serge Pinède**, who helped me to program the task, and **Fidji Francioli** for the animal care.

I wish to thank **Virginie van Wassenhove** and **Charlie Wilson**, for being part of my *Comité de Suivi Individuel Doctoral* over 4 years, and for the helpful conversations and advices.

I want to thank all the students and former students at the *Institut des Sciences Cognitives Marc Jeannerod*. Through their kindness and interest in others, they actively promote cooperative research instead of a competitive one. Many thanks to **Rémi Philippe, Rémi Janet, Sébastien Kirchherr, Mathilda Froesel, Valentin Guigon, Alice Massera, Marie Véricel, Yann Bihan-Poudec, Maëva Gacoing, Étienne Abassi, Nicolas Goupil, Éloïse Disarbois, Antoine Ameloot, Yidong Yang, Matthieu Malherbe, Marie Habart, Jacopo Baldi, Maxime Gaudet-Trafit, and Toan Nong**. I also thank the engineers **Lucas Maigre** and **Thomas Perret**.

A great thank to **my parents**. Somehow, they always manage to give me good advices even if most of the time they don't know what they are talking about. Congratulations for that.

I address a huge thank **my sister**, for showing that nothing is defined in advance.

I want to thank **Quentin Lachaud, Clément Gaboulaud, Aymeric Filleux, Hadrien Rouby, Vincent Maillhol** -and congratulate him for his newborn kid-, **Paul Cormary, Maxime Puech, Hugo Rey** and **Maxime Vion** even if they will never read these words.

Finally, and most importantly, I want to thank **Marlène Méchiche**, my partner in life, for its full help, patience, and support, no matter what.

Table of Contents

Résumé (Français)	1
Abstract (English)	2
Acknowledgements	3
A. Introduction	9
I. Time in the brain	9
I.1. The concept of time: from physics to neurosciences	9
I.2. Temporal and spatial processing: a common integration?	12
I.3. Cognitive models and neural substrates for time integration	14
I.4. Is time processing influenced by time-range?	26
II. The striatum and hippocampus	31
II.1) The caudate-putamen ensemble in the striatum	31
II.2. The hippocampal formation: <i>where</i> am I in time?	40
III. How neurons can tell time: single cells and populational level	49
III.1. Single-cells can tell time.	49
III.2. Populational codes	57
B. Problematics.....	63
C. Chapter 1. A differential adaptation of neural codes to time in the striatum and hippocampus .	65
C.1. Abstract	66
C.2. Introduction	67
C.3. Results	69
C.3.a. Monkeys successfully categorize three ongoing durations	69
C.3.b. Monkey's subjective perception of duration varies with time range	69
C.3.c. A strong recruitment of striatal cells that adapts to processing demand over time	70
C.3.d. A mix of ramping and sequential peaks across structures.....	71
C.3.e. Time-modulated cells display response to other task events.....	72
C.3.f. A slow speed but steady progression in caudate	73
C.3.g. Caudate and putamen accurately predict time across sub-second and supra-second ranges	74
C.3.h. Higher discriminability between two time-points adapts to processing demand	76
C.3.i. A second's encoding is contextually relevant across ranges.....	77
C.4. Discussion.....	78
C.4.a. A prospective categorization based on ongoing elapsed time in the non-human primate from sub-second to supra-second ranges	78
C.4.b. A strong and adaptive recruitment of striatum	79
C.4.c. Time cells presence but poor time prediction in the hippocampus	81

C.4.d. Moment-to-moment adaptation of temporal discrimination in striatum and hippocampus	82
C.5. Methods	84
C.5.a. Animals and behavioral set up.....	84
C.5.b. Behavioral training.	84
C.5.c. Retiming sets	85
C.5.d. Behavioral analysis.	85
C.5.e. Electrophysiological recordings	86
C.5.f. Information content computation.	86
C.5.g. Definition of the neural pattern of single-cells	87
C.5.h. Selectivity to features of the task.....	87
C.5.i. Principal Component Analysis.	88
C.5.j. Multi-class decoding using linear regression	88
C.5.k. Pair-wise analysis using Support-Vector-Machine.....	89
C.6. Bibliography of Chapter 1.....	91
C.7. Figures and Legends	96
D. Chapter 2. Parallel absolute and relative codes in the striatum	117
D.1. Abstract.....	118
D.2. Introduction	119
D.3. Results.....	120
D.3.a. Behavioural results indicate a context dependant categorization of the durations	120
D.3.b. Classification of absolute and relative neurons across different time-ranges.....	120
D.3.c. Caudate adaptation to contexts can be explained by a shift in the centre of masses.	122
D.3.d. Caudate population activity between sets correlates stronger with an absolute pattern when time is rescaled down	123
D.3.e. Caudal population activity is maintained between 1 and 2 seconds.....	124
D.4. Discussion	127
D.5. Methods and supplementary results	129
D.5.a. Baseline comparison across sets	129
D.5.b. Behavioural analysis.....	129
D.5.c. Relative and absolute patterns defined by the centre of masses.....	129
D.5.d. Relative and absolute patterns defined by the correlations	131
D.5.e. Leaving-one-out method for linear regression.....	132
D.5.f. Populational correlations	132
D.5.g. Temporal multiclass decoding.....	133
D.6. Bibliography of Chapter 2	134

D.7. Figures and Legends.....	136
E. General discussion	151
E.1. Time categorization differs across ranges.	151
E.2. Is there a shift of timing strategies?	152
E.3. Time categorization follows a sequential rule	152
E.4 TM-cells are not directly recruited as a function of movement	153
E.5. Can we decode time from neural activity?	154
E.6. Are all neural structures equally recruited?	155
E.7. Striatum scales duration better	155
E.8. Striatum predictability decreases over ranges	156
E.9. Linking ramping activity to reward anticipation	157
E.10. Can be time decoding linked with ramping activity?	157
E.11. Is time processed in sequence or in a parallel way?	158
E.12. Future perspectives	159
F. General bibliography	161

A. Introduction

For Jean Giono, “time is what passes when nothing passes” -happens-. Somehow, this citation reveals the difficulties to define time. Indeed, it says that time “passes”, but time does not pass. The figures of speech we use to talk about time distort time definition. Indeed, as we say that “time flies” or “time flows” it is not true. Time is not an object, but rather the container allowing objects to exist. Indeed, the metaphor of the flowing river to define the flow of time is obsolete, because it confuses the container and the content (Klein, 2007). Time is not the river, but rather the borders, the container of the river, allowing the streams to flow. Time does not pass, but reality passes over time. The citation also raises another important question: what if nothing happens, does time still pass? For humans, this is linked with the ability to perceive time: do we need to perceive time for time to be real? To experience a sense of time, the brain must keep a track of changes. This raises the question, how is time process by the brain?

I. Time in the brain

Before going into details of neuroscientific and cognitive definitions of time, we will first try to restrict its conceptual definition. To provide a complete definition of time seems a pretentious statement given the difficulty to capture what time is at a psychophysics and neurobiological levels. Time is a non-sensitive feature of our environment, as space is. The understanding of temporal processing is related to the understanding of spatial processing, we will try to see why. Then, we will present a -non-exhaustive- list of examples of cognitive models explaining timing, that have been more or less successively linked with neural substrates, but often ignoring the role of time-range in time processing.

I.1. The concept of time: from physics to neurosciences

Time is a concept that neuroscience has borrowed from philosophy and physics. Recently, it has been argued how important it is to define properly the phenomenon -or function- we are talking about in neurosciences (Buzsáki, 2020). Indeed, as neuroscience is a “young science”, most of the vocabulary used comes from psychology and philosophy. Even if the same terms can be transposed to neuro-biological phenomenon’s, it is important to precise in which framework they are mentioned. This is also true for time (Paton & Buonomano, 2018). Likewise, when we talk about time in neurosciences, we are not talking about time *per se*, but about the “inner sense of time” (Wittmann, 2013): the neural activity transcribing the information that something is *going* on. If we consider time as it is defined in physics, it has for a *long* time being defined by three characteristics that were not supposed to be malleable: its **direction**, its **speed**, and its **unicity** (Rovelli, 2017). Those are

characteristics that influence our perception of time, helping our understanding of it. But modern physics have redefined what common sense tells us: time can flow with multiple speeds, leading to several presents. However, the direction of time goes only in one way, from past to future. As we move from time in physics to neuroscience, we could first ask: do these characteristics hold?

Relevant to the directionality of time, in physics, there is only one equation that differentiates the past state of objects with their future state: the entropy's equation. It stipulates that elements go from a low state of entropy to a higher state of entropy; and this is their unique direction, from past to future. In neurosciences, this statement holds. Indeed, many equations accept time as a variable in neurosciences. This suggest that the brain and cognition are subject to biological laws that are time-dependent. For example, Hebbian learning or the mechanism of action potential itself at the cellular level, Pavlovian conditioning at the behavioural level, or still -episodic- memory recall need to occur in a defined temporal order. One could argue that episodic memory allows us to retrieve memories from the past but also to project us into the future, losing so the unidirectionality of time. Indeed, the common process for mental time travel to the past or to the future is the ability to retrieve detailed information about an episode that is 'not present'. The link between episodic memory and mental time travel to past and future has been demonstrated with brain imagery (Okuda et al., 2003) and clinical studies (Klein, Loftus, & Kihlstrom, 2002). Although, 1) we are not physically projected nor to the future nor to the past, 2) and the common process for remembering past events and planning futures ones lay on sequencing operations that goes in one direction only (D'Argembeau et al., 2015).

At the neural level, for long-term potentiation (LTP), neuron A must spike before neuron B in order to decrease threshold excitability threshold of neuron B. If neuron A does not spike, neuron B is not active. If neuron B discharges before neuron A, the causal link between neuron A and B does not occur (Montague & Sejnowski, 1994; Nicoll et al., 1988).

At the behavioural level, learning processes are possible after making a link between two stimuli of the environment (Pavlovian conditioning) or a stimulus and an action (instrumental learning). Pavlovian conditioning refers to the association between two or more stimuli: a conditioned stimulus (CS) is learned to be announcing the second one, an unconditioned stimulus (US), that provokes a physiological response. With learning, after multiple repetitions, the physiological response can be provoked by the presentation of CS. This process involves an ability 1) to learn a sequence that must respect a temporal order: CS must become first in time, in order to be an announcer of US; and 2) to assimilate a duration: the temporal *distance* of CS-US must be short enough to consider CS-US linked between each-other, by temporal pairing (Balsam & Gallistel, 2009; Rescola & Wagner, 1972). If the duration is too long, there is no learning because CS and US are not integrated as a unique memory. On the other hand, instrumental learning does not refer to the association between external stimuli, but rather to the association of a response in presence of a particular stimulus to get the desire

outcome -reinforcement or avoidance- (O’Doherty et al., 2017). The effect produced by the action following the stimulus presentation allows learning. Although, if the outcome occurs before the action production, the association between the sequence stimulus-action-outcome is weakened.

These observations indicate that in the brain, as in physics, time goes only in one direction. The two other characteristics of time identified as multiple in physics, its speed and the unicity of present, can also be described as multiple in neurosciences.

For example, relevant to the speed, it was shown that if a clock is in movement, it will slow down. This has been proved by testing two atomic clocks, one immobile, and the other moving around the world. At the end of the experiment, the clock that was moving was delayed with respect to the clock that stayed immobile; indicating that time did not move at the same speed in both cases (Hafele & Keating, 1972). Movement is not the only factor available to modify time speed. It is also influenced by gravity: the closer to the centre of the earth, time slows down. Without going into details, it means that next to points with high gravity, time is slowed down for the objects closed to it. In physics, it is now widely accepted that time speed is not unique. In neurosciences, the multiplicity of time speed can be easily understandable, as we have previously defined time as “the inner sense of time”. So, the transformations operated by the brain, that are biochemical mechanisms mainly involving dopamine (Cheng et al., 2016), can speed up or slow down subjective time perception. Time perception is then logically influenced by our emotional states (Efron et al., 2006) or cognitive and attentional loads demanded by the tasks (Politi et al., 2018) for example.

Whether time has a unique present frame is questioned. Indeed, contemporary physics consider that the present is a valid concept when it refers only to objects near by the reference point; and there are as many presents as there are elements in the universe. The idea that all the objects were moving within the same time line is obsolete. Indeed, there are as many time-lines as there are objects. We do not go from a common past to a common future, but each element of the universe has its own past and its own future, that sometimes interplay, sometimes do not. In neurosciences, temporal multiplicity cannot be illustrated in the same way, but rather by the multiple ways to process time. It is possible to distinguish between circadian -temporal- rhythms, processed by the suprachiasmatic nucleus and widely documented (Hastings et al., 2018), and interval-timing for example, for which the understanding of its neural bases is still an ongoing debate. This is why from now on, **the topic of interest is interval timing**: we introduce a new task to test time processing by focusing on two structures that might sustain it. Interval timing differs from circadian rhythms as it is 1) more flexible, and adapts across different ranges -with some limits-; but 2) is less accurate than circadian rhythms.

Even within interval timing processing, we can distinguish between multiple forms of time. Explicit and implicit timing for example, correspond respectively to an active engagement in timing -

measurement- and to an automatic temporal perception. One can also distinguish between time-production and time-estimation: time-production -or reproduction- is internally generated and depends on an outcome conditioned to a specific time production, while time-estimation relies on the capacity to perceive time and evaluate duration afterwards. There is also another key distinction between timing of an event (keeping a track of a duration) and event sequencing (ordering the events in time). This last capacity is needed for learning and memories formation, and does probably not involve the same cognitive processes as interval timing.

As a conclusion, the heuristics provided by physics offers a framework that is relevant to probe the neuroscience of time, leading us to question its direction, speed and unicity.

I.2. Temporal and spatial processing: a common integration?

To process temporal information, there is a need of quantification. Thus, it makes sense to propose temporal models linked with other types of quantification, such as counting (Gallistel & Gelman, 2000) but also spatial processing (Walsh, 2003; Gallistel, 1989).

Indeed, more recent findings suggest that temporal processing is linked with spatial processing (Mendez et al., 2011): similar behavioural patterns were found in temporal and spatial bisection tasks (Figure 1). Note, a bisection task requires to categorize a target as being shorter or longer -binary outcome- than a sample cue. In a temporal bisection task, the cue and target are durations, in a spatial bisection task they are distances. Usually, the performances in these tasks lead to a psychometric curve where the durations best categorized are the extremes, and the closer to the cue, the performance tends to chance level. Performance is represented by the probability to respond long at each standard stimulus. Here, we can also note that humans and monkey's performance was more similar when judging a duration at the second range than when judging a distance.

Time and space have first been linked in Physics: Aristotle defended the thesis that without movement, there is no time, because time is only a variable to quantify change. On the other hand, Newton proposed the idea that time, "true time", also exists when nothing exists and that it is only accessible with mathematics. Also, another example of how time and space are linked in Physics is that both of them share the common physical characteristic that there is a smallest unit possible for each one. They are not infinitely small.

In addition to the fact that space and time are intrinsically linked in Physics, that can influence our way to understand them, we are also used to speak with spatial metaphors when we talk about time. This influences our temporal processes too. It has been demonstrated in humans: temporal and spatial judgements are asymmetrical. It means that spatial stimuli -its length- influences a duration's estimation but not the opposite. A Theory of Magnitude (AToM) explains this phenomenon because in humans, semantic metaphors about time often rely on spatial metaphors, thus, space influences

temporal perception but the contrary is not true. In monkeys, such effect was not found (Merritt et al., 2010).

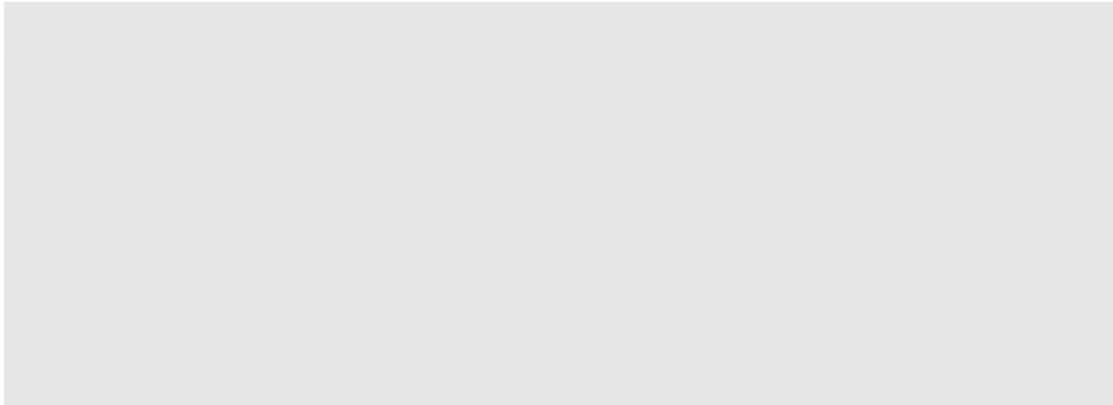


Figure 1. Psychometric curves for monkeys and humans in a temporal bisection task (left panel) and a spatial bisection task (right panel). In the temporal bisection task, cue durations were 350, 685 and 1195ms. In the spatial bisection task, cue distances were 2.85, 4.8 and 6.9° (Mendez et al., 2011).

Another possibility of why time and space are linked in our mind, is because of our environments: they are correlated when we perceive and when we act. Time and space are commonly integrated to allow anticipation of the trajectories of surrounding stimuli in movement. It has been established that in timing tasks, animals develop stereotypic movements to track time (Gouvêa et al., 2014) and when they are unable to do so, their timing abilities decreases (Safaie et al., 2020). Basically, time perception would result from the signals of our movements: during an interval timing task, where we are in space would tell “where” we are in time. Further, it has been demonstrated that timing and sensorimotor control are tied in primates at the milliseconds scale (Balasubramaniam et al., 2021). For example, training in a motor sequence improves time discrimination at the range of the movement performed (300ms), and time perception does not improve without motor training (Guo et al., 2019). Motor production and time perception at the millisecond range are likely to be sustained by very close processes. In non-human primates (NHP) motor cortex for example, there is a time modulated activity during time-production and time-estimation tasks, although neural codes for time are embedded in the neural codes for movement (Roux et al., 2003). Following the idea of “phylogenetic refinement” (Cisek, 2019), time code for perceptual and cognitive function could emerge from neural circuits for movement, as these later ones are phylogenetically older. In addition, attentional spatial and attentional temporal neural substrates partially overlap signifying that they share cognitive processes; but time and space do not share the same cortical circuitry, respectively distributed among right and left hemispheres (Coull & Nobre, 1998). Although, even if animals, and humans (De Kock et al., 2021), use motor -spatial- strategies to improve the tracking of time, it does not mean that there is no time

code in the brain possible without movement, but rather that these processes are sustained by very close networks.

Thus, as we know, primates -humans and other primates- have a more developed somatosensation¹ than rodents (O'Connor et al., 2021). If we consider time processing interlinked with somatosensory processes, we can expect to see differences in the temporal processes between primates and rodents.

Finally, time and space are also related in episodic memory. Episodic memory refers to the ability to retrieve an episode experienced in the past, associating an event -what-, a place -where- and a moment -when-. The definition of episodic memory also includes a specific retrieval process, which is the autonoetic consciousness or, more precisely, the self-awareness which retrieves the past experience from a subjective point of view (Tulving, 1993). Is episodic memory unique to humans? This is still an ongoing debate, but one can assume that the difference between humans and animals is in the retrieval process and not in the memory formation, as other animal species are able to guide their behaviours in function of “episodic-like” traces of information (Zhou & Crystal, 2009; Ergorul & Eichenbaum, 2004; Clayton & Dickinson, 1998). Thus, an information stored in memory associates a place and a time, leading to a memory track where both features are connected. As many species are able to make spatiotemporal associations during memory formation, this indicates that the ability to place an event in time is critical for behavioural adaptation and survey.

Thus, in neurosciences time and space are coupled by movement and episodic memory.

Here, we highlight the fact that basal ganglia, which group several nuclei, are involved in motor movements, and hippocampal formation is the region involved in episodic memory and spatial processing. Therefore, given the link between time, movement, space and memory, it is not surprising that cognitive models of time processing have given an important role of these two regions as neural substrates needed for timing.

1.3. Cognitive models and neural substrates for time integration

There are different types of models of timing in the literature, that can be grouped as pacemaker-based models, coincidence-detection models and process-decay models (Matell & Meck, 2000). Here, we describe their principles and, without giving an exhaustive list of the models found in

¹ Somatosensation is the “sixth sense” allowing to a subject to interact with its environment. It groups several sensory systems (Ager et al., 2020): thermoception (temperature), nociception (pain), equilibrioception (balance), mechanoreception (vibration, discriminatory touch and pressure) and proprioception (positioning and movement). In O'Connor et al. (2021) the authors show that the differences in whiskers and hands lead to differences in the somatosensory system.

the literature, we focused on models that have implications for neural underpinning of time, which is the main topic of this thesis.

1.3.a. The Scalar Expectancy Model

The pacemaker-based models describe time integration by the brain as a stopwatch. There is a pacemaker in the brain ticking at a regular frequency -with an accepted (slight) variability-: the number of tick accounts for ongoing time. For example, at a frequency of 2Hz, four ticks code for 2 seconds. These models are defined as dedicated model to time: their function is to estimate time (Wittmann, 2013); and it implies that there would be a structure in the brain that has this specific function: to be the pacemaker.

The most accepted model of the pacemaker's ones is the Scalar Expectancy Model (SEM). It follows from the Scalar Expectancy Theory, which stipulates that after learning, and over multiple time intervals, the noise in time estimation increases linearly with time. Such a property of timing behaviour was first observed and well documented with Fixed Interval (FI) protocols (Gibbon, 1977).

FI protocols are based on instrumental learning: a conditioned stimulus (CS) is presented, announcing a reward at time t after its onset. If the subject responds before t , he has no reward. Its behaviour is rewarded only when he responds at time t -or after it-. With training, the subject learns to respond closer to the expected event, the time t of reward. If the subjects are trained at multiple times, from t_1 to t_N , the distribution of response probability is transformed with a constant coefficient of variation (CV) from t_1 to t_2 , for example. If the probability to respond at t_1 follows a normal distribution of mean μ_1 and standard-deviation σ_1 , then the probability to respond at t_2 will follow a normal distribution of mean $2 \times \mu_1$ and standard-deviation $2 \times \sigma_1$. More generally, the probability to respond at t_N follows a scalar rule such that $\mu_N = N \times \mu_1$ and $\sigma_N = N \times \sigma_1$. The CV, also named k , is then given by the formula: $k = \mu_1 / \sigma_1 = \mu_N / \sigma_N$ (Gibbon & Church, 1990) and suggests that timing follows a Weber Law².

Concretely, what does it mean at the behavioural level?

The scalar property of timing behaviour implies that the performance at t_1 is as good as the performance at t_N , once both durations have been transformed on a relative scale such as $t_N = k \times t_1$ (Figure 2).

² Weber-Fechner laws describe how perception is influenced by the actual changes in a physical stimulus (visual, for example). The Weber law stipulates that perceptual sensitivity to a stimulus is proportional to the changes occurring in the initial stimulus. Could the fact that time perception follows a weber law induce the -wrong- idea that time is processed as any other physical stimulus?

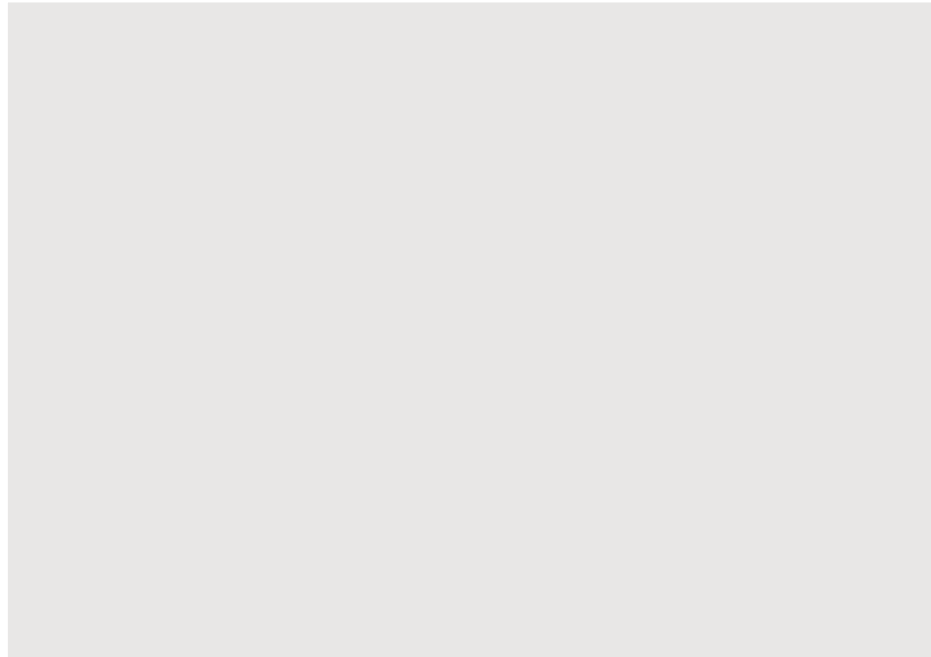


Figure 2. Proportion of responses during FI tasks in rodents represented in absolute times (A, C) and in relative time (B, D). Scalar property of timing behaviour holds from seconds to minute range (Mattell and Meck, 2000).

There are a few variants of the FI task, such as the Peak-Interval (PI) procedure. First, subjects are trained on a FI task. Once they perform well enough, they are tested on probe trials, where the response at time t is not reinforced: trial keeps going on. These probe trials allow a better understanding of timing behaviour accuracy. Indeed, in a FI task the proportion of response will be highest just before or at the time of reward delivery: on average, the proportion of response increases until the reward. PI procedure is more informative than FI task: during probe trials, the peak of responses (peak-time) occurs at time t if the duration is well estimated, and the proportion of responses decreases after time t , reflecting the drop of reward expectancy. This protocol allows to understand the subject's time accuracy: if peak-time is inferior to t (leftward shift), the subject underestimates the duration. If peak-time is superior to t (rightward shift), the subject overestimates the duration. In addition, the moments at which subjects start and end responding within the interval, respectively called 'start' and 'stop' times, are informative about subjective perception, impulsivity and inhibitory capacities. Furthermore, peak-spread (the width of responses' distribution over time) also carry information about timing, indicating temporal precision, while peak-rate (the normalized amount of responses) reflects the subject's motivation (Coull et al., 2011). Scalar property of timing behaviour has been found on rats (Tallot, Capela, Brown, & Doyère, 2016; Meck & Church, 1984), birds (Gibbon, 1977), monkeys (Mendoza, Méndez, Pérez, Prado, & Merchant, 2018; Mita, Mushiake, Shima, Matsuzaka, & Tanji, 2009) and humans (Rakitin et al., 1998), and thus seems to be a property common to all species.

The scalar property of timing behaviour implies two things. First, timing relies on the anticipation of the reinforced event, because during retiming conditions -from t_1 to t_N for example-, estimations are tied to the end of the interval and not to its onset. Temporal processing is dependant of an expected event. Second, timing is relative. Indeed, the time occurrence of expected reward is constantly updated between different intervals, and matched in a relative scale but not in an absolute scale. This suggests that the expectation of the event is represented, but not the durations *per se*.

Later on, the SEM proposed several components to account of this behavioural property (Gibbon et al., 1984) derived from an older model (Treisman, 1963).

The SEM contains three processes that allow temporal integration: a clock, a memory and a decision process. Initially, the clock process was composed of a pacemaker, generating pulses at a constant rate, and a switch -an attentional component-, that transfers the signals into an accumulator when timing is involved in the cognitive task. The memory process was composed of the accumulator, also called the integrator -which is sometimes defined as a working memory component-, and a storage component, which contains reference memories. Finally, the decision process is composed of a comparator, that compares the durations in the integrator (ongoing time) with the durations retrieved from reference memory (Figure 3A). Temporal processing by this model translates a sequential treatment of temporal information, where each component treats the information in a well-defined order. First, a pacemaker acts as a stopwatch, then, the switch works as an attentional process to transfer the pulses to the integrator. The integrator keeps in mind the ongoing duration, and sets a beginning and an end to it. This duration is next conducted to the comparator. Meanwhile, the comparator also receives information about long-term memory -storage component- and finally, it is able to compare the ongoing duration with the one stored in the reference memory -possibly set as a threshold-. This comparison between ongoing and long-term memory leads to an outcome, if the durations are judge close enough. In function of the feedback, if there is a reinforcement, the duration in working memory -or integrator- is stored in the reference memory, allowing an update of the track leading to a thinner representation. However, the main idea of the authors is not about this sequential processing, because as mentioned it is replicated from an older model (Treisman, 1963), but it is rather about the origin of the scalar noise in this model, that would be induced by the pacemaker, the working memory component, the storage component, or the threshold of the reference memory. More recently, the working memory component has also been considered as part of the clock process (Figure 3B): this distinction can be important as one can consider memory and clock processes sustained by different brain regions.

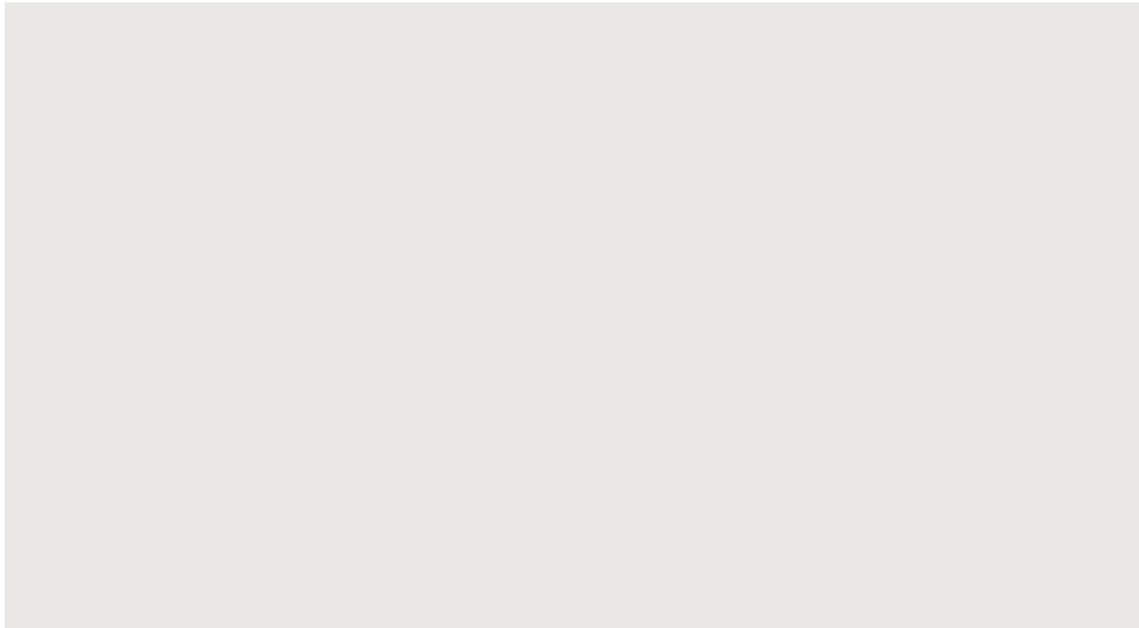


Figure 3. A. The scalar expectancy model and its components, as it has been proposed initially (Gibbon et al., 1984). **B.** The scalar expectancy model by placing the working memory module (integrator) as a clock component (Meck, 1996).

Afterwards, the distinction between clock process and memory processes has been linked respectively with dopaminergic and cholinergic systems (Meck, 1996). Warren Meck highlights the fact that variations in timing performance can be due to variations in clock, memory, or comparison process; referring to the SEM. He assimilates the clock process with dopamine (DA) circuitry in the basal ganglia, and the D2 receptors playing an important role. A series of experiments shows that the pulses for time-keeping are generated by substantia nigra (SN) in rodents, while dorsal striatum - equivalent of Caudate-Putamen ensemble- gates the pulses for accumulation. The SN projects to the striatum: in the clock process of the SEM, this is equivalent to the pacemaker generating pulses to the accumulator through the gating. In a schematic way (Figure 4), the firing of the dopaminergic neurons in the SN always generates the pulses. When timing is involved, the striatum is responsible of the read out of these pulses and transfers them to the integrator, that could be the globus pallidus. However, this last proposition is challenged by the more recent models (Matell & Meck, 2004; Matell & Meck, 2000), suggesting that the striatum would directly play the role of the integrator. On the other hand, the memory processes are considered as cholinergic dependant. Indeed, the author shows that choline acetyltransferase (ChAT) is also involved in temporal perception, but in relation with working memory and reference memory. The working memory process is not considered as part of the clock process here, therefore it is distinguished from the integrator. Concerning the cholinergic system, the author focuses on frontal and hippocampal regions and reviews several studies in rats with hippocampal and frontal damage during a gap-procedures. Gap-procedures follows the same design as a PI task, except

that a gap is introduced in the stimulus to be timed (Figure 4). In this case, the stimulus to be timed is in general a sound, that last for several seconds (10 or 15 for example). Then, in function of the shift observed for the peak-time and its relation with the gap, one can see if the tracking of the event is impaired: after the gap, a shift of peak-time equal of the duration of the gap illustrates an accurate temporal tracking paused during the gap. In our example (Figure 4), it is illustrated by a suppression of the behaviour during the gap and after the gap, the animal resumes its timing behaviour. This phenomenon is called the 'stop rule' (Tallot et al., 2016). Thus, when there is no 'stop rule' observed after the gap, the behaviour can be reflecting a working memory damage: the animal is unable to resume its timing behaviour, it has lost the track of the time preceding the gap. Hippocampal damage involves an amnesia for the stimulus -the time- prior the gap and frontal lesions did not, suggesting that the hippocampal system is involved in "working memory" but not the frontal lobes. Besides, during a simultaneous temporal procedure (STP), lesions of the frontal lobe impaired the timing of two stimuli presented simultaneously. This later result illustrates the role of frontal cortex in divided attention, while hippocampal lesions did not impair the performance in STP. STP follows the same rules than FI and PI procedures, except that two stimuli are presented simultaneously. A correct timing of both stimuli leads to two peak-times matching the durations of both stimuli. Taken together, these results indicate a distinction of the DA system as being responsible for clock process, and the cholinergic system being responsible of memory formation of temporal durations (Figure 5). Thus, cholinergic system and hippocampus could be linked in the temporal processing as they sustain temporal memory formations. To sustain this assumption, it has also been highlighted that in rodents, timing impairment after nigro-striatal pathways lesions or drug administration occurred right after surgeries, suggesting an alteration of the clock process. Meanwhile, lesions and drug administration's acting on the cholinergic pathways impacted the behaviour after several sessions of training, suggesting an alteration of the encoding memory process rather than the clock (Coull et al., 2011).

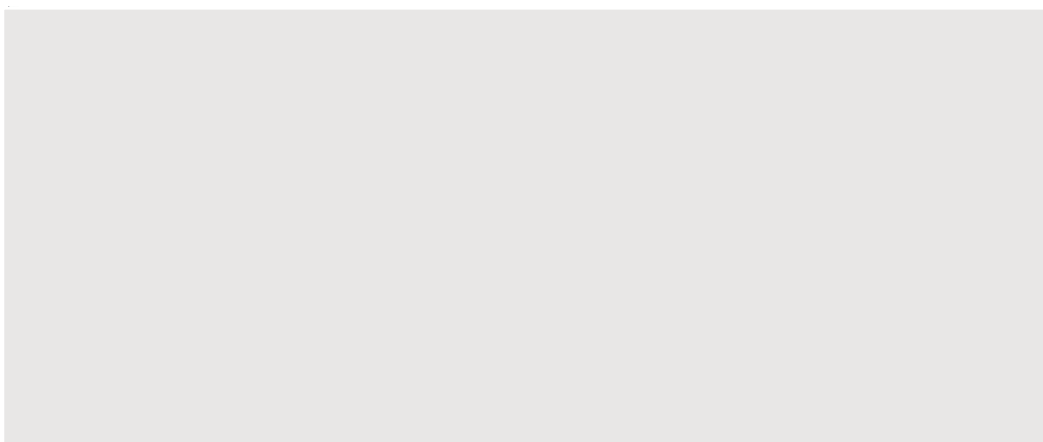


Figure 4. Gap procedure from Tallot et al. (2016). Legend is preserved. A–B. "The mean suppression curve across time is represented with the gap as a grey area (lasts 3s with an onset at 3s for the US@15s group (A) and lasts 2s with an onset at 2s for the US@10s group (B))"

One important point to understand about SEM, is that it gives an important role to neurons activity: pacemaker, accumulator, comparator and even reference memory can be seen as brain areas coding ticks by single cells or neuronal populations activity.

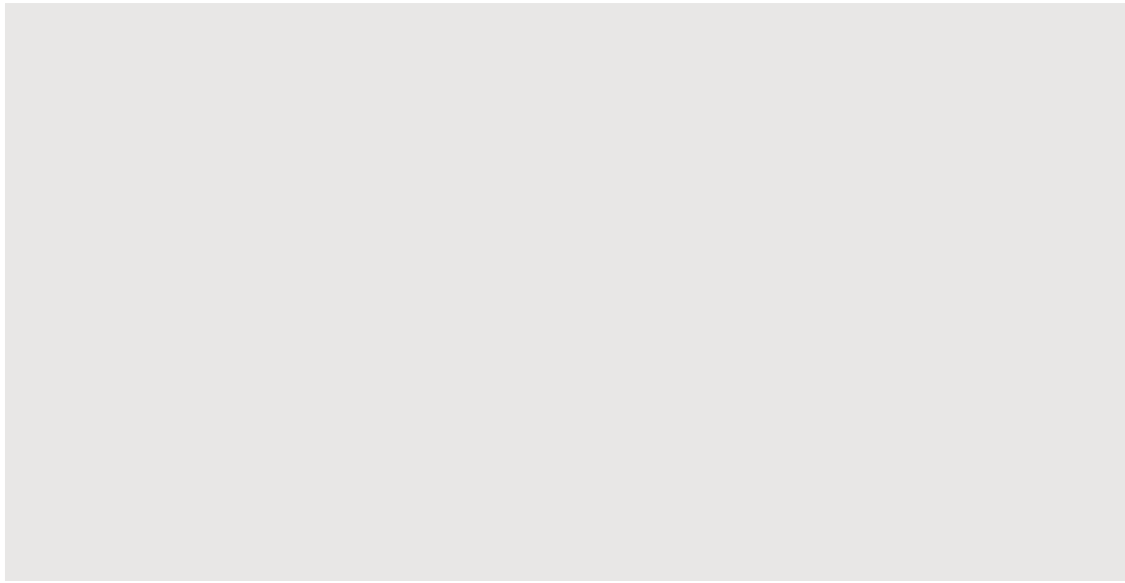


Figure 5. Dopaminergic (A) and cholinergic (B) drugs effects on peak times (y-axis) during fixed intervals procedures across sessions (x-axis) in rats (Meck, 1996). **A. Clock Patterns.** Rats treated with methamphetamine (close symbols) and haloperidol (open symbols), that respectively increased and decreased levels of DA. Left. Drugs administrations on well-trained rats (2 groups, trained on 20s and 40s intervals). Increased levels of DA leads to an underestimation, and decreased levels of DA leads to an overestimation. However, the adaptation - new memory formation- is efficient as over sessions, rats' peak-times are getting closer to 20 and 40s for respective groups. Then, with no drug administration, intervals are overestimated in the methamphetamine group and underestimated in the haloperidol group. This reflects the changes of the internal clock suffering from the drug administration's sessions that have altered the reference memories. Over training, peak-times are back to 20s and 40s for respective groups. **B. Memory Patterns.** Rats treated with physostigmine (closed symbols) and atropine (open symbols), that respectively increased and decreased cholinergic activity. On the contrary of DA drugs, cholinergic drugs do not influence the peak-time at the firsts sessions of under drug administration (left) for 2 groups of rats trained on (20s and 40s intervals). However, cholinergic modulations lead to a distortion of the new memory formations: increased cholinergic activity reduces peak time and decreased cholinergic activity leads to increased peak-time. As peak-time during the first sessions under drug administration are not shifted, this can be interpreted as a preserved clock process. The fact that peak-time, on the contrary of DA modulations, is shifted over training, is interpreted as an alteration of the temporal memory formation, or an update. When cholinergic drugs are not administrated anymore (right), the overestimations and underestimations pattern are consistent with the erroneous memories. New memory formations are consistent with a return to 20s and 40s peak-times respectively for each group.

Following these results, a temporal map hypothesis of the rodents' hippocampus advances the idea that durations are stored in the hippocampus. According this idea, short durations -around 8s- could be stored ventrally and longer durations -around 12s- could be stored dorsally (Oprisan et al., 2018). The authors advance several arguments and results from the literature. The model is convincing if one considers the hippocampus as a storing structure and not a memory formation structure, but is documented only for a defined time-range at the tens of seconds. However, what would be the neural signatures for temporal memory remains unclear.

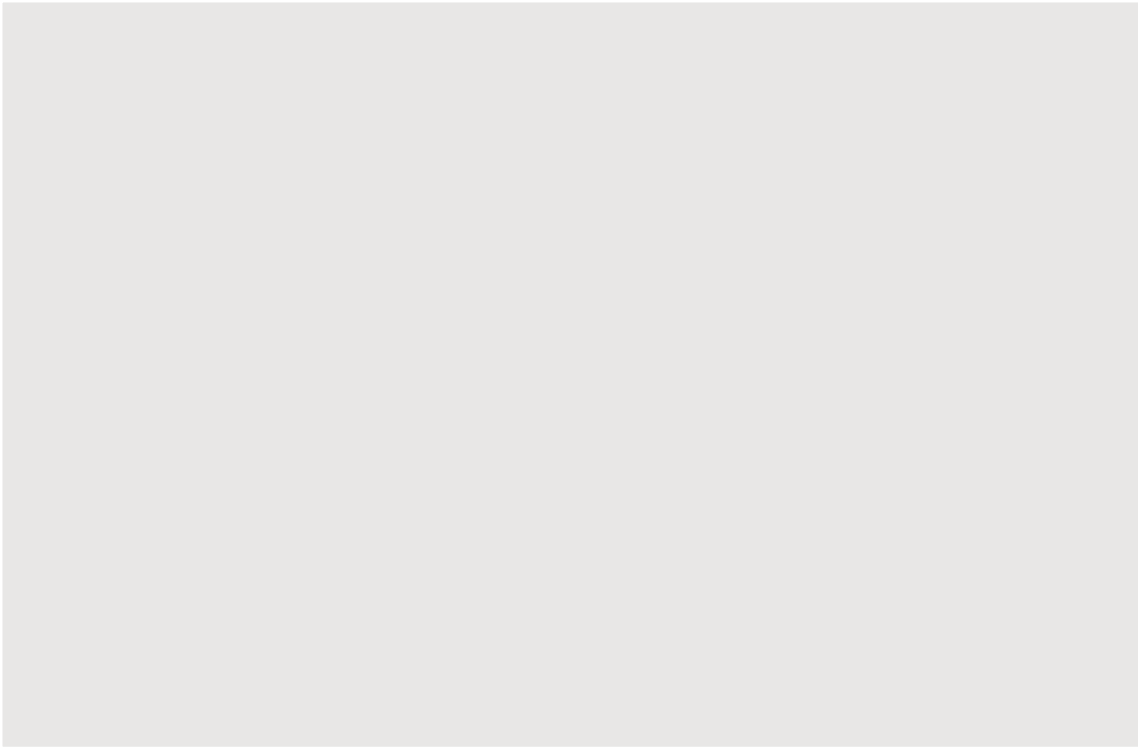


Figure 6. The components of the scalar expectancy model as proposed by Meck (1996) and Oprisan et al. (2018).

Some of the components of the SEM have been placed in neural substrates but not all of them: nor the reference memory -except for the topological map of hippocampus mentioned above-, nor the comparator process for example. It also remains unclear what neural substrate act as the working memory component: it is not directly represented in the Meck's model for example (Figure 6). Whether the integrator and the working memory components are the same remains unclear, as the first one is proposed to be sustained by the globus pallidus and the second one by the hippocampus in the text (Meck, 1996). This can be a limit of the serial representation of temporal processing. Later on, some regions have been suggested to play the role of comparator process at the second range: the Supplementary Motor Area (SMA) and the dorsolateral prefrontal cortex shows activations during comparisons of time intervals (Rao et al., 2001), but also the striatum (Harrington et al., 2011). Although, there is not direct pathway between dorsal striatum and hippocampus that would attempt for the connection between the gate and accumulator nor between the accumulator and comparator modules. Thus, this information must go through the cortex.

Regarding the reference memory component, we prefer to consider a temporal consolidation in long-term memory of the durations in the cortex, exactly of what would be expected for any type of memory formation (Moscovitch et al., 2005) as it is described by the multi-trace theory (MTT). Indeed, one of the weak points of the SEM model and the neural substrates suggested, is the lack of importance it gives to cortical areas, except the slight mention they could play as a comparator process. Cortical

areas are more often considered in the multiple-oscillator models. Gradually, the representation of interval timing has been disengaged from pacemaker models to move to Coincidence-Detection models, as more evidences of the role of cortical areas in timing appeared. Thus, cortical areas are probably not placed into the SEM because they have been directly placed into the coincidence-detection models afterwards.

Although an important point that the SEM leaves us with, is that it accounts for scalability in behaviour: the code for time is relative to an upcoming event. So, as behaviour is scaled in a relative way, there must be a relative -neural- code at the neural level for the duration estimated. But SEM also implies that there must be a code for memory storage in the brain. We advance the idea that such a storage memory code could be an “absolute time code”, even if it can be adjusted by a coefficient later on (Oprisan et al., 2018).

1.3.b. Coincidence-Detection models

Coincidence-Detection models (CDm) are based on the principle that there are multiple pacemakers in the brain, and that their signals are integrated by a detector. Then, the detector is activated by the reception of the simultaneous input, and acts as a stopwatch. Usually authors refer at this detector component, at this stage of time perception, as a clock (Matell & Meck, 2000), but we prefer the term stopwatch. The use of the terms “clock” or “stopwatch” infers the fact that temporal processing at this stage is invariable and insensitive to noise, but it is. The CDm are not incompatible with pacemaker-based models, such as the SEM. They can easily be compared and are based on similar properties: CDm consider cortical areas as pacemakers, but they are also based on clocks, memory and comparator processes (Treisman, 1963): the detector from the CDm can be assimilable to the integrator of the SEM (Figure 7). CDm complete the SEM by including cortical areas and cortical oscillations in time processing. For example, in the beat-frequency (BF) model, pacemakers could be either the neural oscillations from cortex, or even a group of cortical neurons spiking at a regular frequency (Kononowicz & van Wassenhove, 2016). The main point, is the idea that the brain has multiple oscillators -not only one-, and all of them are acting at a unique frequency. Then, the beat frequency of any pair of them is defined as the frequency at which they discharge simultaneously: their beat frequency is lower than their intrinsic oscillations (Miall, 1989). This operation allows to time from milliseconds scale to minutes. Thus, the encoding of a duration from t_i to t_j can be computed by finding the oscillators firing simultaneously at t_i and at t_j . The retrieval of the interval can be processed by selecting the pair -or the group- of oscillators that fire simultaneously again. The neural substrates for the pacemakers of this model are the cortical areas -cortical activity is synchronized by a stimulus onset- and the striatum: the striatal spiny neurons detect the synchronization of the cortical inputs, signifying the beginning and the end of the duration (Matell & Meck, 2004; Matell & Meck, 2000).

Thus, the striatum is proposed to be a neural candidate for the coincidence detector, because of its large cortical afferent. The model underlying this architecture is referred as the striatal beat-frequency (SBF) model. The striatum plays a role similar to the integrator described in the previous model, therefore integrating information from the cortical areas. This model integrates into a unique framework the time codes in multiple cortical area such as frontal cortex, supplementary-motor areas, parietal cortex, or even auditory cortex and also the circuitry in time-attention based task (Coull et al., 2004). However, studies are restrained to second-range discriminations.

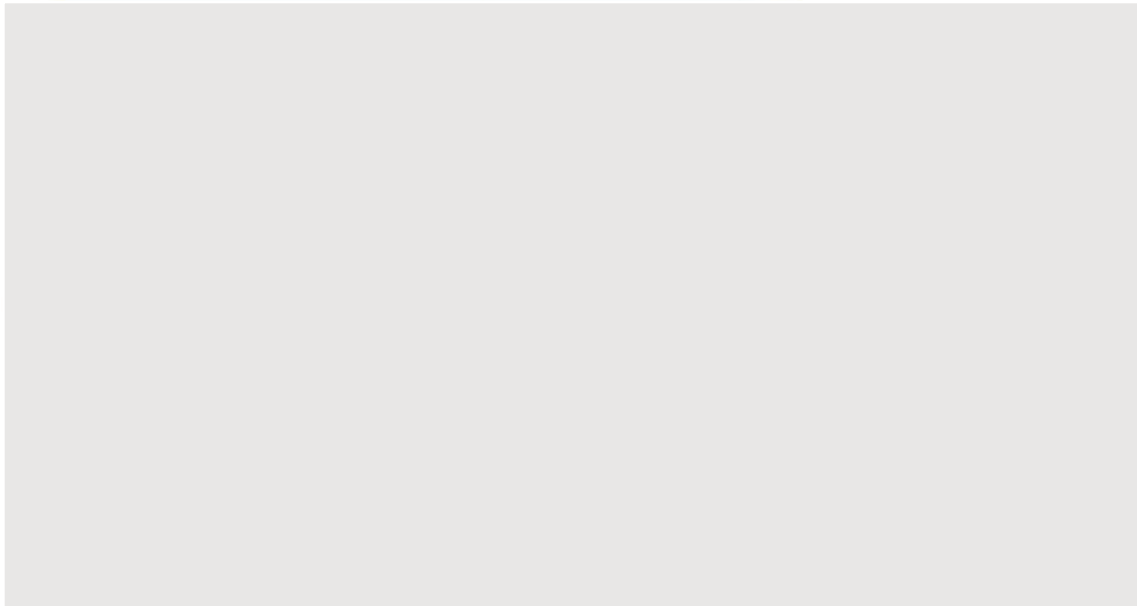


Figure 7. Cortico-striatal circuits in interval timing as described in Coull et al. (2011) based on the SBF. Taken together, SEM and SBF models, pacemakers could be sustained by midbrain regions and cortical areas, integrators could be played by striatum or GP. In addition, suggestions in link with connectivity are represented in dot orange: the thalamus and the cortical areas could play a role of reference memory components. Blue lines represent dopaminergic inputs, and red lines glutamatergic inputs are excitatory (purple). Red lines represent GABAergic inhibitory inputs (green).

It is tempting to find neural candidates for the elements making the coincidence detection model. Indeed, neural oscillations at the cortical level are strong candidates to represent ongoing time (Grabot et al., 2019), but no particular frequency band is a preferred candidate (Kononowicz & van Wassenhove, 2016), and the SMA acts as a stopwatch process -pacemaker-. In addition, the basal ganglia, and more specifically the putamen, may play the role of coincidence detector as part of the striatum, by being involved in short-term memory process at the second range (Harrington, Zimelman, Hinton, & Rao, 2010; Coull, Nazarian, & Vidal, 2008; Rao, Mayer, & Harrington, 2001). This has been tested with time-discrimination tasks. In brief, subjects have first to encode a standard duration, to keep the duration in mind during a short delay, following which a second duration is presented. Then a comparison must be done, as in a temporal bisection task defined previously: is the second duration shorter, longer or -sometimes- equal to the first on? Such a task allows to distinguish

the encoding, storing and retrieval phases of timing. SMA is equally engaged -revealed with functional Magnetic Resonance Imagery (fMRI)- during both perceptual phases, in link with its “pacemaker” role. Putamen instead is involved in the storing phase, for short delays, between two cues presentation; while the superior temporal gyrus could be the one retrieving and comparing the durations. These results do not fit well the SEM neural bases described earlier: indeed, temporal areas are involved in the duration processing but not as working memory. Here, the striatum acts as the working memory process. Thus, the distinction between clock processes and memory processes remains unclear, as we mentioned, sometimes working memory component is part of the clock process. In addition, prefrontal cortex (PFC) shows strong synchrony with the striatum during learning (Antzoulatos & Miller, 2014) and PFC could also play an important role as a pacemaker in SBF model (Kononowicz & van Wassenhove, 2016), validating the idea that multiple cortical areas are involved in timing. It also remains unclear, from fMRI observations, how the striatum can act as a coincidence-detector if it is not involved at every step of timing or decision processes. From electrophysiological data although, the striatum shows timing activity at multiple periods of timing tasks in rodents (Zhou, Masmanidis, & Buonomano, 2020; Emmons et al., 2017; Mello, Soares, & Paton, 2015; Gouvêa et al., 2015) and monkeys (Wang, Narain, Hosseini, & Jazayeri, 2018; Chiba, Oshio, & Inase, 2015), particularly during memory phase and comparisons phases; which is more convincing for its detector role. There is also a lack of information for discrimination of longer durations, and the evidences that the basal ganglia would also be involved in timing at longer ranges for primates.

Furthermore, temporal distortion under the influence of emotional load could be due to the sensitivity of cortical oscillators to DA level. Indeed, DA could be responsible of the resetting of the stopwatch at the cortical level (Oprisan et al., 2014). Its release from SN into the striatum acts as a reinforcement signal to represent a particular duration within the cortico-striatal connectivity (Matell & Meck, 2004) matching the role of the connection between cortex and striatum to time intervals.

In brief, SBF supports a dedicated model of timing, for which there is a dedicated network for temporal processing. Although, more or less recent observations support the idea of intrinsic temporal process in the brain: time estimation emerges from the properties of the neurons and neural circuits (Balasubramaniam et al., 2021; Karmarkar & Buonomano, 2007).

1.3.c. The “process-decay” models as examples of intrinsic models of timing

The scalar expectancy theory stipulates that the noise in time perception follows a scalar distribution at second to minutes ranges. A second interpretation of timing behaviour relates on the decay of information as time goes by. Models supporting such an explanation of the temporal processing are defined as intrinsic models of time, as opposed with the SEM or SBF that are dedicated models. Intrinsic models do not compute time *per se*, but the information they code for reflects time.

For example, the Multiple-Time-Scale (MTS) model advances the idea that time estimation can be read as the decay of memory trace (Staddon, 2005; Staddon & Higa, 1999). On FI procedures, the illustration is that the subject could start to respond when the memory trace induced by the stimulus onset drops below a threshold. The key point of this model is that habituation, forgetting and interval timing are underlied by the same dynamical processes which is the formation, the maintenance and the degradation of the memory trace. Thus, memory is interlinked with timing within a working memory framework.

Similar observations have been modelled in a 3-layer neural network, the Timing from Inverse Laplace Transform (TILT) where the stimulus history is reconstructed according to its onset (Shankar & Howard, 2012). The three layers of this model are f , τ , and T . In sum, f is the function that denotes the presentation of a stimulus over time, $f(t_i)$ is the code for the stimulus f at t_i . At each moment, the stimulus layer f activates a column in τ -layer, composed of leaky integrators -a component that leaks a small amount of input over time-. Each integrator decays at a distinct rate, and keeps a track of stimulus history (Figure 8). Each τ column is then transformed in the T -layer, which is modelled by time-cells: neurons that always peak at the same moment within an interval. The association of $f(t_n)$ and corresponding T -layer are stored in memory. This model is relevant because it gives a particular role of time-cells, suggesting that these neurons do not peak in a sequential order because they are sequentially organized, but rather because each node of the time-cell layer is activated after a certain decay of the presentation of the stimulus f . With learning, the association between $f(t_n)$ and $T(t_n)$ grow stronger, thus the T -layer induces activity in the f -layer, and by doing that allows the prediction of $f(t_{n+1})$ in function of the state of $T(t_n)$: this phenomenon accounts for temporal predictions. Although, the key is that temporal learning is successfully coded by the decay activity in a f -layer composed of leaky integrators that could be played by cortical and sub-cortical structures.

A different process-decay model is the Dual Klepsydra Model (DKM). This model does not consider any pacemaker neither (Wackermann & Ehm, 2006), but it is convincing to explain a particular phenomenon: the bias-to-short in time-reproduction-task (TRT). In a TRT, a first duration is presented to the subject, that the subject must reproduce the most accurately afterwards. The bias-to-short in TRT is the fact that the reproduced duration is shorter than the presented duration. The key point of this model is to propose, instead of a counting stopwatch such as the pacemaker, a cumulative clock, like a water-clock. Two mechanisms are described in this model: a cumulative process that is informative about ongoing time, and a relaxation process inducing a loss of information as time keeps going after the end of the duration. The model describes inflow/outflow systems combining both, the integration of the external event in a cumulative way and the spontaneously relaxation following its end. Although, this model does not account for consolidation of temporal information nor comparisons of durations with stored ones.

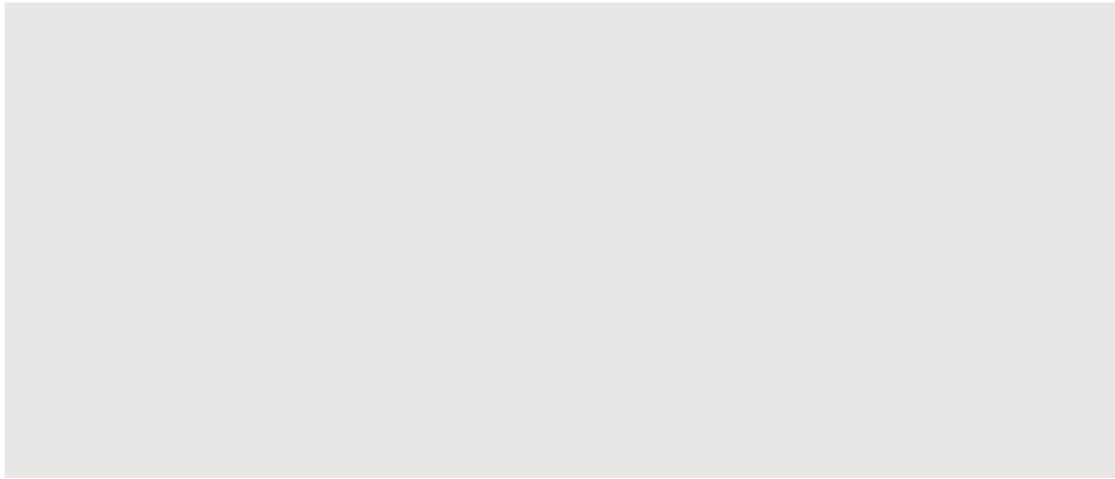


Figure 8. The TILT model from Shankar and Howard (2012). Legend is preserved. “**(a) Timing mechanism.** The stimulus function activates a τ column of leaky integrators. Each node in the τ column has a distinct decay rate s . The activity in the \mathbf{t} column is mapped onto the column of time cells \mathbf{T} via the operator L_k^{-1} . At any moment, the activity distributed across the \mathbf{T} column represents a fuzzy but scale-invariant presentation history of the stimulus. **(b) Associative learning.** For each node in the stimulus layer \mathbf{f} , there is a column of nodes in the τ and \mathbf{T} layers, as represented by appropriate shading. The \mathbf{T} -layer activity at each moment is associated in a Hebbian fashion with the \mathbf{f} layer activity, and these associations are stored in \mathbf{M} . The associations stored in \mathbf{M} and the instantaneous \mathbf{T} -layer activity induce activity in the \mathbf{f} layer. This internally generated activity in the stimulus layer is interpreted as the prediction \mathbf{p} for the next moment.”

Intrinsic models of time are relevant as they support the idea that time is not processed by a central clock in the brain, but rather by different processes according to the task. In the models I have mentioned, one is efficient to explain behaviour in FI tasks, another one is efficient explaining behaviour in a TRT. This observation leads to the idea that time is processed in different areas of the brain in function of the cognitive demand and in function of the time ranges (Buhusi & Meck, 2005).

1.4. Is time processing influenced by time-range?

Yes.

A dedicated model of time should not make any distinction between different time-ranges. For example, temporal reproduction task at the supra-second ranges (2.2, 2.7 and 3.2s) and tens of seconds (9, 11 and 13s) showed the same pattern of activation in cortical areas in both conditions (Macar et al., 2002). The scalar property of timing behaviour also predicts a dedicated timing computation in the brain with linear link from seconds-to-minute range. Although, whether the supra-second ranges below ten seconds, the tens of seconds ranges, and the minute range support the same timing mechanism is still unknown, and electrophysiological data from rodent’s literature gives contradictory arguments about the distinction between tens seconds and minutes as being part of the same range or not (Shikano, Ikegaya, & Sasaki, 2021; Sabariego et al., 2019; Robinson et al., 2017). Indeed, hippocampal “time-cells”, believed to carry a code for time in interval timing, are not always

found at the minute range, but they are found at the tens of second range (Mau et al., 2018; MacDonald, Lepage, Eden, & Eichenbaum, 2011; Pastalkova, Itskov, Amarasingham, & Buzsáki, 2008).

Another recurrent division made in the literature is between the sub-second and the second ranges (Mauk & Buonomano, 2004). To develop further this distinction, sub-second timing would be automatically processed, while second range timing would involve attentional demands (Lewis & Miall, 2003). For example, neural basis of such distinction have already been proposed, between cortico-striatal (top-down) and cortico-cerebellar (bottom-up) circuits, respectively involved in second-to-minute and milliseconds processing (Meck, 2005). Such a distinction has been challenged recently: in monkeys, cerebellum is involved in 'self-timing' -movement self-initiated with a delay- at sub-seconds but also second-range (Ohmae et al., 2017); and also times movements in rodents at the supra-second range (Gaffield et al., 2022).

However, a distinction between milliseconds and second-range timing is likely to exist. Another argument for such a distinction lays on the fact that scalar property for timing is not observable below 100ms in humans (Wearden & Lejeune, 2007), but is only observed for durations from 200ms and above (Mauk & Buonomano, 2004). Further, supra-seconds discrimination could be enhanced by language acquisition in humans: pre-school children discriminate sub-second (200-800ms) and supra-second (1000-4000ms) durations with no difference between each other, while older children (8 years old) performed better at the supra-second range, as adults do (Hamamouche & Cordes, 2019). This could reflect a strategy adopted by older children and humans in general, and involve "numerical counting" when humans time a duration. Indeed, counting becomes useful when the durations to time are longer than 1s (Grondin et al., 1999).

Still, it is complicated to set different thresholds between the time-ranges, and probably there is more than one threshold to set.

A distinction between sub-second and seconds ranges can be made based on the information integration by the brain (Pöppel, 2009). This distinction is not based on time-perception, but it rather argues that the window of 30-40ms is the time needed to reconstruct information conveying from multiple canals (visual, auditory) in the brain. Thus, specifically to humans, time cannot be discriminated within -or below- this window. These properties could define the neuropsychological basis of a moment: a duration that is indivisible. It is striking how timing performance in the same task (an -auditory- interval discrimination task) can be improved at 100 and 200ms, but that such improvement is not transferable from one duration to another (Karmarkar & Buonomano, 2003), and improvement timing estimations around 300ms does not affect timing at other ranges (Guo et al., 2019). This suggests that different temporal processes are recruited for different time scales in the brain. To the millisecond window for time integration just described, Ernst Pöppel opposes another

window of 2-3s size that would give a pre-semantic window of temporal integration needed to construct a conscious episode. Time within this second temporal window is better integrated.

At this supra-second range, one major consideration is the distinction between proactive and retroactive timing. Proactive timing reflects the cognitive processes to time a duration *a priori*: the instruction is given before the timing interval. On the other hand, retroactive timing demands to estimate a duration afterwards: no active timing was involved, the estimation rather lays on the recollection of the events that had elapsed. This second type of timing relies more on an episodic memory retrieval (MacDonald, 2014). It is not studied with animals as it needs the comprehension of an oral instruction following a different ongoing task. Thus, even if there is no empirical evidence for it -yet-, one could hypothesize that proactive timing demands attentional process, and that as time goes by, a duration could be better estimated by using a retrieving strategy rather than an explicit timing. This later strategy is more demanding and thus, maybe not adapted for longer durations. A suggestion is that such a phenomenon would be observable with reaction times: after proactive timing, reaction times would be faster and reflecting anticipation of the end of the interval, as the subject is engaged in timing. After retroactive timing, reaction times would be slower, there is no more anticipation of the end of an interval and the retrieval of the information in memory would increase responses times. Thus, if tested on the same type of timing task, by changing the length of the durations, one could argue that there is a difference in temporal processing depending on the time-range.

Therefore, even if scalability is observed from seconds-to-minutes intervals, we can imagine that second and minutes are not processed in the same way in the brain. For example, patients suffering from Parkinson's disease show impaired time discrimination at the second range in a time discrimination task (short interval at 0.2 or 1s, long at 1.25, 1.5; 2 or 3 times longer than the shorter one) but did not perform differently than controls subjects while discriminating duration at the tens of seconds to minute ranges: 12, 24 or 48s (Riesen & Schnider, 2001). Following this idea, a distinction between short-term and long-term episodic memory has already been suggested, based on the scale from minute to hours to days, but also in function of the cognitive load of the task (Kesner & Hunsaker, 2010). As we argued that timing is interlinked with memory when we described the cognitive models of timing, we can assume that such a distinction could also be made for temporal processing.

We must ask: what are the time limits of the other cognitive process involved in time discriminations, such as attention or working memory? For example, in delay matching-to-sample task (DMTS) that involves working-memory, performance decreases as the delay between stimuli increases from seconds to minutes (Lind et al., 2015); and visual recognition memory is impaired at delays longer than 6s but preserved for delays ranging from 0 to 2s after perirhinal damages (Buffalo et al., 1998). Thus, does it mean that the same cognitive task does not involve the same memory -or cognitive-

processes as a function of time? If so, one can expect that the temporal processing in such a task would be different for 2 and 6s. The same type of arguments can be found in the attentional system for example: reaction times also increases when the periods preceding a target increase from 0.5 to 3.5s (Karlin, 1959), suggesting a decay in arousal that is time-dependant. In monkeys, motivation also drops when delay to reward increases from second to tens of seconds (Minamimoto et al., 2009) suggesting that the interval is not perceived in the same way in one range or the other.

At the neural level, a similar hypothesis suggest that temporal scales are distributed hierarchically across the primate cortex, with prefrontal areas computing longer timescales than sensory areas (Murray et al., 2014). This difference would be related to the cognitive functions processed in the corresponding areas, as intrinsic models of time suggested.

Inter-species comparisons could be relevant to investigate these differences between time-ranges. For example, because of the role of language in human and its impact in time processing, or because of the species differences in somatosensory processes and how these differences can influence temporal integration at different time ranges. Thus, differences or common observations observed across species could help to understand what is at the origin of temporal processing. Although, it is complicated to make direct comparisons between rodents and non-human primates, specifically because of the time-ranges studied up to now in both species differ empirically: seconds in monkeys, tens of seconds in rodents. One can ask if time-range is an intrinsic limitation relative to each specie instead of being a topic of study. In other words, is there a set of durations too short in rodents and a set of durations too long in primates to be studied? Or it can also be due to physical limitations of the animal models: freely-moving rodents and head-fixed monkeys. To provide an element of response to this question, we referred to a recent review (Tallot & Doyère, 2020) to compare the time-ranges usually tested in rodents and the time-ranges usually tested in monkeys. The aim is to see if there is a difference between time-ranges in rodent's studies ($n=66$) and time ranges in monkey's ($n=51$). From the studies of this review, we create a dataset of durations tested in rodents and monkeys, where explicit and implicit timing tasks are put together. We removed of the dataset the studies above the minute-range, and added one study in monkeys of time categorization task (Mendoza et al., 2018). For the studies in which there was more than one duration, in time-discrimination tasks or FI with variable delays for example, we used the median of the intervals as the representative duration of the study. We show that time-ranges studied in rodents and monkeys are different (1-way ANOVA, $F(1,115)=10.51$, $p=.0016$). Time ranges in rodent's studies are higher than time ranges in monkey's studies, as illustrated in Figure 9. This is an important point to consider when trying to extrapolate results obtained from an animal to the other, and may result from very different testing conditions in rodents and primates.

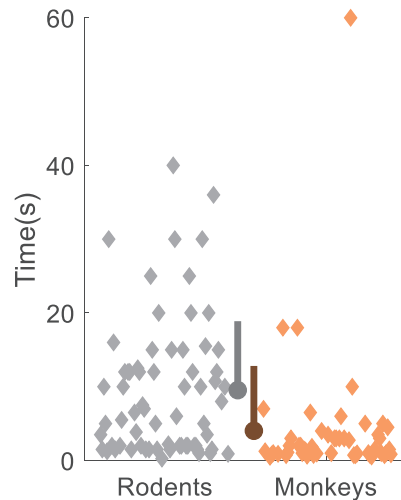


Figure 9. Survey of time-ranges studied in rodents and monkeys. Each diamond is the duration representative of a study. Mean and standard deviation are represented by dot and solid line. Dataset created from studies reviewed in Tallot and Doyère (2020).

By showing 1) that the hypothesis that time processing at different time ranges could be sustained by cortico-striatal and cortico-cerebellar networks has been challenged, 2) contradictory electrophysiological data in rodents, 3) that there is some variability of performances in cognitive tasks as a function of time; it is complicated to set a unique threshold for time processing between time ranges. We can imagine the fact that there would be more than one threshold between time-ranges for time integration, in humans at least. The 100ms threshold is accepted in the literature, but we posit the fact that between several seconds to tens of seconds range there would be another threshold -and not the only one-.

This question is not assessed with temporal processing, although in the attentional system, there is a time-dependant difference between different attentional states: a brief arousal state that is not comparable to a longer sustained attentional state (van Zomeren & Brouwer, 1994). Thus, it would make sense that time processing would integrate durations differently in function of their length.

To investigate further the possible differences between time-ranges, we developed a discrimination task that involves several durations to categorize -a short, an intermediate and a long one- across multiple time ranges, and we asked whether the accuracy of temporal categorization was constant across ranges or if there was an effect of the time range in the temporal accuracy.

So far, there are two brain areas coming up often when we talk about time integration: the striatum and the hippocampus. Whether it is about time and space, cognitive models of time estimations, or the link between time and learning processes, the hippocampus and the striatum are two potential candidates to integrate time.

Thus, let's present these structures more in details.

II. The striatum and hippocampus

Both the striatum and the hippocampus receive cortical inputs, but they have been associated to very different functions, likely resting on very different sets of connections. The striatum receives its inputs from multiple cortical areas, while the hippocampus funnels in a cortical input from the entorhinal cortex. This is a first distinction between the two areas. Although, both brain regions play a part conveying a large amount of information in the aim to, schematically, select an outcome for the striatum, and to create a memory track of an event for the hippocampus.

For each structure, we can ask how their cellular characteristics, their connectivity and their functional role would give them an important part in temporal processing.

II.1) The caudate-putamen ensemble in the striatum

The striatum is the main input of the basal ganglia (BG) which also includes the substantia nigra, the globus pallidus and the subthalamic nucleus. Striatum can be divided in three different sub-regions: the caudate, the putamen and the nucleus accumbens (ventral striatum). These regions do not differ by their cellular characteristics, but they do differ by their connectivity and their cognitive functions. We will present striatum connectivity, its imbrication in the cortico-striatal-thalamic loops, and striatal cellular characteristics. We will mainly focus on the caudate-putamen ensemble, as it has been proposed as neural substrates for time processing, by detailing their functionalities.

II.1.a. Connectivity

Striatum receives glutamatergic afferents from multiple cortical areas, thalamus, and dopaminergic afferents from the midbrain: the striatum is one of its larger efferent. Substantia nigra compacta (SNc) projects to caudate-putamen ensemble and ventral tegmental area (VTA) projects to nucleus accumbens (Haber, 2014). Even though most of the dopaminergic inputs to the striatum modulate the cortical inputs by phasic activations (Matell & Meck, 2004), there are also tonic discharge from dopaminergic neurons (Howe et al., 2013), that could allow to continuously track reward changes (Wang, Toyoshima, Kunimatsu, Yamada, & Matsumoto, 2021).

Although, most of the striatal inputs come from cortical areas. Motor cortices project mainly to median-dorsal putamen (Künzle, 1975). On the other hand, striatal most anterior territories of caudate-putamen ensemble and ventral striatum, received most of its inputs from prefrontal cortex (Haber, 2016). Ventral striatum also receives inputs from the hippocampus and the amygdala. Most of the projections to the anterior part of the striatum are dorsally to ventrally segregated, respectively receiving inputs from: dorso-lateral prefrontal cortex (DLPFC), dorsal anterior cingulate cortex (ACC),

orbito-frontal cortex (OFC), and ventro-medial prefrontal cortex (Figure 10). This wide connectivity makes the anterior striatum a complex structure processing information for learning (Haber et al., 2006). The organization of cortico-caudal projections combines two schematics approaches. The first one, is the organization from anterior to posterior parts: frontal cortex projects to anterior striatum, parietal cortex projects to median part, occipital to posterior and temporal to ventral. The second schematic organization concerns the caudate. Posterior-parietal cortex on one side, DLPFC and OFC on a second side, anterior cingulate and superior temporal cortex on a third side, respectively project to caudate in an organization from medial to lateral axis (Selemon & Goldman-Rakic, 1985).

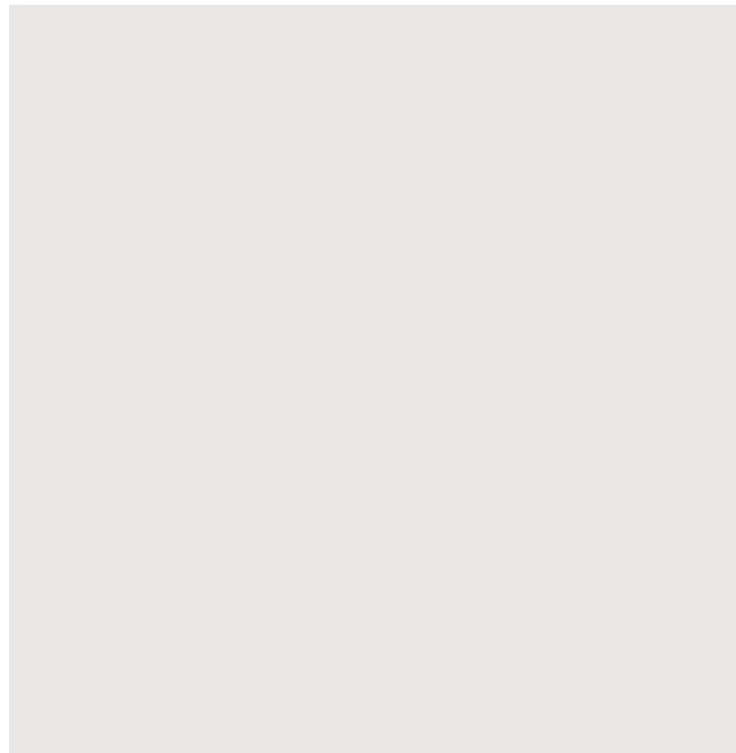
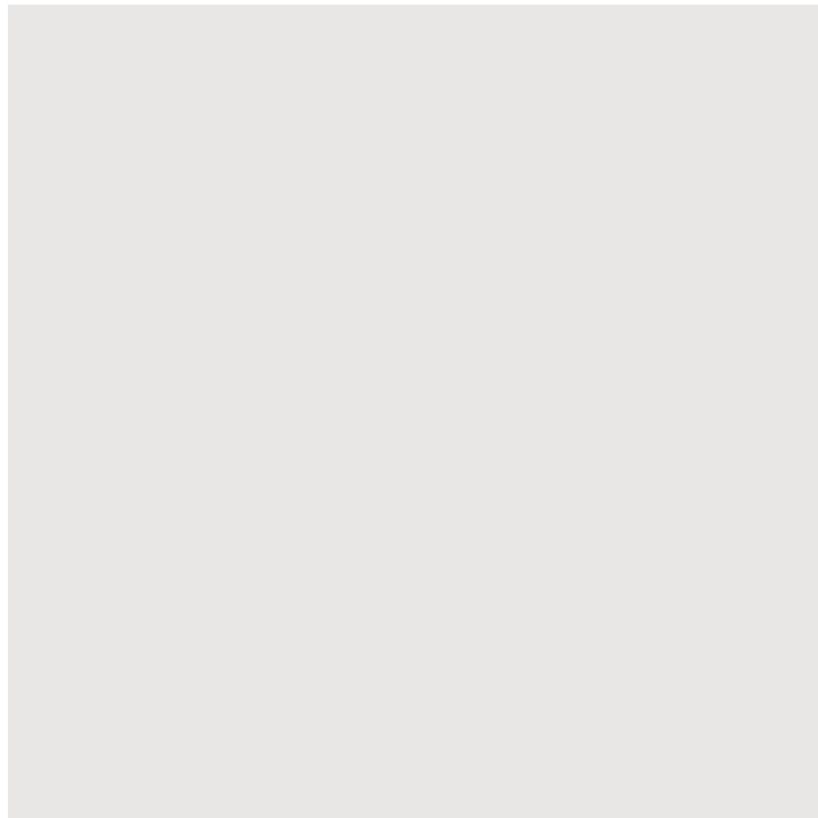


Figure 10. « Schematic illustrating the general topography of frontal inputs to the rostral striatum. dACC, dorsal anterior cingulate cortex; dPFC, dorsal prefrontal cortex; OFC, orbitofrontal cortex; vmPFC, ventromedial prefrontal cortex. » (Haber, 2016).

The striatum projects i) via the “direct way” to globus pallidus internal (GPi) and substantia nigra reticulata (SNr), or ii) via the “indirect way” that pass by the globus pallidus external (GPe) and subthalamic nucleus -as it was mentioned already-. GPi/SNr project then to the thalamus, which in turn project back to the striatum and to cortical areas (Hunnicut et al., 2016) forming a cortico-striatal-thalamo-cortical loop. Cortical areas are the main output of the basal ganglia circuitry. Thalamo-striatal projection allows inhibitory control (Saund et al., 2017), and we assume that to keep a track of time without any new cortical input, such a loop is needed (Figure 11). In the same way, the retro-projection from SN to striatum could also be involved in timing. In addition, striatum also projects to the hippocampus via the lateral entorhinal cortex (Sørensen & Witter, 1983).



Indirect pathway: inhibits
Direct pathway: facilitates

Figure 11. Cortico-striatal-pallido-thalamico-cortical circuitry. Adapted from Meck (1996). Glutamaergic (Glu) inputs are presented in red, dopaminergic (DA) in blue and GABAergic in green to match Figure 6. Direct pathway (dark grey) from striatum to GPi/SNr facilitates action selection, indirect pathway (light grey) from striatum, to GPe to STN to GPi/SNr inhibits actions. Two loops presented in orange illustrates a possible circuitry allowing temporal processing without the any new cortical or sensory input. SNc/SNr: substantia nigra compacta/reticulata; GPe/GPi: globus pallidus internal/entopeduncular; STN: subthalamic nucleus.

The first segmentation of cortical-basal ganglia circuitry has divided five cortico-striatal-pallidal-thalamo-cortical loops (Alexander et al., 1986). Based on the inputs, a functional role has been proposed to different regions of the striatum: the SMA projects to the putamen in the motor circuit, the frontal-eye-field (FEF) project to the caudate body in the oculomotor circuit, the DLPFC projects to the head of the dorso-lateral caudate in an “association” loop, the lateral OFC to the head ventro-medial caudate and the anterior cingulate to the ventral striatum. Such a physical parallelization of these loops allows a parallelization of the cognitive functions. Caudate head, anterior part, and caudate tail, posterior part, also received different cortical and sub-cortical inputs (Griggs et al., 2017).

Therefore, we can consider that the striatal circuits, the motor one (motor cortex to putamen), the associative one (DLPFC to caudate) and the limbic one (anterior cingulate cortex to the ventral striatum) play a role in proactive inhibition, which is the ability to inhibit actions voluntary after learning. It can be opposed to the reactive inhibition, which is automatic, and does not go through the

striatum: the inhibition of an action in reaction to an external stimulus goes directly from cortex to subthalamic nucleus by the “hyperdirect pathway” (Jahanshahi, Obeso, Rothwell, & Obeso, 2015). Thus, striatal connectivity allows to maintain outcomes during a delay. This ability could also be allowed by the properties of medium spiny neurons.

II.2.b. Striatal cells

Striatal cells are divided into two main classes: spiny projection neurons, or medium spiny neurons (MSNs), and aspiny interneurons (Kreitzer, 2009). MSNs, that represent more than 95% of the striatal neurons (Yelnik et al., 1991), are phasically active in response to a spontaneous stimulus (Wilson et al., 1990) with a low spontaneous discharge rate (Kimura et al., 1990). There are two types of them: the ones projecting to the substantia nigra (SN) via the direct pathway, the others projecting to the globus pallidus (GP) via the indirect pathway. The direct pathway facilitates behavioural outcome, and the indirect pathway suppresses it: stimulation of the direct pathway induces motor activity while stimulation of the indirect pathway inhibits motor activity (Kravitz et al., 2010; Macpherson, Morita, & Hikida, 2014 for review). However, the respective roles of the two pathways is likely to be more complex, both pathways regulate movement initiation and ongoing behaviour in different ways (Tecuapetla et al., 2016). Both circuits are GABAergic, their discharges inhibit the projection from SN to thalamus, which is also GABAergic, and by double disinhibition, they provoke the selected output. In the striatal beat frequency (SBF) model, the MSNs neurons are associated with the coincidence detection module (Kononowicz & van Wassenhove, 2016; Oprisan & Buhusi, 2014) because of their -very- large amount of input and because they show high synchrony during their transitions from depolarized to hyperpolarized states (Stern et al., 1998): the striatal neurons have the biological needs to compute time.

Another argument that makes striatum a good structure for timing, is the organization of its intrinsic circuitry. MSNs -projections neurons- can exert lateral inhibition within the striatal circuitry, to other MSNs, to inhibit them. This lateral inhibition allows to balance the actions selections and suppressions during a task (Burke et al., 2017). One can suppose that this lateral inhibition allows to maintain a selected behaviour in time, and to produce it when a selected threshold is reached or when it receives the proper input from thalamus or substantia nigra (Figure 12).

The taxonomy of interneurons is more heterogeneous: fast spiking interneurons (FSI) and low-threshold spiking (LTS) interneurons are also GABAergic neurons, but tonically active interneurons (TANs) are cholinergic. Although, this classification is not exhaustive (Burke et al., 2017). The last category are distinguishable from the others because of their electrophysiological parameters: they display mainly a tonic spontaneous discharge rate around 5Hz (Kimura et al., 1990). They also respond to reward by suppressing their tonic discharge after reward delivery, exhibiting a brief pause, followed

by a brief rebound in their tonic activity. This electrophysiological signature is also observed after the presentation of a stimulus announcing a reward after Pavlovian conditioning (Apicella et al., 1991). The innervation of striatum by dopamine from the substantia nigra modulates the response of -caudal-TANs after learning (Aosaki et al., 1994): their proper responses are a fundamental need for associative learning. Also, recent evidences suggest that they trigger more information than just reward processing and learning, but also are informative about context recognition, movements and stimulus detection (Apicella, 2007). By themselves, they give an idea of the wide range of cognitive processes computed by the striatum. For example, besides the recognition of a rewarding stimuli, TANs also contributes to motor processes by coding for the probability that the stimulus will trigger a movement (Blazquez et al., 2002).

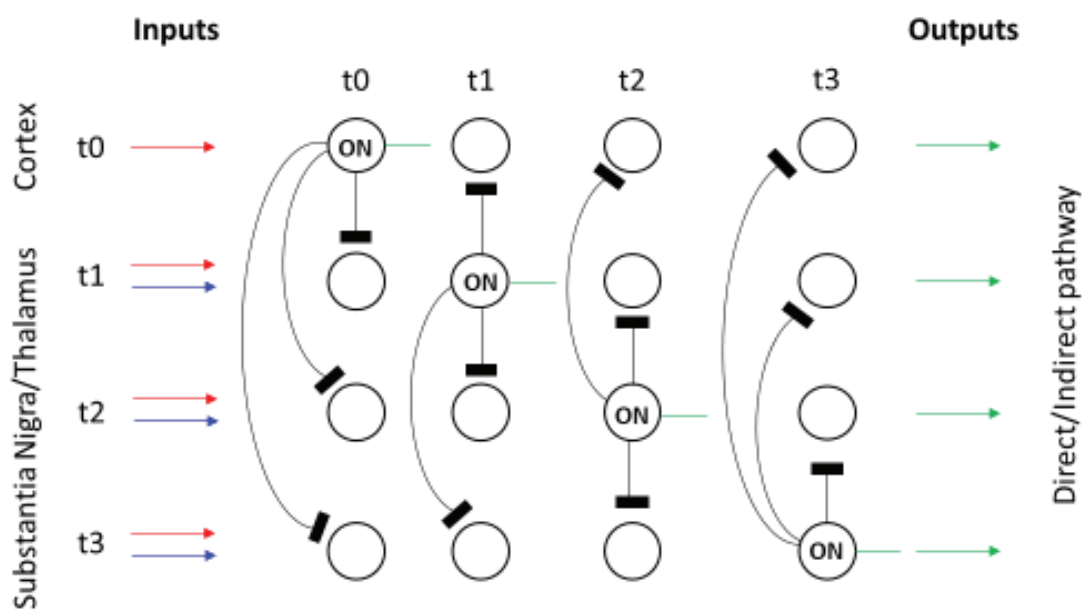


Figure 12. Medium spiny neurons and their collateral inhibitions (black lines with rectangles) coupled with GABAergic outputs (green) allow action selection at time t. At t0, neurons responsible for outputs at t1, t2 and t3 are inhibited, and output is allowed by t0 projection. At t1, t2 or t3, the same logic is applied but inputs are proposed to come from other regions of the cortico-striatal-thalamic loops (dopaminergic in blue or glutamatergic in red).

Thus, one could define as many cognitive functions for the striatum as the number of cognitive functions computed by its dopaminergic and cortical afferent, and the heterogeneity of striatal cells allow so many different computations.

II.2.c. Functions

Dopamine regulated functions

Besides movement production (DeLong, 1990), the cortico-striatal-pallidal-thalamo-cortical loops are involved in many cognitive functions such as -habit- learning (Seger & Spiering, 2011), goal-

directed action selection (Pernía-Andrade, Wenger, Esposito, & Tovote, 2021; Kimchi & Laubach, 2009) and reward evaluation (Humphries & Prescott, 2010) via dopamine regulation (Schultz, 2007). Neuronal loss from SN, that projects to striatum, causes a dopamine deficiency in Parkinson's disease (Jellinger, 2015). The main symptoms of Parkinsonian patients, at early stages, are motor symptoms; and one of the collateral effects of treatment is related to reinforcement -gambling-. Thus, neuropsychology informs us about the main roles of the striatum: movement and reward processing. Even if dopamine is believed to be one of the main neurotransmitters involved in timing, it is important to note that dopaminergic depletion does not provoke timing complaints in these patients. Although when they are tested, there is indeed a deficit in timing durations (Parker et al., 2013). The first role of dopaminergic neurons is to signal rewards. Unexpected rewards elicit increase of dopamine neurons located in substantia nigra (SN) and ventral tegmental area (VTA). With learning of an association between a conditioned stimulus and a reward, dopaminergic neurons increase their activity to the CS presentation. During the delay -in an instrumental task- dopaminergic neurons do not show a tonic transient activity, indicating that they do not reflect any working memory process but rather mark the time of events (Schultz, Apicella, & Ljungberg, 1993). When an expected reward is omitted, there is a suppression activity at the moment when reward would have been delivered (Sarno, De Lafuente, Romo, & Parga, 2017; Schultz, Dayan, & Montague, 1997). Dopaminergic responses also occur when rewards are either unpredicted or when they occur at unexpected times (Hollerman & Schultz, 1998) after learning: by definition, dopamine codes for the occurrence of a reward and its time. A partial conclusion is that reward-related dopaminergic activity codes time of events. In rodents, dopaminergic modulations explain temporal judgements during a bisection task (Soares et al., 2016). Indeed, activation of dopaminergic neurons from SNc leads to an underestimation of the durations at the same range, and the inhibition of the dopaminergic cells lead to an overall overestimation of the durations, illustrated by the increased proportion to respond long. Even though this result is striking, and confirm the role of dopamine in timing, they do not match the theory were dopaminergic pulses act as a pacemaker, and increasing dopamine activity increases time estimations (Buhusi & Meck, 2002; Maricq & Church, 1983). Indeed, following this last assumption, the activation of dopamine neurons should lead to an overestimation of time, and an underestimation should be observed after inhibition. This illustrates perfectly the following point: the dopaminergic and striatal systems are involved in timing, without raising any doubt, although how they do, it is still unclear. Thus, one could make the hypothesis that striatum is highly involved in timing because of its dopaminergic afferent that encode information about rewards and time needed for learning. In addition, to the phasic inputs, dopamine neurons also provide tonics signal from VTA and SNc to striatum (Howe et al., 2013) that may continuously evaluate possible rewards (Wang et al., 2021), and permit a continuous updating of information over time - leading to a temporal representation-.

Functional map based on cortical afferences

Besides its dopaminergic inputs, the classical way to draw a functional map of the striatum, is to map it in function of its cortical afferences. Following the motor, associative and limbic loops assumptions, putamen is involved in motor action-selection and habit learning (Grahn et al., 2008). Indeed, while putamen shows a rostro-caudal somatotopic organization, with sensory-motors and motor actions from leg area located dorsally, face more ventrally and arm -or hand- in between; there is no such activation or neural code in caudate: it is not involved in motor movement (Gerardin et al., 2003; Alexander & DeLong, 1985), except saccadic eyes-movements (Hikosaka, Sakamoto, & Usui, 1989). Caudate plays more of an associative role: it is sensitive to feedbacks in learning, and allows updating information about ongoing behaviour (Delgado, 2007), it encodes multiple features relevant to decision making, including evidence accumulation -over time- (Ding & Gold, 2010). Finally, ventral striatum codes for motivation (Marche et al., 2017) and reward expectancy (Schultz, Apicella, Scarnati, & Ljungberg, 1992). Although, these loops, and so the functional territories, are not perfectly segregated and they do overlap (Draganski et al., 2008). In another primate study, the disruption of striatal activity by increasing MSNs neural activity with bicuculline (a GABAergic antagonist), induced movement disorders in the dorsal striatum and impaired motivational behaviours in the ventral striatum (Worbe et al., 2009). In addition, another distinction that can be done within striatum, is the division between rostral and caudal territories in motor learning: the rostral part sustains a learning mechanism while the caudal part impairs performance in behaviours already learned, sustaining a memory mechanism (Miyachi, Hikosaka, Miyashita, Kárádi, & Rand, 1997; Miyachi, Hikosaka, & Lu, 2002), or an intentional versus an automatic mechanism as it has been discussed and confirmed later on (Kim & Hikosaka, 2015). A motor task dissociating selection, preparation and execution of a movement also illustrates different involvement of the striatal territories. While action-selection was sustained by the caudate nucleus, preparation and execution activated respectively rostral and caudal parts of the putamen with respect to the anterior commissure (Gerardin et al., 2004) confirming a functional distinction in the rostral-caudal axis in addition to the sub-structures of the striatum. Such a distinction is also made within caudate nucleus: even if caudate circuits code for saccadic eye movement to a rewarded object, caudate-head circuits codes are sensitive to recent experiences and short-term memory, while caudate-tail circuits codes in function of long-term memory with outputs more stable (Hikosaka et al., 2019). These arguments lead us to define a map of the striatum that is not solely based on the three different sub-territories, but that is also organised in an anterior-posterior axis where the most rostral areas are involved in executive functions and caudal areas are influenced by long-lasting codes and processes.

Thus, the striatum receives inputs from anterior cingulate cortex, and orbito-frontal cortex which process reward information and motivation (Setogawa et al., 2019; Shidara & Richmond, 2002;

Tremblay & Schultz, 1999). Frontal cortex plays an important role in working memory (Riley & Constantinidis, 2016), carrying information over time without sensory cues. For example, frontal lobe lesions induce deficits in performing delayed responses (Jacobsen & Nissen, 1937). Frontal cortex projects widely to the striatum. Considering this, the striatum receives inputs about all these information and codes for reward and time: reward codes in the striatum are widely distributed from dorsal to ventral (Bowman et al., 1996), neurons in the anterior striatum codes the values -reward magnitude- of an action-selection and not the action itself (Samejima et al., 2005), and reward expectation is coded in caudate head (Kawagoe et al., 1998).

Reward processing in the striatum and time

The previous paragraph described results showing that striatum processes reward expectancies, reward times and movements. These functions can easily be linked to proactive inhibition during reward discounting processes.

Reward discounting refers to the fact that the same reward -size, amount, usually defined by magnitude- has a higher “subjective value” as it occurs earlier in time. Or, in other words, that waiting for reward devaluates its value. The subjective value can be measured by proposing a choice between two rewards, R1 and R2, where R2 is bigger than R1. R2 can be associated with a variable delay, from t_0 (immediate delivery of the reward) to t_n , and R1 with a fixed delay t_{R1} . In a forced-choice task between receiving R1 or R2, if R2 is associated with “short” delays, from t_0 to t_n , the probability that the subject picks the bigger reward is high. To do so, the inhibition of selecting the immediate reward must occur. Reward evaluation and proactive inhibition interplay. If R2 is associated with “long” delays, from t_{n+1} to t_N if we follow the same example, the subject has higher probability to choose R1 if it is associated with a shorter delay. Usually, the probability to pick R2 over R1 follows an inverse logarithmic curve in function of the delay it is associated with: it's the discounting value of R2 (Frost & McNaughton, 2017; Green, Myerson, Holt, Slevin, & Estle, 2004). Usually, t_n is longer than t_{R1} : the subject waits more but receives a higher reward. So, the association between R2 and t_n (R2- t_n) has a higher value than R1- t_r . But at t_{n+1} , the subject prefers to pick R1: the association R2- t_{n+1} has a lower value than R1- t_r . With delay discounting, time becomes a feature of our environment influencing decision making and goal-directed behaviour. Of course, prefrontal cortex codes for differential values of these associations needed to process a choice (Kim, Hwang, & Lee, 2008), and we know to prefrontal cortex projects to anterior striatum.

Striatum -caudate and accumbens- neurons code the information (sum of reward and difference between two rewards) needed for decision in this type of task (Cai et al., 2011). Caudate neurons represents temporally discounting values combining the information about reward size and delay at the supra-second range (up to 6.9s) during cue presentations, and its inactivation impairs the integration of reward and cue leading to a drop in motivation (Hori et al., 2021). In the ventral striatum,

TANs code for temporal discounting during the cue period by scaling their neural pulse or their pause-pulse responses. Such a code is informative about the subjective value of the reward leading to a decision, but not to time *per se* (Falcone et al., 2019). In addition, caudate dysfunction induced by dopamine agonist in non-human primates alters temporal discounting in monkeys, avoiding larger rewards delayed in time and seeking for smaller immediate rewards. It is likely that this disturbance is due to the fact that time, in this case waiting for a delayed gratification, is perceived more aversive, but this could also be due to the activation of the direct pathway inducing seeking behaviours for direct rewards (Martinez et al., 2020). Such a pattern was not found after dopamine dysregulation in putamen or ventral striatum. Once more, these results confirmed the different involvement of the striatal sub-structures in information processing (Dalley & Robbins, 2017).

Striatum and behavioural conditioning

We have mentioned the importance of time in behavioural learning, such as Pavlovian and operant conditioning. Now we will show that the striatum plays a role in such learning. During Pavlovian conditioning, temporal information between CS and US is coded by the amygdalo-prefronto-dorsostriatal circuit in rats for aversive learning (Tallot et al., 2020) and dysregulation of dorsal striatum slows down appetitive learning of CS-US associations (Cole et al., 2017). Indeed, dorsal striatum in rats is required to link stimulus-output and response-output associations in Pavlovian and instrumental learning (Corbit & Janak, 2010). As we already showed, FI procedures are instrumental learning task. During the CS-US delay, striatal neurons showed scalability from 12 to 60s to optimize behavioural anticipation of the reward (Mello et al., 2015). Indeed, striatum controls temporal behaviour by dopamine regulation (Kamada & Hata, 2021; De Corte, Wagner, Matell, & Narayanan, 2019) but also with cortical signals (Emmons et al., 2017). Striatum is not involved in behavioural conditioning only because of its responsiveness to rewards, but also because it has the function to time CS-US durations and to link these events in time. Striatal neurons also code expected events -rewards- in time, after 10s or 40s, during a FI task; indicating that they do not necessarily map the durations *per se* but they can code for expected events (Matell et al., 2003). Furthermore, during an instrumental task, choice can be based on stimulus duration only. During Pavlovian conditioning, timing is linked with the expectancy to reward or CS-US integration, but not needed to produce an outcome. On the other hand, during instrumental task, timing is needed to produce an action: timing is not directly related with reward expectancy nor with temporal pairing between two events in this case. This is the case for bisection tasks: to get rewarded, subjects must discriminate a standard duration as shorter or longer than a target duration. We know that in this type of task at the second range (duration-target at 1.5s, duration to distinguish went from 0.6 to 2.4s), striatal activity is linked with durations-judgements (Gouvêa et al., 2015). This result shows that striatum codes for time in order to produce time-based outcomes.

Time processing and sequencing are functions that are also treated by the hippocampus (Pezzulo et al., 2014). For example, striatum and hippocampus are involved during acquisition of motor-learning sequences (Gann et al., 2021) but the proper functioning of both structures is also needed to correctly process time at the minute-range. Indeed, striatum encodes durations at the minute range, up to 5 minutes, in a task similar of an FI task, but the organization of its neural activity is impaired after hippocampal inactivation (Shikano, Ikegaya, & Sasaki, 2021).

II.2. The hippocampal formation: *where am I in time?*

The hippocampus is a structure of the medial temporal lobe of three neural parts: CA1, CA2 and CA3 that stand for Cornu Ammonis. The hippocampal formation groups the hippocampus and its most neighbouring structures: the entorhinal cortex (ERC), the subiculum and the dentate gyrus (DG). Its cytoarchitecture has an ancient phylogenetic origin with very few changes from rodents to primates. One of its main accepted function supports an involvement in spatial navigation which also support a cognitive map within which mental navigation is possible (Milivojevic & Doeller, 2013; O'Keefe, 1990). Further, it plays a role in the so-called episodic memory as its lesion induces a strong anterograde amnesia.

II.2.a. Cells and internal circuitry

The components of the hippocampal formations have 3 cells-layers, except the entorhinal cortex (ERC), making them different from the neocortex that is composed of 6 cells-layers of neurons. Most of the connections within hippocampal formation are unidirectional. The ERC is the main excitatory input to DG, projecting to CA3, that transmits the information to CA1: this structures a trisynaptic circuit of information processing (Lopez-Rojas & Kreutz, 2016). Nevertheless, ERC also has direct projections to CA3. Most of the excitatory neurons of the DG are granule cells, different from pyramidal cells of CA regions (Amaral et al., 2007). Their axon projections to CA3 are called the mossy fibres. They largely innervate collaterally DG and a larger number of CA3 interneurons, more than CA3 pyramidal cells, providing a sparse code of information (Figure 13). What does it do? The role of DG is to disambiguate similar but different information -pattern separation-: it has more cells than its cortical inputs, that allows to increase information with respect to the conveying one (Schmidt et al., 2012). The final result is to be able to distinguish between two similar memories. Although, whether such a computation takes place in the hippocampus is an ongoing debate: there is evidence for hippocampal activity responding to a same concept -conveying information- (Quiari Quiroga, 2020), opposed to a vision where pattern separation is needed to memory formation, at the condition they take place into the DG and CA3 only (Rolls, 2021).

Neurons in the CA regions of the hippocampus can be distinguished into inhibitory interneurons -around 10% of them- and excitatory pyramidal cells in rodents and humans (Viskontas, Ekstrom, Wilson, & Fried, 2007; Csicsvari, Hirase, Czurkó, Mamiya, & Buzsáki, 1999) that differ by their average activity -higher for the interneurons- and their waveform. CA3 also projects 1) collaterally to other pyramidal CA3 neurons 2) and to CA1 via the Schaffer collaterals. CA3 collateral projections allows auto-associations between inputs that come from different part of the cerebral cortex -via the dentate gyrus- but are associated in CA3 via their recurrent network: this permit the formation and the storage of episodic memories in CA3 network (Treves & Rolls, 1994). For example, a colour-shape association is learned: colour activates neuron CA3-a and shape activates neuron CA3-b. The presentation of the colour recalls the shape in memory because CA3-a also activates CA3-b by the collateral. To retrieve a memory, the whole pattern of CA3 activations activates the CA1 pattern following. Then, CA1 neurons would in turn activate entorhinal cortex that projects back to the cerebral cortex areas originally providing inputs to the hippocampus. These back projections could re-activate physical, emotional or semantic features of an episodic memory. CA1 also receives direct inputs from the entorhinal cortex, where the information is coded with more details than in the other structures of the hippocampal formation.

We have also mentioned CA2 area in the hippocampus. One of the properties of CA2 neurons is to have a reversed synaptic strength rule: they are weakly activated by their proximal inputs from CA3, and strongly activated by their distal inputs from entorhinal cortex. Then, CA2 projects to CA1 (Chevalyere & Siegelbaum, 2010). CA2 plays a critical role in social memory (Lopez-Rojas, de Solis, Leroy, Kandel, & Siegelbaum, 2022; Chevalyere & Piskorowski, 2016; Hitti & Siegelbaum, 2014), but not in spatio-temporal associations.

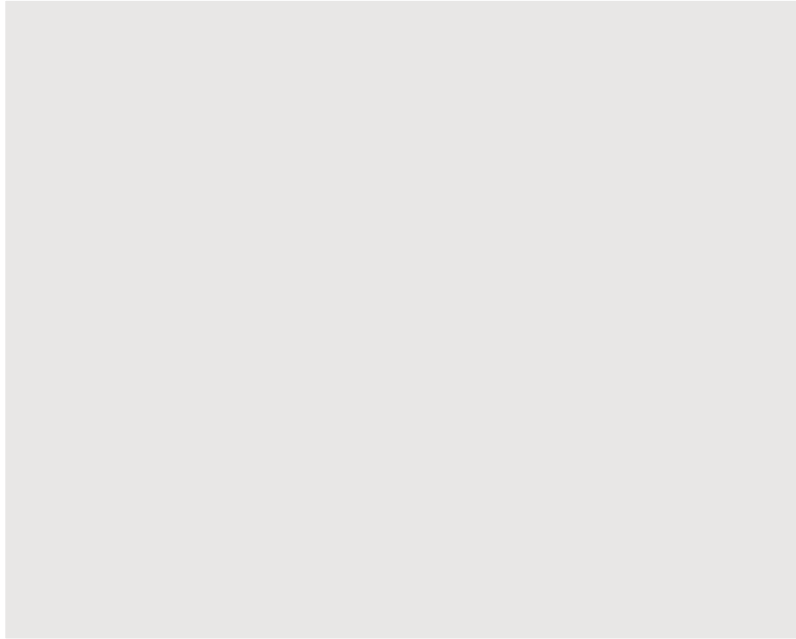


Figure 13. Connections of the hippocampus and pattern separation (Rolls, 2021). Legend is preserved. “Inputs reach the hippocampus from different parts of the neocortex (A) through the perforant path (pp) that makes synapses with the dendrites of the dentate granule cells (DG) (B). The DG cells are hypothesized to produce pattern separated representations in CA3 by operating as a competitive network that projects via the sparse mossy fibre inputs to the CA3 cells. The recurrent collateral system of the CA3 cells (red) is proposed to operate as a single attractor network to associate separate ‘where’ with ‘what’ or reward representations in one trial for episodic memory. The CA3 pyramidal cells project to the CA1 pyramidal cells that are hypothesised to produce conjunctive representations from the separate representations of ‘where’ and ‘what’ in CA3. These conjunctive CA1 representations are efficient as the first stage of the multistage recall process back to the neocortex (green). Time and temporal order are also important in episodic memory, and may be computed in the entorhinal–hippocampal circuitry [...]. The thick lines above the cell bodies represent the dendrites. S and D – superficial versus deep layer pyramidal cells. F – forward inputs to neocortical neurons from earlier neocortical areas. The numbers of neurons in different parts of the hippocampal trisynaptic circuit in humans are shown in (A), and indicate many DG cells, consistent with expansion encoding and the production of sparse uncorrelated representations prior to CA3. [...]”.

How does time emerge from such a complex circuitry? In theory, time is not coded in the same way by the entorhinal cortex than by CA regions because the activation of these sub-population - networks- depends on the cortical inputs. One hypothesis is that temporal information is widely encoded in the entorhinal cortex -with neurons maintaining a monotonic increased or decreased firing rate over time-. In the hippocampus, CA neurons code for time with phasic -transient- activity. CA3 is able to associate temporal information from ERC with other features. On the other hand, CA1, that has the cytoarchitecture allowing competitive network processing, would allow time-sequencing for episodic memory formation (Rolls & Mills, 2019).

In conclusion, the circuitry of hippocampus allows memory formations by auto-association and pattern separations via the trisynaptic circuitry. It is likely that any time code in the hippocampus will be due to memory formation and associative learning. Although, time integration in the hippocampus that does not involve episodic memory might not be coded in the hippocampal circuitry.

II.2.b. External connectivity

The hippocampus receives its inputs from the DG and the entorhinal cortex. Entorhinal cortex receives its inputs from other associative temporal and parietal cortices. In primates, CA1 receives also cortical inputs from temporal and parietal lobes, revealing that the circuitry of hippocampal connections is, in reality, more complex than the trisynaptic connections (Rockland & Van Hoesen, 1999). Then, CA1 1) projects directly to cortical regions -orbital and lateral frontal cortices, anterior cingulate cortex- via the fornix (Insausti & Muñoz, 2001), or 2) projects to the subiculum which projects back to the rhinal cortices and parahippocampal region (Suzuki & Amaral, 2003).

Entorhinal cortex receives its inputs from temporal areas around it, mainly perirhinal and parahippocampal cortices (Van Hoesen & Pandya, 1975). It also receives various inputs from (orbito-) frontal regions (Van Hoesen et al., 1975). These wide patterns of connection allow integration of multiple information.

The hippocampal formation also projects to the striatum, to the nucleus accumbens, from the subiculum via the ventral tegmental area (VTA). This connection is part of the hippocampal-VTA axis regulating dopamine release after the experience of novelty (Lisman & Grace, 2005). The inputs from ventral subiculum to the accumbens regulates the phasic release of dopamine neurons in the striatum, driven by relevant events (Grace et al., 2007). This connexion is critical to decision-making in a reward-delay judgement: the damage of ventral hippocampus and accumbens impaired the selection of large delayed rewards, and induces preference for small immediate rewards (Abela et al., 2015).

II.2.c. Memory Function

Clinical neurosciences established pioneering discoveries on the role of the medial temporal lobe in memory formation (Scoville & Milner, 1957) as patients with hippocampal lesion display strong anterograde amnesias for everyday life events, the so called episodic memory (Tulving, 1993). To what extent, hippocampal memory only deals with episodic memory and whether it englobes other processes beyond acquisition, such as consolidation, retrieval or even working memory is still a matter of debate (Ergorul & Eichenbaum, 2004; Eichenbaum, 2001).

From learning episodes to consolidating them

According to the multiple-trace theory, learning involves cortico-hippocampal circuitry: cortical areas activate hippocampus for associations during learning and this signal is then send back to neocortex. Then, with the “consolidation” of the track, the activation of cortical areas does not go through hippocampus anymore (Moscovitch et al., 2005). This theory explains why episodic memory is altered after hippocampal lesions or at early-stages of Alzheimer disease, and why older memories are preserved. Similarly, hippocampus is involved in explicit memory, while striatum sustains implicit - automatic- memory (Geddes, Li, & Jin, 2018; Tecuapetla et al., 2016) . This means that during learning,

a consolidation of the information occurs and hippocampus is disengaged from information processing, in opposition with striatum, that supports stabilized memories (Albouy et al., 2015). In the aim to “create” a new episodic memory, there must be an association between a time, an event and a place (Tulving, 1993). For this, many different codes in the rodent’s hippocampal formation allow spatial representation: 1) self-position in allocentric space, such as place-cells (O’Keefe & Conway, 1978; O’Keefe & Dostrovsky, 1971) and grid cells (Boccaro et al., 2010), reward location (Gauthier & Tank, 2018) and various aspects of space such as border cells (Bjerknes, Moser, & Moser, 2014; Lever, Burton, Jeewajee, O’Keefe, & Burgess, 2009). The model for space representation in hippocampal formation is that grid cells from ERC provides hippocampal place cells with distance and self-motion information (Poucet et al., 2014). These codes are interpreted to be a track of spatial memory in a convincing manner (Nakazawa et al., 2004). A striking observation for memory formation, is the fact that during spatial exploration, place-cells that fire sequentially in overlapping places “played back” their sequential activity during sleep episode (Wilson & McNaughton, 1994). Such organisation decayed across time -days- reflecting synaptic modulations modified by behavioural experiences. Replayed activity maintain their temporal structure on subsequent sleep episodes (Lee & Wilson, 2002; Louie & Wilson, 2001): the temporal order during information coding can be maintained and reproduced from tens of seconds to minutes. In addition to single-cells code, sharp-wave ripples (SWP-R) are believed to transfer information to neocortex during sleep. Indeed, their inactivation during sleep leads to an impairment of spatial-reference memory task -food retrieval-. It is accepted that sleep episodes are necessary for memory consolidation (Girardeau & Lopes-Dos-Santos, 2021). Although, even if during awoken episodes place cells code for space, their subsequent episodes, from the studies we mentioned, may consolidate temporal sequence in memory and not space *per se*. In addition, replay patterns have also been observed during awoken episodes. The sequentially discharge of hippocampal cells is taking place in a reverse order during stop episodes following a running episode (Foster & Wilson, 2006). Such a replay pattern is believed to encode with precision temporally closed events, bringing temporal parameter in the memory formation role of place cells. It remains unclear whether some of the reverse replays are due to anticipation -as rats must run in the opposite direction after the stop episode-, or whether they could code for time information instead of space. These reverse replays are more readily observable in new environments than old ones, in line with the role of hippocampus in memory formation. In addition, spatial codes can also carry temporal information. Indeed, place cells in CA3 show robust pattern representation stable between different episodes of recording from several minutes to several hours (up to 6), while place cells in CA1 regions showed variability below 1h and the similarity decreased as time went by (Mankin et al., 2012). This temporal code reflects a “process-decay” temporal representation.

Cross species place codes?

Space codes in the primate hippocampus differ from rodents, most likely due to foveally dominated vision in primates (Rolls & Wirth, 2018). Indeed, spatial view cells have been described in primates to code gaze position instead of place leading to a representation of space (Rolls, 1999). Although, there is also allocentric and egocentric representation of space in the primate hippocampus (Feigenbaum & Rolls, 1991), and hippocampus is also involved in spatial memory formation (Wirth et al., 2009). Hippocampus is needed to retrieve spatial information -already learned- (Hoscheidt et al., 2010), and for allocentric navigation, as demonstrated with an impairment of food retrievals for monkeys after hippocampus lesions (Lavenex et al., 2006). But it codes also during learning to make new associations -memory formation- between two unrelated stimuli, a scene -what- and a spatial position -where- (Wirth et al., 2003). Other regions of the medial temporal lobe (Messinger et al., 2001) are also involved in learning spatial associations. But the circuitry of hippocampal formation allows both, spatial and nonspatial memory (Rolls, 1991).

Schemas in hippocampus

In rodents, hippocampus supports memory recall when spatial components must be processed or when there is a recency -temporally close- component (Barker & Warburton, 2011). In humans, -visual- recognition memory can be distinguished into two different processes: familiarity, which only induces a feeling of knowing, or recall, which induces a full remembering of the source and context of a memory (Besson, Ceccaldi, Didic, & Barbeau, 2012; Tulving, 2001). Familiarity is limited to a recognition without being able to place the memory back into context. Recall refers to the ability to retrieve the contextual details encountered during encoding experience. The first allows a fast information processing whereas the other requires more cognitive resources and it is not hippocampal-dependant (Barbeau et al., 2011) but it is ventrally -rhinal cortices- sustained. On the other hand, the ability to recall detailed information is supported by hippocampus. The ability to recall in details information leads to the ability of constructing higher mental representations computed in the hippocampus. For example, hippocampal cells are responsive to more complex physical features such as social stimuli, faces and voices independently in macaques hippocampus (Sliwa et al., 2016). Furthermore, in humans, medial temporal lobe (MTL) also shows selectivity to “concepts”, coded with neurons firing in response to landmarks, objects or persons, presented in different visual modalities -pictures or letters- (Quiroga et al., 2005). By creating concepts, hippocampus can incorporate new information into “schemas” already existents, allowing quicker learning (Tse et al., 2007). Schemas also allow the organization of past experiences. In monkeys hippocampus, schema cells allow to quick learn how -where- to navigate in a spatial navigation task based on previous experiences by integrating multiple features of similar environments (Baraduc et al., 2019). Space is integrated within a larger mental representation.

Short-term information processed in the hippocampus

Because, hippocampus is involved in long-term memory formations, one can doubt whether any short-term memory processes can also depend on the same structure. The short-term computations in the hippocampus and in the cortico-hippocampal loop may be involved in memory formations by computing associations; but it has also been suggested that they can support short-term and working memory (Laroche et al., 2000). Short-term memory differs from long-term memory as it demonstrates temporal decay and chunk capacity (Cowan, 2008). Working memory has also these limitations, but it involves cognitive manipulation of the mental representations.

Delayed-match-to-sample tasks are recognition memory test, that involve also short-term memory, and they are hippocampal-dependant (Gobin, Wu, & Schwendt, 2020; Sloan, Döbrössy, & Dunnett, 2006; Jagielo, Nonneman, Isaac, & Jackson-Smith, 1990). In these tasks, subjects must retrieve cue-targets associations. In general, cue-1 is presented first -sample phase- followed by a delay. After the delay, several targets are presented -match phase-, and the subjects must choose the correct target, *i.e.* target-1, according the cue. If the choice is correct, it means that cue-1 has been kept in memory during the delay in order to produce the appropriate outcome. Then, in another trial for example, if cue-2 is presented, the subject will have to pick target-2 after the delay. In rodents, hippocampal cells fire at the presentation of the sample, the delay, the match and the reinforcement (Hampson, Heyser, & Deadwyler, 1993; Otto & Eichenbaum, 1992), implying that hippocampus is needed to process information at every step of the task, with a more important role of CA1 associating nonspatial objects (Kesner et al., 2005). Later on, it has been shown that both CA3 and CA1 are involved in keeping a track of events in this short memory task, indicating that CA3 role is not limited to spatial processing and CA1 is needed to associate stimuli when there are delayed of 10s (Farovik et al., 2010). In monkeys, inferior temporal lobe codes to retrieve information (Naya et al., 2001) and during the delay of delayed sample-to-match task (Naya et al., 2003). In line with this observation, hippocampus also is active in humans during retention in a working memory task (Zhang & Naya, 2022). Although, even if hippocampal lesions impaired animal performances in a -variant- delayed nonmatch-to-sample: even if they were able to recognize a novel object presented 8s after the 'sample object'; their recognition capacity decreases quicker than intact monkeys at the increased at 15s, 60s, 10 minutes and 40 minutes (Zola et al., 2000; Zola-Morgan, Squire, Rempel, Clower, & Amaral, 1992). This suggest that hippocampal was necessary for information processing beyond 10 seconds. Nevertheless, in the cognitive model of working memory, the hippocampus is not proposed to be a neural substrate for working memory. Working memory would be rather supported by a distributed system (Baddeley et al., 2011).

Hippocampus and temporal order

In addition to keep information in mind for a certain time, hippocampus is also needed for sequencing events in time (Ranganath & Hsieh, 2016). This allows the organisation of events in episodic memory, and answer two questions: what comes first and what announces something. Thus, hippocampus allows temporal-order memory in rodents (Manns, Howard, & Eichenbaum, 2007; Fortin, Agster, & Eichenbaum, 2002) and its neural codes detects the presentation of stimuli -odours- in sequence or out of sequence (Shahbaba et al., 2022; Ranganath & Hsieh, 2016). In non-human primates, medial temporal lobe codes for temporal order items-based and link the items between them during the encoding phase of a 2-items sequence order task (Naya, Chen, Yang, & Suzuki, 2017; Naya & Suzuki, 2011). Time related activity is informative about time elapsed since cue-1 and time remaining to cue-2, needed for working memory and episodic memory formation. This is in line with previous results showing that during an object-place association task, hippocampal activity showed increased selectivity between the stimuli association and the outcome, carrying memory through time (Sakon et al., 2014). In humans, neurons recorded in MTL show anticipatory responses to their responsive stimuli when there are placed in a well-known sequence (Reddy et al., 2015). These results illustrate how time code in the hippocampus seems to be related to sequencing events, needed to memory formation. In fact, it has recently been proposed that hippocampus does not represent space nor time *per se*, but rather organizes sensory events into sequences to construct an internal representation of the environment (Buzsáki & Tingley, 2018).

Remember, the order of events -sequencing- is crucial for associative learning.

During Pavlovian conditioning, hippocampus plays an important role to create a context associating environmental stimuli in order to prevent a positive or an aversive event (Holland & Bouton, 1999). Whether it links the events in time does not remain clear. During a FI task, lesions within the dorsal hippocampus impaired timing behaviour up to 40s in a Pavlovian task (Tam & Bonardi, 2012), in line with the previous results showing that cholinergic level in hippocampus -and medial prefrontal cortex- was higher during Pavlovian associations delayed for 10s than for non-delayed associations (Melissa Flesher et al., 2011).

It has also been established that at the minute range, hippocampal inactivation impaired 3-intervals discrimination at the minute-to-tens of minutes ranges (Jacobs et al., 2013). In an instrumental learning task, a short, intermediate and long intervals were presented to rats that have to select a port in function of the length of the interval. Short and long intervals were always the same, 1 minute and 12 minutes; and intermediate duration varied: 1.5, 3 or 8 minutes. Overall, the results show that time-discrimination for durations with large temporal differences (1-3-12 minutes) does not involve hippocampus, but the discrimination of durations close to each other (1-1.5 and 8-12) is hippocampal-dependant. This is in line with the role of events sequencing, hippocampus allows high-

temporal discrimination to segment episodes. At another scale, lesions of the medial entorhinal cortex (mERC) impaired performance on a temporal-bisection task -10 vs. 20s- but only for the longer duration (Vo et al., 2021), suggesting that keeping track of events exceeding 10s is sustained by the mERC, but not the shorter delays.

As hippocampus supports mental navigation through concepts and memory (Theves, Fernández, & Doeller, 2020; Schiller et al., 2015), it is possible to navigate through time (Gauthier, Prabhu, Kotegar, & van Wassenhove, 2020). Thus, we mentioned spatial codes that carry temporal information and temporal activity reflecting memory process. Although, time-related activity and hippocampus involvement in time-processes seem to be related with -working or episodic- memory. If there would be a time code in the hippocampus for time *per se*, that would track a precise moment in time, as place cells code for a precise location in an environment, such a neural correlate should be observed in the hippocampus. The existence of such code has been argued with the discovery of time-cells in the hippocampus.

III. How neurons can tell time: single cells and populational level

At the neural level, successful time integration could result from neural activity different between t_i and t_j . As for discrimination codes, neurons selective for t_i but not for t_j would situate time at t_i , and conversely for t_j . For a neuron, this would be coded by firing at a well-defined moment within in a wider interval, such as time-cells do. We distinguish this temporal code, the modulation of a neuron's activity by time during an event, from the neuronal responses relative to temporal judgments as what has been observed in macaques frontal cortex (Genovesio et al., 2009) and striatum (Chiba et al., 2015) for example. At the populational level, the state of neural population would reflect a change between t_i and t_j , to be able to situate in time -decode time- by reading the code of the population. Although, are these two patterns the only-ones?

III.1. Single-cells can tell time

In a recent review, three distinct pattern of single cells have been identified to carry temporal information: phasic activation within a delay, ramping activity, and sustained activity over a duration (Tallot & Doyère, 2020). Here, we do not consider neural sustained firing rates at a constant level as a temporal signal, but rather as a signal carrying information over time. Although, phasic activity in a time interval, whether it marks expected events in time -onset and offset of durations for example- or a precise moment in a duration, as time-cells do, and ramping activity -up or down- over time, are the two codes carrying information about time (Tsao et al., 2022; S. Zhou & Buonomano, 2022). Thus, time can be encoded at the single-cell level. We will present the characteristic of these two temporal codes and their properties.

III.1.a. Time cells

The first appellation of "time cells" found in the literature does not refer anymore to the definition we know of them. Indeed, it classified neurons that preferentially encode for cue-1 or cue-2 during the encoding phase of a 2-items sequences, as opposed with "item cells" -item selective-. These neurons cover periods lasting for 320ms, to code in a binary way period-1 versus period-2. Thus, the first definition of "time cells" were embodied in a code for temporal sequence of events (Yuji Naya & Suzuki, 2011). Twenty days later, another study, in rodents, defined "time-cells" hippocampal neurons that fired at a specific moment of a larger defined interval -up to 10s- (MacDonald et al., 2011) consistent across trials. This specific moment, time t , within the interval was defined as the time-field of the time-cell. It is expressed by a phasic discharge at time t for each interval presentation. During a delayed go/no-go task, these neurons form sequential organization of peak time, in such a way that they 'bridge the gap' between cue and response periods: the entire delay duration was filled by

successive peak activity of the time-cell population. Time-cells sequence an event, the delay, that lies within a larger sequence of events, cue-delay-response, that are already distinguished by hippocampal neurons, confirming the role of the hippocampus in representing sequencings of events. The concept of time cells has been built in analogy with the “place cells” concept, assigning them a role in memory consolidation as was developed for place cells. Some of these time-cells displayed different activity in function of the object presented in the cue period, indicating that their temporal modulation can depend on the memory load. Time-cells also responded to two properties: 1) their time-field -width- increased as the time-field arrives later in the interval; and 2) there are more neurons peaking at the beginning of the interval than at the end of it. Thus, beginning of durations is more strongly encoded than the end of a duration. In the same study, when the delay was multiplied by two -up to 20s-, there was evidence to show that some neurons displayed an absolute pattern of retiming, with a high correlation between their activity at 10s and the first half of the 20s; indicating that there is a code for absolute time in the brain. If a duration is stored in memory as time *per se*, such a code would be needed. On the contrary, very few neurons displayed a scaling pattern -5 out of 89- with high correlation on normalized time. The rest of the cells did not show strong pattern of absolute or relative “retiming”, but rather a total “remapping” between durations. The sequencing of an event with this type of code was already documented (Pastalkova, Itskov, Amarasingham, & Buzsáki, 2008). Indeed, in a previous study in which rodents had to complete an alternation task -left or right- after running in a wheel for 10-20s, hippocampal neurons showed a robust reproducibility in their peak activity across trials, generating a sequence during the running episode. The alternation task is defined in the study as a memory task, and the same pattern of sequential activity was not found in a nonmemory task; suggesting -again- a memory role of these hippocampal cells. As for time-cells, there was more neurons peaking at the beginning of the running episode than at the end. Furthermore, the pattern of these cells emerged quickly during learning and they carried information about subsequent behaviour in the alternation task, indicating that they do not carry only time information but rather time within an episode (Gill et al., 2011). In this type of task, neurons can also be sensitive to distance travelled, space, or even speed, instead or in addition of elapsed time. Indeed, when time and distance are the prominent dimensions of a task, time and space both modulated single-cell activity. On the other hand, a few neurons were influenced either by time, either by distance. Funnily, these cells modulated by only one feature -time or distance- regularly fire together, suggesting even though a strong dependence between time and space in the hippocampus (Kraus et al., 2013). When animals are immobilized, sequences are also generated in the hippocampus. In addition, most of the time-cells active during the delay match-to-sample task are selective to a specific sample; and each sample is represented by a distinct pattern of time-cells population (MacDonald et al., 2013). The neural sequences in a 10s-running episode allows to decode time, which means that in function of the neural

activity at time t it is possible to know time t . Also, the overall sequence of time-cells is stable across days -up to 4-; sufficiently enough to predict time within the interval of a day depending on another day activity. But it was also different enough to distinguish the sequences in function of the day (Mau et al., 2018). These results suggest that time code in the hippocampus is strong enough to code time at the tens of seconds range but also to distinguish between different episodes -days-.

All the results mentioned above are from CA1 region, but time-cells have also been found in CA3, with the same prevalence, and displaying the same characteristics (Salz et al., 2016). The question about a difference between CA1 and CA3 remains, especially given their respective position in the hippocampal circuit: CA1 receives input from both CA3 and ERC, while CA3 mainly receives input from dentate gyrus.

The proper organization of CA1 cells hippocampal time-cells and its memory function was suggested to depend on the proper inputs it receives from the ERC. Indeed, inactivation of medial ERC (mERC) in rodents during a delay match-to-sample -delay was 7s- induces a performance deficit in the task, and it impairs the sequential pattern of time cells. Although, mERC inactivation did not affect the place code of CA1 nor the selectivity to objects (Robinson et al., 2017). This result contrast the finding that mERC is involved in temporal processing for durations above 10s (Vo et al., 2021). In line with this last point, another study indicates the opposite. First, rats with mERC lesions and rats with mERC lesions plus hippocampus lesions ran an alternation task with no delay, 10s and 60s delays. Performance was impaired only at the delayed conditions for both groups; thus the electrophysiological results challenged several findings. First, during 10s-delay, sequential activity of time-cells did not differ between the two conditions of the alternation task -right or left- in either mEC lesioned groups nor control. Then, mERC lesions reduced more importantly spatial code in CA1 than in CA3 but did not alter the sequential firing of time-cells in none of the hippocampal regions; as opposed of what would have been expected from the previous study. In contrast, mERC lesions impaired the spatial code in both regions, more importantly in CA1 than in CA3. In addition, even if the sequential activity of time cells is similar between the 10s conditions and the first 10s of the 60s delay -absolute code-, the time cells do not “bridge the gap” of the 60s interval, suggesting that there is a temporal threshold above which time is not sequenced in the brain (Sabariego et al., 2019). The difference between this last study and the previous one might rely on the difference of the tasks: the delay match-to-sample and the alternation task might not require the same memory load.

Another paradox in time cells relates to their relative or their absolute code for time. Until now, it has been pointed out twice that there is an “absolute” code for time in rodent’s hippocampus. Although, a more recent study shows that time-cells in the hippocampus adapt their discharge rate from 10-to-20s and then back from 20-to-10s in relative way, by adjusting their responses extending or shrinking their temporal firing rate as they perform a temporal discrimination task -short vs. long-

(Shimbo et al., 2021). Thus, it seems evident that, even if a definition of time-cells linked with a functional role was emerging, a concluding remark has not been established yet, as there are still contradictory observations regarding their absolute versus relative code, the importance of mERC inputs to generate the sequence and their ability to time durations at the minute range. For example, a recent study also contradicted the non-mapping of minutes by time-cells in the hippocampus, as they show sequential activity up to 5 minutes (Shikano et al., 2021). In a fixed-time task where reward was delivered every 5 minutes, hippocampal neurons also presented a sequential activity mapping the entire duration, and this sequence emerges with learning.

The question raised: are time-cells also present in primates?

As we already reported, time-cells in the primate were first defined as time-cells because they were selective to a temporal position in a sequence-order task during the encoding phase (Yuji Naya & Suzuki, 2011). More recently, studies with patients suffering from pharmacological intractable epilepsy have also identify time-cells in humans hippocampus. In a first study, patients were asked to complete a declarative-memory task where they had to remember a list of word -encoding phase-, and retrieve them -recall phase- after a delay -lasting more than 20s-. Encoding periods last 30 or 40s, retrieval periods lasted 30 or 45s. Time-cells covering these two phases have been found, most of them covering one of the two phases but some of them timed both, encoding and retrieval phases. Further, the more the time-cells pattern were consistent, the more the patients were inclined to retrieve the information in a temporal clustered manner during the retrieval phase (Umbach et al., 2020). In another study, two experiments were performed. First, patients learned sequences of images and memorized them to be able to retrieve any image missing. A sequence lasted 6.5s approximately. The second experiment was the same as the first, but image sequences were interspersed with a 10s gap. Time-modulated neurons were observed during both, image sequences and gaps periods; covering the entire periods. Taken together, these neurons allow better time-estimations than non-time cells, indicating that the time cells population is informative about the time within the periods (Reddy et al., 2021).

Time cells have not only been reported in other species than rodents, but also in other brain areas.

Time cells have also been recorded in the rats -medial- prefrontal cortex (mPFC) and motor cortex. In mPFC, which is also involved in working memory, neurons displaying the same characteristics as time cells have been recorded in a temporal bisection task at the supra-second range (Tiganj et al., 2017). The fact that these neurons are found in an area that is also involved in working memory suggests that “time cells” code is relevant for memorisation. In addition, the same pattern of discharge has been recorded in orbitofrontal cortex during Pavlovian conditioning (Bakhurin et al., 2017) and in motor cortex while rodents actively timed rewards expectancy in a 2-fixed-interval (FI) timing task

between 3 or 6s. In another study, peak activity from neurons in the motor cortex are organized in sequence, and most of these cells show a scalable activity between the two durations. Although, some neurons also display an “absolute” code and a “remapping” in-between (Zhou et al., 2020).

In the last study mentioned, authors recorded also from dorso-lateral striatum (DLS). The organization of striatal peak sequence was more strongly organized in DLS than in motor cortex. In addition, most of the neurons also displayed a scalable code; but absolute patterns and remapping patterns were also found at the supra-second range (Zhou et al., 2020). More studies have identified time cells like in the rodent’s striatum. The scalability of striatal time cells is also robust from tens of seconds-to-minute range (Mello et al., 2015), unlike of what we found in hippocampus where data is less striking (Sabariego et al., 2019). Striatal neurons display the same characteristics as time cells, which are 1) more neurons peak at the beginning of the interval compared to the end, and 2) time-field increases as peak position moves away from the beginning. In addition, their sequential organisation maps the interval from 12s to 60s, by scaling their firing pattern adjusting their centre of mass. In another study we already mentioned, striatal neurons peak sequences were observed during a 5-minutes fixed-time task and map the entire interval. As in the hippocampus, striatal time cells presented the characteristic to have broader time-fields when peak time occurred later time, and striatal sequence of peak activity emerges with learning. In addition, the authors showed that when hippocampus is inactivated, the time selectivity for striatal cells significantly decreased, suggesting that the minute encode process is dependant from striato-hippocampal circuits. In a temporal-bisection task, striatal neurons showed a preferred time-field across trials, with more neurons peaking at the beginning of a trial than at the end in a complete different time-scale: second-range discrimination from .6 to 2.4s (Gouvêa et al., 2015); and at second range during Pavlovian conditioning (Bakurin et al., 2017). In the monkey striatum, there is also some sequential activity in the responses profile of the neurons. During a Pavlovian task, putamen neurons can be grouped into 3 distinct sequences within a 2s-window of cue presentation (Adler et al., 2012). Even though, these neurons do not show an acute time-field, they do map the entire duration by maintaining their discharge rate in a more or less sustained state compared to baseline.

We have mentioned pre-supplementary motor area (pre-SMA) as a key area to process temporal information. One of the neural correlates for time-processing in pre-SMA are “boundary-cells”, found in primates (Mendoza et al., 2018). These boundary-cells also show a phasic discharge at a specific time of an interval, except that they differ of the neurons defined as time cells because the specific time they represent is of interest in the temporal task. Indeed, when monkeys performed a bisection task across different ranges, from sub- to second-range, with boundaries between short and long durations defined respectively at 350, 685 and 1195ms; “boundary cells” peak relatively close to the boundary at each condition. One quarter of them show retiming patterns, by scaling their activity.

They are also linked with behavioural outcome: the closer the peak is from the boundary time, the higher are the chances of the monkey to correctly evaluate short as short or long as long. In the same study, authors have identified 1) category-selective cells, that fire after the interval to be timed as ended but before the choice, and carry information about the outcome: short or long; and 2) trial's outcome neurons that fire during the inter-trial interval in function of the presence or absence of reward. In line with these results, imaging study show that pre-SMA is recruited in human performing a similar timing task (Coull et al., 2008). In conclusion, in pre-SMA, single-cells carry code about time perception, decision, and reinforcement with transient -phasic- activity. These properties are well studied for the temporal control and motor execution of actions.

Further, time-cells like neurons could be found in other regions, as long as the function sustained by the region is time-dependant or time-indicative. For example, in monkey's amygdala, single cells code for time to break a social gaze engagement (Gilardeau et al., 2021), as dopaminergic neurons code for time of reward as mentioned above, or TANs also code for immediate time after stimulus announcing a reward. These codes give an acute temporal information, even if they do not code time *per se*. The fundamental hypothesis behind time-cells, or even boundary-cells in the study described, is that they do code for time.

III.1.b. Ramping neurons

As opposed to time-cells that are time selective within an interval, therefore generating an acute code for time from which a duration cannot be decoded from a single time-cell; ramping-neurons show instead a monotonic increased -or decreased- activity through time, and generate a global code for a duration. Indeed, with a perfect ramping neuron from t_0 to t_N , one could know the time by looking at the neural activity of one single-neuron.

In the hippocampus, is there a ramping pattern activity complementary to the phasic one?

Such activity has not been much reported in the primate hippocampus. Although, in the humans studies we mentioned, some neurons in the hippocampus matched better a ramping pattern than a phasic one, and were thus characterized as ramping neurons but they were always less prominent than time-cells (Reddy et al., 2021; Umbach et al., 2020). In monkey's hippocampus instead, "incremental timing-cells" (ITCs) were recorded in a working memory task. These neurons played a role carrying information over time -750ms- between an object-place association and the outcome. Some of these neurons were not selective to cue nor associations -agnostics cells-, and just ramped no matter what. Other ITCs carried information about the object-place association, and a third type of neurons were selective for the outcome. These two last patterns of responses are linked with memory load, allowing to carry information about association and to respond over time (Sakon et al., 2014).

In rodents, ramping neurons have been identified at the minute range in the hippocampus and the striatum. At the minute range, 'pure' ramping neurons were more prominent than 'pure' time-cells in both structures (Shikano et al., 2021), suggesting that at longer ranges an acute code for durations is not needed but it's rather more efficient to code a wider duration. Actually, ramping neurons in rodents are usually more prominent in mERC. Remember, there is this hypothesis that mERC codes time in a wider manner, and hippocampus codes in a more precise way (Rolls & Mills, 2019). In humans, the proportion of ramping-cells in ERC is 50% (Umbach et al., 2020), thus higher than in hippocampus. In rodents too, ramping neurons are more prominent in lateral ERC than in mERC or CA3 (Tsao et al., 2018) during 250s periods, at the minute scale. Another time-code that has been found in the primate ERC, named "relaxation cells", is similar to the ramping pattern of neurons (Bright et al., 2020). These neurons showed a selective response to visual cue, and then decreased their firing rates. Relaxation time was defined as the time it took neurons to decay back to 63% of baseline firing. Even if all the neurons had a quick response latency (<1.5s), the relaxation time varied from 0.1s to 20s; allowing a wide representation of elapsed time, exactly like what would be predicted by decay-process models of time. In line with this theoretical approach, the time-code of these neurons reflects an intrinsic time representation from neural activity, triggered by something else -visual cue-. This remark can be done for all the codes involving ramping activity. Is ramping activity coding time *per se*, or is it the following signal left by a sensory cue triggering information integration or expectation (Reutimann et al., 2004)?

For example, ramping activity in macaque's frontal cortex is indicative about outcome, keeping a track of it but decaying over time. This ramping activity is not necessary a time-code, but rather a code for outcome that decays over time, and also fits the intrinsic code for time in the brain via process decay (Marcos et al., 2016). A basic sensory code that could be translated in temporal code but might not truly be one, is the ramping activity anticipating reward; as what has been found in the rodent's orbitofrontal cortex (Xiao et al., 2016) and PFC (Emmons et al., 2017; Narayanan & Laubach, 2009). In macaques, most of the prefrontal neurons show an increasing activity during a delay -12s- that is linked with future outcome, and its slope is higher when the outcome is 100% predictable (Quintana & Fuster, 1999), also suggesting that this activity is not related with time *per se* but rather with sensory expectations. Another ramping code that is not related with time is the dopaminergic tonic discharge triggering reward value: their discharge rate display a ramping-up activity when reward-value increases (Wang et al., 2021).

One way to address whether temporal organization of neuronal activity reflects time or other variables related to time, is to ask what kind of code is observed during purely temporal task. Thus, when macaques performed a time production task, only 10% of the neurons in medial frontal cortex (MFC) were categorized as ramping neurons (Wang et al., 2018). These data suggest that the ramping

neurons give a code in time not a code for time. In line with this assessment, ramping neurons in lateral intra-parietal (LIP) macaques cortex signals the probability of an event to occur -hazard rate- (Janssen & Shadlen, 2005; Quintana & Fuster, 1999) or the relevance of a cue as time goes by (Leon & Shadlen, 2003) and can be linked with attentional mechanisms. Still in LIP, ramping activity is also related with motor outcome: when a threshold is reached, the outcome is produced (Maimon & Assad, 2006). LIP ramping activity also codes for time integration and scales time (re)production (Jazayeri & Shadlen, 2015); maybe reflecting a code for time *per se* in the ramping activity of single cells. In rodent's mPFC, ramping neurons are the more prominent during a temporal bisection task at the second range, confirming the importance of this type of code for timing (Kim et al., 2013). As we mentioned in waiting tasks, FI at supra-second and tens of seconds range and a similar FI task at 5s, ramping activity is prominent in rodent's PFC but also in rodents dorsal (Emmons et al., 2017) and ventral striatum (Donnelly et al., 2015). Striatum receives a large quantity of inputs from cortical areas. It is possible that ramping activity from cortical areas drives ramping activity in striatum.

Indeed, in the same study (Emmons et al., 2017), the authors reported that the majority of striatal neurons active during the delay of the FI -3 or 12s- had a ramping activity. As for striatal time-cells like, those neurons also scale their activity between the two durations. Furthermore, most of these ramping neurons -72%- did not respond significantly to lever-press. These observations suggest that the ramping neurons "time" the interval, but are not anticipatory to the response. In ventral striatum, ramping activity is also linked with reward expectation (Schultz et al., 1992). Ramping activity in ventral striatum and mPFC triggers the behavioural outcome when it reaches a threshold: the monotonic increased firing rate acts as a go signal in time (Donnelly et al., 2015). Although, in monkeys caudate, the responses of single cells were heterogenous and not dominated by ramping activity. The pattern of neurons was similar between caudate and MFC (Wang et al., 2018). Taken together, these results suggest that the activity profile between frontal cortex and striatum was similar during the same task: when there is ramping in frontal cortex, there is ramping in striatum. When there is not a dominant ramping pattern in cortex, striatum is not dominated by ramping activity neither. Although, even if ramping activity is observed in monkey's frontal cortex and in caudate nucleus, activity in FEF is related to sensory incomes and activity in caudate is related to reward expectancy.

Several observations about ramping neurons seem to link this pattern to other features than time, whether it is at the cortical level or in the striatum. Although, this does not question the assumption that the best time code carried by a single cell is the ramping one.

III.2. Populational codes

The more data, the more reliable the information is, therefore neural population may carry much better information about time. Despite the role of the oscillations to tell time, here we will detail the pictures of neural populations throughout time.

To tell time at the populational level, the “state” of the population must evolve over time (Buonomano & Maass, 2009). At time t_1 , a neural population is defined by D-coordinates, or D-dimensions, where D is the total number of neurons in this population. If we consider a 2-neurons population, the state of the population at time t_1 is given by the activity of neuron-1 and the activity of neuron-2 at t_1 . If neuron-1 and -2 keep a constant activity during an interval, it is impossible to read-out time within the interval because the state at each moment is defined by the 2 same coordinates: $t_{1(x1,y1)} = t_{2(x2,y2)}$ where $x1$ and $y1$ are respectively the states of neuron-1 and -2 at t_1 , and $x2$ and $y2$ the states of neuron-1 and -2 at t_2 . In this case, activity at t_2 is not dependant of activity at t_1 (Figure 14-A). If one of the neurons has a time-modulated activity, it becomes more evident to read time, as shown in Figure 14-B: a gradient appears in the x-axis. If both of the neurons change their firing rates over time, it becomes possible to read-out time: all the coordinates at each time-point are informative, $t_{1(x1,y1)} \neq t_{2(x2,y2)}$. The gradient appears in both axis, x and y, as shown in Figure 14-C. In this second case, activity at t_2 is “predictable”, or is “due” to the activity at t_1 . As the number of coordinates increases, so does the probability to be able to read time. Now, if we consider a population made of 1 time-cell and 1 ramping neuron, it becomes clearer how we can read time in function of the ramping neuron activity, and in addition, the time coded by the time-cell is more distinguishable from the rest of the interval (Figure 14-D).

Once we consider this, it brings two important ideas to time code by neural population.

First, by placing the neural population in a Euclidean space with n-dimensions, it becomes possible to compute the amount of change between the two time-points. Indeed, the change between time t_1 and t_2 is the distance between $t_{1(x1,y1)}$ and $t_{2(x2,y2)}$ given by the formula:

$$t_1-t_2 = \sqrt{[(x1 - x2)^2 + (y1 - y2)^2]}$$

or

$$t_1-t_2 = \sqrt{[\sum_{d=1}^D (d1 - d2)^2]}$$

where D is the total number of dimensions.

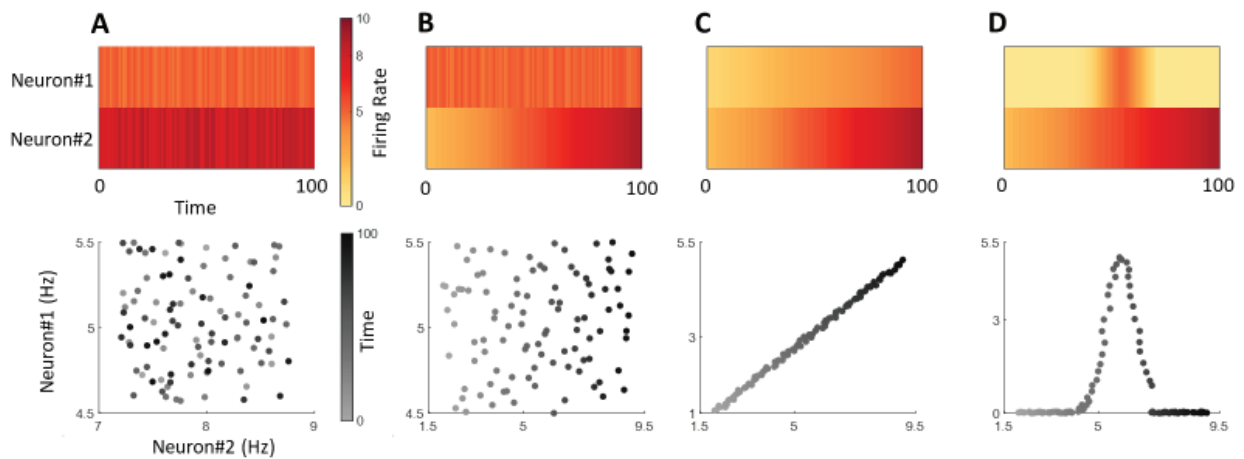


Figure 14. Two-neurons populations and their trajectories. **A.** Top row. 2 neurons displaying constant activity over time, Neuron#1 at 5Hz, Neuron#2 at 8Hz, with random noise at 10% of the mean. Bottom row. Neural trajectory of such a neural population, not organized over time (c-axis). Time is represented from 0 to 100. **B.** Top row. 2 neurons population, with Neuron#2 displaying monotonic increase of its activity over time. Neuron#1 is the same as in A. Bottom row. Neural trajectory of the population. Temporal pattern appears over the x-axis (Neuron#2 activity). **C.** Top Row. Neuron#1 also display monotonic increase of its activity over time. Neuron#2 is the same as in B. Bottom Row. Time-points are well distinguishable in both axes. **D.** Top Row. Neuron#1 is a time-cell peaking around Time 60. Neuron#2 is the same as in B. Bottom row. Neural trajectory is well discriminated over the x-axis, but only peak time of the time-cell is distinguishable in both dimensions.

If the distance between two time-points t_1 and t_2 within the interval is always constant, the Euclidean distance between t_1 and t_2 can be defined as the instantaneous speed. It also becomes possible to compute the total amount of change, from t_n to t_1 for example, where t_n can be any time-point of the interval; or simply by computing the cumulative sum of the instantaneous speed from t_2 to t_1 to t_N to t_{N-1} , where N is the last timepoint of the interval. To simplify this computation, one method accepted is to compute principal component analysis (PCA) on the neural data to reduce the dimensionality of the data. This dimensionality reduction method allows to create new abstract variable from the set of the data -the neural population- by catching the components that explained the most the variable of the data. Thus, instead of computing the distances on D-dimensions, it becomes possible to compute the distances on 3-dimensions if one considers that the 3 first component catch enough variance in the data.

Second, if the amount of change is large enough between t_1 and t_2 , then one should be able to “know” time by looking at the populational state and answer two different questions: is t_1 different from t_2 ? and “what time is it”? The first question can be answered by running a pairwise-decoding on the data, and the second by running multiclass-decoding (Cueva et al., 2020). With pairwise-decoding, for each pair of time-points within the interval, one could say which pair are close to each other -state proximity- and which ones are distinguishable -state distality-. On the other hand, multiclass-decoding allows to identify neural populations that are reliable on time predictions. Such a populational code would be useful to tell time any time one refers to it.

III.2.a. Neural populations speed: a tool to scale durations?

Scalar codes at the population levels have been identified in cortical -MFC- and caudate nucleus as monkeys performed a time-production task at the sub-second and second range. Indeed, even if the population in both brain areas were composed of an heterogeneous set of neurons, one key point at the populational level was that between 'short' and 'long' conditions, neural activity rescaled the temporal production by adjusting its speed (Wang et al., 2018). So, the neural population in two different intervals, 'short' and 'long', covers the same distance from t_1 to t_N . Although, the amount of change between, t_n and t_{n+1} is not the same during 'short' and 'long' time-production: the speed between each time-point is scaled in such a way that the total duration is covered by the same amount of change in both conditions. The evolution of the population state over the interval is called the neural trajectory. So, the fact that this population code was found in MFC and caudate, but not in the thalamus, implies that the temporal scaling occurs before the thalamic signal. After observing scalar patterns in striatal single cells, there is evidence for scalability also observed at the neural population. Similarly, durations are also encoded in frontal cortex by scaling the speed of neural population in function of a prior expectation (Meirhaeghe et al., 2021). Thus, this code is not simply due to temporal production, but is also involved in time estimation, at least in the frontal cortex.

III.2.b Time prediction: which structure is the best time-predictor?

There can be two ways to predict time: at a wide timescale or at a precise time scale. For example, in a temporal bisection task, there is only a need for short versus long estimations: the code can be wide. Indeed, when rodents perform a temporal bisection task, two distinct sub-populations emerged from the time-cells of the striatum. One of these sub-populations will be active preferentially before the boundary, the second one will be more active after it. Thus, by looking at the average activity of these two sub-population, one can predict where we are in time but on a binary way: before or after the boundary (Gouvêa et al., 2015). Furthermore, the activity of these two sub-populations predicts the temporal estimation, if the 'short' sub-population is higher than the 'long' one, the outcome of the animal will likely be 'short' estimation, even though time was 'long'. Same observation is done looking at the 'long' sub-population: when its firing pattern the highest, the estimation is 'long'. In sum, striatal activity is informative about time perception, at least in a binary way: by looking at its neural activity, one can predict the behavioural outcome at the second range. At the tens of seconds-to-minute ranges, striatal activity is also able to predict time accurately from 12 to 60s intervals. More studies in rodent striatum revealed that even if striatal neurons display the same characteristics than cortical neurons at the single-cell level (OFC and M2), and at the populational level -composed of time-cells like neurons- time is best decoded in the striatum than in the others structures; because of the well-organized sequence of activation. All together, these results indicate that even if time is processed

in multiple brain areas, striatum times more accurately, probably because of its wide inputs (Zhou et al., 2020; Bakhurin et al., 2017). Thus, at least in rodents, if one asks the question “what time is it” during interval timing, one should look at the striatum to answer it.

Another question one can ask is whether time can be decoded from the neural populations depending on the nature of the timing tasks. For example, during an explicit and an implicit temporal task -explicit temporal task requires to keep a track of time to produce a corrected output; while an implicit temporal task does not require the active tracking of time between two events-, it is possible to decode time in multiple structures -OFC, PFC, amygdala, anterior cingulate cortex-. Without looking at which structure time the best, it is demonstrated that when explicit timing is involved, temporal decoding from the neural activity is best. This implies a stronger temporal modulation in neural networks when time is tracked (Cueva et al., 2020). In addition, the authors demonstrated that the most important component in timing activity, the one that allows the best temporal prediction, is the ramping component, suggesting that a monotonic increase of the activity in time allows the best time-prediction.

From this last observation, some results remain unclear. Somehow in line with this last observation, ramping neurons from rodents LEC accurately inform about time as it is segmented in temporal epochs of 20s, thus it seems that they carry information about a large range of time (Tsao et al., 2018). On the other hand, in the entorhinal cortex also, relaxation-cells -that we defined as the neural basis of the “process-decay” model of timing- exhibiting a similar pattern of the ramping neurons, are very good temporal predictors of the beginning of an interval up to 5s, but not good predictors for the end of it -approximately 4/5th of the interval-. Thus, entorhinal cortex carries information about time at different ranges, but the differences could also be due to the animal model. Without any strong conclusion on the temporal codes of the entorhinal cortex, we can nevertheless argue that the temporal predictions are behind the expectations of what would be expected from a ramping-neurons population.

Strangely, temporal prediction based on neural activity was not often computed. For example, even if time-cells were first documented 2011, the first decoding analysis on hippocampal time-cells appears seven years later by showing that time-cells allowed to decode time during intervals of 10s (Mau et al., 2018). Further, time predictions are better at the beginning of the interval than at the end of the interval: errors increased as time to be decoded arrives later in the interval. This is the same observation that has been done from relaxation-cells in the entorhinal cortex. The phenomenon here can be explained by the fact that the time-cells intrinsic organization fire mostly at the beginning of the interval. With this kind of population, it is easiest to distinguish between the beginning of the interval and the rest, but not to predict time at any moment of the interval. Similar results are reported

in time-cells decoding from humans (Reddy et al., 2021) for the shortest duration tested (6.5s), but when the interval to be decoded increased (up to 30s), time prediction decays.

In conclusion, time codes differences could emerge between structures, between pattern of cells or even between tasks demands. Although, the striatum seems to be the best structure predicting time, from what is observed in empirical data, while whether ramping or sequential activation of neurons is the best pattern for time decoding is still in debate.

B. Problematics

We have highlighted that, on the contrary of rodent's studies in the timing field, few studies have reported behavioural patterns and neural signatures across several seconds' range in primates. Because the striatum is involved in movement and actions selection and the hippocampus is involved in episodic memory, these two structures have been proposed to play an important role in temporal processing. Thus, we have targeted these two structures in the macaque brain, as monkeys performed an ongoing temporal categorization task, from sub-second to several seconds' range.

The aim of this thesis is to **1)** document the temporal behaviour across different time-ranges in non-human primates, during a time-categorization task. We developed a discrimination task that involves several durations to be categorized, as short, intermediate or long. On the contrary to time production task, responses associated to each duration were produced after the duration had elapsed. Between sets, the durations were changed, decreased or increased proportionally: sub-second (0.25, 0.5 and 1s), second (0.5, 1 and 2s), supra-second-1 (1, 2 and 4s) and supra-second-2 (2, 4 and 8s) ranges. At the behavioural level, this design allows to investigate several points. First, we can do between-sets comparisons: we asked whether non-human primates perform temporal categorization with the same accuracy when durations to be timed ranged below the second and when they range at multiple seconds? Second, because some of the durations we use are the same between ranges, another between-sets comparison we can address is if the temporal categorization of a duration is set-dependent. This allows to test relative judgements as a function of time ranges. Third, within a set, we can identify the behavioural pattern of temporal categorization when it includes 3 durations to discriminate: which one of the intervals is best discriminate, the short, the intermediate or the long? In bisection tasks, shorter and longer intervals are the best categorized (Figure A.1). This pattern of behaviour could be retrieved in our task, or the intermediate one could be better categorized as it can be used as a reference time.

As monkeys performed the task, we recorded single neurons activity in the striatum: mid-parts of the caudate and putamen, and the anterior hippocampus. We want to highlight **2)** the differences of the brain areas, striatum and hippocampus, during a time-categorization task. Indeed, the striatum has been shown to support time-related activity in rodents from second-to-minute ranges (Zhou et al., 2020; Bakhurin et al., 2017; Emmons et al., 2017; Mello et al., 2015; Gouvêa et al., 2015) and the hippocampus at the tens of second ranges (Shimbo et al., 2021; Mau et al., 2018; Kraus et al., 2013; MacDonald et al., 2011; Pastalkova et al., 2008). Nonetheless, there are less studies in the non-human primates documenting these structures activity during timing tasks. We know that caudate scales its neural speed during temporal productions at the second range in time production task (Wang et al., 2018), and that in human hippocampus, time-cells have been identified during learning sequences of

images and lists of words (Reddy et al., 2021; Umbach et al., 2020). Here, we report for the first time the pattern of neural activity in these two structures, and compare their activity in the same task. We are going to ask if, in primates, striatal activity changes over time during a temporal categorization task, and if its activity maintains the same dynamics across different time-ranges. On the other hand, we asked how good is hippocampus to code time when there is no sequence-learning, movement, nor any kind of episodic memory involved in the task. In the first chapter of this thesis (Paper 1), we show how the speed, the trajectories (Figure A.14), the time predictability and the time discrimination based on single-cells activity is different between striatum and hippocampus. We explained these differences in function of the external connectivity's of the structures and in function of their functional role. For example, does the striatum sustain a time for action and the hippocampus a time for memory? This implies that temporal codes are due to a cognitive involvement during time. Thus, in addition, we asked whether the time code for a duration is dependent of the cognitive load engaged during this duration. In the second chapter of the thesis (Paper 2), temporal dynamics are addressed differently. Even if we still focus on the differences between structures, we also described different subpopulations coding time in two different ways: following either an absolute or a relative pattern. We aim to identify the structure of the unravelling of cell recruitment during the interval durations. We will test the robustness of these subpopulations between structures and across sets and ask which coding pattern, absolute or relative, drives the dynamic of the entire population.

Finally, another point of this thesis is to **3)** identify possible differences between caudate and putamen during timing. Indeed, even if they part of the striatum, they are both part of different basal ganglia loops (Alexander et al., 1986), and process information in parallel. Thus, time could be processed in a parallel way, in function of the cognitive task involved.

C. Chapter 1. A differential adaptation of neural codes to time in the striatum and hippocampus

Felipe Rolando¹, Tadeusz Kononowicz^{1,2}, Jean-René Duhamel¹, Valérie Doyère² and Sylvia Wirth¹

¹ Université de Lyon, CNRS, Institut des Sciences Cognitives Marc Jeannerod (UMR 5229), 69500, Bron, France.

² Université Paris-Saclay, CNRS, Institut des Neurosciences Paris-Saclay (NeuroPSI), 91190 Gif-sur-Yvette, France.

C.1. Abstract

Tracking time allows an adaptive anticipation of events when supported by memory. The striatum and the hippocampus display strong time-related activity suitable to time processing at different scales. However, no previous study directly compared their activity to understand how their neural population adapts to different time-ranges. Here, we recorded single-cells in caudate, putamen and hippocampus as monkeys performed a time-categorization task. The task is based solely on cumulative elapsed time, nesting two duration probabilities (short and intermediate) into the longer one, which ranged from 1 to 8 seconds. While time-modulated cells were identified in all structures, we revealed strong differences between structures. There were overall more time-modulated cells in the striatum compared to the hippocampus. Further, the larger moment-to-moment changes in striate neural dynamics supported better time prediction and higher temporal discriminability between two time points compared to hippocampus. In addition, we discovered a difference within striatal sub-regions, and identified the caudate as a better predictor than the putamen. Despite strong differences in striate and hippocampal activity, we show that temporal discrimination adapted from fine to coarse as a function of time range, but in a region-specific manner. Striate activity supports an overall finer discrimination than hippocampus, which may relate with its functional specificity in fine control of action, as opposed to hippocampus which may represent time for memory.

C.2. Introduction

The use of precise time to control our daily life is extremely recent in human evolution. However, on a daily basis, in addition to relying on electronic agendas, one continuously tracks time to optimize schedule and prepare for next actions. This planning entails that the brain contains neural signals that can represent events' times and durations, and further intervals between them, thereby supporting the ability to adaptively anticipate events and prepare adequately (Tallot & Doyère, 2020; Tsao, Yousefzadeh, Meck, Moser, & Moser, 2022). Indeed, we can learn that an event causally predicts another one if the latter follows after a short elapsed time. Once we learned to anticipate an event, we know when too soon is too soon, and when too late is too late (Rescola & Wagner, 1972). Recently, several findings shed light on how the brain achieves this, but whether and how neural activity adjusts to different time scales is not yet well understood, despite many reports on time-modulated neural activity in many brain regions during motor or cognitive tasks (Tsao et al., 2022; Tallot & Doyère, 2020; Mauk & Buonomano, 2004). While the presence of a temporally organized pattern of spiking activity is ubiquitous, how this supports a neural map of time adapting to different event orders, durations and time ranges is still unclear. Indeed, evaluating events' time order or duration may not necessarily be supported by the same processes or involve the same brain regions. Further, different patterns of time modulation have been identified in humans or animals as they timed events or intervals between events, with or without an explicit task demand (Tallot & Doyère, 2020; Mauk & Buonomano, 2004). For example, analogous to place cells, so called "time cells" identified in the rodents hippocampus (Shimbo, Izawa, & Fujisawa, 2021; Mau et al., 2018; MacDonald, Lepage, Eden, & Eichenbaum, 2011) and humans' cells (Reddy et al., 2021; Umbach et al., 2020) display increased rates at specific moments during time intervals. Cells alike to time cells were also identified in the rodents striatum and display peak of activity spanning a time interval (Mello et al., 2015). Next, cells displaying "ramping" activity were identified in the striatum (Emmons et al., 2017), the hippocampus (Sakon et al., 2014), the entorhinal cortex (Tsao et al., 2018) or the parietal or prefrontal cortices (Jazayeri & Shadlen, 2015; Kim, Ghim, Lee, & Jung, 2013). These cells present a rise in activity as event's occurrence approaches (Tsao et al., 2018; Janssen & Shadlen, 2005) or, at the opposite, a slow decrease in rate as a function of time from an event (Bright et al., 2020; Tsao et al., 2018). Based on these different patterns, modelling works tested different architecture determining parameters affecting encoding efficiency (Zhou et al., 2020). It was shown that cells displaying peak well distributed along an interval is the neural organization that supports best decoding of time (Tsao et al., 2022; Zhou & Buonomano, 2022; Zhou et al., 2020). However, experimental data showed that both peak and ramp activity were found in the same brain regions at different time ranges and in different tasks (Shikano, Ikegaya, & Sasaki, 2021; Reddy et al., 2021; Umbach et al., 2020; Sabariego et al., 2019; Mau et al., 2018; Tiganj, Jung,

Kim, & Howard, 2017; Mello et al., 2015; MacDonald et al., 2011; Pastalkova, Itskov, Amarasingham, & Buzsáki, 2008), which suggests that peak and ramp activity may arise from different local or external connectivity and subserve different functions.

Here we focused on two brain regions that share an involvement in neural representation of time: the striatum and the hippocampus. The striatum has a majority of inhibitory medium spiny neurons, and plays a major role in the cortico-striatal-thalamic loops in the control and selection of time for action (Jahanshahi et al., 2015). The hippocampus, whose principal cells are part of the tri-synaptic circuit connecting with entorhinal cortex, is likely involved in processing time supporting building of episodic memory (Rolls, 2010). While the two regions are clearly separated by their neuroanatomy, cellular types and functional roles, several studies described similar neural patterns during time intervals (Shikano et al., 2021; Pilkiw & Takehara-Nishiuchi, 2018). How these regions differentially process time remains unknown. Further, many studies relied on rodents, and those performed in monkeys or humans rarely exceeded 1 or 2 seconds (Tallot & Doyère, 2020). Whether there is a difference in time processing ranging from sub-seconds range to several seconds is also an important issue. For the first time, we probed neural activity in the striatum and the hippocampus as monkeys tracked elapsed time at different time resolutions within the second (.25-.5-1s) to between several seconds (2-4-8s). In this new task, 3 ongoing durations are categorized as time elapsed since a start signal into nested short, intermediate or long durations. We describe the presence of time-modulated cells in monkeys, in the striatum (caudate and putamen) and in the hippocampus. However, despite a seemingly similar neural representation, our results show a strong striatal recruitment during the task together with an adaptation of respective codes to different time ranges, in contrast to the hippocampus that showed very little time modulation. Overall, these results provide the first data comparing directly caudate, putamen and hippocampus, shedding light on the task's specific recruitments of these brain regions and their adaptations as a function of time range and task demand.

C.3. Results

C.3.a. Monkeys successfully categorize three ongoing durations

We trained two female Rhesus macaques to categorize elapsed durations following a cue as short, intermediate or long (see Methods, Figure 1A). A trial started when a white square was briefly presented on the screen (200ms), its offset marking the beginning of the duration to-be-timed, and ended when three blue squares (responses targets) appeared at the bottom, left and top of the screen (Figure 1A). Depending on the elapsed duration, via a joystick, the monkey moved a pointer to the bottom square for short, the left one for intermediate, or the top one for long. Movements performed too early resulted in aborted trials. Monkeys were first taught the 0.5, 1, and 2s discrimination (reference set termed set-2s long). Then, they performed within-session retiming sets (Figure 1B) to sub-second range (durations divided by 2, termed set 1s-long in which durations were 0.25, 0.5 and 1s) and to two supra-second sets, termed set 4s- and set 8s-long (see Methods for details). Both monkeys categorized the three intervals well above chance, (χ^2 -test for each monkey separately, $\chi^2(6)=3.3193e4$, $p<0.0001$ for monkey 1; $\chi^2(6)=2.6853e4$, $p<0.0001$ for monkey 2) showing that animals discriminated intervals ranging up to 8 seconds (figure 1C). A general-linear mixed-effect model (GLME, see Methods), with interval and set as fixed factors, revealed a significant modulation of behavioral accuracy by time range across and within sets. Overall, performances were the highest for reference set 2s-long, which was also the first one animals were initially trained on, followed by 1s-, 4s- and 8s-long. Within the sets, the long interval was better discriminated for set 2s-, 4s- and 8s-long, while for set 1s- the short interval was better discriminated. Performances for intermediate intervals were always lower for sets 2s-, 4s- and 8s-, except at sub-second range where intermediate and long intervals were categorized with the same accuracy (Figure 1C, supplementary Table 1).

C.3.b. Monkey's subjective perception of duration varies with time range

To evaluate monkey's perception of elapsed time at different time ranges, we tested whether the nature of the errors for the intermediate interval changed as the duration range increased (Figure 1E). A GLME (see Methods) showed an unequal distribution of the nature of the errors that varied across time. Indeed, the proportion of intermediate intervals erroneously categorized as short decreased with increasing time range in favor of long. Thus, when facing an intermediate duration (e.g. 0.5s), animals more likely labelled it as short (0.25s) at sub-second range than long (1s), i.e. showing underestimation. When the ranges increased, monkeys mistook more frequently intermediate trials with longer durations, showing overestimation. Next, as response latencies reflect readiness to act, they can be a proxy for the animal's anticipation of an event. We tested whether response latencies changed as a function of intervals and of the range of discrimination (Figure 1D). A Linear Mixed Model

(LMM) performed on normalized response latencies (see Methods) for correct trials revealed an effect of set ($F(3,61185)=1.2962e3$, $p<0.0001$), duration ($F(2,61185)=549.9881$; $p<0.0001$), and an interaction between the two ($F(6,61185)=700.19$, $p<0.0001$). Across sets, normalized response latencies (see Methods) were smaller at sub-second and second ranges compared to longer sets (see supplementary Table 2). The distribution was also significantly shifted negatively for sub-second and second range suggesting that animals anticipated more at these sets compared to long ones. Within sets, reaction times were much smaller for long intervals at sub-second and second ranges compared to short and intermediate. For supra-second ranges, the opposite was true: responses were faster for the shorter intervals. The overall pattern of response latencies' distribution suggests that the monkeys anticipated the end of the long interval at sub-second and second range only. We wish to emphasize that the task is not dependent on the animal's speed to respond. Animals were only rewarded if they made a movement to categorize the trial once the targets were on. Anticipation of response before the end of the interval signaled by the target appearing on the screen (joystick movements) resulted in an aborted trial. Such aborted trials were rare (1.1%, 0.28%, 1.38% and 1.16% of trials for monkey 1, respectively at sets 1s-, 2s-, 4s- and 8s-long, and 3.99%, 1.38%, 4.44 %and 3.98% for monkey 2), and their distribution was consistent with an anticipation of the longest sub-second and second ranges duration as shown in Figure 1D. In summary, the animals categorized durations well above chance at all ranges, and appeared to be able to withhold motor responses. Therefore, the task is likely dissociating evaluation of elapsed time from motor production itself.

C.3.c. A strong recruitment of striatal cells that adapts to processing demand over time

We first aimed compare time-signals in the caudate, the putamen and the hippocampus. To this end, a rectangular chamber was implanted on the animal's skull, linear arrays were lowered every session, and neural activity was recorded through a laminar electrode while animals performed the task (Alphaomega, see methods). We isolated offline (see Methods) 615 neurons in the caudate, 736 in the putamen and 931 neurons in the hippocampus (Figure 1F and Figure 2 for individual examples). To determine whether neurons displayed time-modulated activity, we analysed the spiking activity during correct long trials, while the animal continually waited to categorize the current interval as short, intermediate and then finally categorized the trial as long. We computed a time "Information Content" (IC in bit per spike, Skaggs et al., 1992) for the longest interval of each set partitioned in 100 bins. We defined time-modulated cells (TM cells) as cells for which the IC computed on actual data was above the 95 percentiles of the distribution obtained from 1000 surrogates with permuted spikes (see Methods). The time IC value reflects the information carried by a spike as a function of a time bin weighted against all time bins, and when tested against chance, allows determining whether actual pattern of firing rate as a function of time differs from chance. TM cells were significantly more

numerous in the caudate, followed by the putamen and the hippocampus across all time sets (χ^2 -test ran on each set, $\chi^2=41.05$, $p<0.0001$, for set 1s-, $\chi^2(3)=117.78$, $p<0.0001$, for set 2s-, $\chi^2(3)=20.75$, $p=0.003$ for set 4s-, $\chi^2(3)=11.35$, $p=0.0034$ for set 8s-long, Figure 1G left pies). The percentage of TM cells remained approximatively constant across sets within regions, suggesting an adaptation to the time range. To control whether this constant proportion of TM cells across ranges was due to the fact that bin size was adapted to the length of the interval (i.e. 10ms for 1s, 20ms for 2 s, 40ms for 4s, 80ms for 8s), we compared the percentage of TM cells obtained from a fixed bin size and number on a fixed interval (i.e. 1s). Thus, we identified TM cells with IC significance computed on 100x10ms bins of the first second of the 2s (cropping the second half), 4s (cropping the next 3s) or 8s interval (cropping the next 7s), and compared them to the 100bins of the long interval of the set 1s-long. Therefore, we identified TM cells using only the first second of all possible ranges, the difference being the processing demand during this first one second. The results showed that the percentage of TM cells in the striatum identified for the first second at the second and supra-second ranges decreased dramatically compared to the number of cells identified when a second is the whole long interval (Figure 1G right pies, $\chi^2(2)=63.4434$, $p<0.0001$ in caudate, $\chi^2(2)=21.5167$, $p<0.0001$ in putamen), but not in the hippocampus ($\chi^2(2)=5.95$, $p=0.051$). These results show that IC contained in one second in the striatum depends on the processing demand of that second: neural activity for one second is more strongly modulated when events are expected within that second, compared to when that second is part of a larger delay and no event is expected (as in 4s- and 8s-long). Overall, the results show that striatal activity is more strongly modulated than hippocampal activity, and further that time within intervals is processed in an adaptive way relative to time range.

C.3.d. A mix of ramping and sequential peaks across structures

The nature of neural activity throughout time has been linked to different computational functions (Zhou & Buonomano, 2022). For example, linearity in neural population with a continuous increase or decrease in activity (ramping cells) carried more time information to prepare action than cells with one or multiple “time fields” (Cueva et al., 2020; Emmons et al., 2017). On the other hand, well-distributed peaks across an interval better support fine-grained time discrimination within the interval than ramping cells (Zhou et al., 2020). Given that our task differed from previously described time bisection or interval reproduction tasks, we asked whether TM cells exhibited ramping or peak activity profiles across brain regions in our time categorization task. We made the simple hypothesis that more cells may peak near expected events, i.e. the potential end of intervals, when the animal expects to make a specific action related to time judgement and receive the reward (dashed lined in Figure 2). However, visual inspection of the population activity through time (Figure 2 for 2s-long interval, and Figure 3A for population time maps) suggested that TM cells exhibited a variety of time-

modulated patterns that did not specifically fit these expectations. Via a stepwise regression method, we tested whether a linear or a quadratic term best explained the neural activity of each neuron during the interval, and classified them into ramping or peak cells (Reddy et al., 2021; Tsao et al., 2018, see Methods). The latter cells exhibited one or more “time fields” and made up the majority of the population in all regions (Figure S3). Overall, the caudate nucleus and putamen had a higher proportion of ramping neurons compared to other regions at all time ranges (Figure S3B). An ANOVA on the absolute linear terms, with regions and sets as factors, confirmed a significant effect of region, but no effect of set, nor interaction (Figure S3, 2-way ANOVA, $F(2, 677)=36.54$, $p<0.0001$ for region, $F(3,677)=1.46$, $p=0.2237$ for set and $F(6,677)=1.34$, $p=0.2357$ for interaction). Notably, ramping cells were virtually absent in the hippocampus. Next, we asked whether neural activity was homogeneously distributed within the long interval, while the animals successively waited for this interval to end following short, intermediate durations. If TM cells were evenly distributed across the interval, then, the average firing rate (superposed black line, Figure 3A) or distribution of peak times (Figure S3C) should be flat. An analysis of the interquartile interval distribution of the peak shows that these were not uniformly distributed for any region at any time range (Figure S3). Further, we found that the majority of cells reached maximal firing rate before the first half of the trial in all the brain regions, suggesting that more cells peaked in the first half of the trial (see Figure S3C). This suggests that TM cells carried more information during the part of the interval containing more time processing demand. Next, we asked whether neuron’s “time field” size (width) increased as a function of time in the interval. We tested a linear and a quadratic model to explain the width as a function of peak times: we found that at set 2s-long, the quadratic model best explained the relation between time-field and peak time for the caudate and putamen, but not for the hippocampus ($R^2=0.0702$ for caudate, $R^2=0.1342$ for putamen and $R^2=0.0069$ for hippocampus, see Figure S3C). Thus, contrary to what is usually found in the literature (Tiganj et al., 2017; Mello et al., 2015; Kraus, Robinson, White, Eichenbaum, & Hasselmo, 2013), time-field size did not increase with peak latency in the interval, but rather around the time of the first and second expected end of the interval (short or intermediate), compatible with fine-grained time discrimination of the first half of the intervals. Next, we tested whether field size increased between time ranges from sub-second to supra second ranges. We found that was indeed the case, as shown in Figure S3E: field size increased with the overall size of the interval. In sum, while field sizes did not increase within the interval, they increased across time ranges from sub-second to supra-second range.

C.3.e. Time-modulated cells display response to other task events

We asked whether TM cells responded to other task events outside of the interval, such as the target presentation, movement or reward delivery. Such response, observed in addition to the activity

modulated during the long interval, could be interpreted as the prediction error of expecting a timely target appearance or a selective preparation of the response that would normally be executed if the interval had ended. To characterize cells response to other events, using all trials (short, intermediate or long), we used a GLME to test whether cells responded to the events (see Methods) compared to baseline. In the caudate, we found 33.1% (49/148) of the neurons responsive to cue, 84.5% (125/148) to target onset, 84.76% (124/148) to response execution and 81.76% (121/148) to reward delivery. In the putamen, 31.9% (29/91), 78% (71/91), 83.5% (76/91) and 73.6% (67/91) were respectively responsive to the same features, and 29% (18/62), 58.1% (36/62), 51.6% (32/62) and 53.2% (33/62) were responsive in the hippocampus. Amongst the caudate neurons, 91/125, 85/124, and 60/121 responded differently to the target presentation, response execution, or reward delivery as a function of the interval. In the putamen, 51/71, 55/76, and 34/67 neurons were interval modulated during target, response and reward delivery. In the hippocampus, 19/36, 19/32 and 17/32 neurons were interval modulated during these other features of the task. To test the link between these interval selectivity and a possible error prediction for target appearance, or movement preparation, we computed the distribution of the cell's peaks during the long trials for 3 groups of cells sorted as a function of their selectivity (short, intermediate, long) to the other task events during all trials. Specifically, we computed the distribution of peaks during the long interval for all cells that responded more to target appearance when in short trial, and compared them to the cells that responded more in intermediate trials, and long trials (Figure S3F). The results show that in all regions, there was a significant effect of the interval preference ($F(2,147)=3.19$, $p=0.0441$), but no effect of brain region. The distribution of the peaks of 'short-preferring' neurons for target presentation preceded that of 'intermediate-preferring' neuron. However, the distribution of 'long-preferring' neurons did not differ from the other two. The peaks' distribution of the short and intermediate preferring neurons only is coherent with a prediction error centred around the expected event. The same analysis applied on neurons selective for motor execution or reward delivery shows no significant relationship between neuron's preferred movement or reward with peaks' distribution. In sum, these results show that the neurons displayed a rich activity outside the interval, but that this activity was not firmly indicative of the peaks' distribution within the interval.

C.3.f. A slow speed but steady progression in caudate

It was proposed that dynamic changes in a neural population's activity can be defined by its trajectory in a n-dimensional space over t times, and constitutes distinct states through elapsed time (Buonomano & Maass, 2009; Karmarkar & Buonomano, 2007). To compare neural trajectories across regions and sets, we performed a Principal Component Analysis (PCA), on a down-sampled population with neurons as variables and 100 time-points as observations (see methods). Therefore, while Figure

3B represents the projection of the PCA for the reference set 2s-long for all TM cells recorded and presented in Figure 3A, the measures described below were calculated on the down-sampled population ($n=28$). We computed 1) the instantaneous Euclidean distances between two consecutive time-points, which is sometimes referred to as the speed of the neural population (Wang, Narain, Hosseini, & Jazayeri, 2018), and 2) the distance between the neural state at each time point and the centroid of the trajectory (crosses in Figure 3B) to capture the overall distribution of the PCA score in the PCA space. Figure 3C shows that these two measures plotted against each other reveal clear differences between regions, and that while the hippocampus displays a higher speed; its distance to centroid is smaller than in the striatum. Indeed, the average speed was significantly different 1) between regions, lower for caudate followed by putamen, and then hippocampus ($F(2,11988)=32314.19$, $p<0.0001$); and 2) across sets (see Figure S3D) with an overall higher speed at sub-second range ($F(3, 11988)=14014.11$, $p<0.0001$) dominated by a smaller speed in the caudate compared to other regions ($F(6,11988)=1361.84$, $p<0.0001$). Next, to test whether the speed changed within the interval, we regressed the neural trajectories linearly. A significant slope indicates that the neural trajectory changes significantly within the interval, with the negative sign indicating a slowing down of the neural trajectories within the interval, and positive slopes an acceleration. This measure was repeated across sets thereby allowing estimating speed and sign of changes within intervals and across sets (Figure 3E). The 2-way ANOVA on the slopes showed that caudate trajectories were negative across all sets and slowed down significantly more than the two others brain regions ($F(2,11988)=1214.62$, $p<0.0001$) with an overall effect of time range ($F(3,11988)=2420.75$, $p<0.0001$), as the amplitude of the slopes decreased across sets. The interaction ($F(6,11988)=1646.58$, $p<0.0001$) revealed changes in the direction of slopes with positive slopes at the sub-second range, except in the caudate, and negative slopes or close to zero otherwise. In addition, slopes in the caudate followed a gradient from the most negatives ones at the sub-second range to near to zero as the time range increased.

C.3.g. Caudate and putamen accurately predict time across sub-second and supra-second ranges

If the intrinsic organisation of neural trajectory reflects ongoing time, then we should be able to predict time through its ongoing neural activity. To test this, we used a decoder based on linear regression analysis. We trained and tested our model on correct long trials within each set, for each brain region separately, using the down-sampling method, as indicated before, because population size was different across regions (see Methods). Therefore, the results were comparable across regions and sets. First, we show that decoding from TM cells in all three regions was significantly higher than

decoding from other cells (Figure 4A). Indeed, the distribution of the slopes obtained from each decoding output (insets in Figure 4A) was higher than that obtained from other cells ($n=5000$, 2-samples T-test, for all structures, $t\text{-stat}(9998)=68.64$ for caudate, $t\text{-stat}(9998)=61.7118$ for putamen, $t\text{-stat}(9998)=52.9489$ for hippocampus, $p<0.001$ for all brain regions), and differed from that obtained by chance (above 95th percentile of the slopes obtained after random shuffling of the labels, $p=0$, $p=0.001$ and $p=0.049$, respectively for caudate, putamen and hippocampus, Figure 4A insets). The other cells did not decode time above chance level.

Next, we asked whether temporal organisation within one segment transferred to another segment and evaluates the specificity of decoding to a unique temporal window, not any other temporal window. Precisely, we tested whether the organization of the first 800ms of the 2s long interval (corresponding to the duration of the inter-trial interval, or ITI) transferred to the 800ms of the ITI. Thus, we trained on the first 800ms and tested on the first 800ms (control, blue in figure 4B) or on the 800ms of the ITI (grey in figure 4B). Decoding was above chance when trained and tested on the first 800ms of the interval in the caudate and putamen ($p=0.001$ and $p=0.0052$, respectively, figure 4B) but was not significantly different from chance when tested on the ITI. Together, the results show that the decoding of time is specific from certain task periods, and that neural activity is not organized in a way to support decoding across any interval. Next, we asked whether the TM cells, which were identified during the time interval, also supported successful time decoding during another time window. Precisely, we asked whether the activity of TM cells outside of the time interval, could also support time decoding. To this end, we trained the model on the activity of TM cells during the inter-trial interval (ITI, 800ms) that preceded the trial, and tested the model on the ITI (Figure S4). The results show that decoding of time during the baseline was not significantly different from chance in any region. Precisely, the intrinsic organization of TM cells' activity during the ITI does not carry information to decode time: time cells identified during the interval relevant to the task, do not support time processing in another interval.

Next, we asked which brain region timed the best across all time-ranges (Figure 4C). We showed that the caudate and putamen (Figure 4C) decoded time above chance-level for any time set, while, in the hippocampus, decoding did not differ from chance. Overall, decoding was better in the caudate, followed by the putamen and the hippocampus (2-way ANOVA, $F(2,1188)=96.83$, $p<0.0001$). Decoding performance was better at second range than at supra-second ranges ($F(3,1188)=6.27$, $p=0.0003$), but did not differ from sub-second range. The interaction ($F(6,1188)=3.75$, $p=0.0010$) revealed that decoding performance was always better in the striatum, with no difference between the caudate and putamen except at the longer set. The hippocampus was the poorer time-predictor, at any set. Overall, the results show a great difference in the ability of neural activity to predict time across regions, and point to a higher ability for the caudate over other regions.

C.3.h. Higher discriminability between two time-points adapts to processing demand

So far, we showed that striatal neural activity supported better time prediction than hippocampus. Next, we asked how activity at any time-point (time bin) within the intervals differed from any other time-point. This allows to quantify the temporal resolution of the discrimination. To this end, we used Support-Vector-Machine (SVM) based decoding on each possible pair of time points (see Methods). As above, we down-sampled the neural data to allow across regions and sets comparisons. Figure 5A shows the results as a time-by-time matrix, where each point is the discrimination probability (accuracy) between two time-points of the interval, t_n and t_m . We first compared the overall accuracy between any time-point and found a significant effect of brain regions ($F(2,59388)=5876.61$, $p<0.0001$) and time range ($F(3,59388)=3517.73$, $p<0.0001$). The post-hoc analysis following the significant interaction ($F(6,59388)=399.83$, $p<0.0001$) shows that the caudate discriminated better 2 time-points at sub- and second ranges, while putamen was better at supra-second ranges, followed by a lower performance at all time ranges in the hippocampus. Then, for each time-point, we calculated the number of other time-points from which it differed significantly (chance at 0.6), and obtained a discriminability score from 0 to 99 reflecting its low to high discriminability from the rest of the interval (Figure 5B). In the caudate, high discriminability scores were maintained through the interval at the sub-second range ($a=-0.0172$, $p=0.3361$), and as the range increased, the scores decreased throughout the interval ($a=-0.0727$, $p<0.0001$; $a=-0.5416$, $p<0.0001$; $a=-0.3452$, $p<0.0001$ respectively for second, supra-second-1 and supra-second-2 ranges). In the putamen, high discriminability scores were also maintained within the interval at the second range ($a=0.0164$, $p=0.1786$), and decreased as a function of time for the other ranges ($a=-0.0973$, $p<0.0001$; $a=-0.2964$, $p<0.0001$; $a=-0.4905$, $p<0.0001$ respectively for sub-second, supra-second-1 and supra-second-2 ranges). In the hippocampus, discriminability was poorer and never constant at any range ($a=0.3841$, $p<0.0001$; $a=-0.2923$, $p<0.0001$; $a=-0.3561$, $p<0.0001$; and $a=-0.3871$, $p<0.0001$ respectively for sub-second, second, supra-second-1 and supra-second-2 ranges).

Next, we examined how much any time point was discriminated from its neighbouring ones (Figure 5C). We defined the temporal resolution as the distance t_i-t_j , where t_j is the closest time-point from which t_i is decoded above chance beyond t_j . The distance between t_i and t_j gives the size of the time window within which neural activity around t_i is too similar to be discriminated from t_i . A small time-window reflects a high temporal resolution. This resolution differed across structures and ranges (2-way ANOVA, $F(2,1188)=80.82$, $p<0.0001$ for structures, $F(3,1188)=149.37$, $p<0.0001$ for sets). The post-hoc analysis following the significant interaction ($F(6,1188)=7.76$, $p<0.0001$) showed that the time window was narrower in the striatum compared to hippocampus at sub-second and second ranges, without differences between the caudate and putamen, and was narrower in the putamen at supra-second-1 (Figure 5C) compared to other brain regions. Further, the comparison across ranges showed

that the temporal resolution was much narrower at sub-second and second range, and increased dramatically at supra-second ranges.

C.3.i. A second's encoding is contextually relevant across ranges

The above results show that pairwise decoding was higher for short durations and that the temporal accuracy decreased as time ranges increased. Here, we asked whether the first second is decoded with the same accuracy whether the animal performs in a sub-second, second or supra-second ranges, and thus tested whether time-points within 1s can be decoded with the same accuracy independently from the time range it belongs to. We hypothesized that the decoding resolution is adapted to the time demand. Therefore, we performed the pairwise decoding, on the first second of sets 2s-, 4s- and 8s-long, using the neurons defined as TM cells for this specific duration across sets (Figure 1G, right pies). Overall, there was a main effect of time range (figure S5): one second was better decoded at sub-second and second ranges compared to supra-second ranges ($F(3,59388)=3094.3$, $p<0.0001$). There was also an effect of the region with decoding obtained from caudate population above that of the other regions ($F(2,59388)=2491.44$, $p<0.0001$). The interaction ($F(6,59388)=881.48$, $p<0.0001$) confirmed overall a pattern of better decoding achieved by the striatum, mixed with less constant decoding at supra-second ranges.

C.4. Discussion

Neural signals representing the passage of time were previously identified in the striatum and the hippocampus, however, no study had yet compared neural activity in these structures directly in the non-human primate. Here, we characterized neural activity as rhesus macaques categorized ongoing elapsed time into serial durations at times from sub-second to supra-second ranges. We identified fundamental differences between the striatum and the hippocampus during temporal processing. Despite the presence of “time cells” in the hippocampus, their overall organization did not support decoding based temporal prediction. In contrast, changes of neural dynamics as a function of time were much stronger in the striatum than in the hippocampus and allowed time prediction more accurately at all-time ranges. Further, we showed that following the same sensory trigger cueing the interval onset, the recruitment of cells and population-based temporal discrimination between neighbouring time windows adapted to contextual cognitive time demand. Caudate and putamen populations displayed a fine-grained neural representation of time with a constant high resolution at the second range, which adapted to poorer discrimination at supra-second ranges, while the hippocampus only provided coarse representation of moments. These results provide a full characterization of the structure of neural changes in striatum and hippocampus, to provide a clue about neural adaptation through time.

C.4.a. A prospective categorization based on ongoing elapsed time in the non-human primate from sub-second to supra-second ranges

Various tasks have been used to test time perception, the most common being 1) temporal bisection, in which a duration is categorized according to reference samples (Mendoza, Méndez, Pérez, Prado, & Merchant, 2018; Gouvêa et al., 2015), and 2) time production, in which the subject has to reproduce an action in a timely fashion (Meirhaeghe, Sohn, & Jazayeri, 2021; Wang et al., 2018; Jazayeri & Shadlen, 2015). However, while rodents were tested in tasks ranging from seconds to several minutes, the time ranges tested rarely exceed 2 seconds in the non-human primate (Tallot & Doyère, 2020). Here, we first trained animals to categorize three ongoing durations at the second range, and showed that they could apply the same rule at sub- and supra-second ranges. Together, this shows first that rhesus macaques can classify ongoing durations into three categories, and second, that the time range at which they can categorize time is higher than what presumed, given the time range tested previously.

The nature of their categorizing error for intermediate intervals shows that they rely on subjective timing, and that the classification confusion is not biased to the mean interval, but rather, consistent with a lack of precision as time range increases. At long ranges, the overall percent correct

was lower than for second or sub-second ranges, which may reflect a higher difficulty to categorize long durations compared to short durations. Indeed, the fact that the percentage of aborted trials was less than 2 % of trials even in supra-second blocks, pleads for a lack of discrimination ability in long ranges rather than a low performance related to poor motivation. Further, response times increased as a function of time-ranges, which can be linked to a higher uncertainty that slows down choices. Such difficulty has been reported in pre-school children who discriminate better durations at sub-second ranges compared to 1st year elementary school or adults which discriminated equally durations at second and supra-second ranges (Hamamouche & Cordes, 2019). In addition to documented bisection (Mendoza et al., 2018; Leon & Shadlen, 2003), order (Yuji Naya & Suzuki, 2011) and time reproduction (Meirhaeghe et al., 2021; Wang et al., 2018; Jazayeri & Shadlen, 2015) abilities, our results demonstrate that monkeys possess a finer ability to classify durations in a levelled structure.

C.4.b. A strong and adaptive recruitment of striatum

Consistent with the hypothesis that cortico-striatal circuits embody a neural clock, many findings showed that striatal cells in dorsomedial rodent striatum or caudate nuclei in the primate display activity patterns spanning a delay interval, with a mix of ramping and peaks that rescaled to the durations fitting the scalar expectancy theory (Zhou et al., 2020; Wang et al., 2018; Mello et al., 2015; Gouvêa et al., 2015). By using a task that does not require a timed motor production, we focused on neural activity as animals waited for the interval to end before producing an adequate movement. We show that the striatum adapts to temporal demand in several ways: 1) the number of cells recruited increased for fine-grained discrimination at sub-second and second ranges compared to coarser discrimination at supra-second ranges, 2) peak width adapted to time range, yielding to 3) a resolution of moment-to-moment population-based discrimination which adapted to the time range. Together, these effects likely influenced the density of neural representation and its dynamics depending on the time range. While the increased number of neurons at short time ranges might mechanically increase time decoding, we showed by systematic down-sampling neural population for all measures that this explanation did not suffice. Indeed, we showed that time could be accurately predicted well above chance across ranges from 1s to 8s in the striatum even from small populations. Precisely, the instantaneous changes in neural states were higher at short time ranges, and temporal resolution was adapted to time range, with a high resolution at short time ranges and low resolution at supra-second ranges. Therefore, even in a down sampled population, time decoding was supported by adaptive changes in spiking activity.

While our results document these neural mechanisms through the elapsed time of the interval very precisely, they also raise the question of what recruited cells in the striatum in our task. Explicitly, in the task, an interval always started by the same event – a white square briefly shown on the black

screen. Depending on the session block, monkeys adapted their responses to the appropriate time range following a few errors at transitions (typically around 10 trials). Therefore, the task context, rather than the cue itself, modified the way cells were recruited throughout the trial. Further, we showed that only few of the time-modulated cells responded to the visual cues, therefore ruling out the possibility that all the cells identified as TM cells actually displayed decay following initial response. Rather, TM cells were made up of a mix of ramping and peak cells, overall constant across sets in all brain regions, which suggests a mechanism of sequential recruitment of cells through cortical input or local inhibition/disinhibition mechanisms (Burke, Rotstein, & Alvarez, 2017; Hunnicutt et al., 2016; Plenz, 2003). Previous results showed that medium-spiny striatal neurons encoded upcoming reward choices and expected reward times (Schultz et al., 1992; Cromwell et al., 2018). Tonicly active striatal neurones also play a role in tracking reward time (Apicella et al., 1991). Striatal cells are also active during preparation, initiation and execution of movements in rhesus macaques (Schultz, Tremblay, & Hollerman, 2003), and in rodents (Sales-Carbonell et al., 2018). In line with this, a large percentage of time-modulated cells also displayed activity for the cue signalling choice time, and during motor response and reward. Striatum territories are mainly responsible for contralateral movements execution (Worbe et al., 2009), and we recorded in the ipsilateral side of the monkey's preferred hand. The location of time field was not directly in relation with these responses outside the interval, which suggests a mixed selectivity resulting from the interplay between cortical and local modulation in the circuit involved for rewarded timed actions. Given these findings, a logical hypothesis is that the organisation of the temporal dynamics within intervals may be coherent with the expected fixed events nested within each interval, *i.e.*, the possibility that an interval will end after either a $\frac{1}{4}$, or a $\frac{1}{2}$ of the total interval length. We observed a higher density of peaks for the first half of the whole interval at any time range, but the specific time of likely event's occurrence were not marked as in dopamine neurons (Schultz, Dayan, & Montague, 1997). Further, our results differ from findings in pre-SMA in which activity reflected decisional borders between two intervals (Mendoza et al., 2018). The neural dynamics measured through the PCA showed a steady change coupled with a constant resolution throughout 1s- and 2s-long intervals. This pleads against a serial recruitment of the three successive motor command preparation, or reward prediction errors. It comes at odds with the fact that the striatum receives projections from midbrain neurons. It suggests that, within the interval, the density of circuits recruited is constant, and may be independent from phasic midbrain dopamine inputs. Rather, striatal recruitment may reflect a self-initiated continuous cortical attractor sustained at short ranges (Wang et al., 2018) and supported by tonic dopamine input (Howe et al., 2013). The fact that population-based decoding showed adaptation depending on time range is consistent with temporal window gated neural plasticity occurring in cortical and sub-cortical neurons (Chaudhuri et al., 2015; Buonomano & Maass, 2009).

One surprising finding is that we observed a previously unreported difference between the caudate and putamen. We showed that the caudate, rather than the putamen, supports the strongest time prediction based on population coding, in a task with no timed motor demand. While the caudate and putamen do not differ in their intrinsic cellular types and organization, making the striatum essentially a unique structure, there are major differences in the cortical inputs each sub-region receives (Ferry et al., 2000; Alexander et al., 1986). Our findings indicate that the caudate is systematically better at time decoding than the putamen, specially at short time ranges. This is shown by larger neural trajectory, better overall time prediction and higher temporal resolution. An interesting finding is that the putamen performed better at longer time ranges than the caudate, and this may be related to the putamen's involvement in motor execution and preparation (Worbe et al., 2009). In line with this, our results identify differences within striatal territories that may well reflect the differential cortico-striatal loops (Jahanshahi et al., 2015).

C.4.c. Time cells presence but poor time prediction in the hippocampus

In line with previous reports, we identified a small proportion of time cells in the hippocampus. Unlike striatal cells, the proportion of cells (~10%) was almost exclusively made of peak cells, in line with previous studies (Reddy et al., 2021; Umbach et al., 2020). This proportion did not vary with time range. The peak patterns identified here differed from the ones identified in the entorhinal cortex in rodents (Tsao et al., 2018) and macaques (Bright et al., 2020). In rodents, entorhinal cells showed a decay of activity over several minutes likely encoding passage of time, while, in monkeys, neurons displayed a decay relaxation time after image offset akin to a ramping down type of activity. While, in our task, there was a cue offset that may have been able to support such temporal decay, the patterns we observed differed drastically from the ones reported in the entorhinal cortex.

Further, measures of neural trajectory or time decoding were strikingly different in the hippocampus compared to the caudate. Indeed, despite the presence of time-modulated cells, time prediction was only slightly different from chance at the range of the second and at chance level at other ranges. This suggests that population activity did not contain sufficient modulations below or beyond the second resolution to support overall time prediction in the trial. While many studies reported time cells in rodents (Pastalkova et al., 2008; MacDonald et al., 2011; Mau et al., 2018; Shimbo et al., 2021) or in monkeys (Sakon et al., 2014; Naya & Suzuki, 2011), to our knowledge, no previous study attempted decoding time from hippocampal neurons during a time discrimination task at the ranges we studied. A strong difference from most previous reports identifying time cells is that, here, animals are waiting for an interval to end, in a context in which no new specific prospective memory has to be formed. By contrast, in previous studies reporting time cells, there was a memory demand, whether working memory (Sabariego et al., 2019; Pastalkova et al., 2008), order memory of

pictures (Reddy et al., 2021; Naya & Suzuki, 2011) or learning a list of words (Umbach et al., 2020). Our results also contrast with time cells identified in rodents placed on a forced treadmill (Mau et al., 2018; Kraus, Robinson, White, Eichenbaum, & Hasselmo, 2013), where the forced locomotion may have promoted the recruitment of cells that did not have an equivalent in our task. The striking absence of strong time-modulated activity may therefore reflect that no stimulus may entrain neural activity in monkeys performing this task. However, an intriguing pattern emerged from the pairwise moment-to-moment decoding (Figure 5): hippocampal activity supported some discrimination (yet at a probability of 0.7, well below that of the striatum) between durations for the second range (Figure 5A second row), while only a very coarse decoding was observed at other ranges, *i.e.* discriminating only the last or first second from all other intervals. Therefore, the best time resolution was observed for the most familiar set, the one to which animals were trained first. This raises the question of a potential role for the hippocampus in representing well-learned information. In sum, we found little evidence that the hippocampus tracks time when memory is not involved in the task, although the TM cells identified had a pattern similar to time cells reported in the rodent literature. Whether and how the recruitment of hippocampal cells depends on specific memory tasks requires further investigation.

C.4.d. Moment-to-moment adaptation of temporal discrimination in striatum and hippocampus.

It was suggested that the temporal processing emerges from the unravelling of internal dynamic states of network triggered by a stimulus, and that short-term neural plasticity influences the dynamics in the network (Buonomano & Maass, 2009). We made two observations that suggest that plasticity influences the state of the striatal population and to a lesser extent of hippocampal population: 1) when the animals were facing a discrimination at a short range, there were more striatal cells recruited compared to longer ranges; 2) the resolution of temporal discrimination between neighbouring times adapted to the time range in the striatum and the hippocampus (Figure 5C). We controlled that the effect was not due a lower sampling size by computing decoding accuracies on the first second of each time range with time-modulated cells identified during the first second (figure S5). Overall, the results suggest that plasticity biased the neuronal circuits recruited as well as their intrinsic information. Further, the fact that the temporal resolution differed in the striatum and the hippocampus has functional implications in line with the observation that hippocampal activity may only support time representation during episodic memory.

Finally, it has been suggested that time related activity in the striatum is inherited from hippocampal circuits at the minute range (Shikano et al., 2021). Our findings show that, at a lower time range, there is a strong time-related signal in the striatum in the quasi absence of time-related signals

in the hippocampus. This suggests that these striatal circuits may be recruited independently from the hippocampus at short ranges, and subserve different functions. How these organizations develop over time remains an open question.

C.5. Methods

C.5.a. Animals and behavioral set up

We trained two naïve adult female rhesus macaques (Monkey 1, 6.5 kg, and monkey2, 7kg, both 5 years old at the beginning of the experiments) on the ongoing-time categorization task. Surgical, behavioral and experimental procedures were authorized by the ethical comity of animal experimentation N°42 and authorized by the minister of research and innovation under the number APAFIS#13212-20180125104191. Under general anesthesia, the animals were implanted with a rectangular nylon chamber (21x15) allowing simultaneous access to the striatum and the hippocampus (coordinates of the center of the chamber relative to interaural line). A head-post was also implanted and covered by bone cement (Palacos®). The anesthesia for the surgery was induced by Zoletil (Tiletamine-Zolazepam, Virbac®, 5mg/kg) and maintained by isoflurane (Belamont, 1–2%). Post-surgery analgesia was ensured thanks to Temgesic (buprenorphine, 0.3mg/ml, 0.01mg/kg). During recovery, proper analgesic and antibiotic coverage was provided. The surgical procedures conformed to European and National Institutes of Health Guidelines for the Care and Use of Laboratory Animals.

C.5.b. Behavioral training

The task was designed using Presentation (Neurobehavioral systems), which controlled reward deliveries conditioned on the movements of the joystick (Sakae Tsushin Kogyo, L.T.D.) depending on task contingencies. Monkeys were seated at a distance of 55cm from a 1024x768 screen with a refreshing rate of 60Hz. The experimental chair allowed reaching a joystick placed in front of the animal. We first trained the two macaques to associate the movements of the joystick to a pointer on the screen. Following the presentation of a brief white square (200ms interval start cue), if the animal moved the pointer via the joystick to a target (a blue square), it was rewarded by a small amount of diluted juice delivered close to its mouth. The square (150x150pixels) was randomly positioned at the top, bottom or left of the screen on every trial. Once the monkey learned the motor movements to reach targets in the 3 positions, three intervals were progressively inserted between the cue and the targets. The screen remained dark during these intervals. We first trained the monkeys to discriminate the durations at the second-range. The monkey had to wait respectively for .5, 1 and 2s (set 2s-long), without moving the joystick, before the bottom, left or top target appeared. Each target was presented individually after each interval. If the monkey moved the joystick before the end of the interval, the trial was aborted without reward given. The inter-trial interval (ITI) started when the monkey reset the joystick position. Once the monkey was able to wait until the appearance of each target separately before moving the joystick, we presented two targets at the time, top and bottom, after short and long intervals. Once the animal mastered that discrimination, we interleaved short or long interval

durations with intermediate durations, before finally presenting the 3 types of intervals and the three possible targets.

C.5.c. Retiming sets

When the monkeys reached 80% of correct responses at discriminating durations at set 2s-long, we tested them on different sets. First, for several blocks, the monkeys started with set 2s-long, and then the duration were halved: long became 1s, intermediate 0.5 and short .25s (set 1s-long). Then, we tested the monkeys on set 4s-long following the same procedure: monkeys started a block with set 2s-long and after n trials (~100), the durations were multiplied by 2: long became 4s, intermediate 2 and short 1s. Once the monkey adapted to this new retiming condition (retiming long), it had to discriminate even longer durations following the same rule: once it performed enough trials at set 4s-long, durations were multiplied by 2 once more, reaching 8s, 4s, and 2s. Once the monkey learned the retiming rules, we tested it on the same durations, but starting from set 8s-long, then retiming to 4s- and finally to 2s-long.

We recorded from both monkeys while they performed one block on one set followed by a second set. Sets could be set 2s-long followed by set 1s-long, or set 2s-long followed by set 4s-long and set 8s-long (see Figure 1B). Therefore, we recorded from many more neurons in set 2s-long, as this was the reference set. For monkey 1, a few sessions consisted of set 2s-long only.

C.5.d. Behavioral analysis

For behavioral analysis, we removed the sets at which the monkeys performed below a threshold, defined as the average accuracy at each set minus standard-deviation, therefore, discarding sessions in which animals performed poorly likely due to a lack of motivation. Analysis was performed on 53, 153, 77 and 54 sets (there are 1 to 3 sets per recording session) for monkey 1, totaling 42109 trials, and 66, 136, 66, and 48 sets for monkey 2, totaling 32588 trials, respectively for conditions 1s-, 2s-, 4s- and 8s-long. Next, we used a General-Linear Mixed-Effects (GLME) model to identify whether the set or the length of the durations influenced discriminability:

$$\text{Response} \sim \text{Interval} * \text{Set} + (1 | \text{Monkey ID}) + (\text{Monkey ID} | \text{Block})$$

where Interval and Set were categorical fixed factors, and the block and monkey's identity were random factors, respectively numerical and categorical. The accuracy followed a binomial distribution, 1 or 0, for respectively correct and error trials. Set, Interval and the interaction had a significant effect on the performance ($F(3,74685)=644$, $p<0.0001$ for Sets, $F(2,74685)=784$, $p<0.0001$ for Interval, and $F(6,74652)=154$, $p<0.0001$ for the interaction). To understand the interaction, we explored further the contrasts within and between each set, presented in the supplementary table 1.

Next, we focused on intermediate trials to analyze the mis-judgement of errors, as they were the intervals the less well categorized. We took all the incorrect intermediate trials, and ran a GLME

$$\text{Type of error} \sim \text{Set} + (1 | \text{Monkey ID}) + (\text{Monkey ID} | \text{Block})$$

with Set as main factor and the type of error as explained variable, with 0 for short and 1 for long. Monkey ID and Block were defined as random factors. Type of errors were significantly influenced by the time range ($F(3,6433)=260$, $p<0.0001$).

Afterwards, we ran a Linear Mixed Model (MME) on normalized response latencies, after selecting correct trials only:

$$\text{Response latency} \sim \text{Interval} * \text{Set} + (1 | \text{Monkey ID}) + (\text{Monkey ID} | \text{Block})$$

Response latencies calculation: The response latency was calculated between the target onset and the action completed (the joystick entering the target), which coincided with the visual feedback and reward delivery. After each block, monkeys were tested on a “motor-control task”, where no delay was inserted between cue offset and targets onset. Only one target was presented at the time, for a total of ~70 trials. At each block, we computed the averaged response latency at this “motor-control task” for each direction, bottom, left or top. Then, we subtracted this average at each trial at the corresponding block. This normalization gives us a result for which responses latencies below 0 reflected anticipation of the end of the interval, as the time was below the time needed for action selection/execution when the monkey did not know to which direction it had to go.

C.5.e. Electrophysiological recordings

Neural activity was recorded using the AlphaLab SNR version 2.0.4 (AlphaOmega®). Single unit responses were recorded using a 16-channel laminar probe with 300- μm inter-electrode spacing (V-probe, Plexon Inc.; LMA Microprobes). Two such electrodes were inserted simultaneously on every recording session, alternatively in the caudate and the hippocampus, or the putamen and the hippocampus. Cells were isolated offline using a semi-automatic method and checked manually using OFFLINE sorter (Version 3 and 4; Plexon Inc.) We recorded 615 neurons in the caudate (151 in monkey 1, 464 in monkey 2), 736 in the putamen (177 in monkey 1, 559 in monkey 2), and 931 in the hippocampus (291 in monkey 1, 640 in monkey 2). Among caudate neurons, 196, 461, 204, 170 cells were recorded respectively in sets 1s-, 2s, 4s- and 8s-long. Following the same order, 199, 574, 333, 239 neurons were recorded in the putamen, and 348, 759, 340, 203 in the hippocampus.

C.5.f. Information content computation

To define our time-modulated cells, we computed an Information Content for each cell following the next formula:

$$IC = \sum \lambda(x) * \log(\lambda(x)/\lambda)$$

where $\lambda(x)$ is the firing rate of the neuron at time t , λ is the overall firing rate, from t_1 to t_{100} . To keep it constant across sets, we used the longer interval for each set and divided it by 100. The size of the bins varied between sets (i.e. 10ms, 20ms, 40ms, and 80ms respectively for sets 1s-, 2s-, 4s- and 8s-long) but the total number of bins did not. Next, we shuffled the spikes within the interval 1000 times, and, at each time, we calculated a fake IC on the shuffled data. With these 1000 iterations, we computed an IC_{fake} distribution. We defined time-modulated cells neurons that had an IC superior to 95% of the IC_{fake} distribution (p -value calculation). We did this for all sets. Then, to get our TM cells for the first second for all sets, we cropped the correct long trials after 1s and then computed the IC value for each neuron after dividing 1s into 100ms for all conditions. We followed the same procedure, as before, shuffling the spikes within trials across the first second for all trials, to get the p -values within the first second.

C.5.g. Definition of the neural pattern of single-cells

To classify the single cells as ramping or peak neurons, we used a stepwise regression analysis. We defined a cell as ramping when the linear term best explained its firing rate across the interval and the R^2 of the fitted model explained at least 66% of the variance. For cells that did not reach those criteria, we tested whether their neural activity exhibited a peak defined as an increase of 80% above their maximal activity followed by a decrease of at least 15%. If they did, and that only one peak was found in the interval, they were classified as 1-peak neurons. If they did and several peaks were found in the interval, they were classified as n-peaks neurons. For peak time analysis, we only took the highest peak time of the n-peaks neurons.

C.5.h. Selectivity to features of the task

To identify neurons that were selective for other features of the task (cue, target, response and reward), we tested GLME models to identify if 1) neurons were responsive to each task epoch in comparison to the baseline and 2) if there was a difference in that epoch as a function of short, intermediate and long trials (interval identity). The GLME was computed on each neuron's firing rate trial-by-trial for set 2s-long following the formula:

$$\text{Firing Rate} \sim \text{task epoch} * \text{Interval} + (1 | \text{Trial})$$

where Firing Rate was expressed in spike/second, Feature is a categorical variable for which the modalities are the baseline (inter-trial interval), and separately, either the cue display (200ms), the targets displayed (400ms), the movement preceding reward (-400ms before reward delivery) and reward delivery (200ms). Thus, GLME were computed separately for each feature. Interval identity is

a categorical variable, either “short”, “intermediate” or “long”. Trial is the random factors. This model allows to identify if the baseline (ITI) activity was different from another task epoch per each neuron. If the task epoch was significantly different from the baseline, then we tested if there was a difference as a function of interval identity. We defined neurons as selective for one interval identity when its activity for that interval was significantly different from the other two intervals and the other two intervals did not differ from each other.

C.5.i. Principal Component Analysis

We computed Principal Component Analysis (PCA) for each set and each structure on correct long trials within the set. For each neuron, we used the raw activity averaged across trials at each time-point, after dividing it in 100 bins for all sets. Thus, bins at sets 1s-long, 2s-long, 4s-long and 8s-long were respectively 10ms, 20ms, 40ms and 80ms large, as for the IC calculation. Each neuron was defined as a variable and each time-point was defined as an observation. To allow inter-structures and inter sets analysis, we performed the dimensionality reduction 1000 times, down-sampling each time (iteration) our neural population to 28 neurons. At each iteration, we computed the distances to centroids of the distributions and the distances between time-points in the 28-dimensional state. The distances to the centroids were expressed in Euclidean distances with the following formula:

$$D(x,c) = (x_{i,j,k} - c_{i,j,k}) * (x_{i,j,k} - c_{i,j,k})'$$

where x is the state of the population at time t and c is the centroid of the distribution X . i , j , and k are the coordinates in the 3-dimensional state. The speed of the trajectory was computed with Euclidean distance formula, using the 28 coordinates at each time-point. The average speed and the average distances presented in Figure 3C-D and Figure S3D, are the average at each iteration for each structure and each set. The slopes in Figure 3E are computed 1000 times on the neural trajectories obtained at each iteration, for each structure and each set.

C.5.j. Multi-class decoding using linear regression

To predict time based on neural activity, we used a linear regression model to decode time. First, to compare the temporal prediction from TM cells and other cells, we trained the model on the neural activity of the two populations separately. Training phase was computed on the 2s-long interval, during 15 correct long trials. Neural activity was cut into 100 bins, of 20ms, and smoothed on +/- 4 bins trial-by-trial. Then, the model was tested on five different correct long trials. The analysis was cross-validated 1000 times. Per each iteration, we obtained a decoding output $Y = \beta + (\alpha * X)$ where Y is a vector of 100 bins. X represents real-time and Y contains predicted time at each time-point (each bin). A perfect decoding would be illustrated by $Y = X$, with $\alpha = 1$ and $\beta = 0$. As we tested the model on five

correct trials and cross-validated it 1000 time, we obtained per each structure and each population 5000 decoding outputs. For each of these 5000 outputs, we calculated the slope of the predicted time (Y). We get a α_{real} distribution of 5000 slopes of decoding for both populations, TM cells and other cells, for each structure at set 2s-long. To define our chance-level, we performed the same decoding analysis after shuffling the time-labels on tested and trained trials. Thus, we also obtained a distribution of slopes α_{shuffle} calculated on shuffle data. Decoding above chance was define by

$$1 - (\sum \alpha_{\text{real}} > \text{P95}(\alpha_{\text{shuffle}}) / 5000)$$

We used the same method to test the temporal predictability of TM cells during the ITI by training and testing the activity on 15 and 5 ITI respectively. For this analysis, the ITI was cut into 100 bins of 8ms and smoothed on +/-4 bins trial-by-trial. Then, we tested if the neural activity during the ITI could be decoded from the activity of the first 800ms of the interval. This time, we trained our model on the first 800ms of 15 trials of 2s-long conditions defined as correct. The cropped interval was cut into 100 bins of 8ms and smoothed on +/-4 bins. The model was then tested on 1) the first 800ms activity of the long interval during 5 different trials and 2) on 5 ITI. To test the performance of the decoding above chance, we used the same method to compute the slopes and calculate the p -values as before. Finally, to test the performance of decoding across sets, we used the same method, with the exception that, at each iteration, we down-sampled our neural population to 28 neurons. This makes comparisons between sets and brain regions possible. For each set, we took the longer interval of the set, and cut it into 100 bins: sizing of the bins at each set matched the one from PCA. The activity was smoothed on +/-4 bins trial-by-trial. As before, we computed, per each set and each structure, the distribution of the slopes of decoding outputs on real and shuffled data to test the temporal predictability versus chance. In addition, we also tested the distances of predicted time to real time to compare brain regions between each other and sets. We averaged our 5000 decoding output to get 1 vector of predicted time. At each time-point, we calculated the distance from predicted time to real time, and then compared the brain regions and sets using 2-way ANOVAs.

C.5.k. Pair-wise analysis using Support-Vector-Machine

To quantify the difference between two time-points t_n and t_m within an interval, we used a support vector machine (SVM) decoding analysis. At time t_n and t_m , the neural state of the population is given by the activity of n neurons. Again, to compare the activity between structures and sets, we down-sampled our populations, to 30 neurons this time. For each set, we binned the activity of correct long trials into 100 bins, sizing and smoothing them as we did for multiclass decoding across sets. Then, we extracted the 3 first components of the neural state at t_n and t_m using PCA on trial-by-trial basis. After dimensionality reduction, the neural state at t_n and t_m were given by 3 coordinates instead of n ($n=30$). Then, we trained a Support Vector Machine (SVM) classifier on the 3 PCs of 10 trials from t_n

and 10 trials from t_m , and tested it on the PCs obtained from 10 different trials. The SVM classifier returns an accuracy value between 0.5 and 1: 1 reflects the absolute certainty to classify each time-point (t_n and t_m) correctly, and 0.5 reflects the chance level to distinguish t_n and t_m . Each pair of time points, from t_1 to t_{100} , was tested versus each other. We did this analysis for 10 iterations, and represented the averaged outcomes of SVM classifier in a time-by-time matrix, averaging the output of the 10 iterations. To test the temporal accuracy between brain regions and sets, we tested the bottom half of the matrix's accuracies between sets and brain regions using a 2-way ANOVA. Next, we computed the same analysis after shuffling the labels on training and test trials. The 95th percentile of the overall distribution of accuracy obtained from shuffled decoding was 0.55. We used a conservative chance level at 0.6. At each time-point, for each interval, we computed the accuracy score from t_1 to t_{100} . Accuracy score of t_n was defined by the number of time-points decoded above chance from t_n , and ranged from 0 to 99. Per each structure and at each set, we regressed the analysis scores as a function of time to test whether they increased or decreased over the interval. Then, to compute the timing resolution of each structure across sets, we calculated at each time-point t_i the distance t_i to t_j , where t_j is the closest time-point to t_i successfully discriminated from it (above 0.6). To do so, we took the diagonal of our matrices and for each t_i we took the closest time-point decoded above chance at the upper half and the lower half of the matrix, and then averaged them to get the width of the decoding. Finally, to test temporal discriminability in the first second of the intervals across ranges, we took the TM cells defined as such during the first second cropped on longer intervals. We computed the same decoding analysis, down-sampling our neuronal populations to 18 neurons for each structure at each set, except for the caudate at set 8s-long where we had 9 neurons only. To test whether time was discriminated successfully within one second as a function of time-range, we ran a 2-way ANOVA on the bottom half of the output matrices.

C.6. Bibliography of Chapter 1

Alexander, G. E., DeLong, M. R., & Strick, P. L. (1986). Parallel organization of functionally segregated circuits linking basal ganglia and cortex. *Annual Review of Neuroscience*, VOL. 9, 357–381. <https://doi.org/10.1146/annurev.ne.09.030186.002041>

Apicella, P., Scarnati, E., & Schultz, W. (1991). Tonicly discharging neurons of monkey striatum respond to preparatory and rewarding stimuli. *Experimental Brain Research*, 84(3), 672–675. <https://doi.org/10.1007/BF00230981>

Bright, I. M., Meister, M. L. R., Cruzado, N. A., Tiganj, Z., Buffalo, E. A., & Howard, M. W. (2020). A temporal record of the past with a spectrum of time constants in the monkey entorhinal cortex. *Proceedings of the National Academy of Sciences of the United States of America*, 117(33), 20274–20283. <https://doi.org/10.1073/PNAS.1917197117>

Buonomano, D. V., & Maass, W. (2009). State-dependent computations: Spatiotemporal processing in cortical networks. *Nature Reviews Neuroscience*, 10(2), 113–125. <https://doi.org/10.1038/nrn2558>

Burke, D. A., Rotstein, H. G., & Alvarez, V. A. (2017). Striatal Local Circuitry: A New Framework for Lateral Inhibition. *Neuron*, 96(2), 267–284. <https://doi.org/10.1016/j.neuron.2017.09.019>

Chaudhuri, R., Knoblauch, K., Gariel, M. A., Kennedy, H., & Wang, X. J. (2015). A Large-Scale Circuit Mechanism for Hierarchical Dynamical Processing in the Primate Cortex. *Neuron*, 88(2), 419–431. <https://doi.org/10.1016/j.neuron.2015.09.008>

Cromwell, H. C., Tremblay, L., & Schultz, W. (2018). Neural encoding of choice during a delayed response task in primate striatum and orbitofrontal cortex. *Experimental Brain Research*, 236(6), 1679–1688. <https://doi.org/10.1007/s00221-018-5253-z>

Cueva, C. J., Saez, A., Marcos, E., Genovesio, A., Jazayeri, M., Romo, R., ... Fusi, S. (2020). Low-dimensional dynamics for working memory and time encoding. *Proceedings of the National Academy of Sciences of the United States of America*, 117(37), 23021–23032. <https://doi.org/10.1073/pnas.1915984117>

Emmons, E. B., De Corte, B. J., Kim, Y., Parker, K. L., Matell, M. S., & Narayanan, N. S. (2017). Rodent medial frontal control of temporal processing in the dorsomedial striatum. *Journal of Neuroscience*, 37(36), 8718–8733. <https://doi.org/10.1523/JNEUROSCI.1376-17.2017>

Ferry, A. T., Öngür, D., An, X., & Price, J. L. (2000). Prefrontal cortical projections to the striatum in macaque monkeys: Evidence for an organization related to prefrontal networks. *Journal of Comparative Neurology*, 425(3), 447–470. [https://doi.org/10.1002/1096-9861\(20000925\)425:3<447::AID-CNE9>3.0.CO;2-V](https://doi.org/10.1002/1096-9861(20000925)425:3<447::AID-CNE9>3.0.CO;2-V)

Gouvêa, T. S., Monteiro, T., Motiwala, A., Soares, S., Machens, C., & Paton, J. J. (2015). Striatal dynamics explain duration judgments. *ELife*, 4(December2015), 1–14. <https://doi.org/10.7554/eLife.11386>

Hamamouche, K., & Cordes, S. (2019). A divergence of sub- and supra-second timing abilities in childhood and its relation to academic achievement. *Journal of Experimental Child Psychology*, 178, 137–154. <https://doi.org/10.1016/j.jecp.2018.09.010>

Howe, M. W., Tierney, P. L., Sandberg, S. G., Phillips, P. E., & Graybiel, A. M. (2013). Prolonged dopamine signaling in striatum signals proximity and value of distant rewards. *Nature*, 500(7464), 575–579. <https://doi.org/10.1038/nature12475>

Hunnicutt, B. J., Jongbloets, B. C., Birdsong, W. T., Gertz, K. J., Zhong, H., & Mao, T. (2016). A comprehensive excitatory input map of the striatum reveals novel functional organization. *ELife*, 5(November 2016), 1–32. <https://doi.org/10.7554/eLife.19103>

Jahanshahi, M., Obeso, I., Rothwell, J. C., & Obeso, J. A. (2015). A fronto-striato-subthalamic-pallidal network for goal-directed and habitual inhibition. *Nature Reviews Neuroscience*, 16(12), 719–732. <https://doi.org/10.1038/nrn4038>

Janssen, P., & Shadlen, M. N. (2005). A representation of the hazard rate of elapsed time in macaque area LIP. *Nature Neuroscience*, 8(2), 234–241. <https://doi.org/10.1038/nn1386>

Jazayeri, M., & Shadlen, M. N. (2015). A Neural Mechanism for Sensing and Reproducing a Time Interval. *Current Biology*, 25(20), 2599–2609. <https://doi.org/10.1016/j.cub.2015.08.038>

Karmarkar, U. R., & Buonomano, D. V. (2007). Timing in the Absence of Clocks: Encoding Time in Neural Network States. *Neuron*, 53(3), 427–438. <https://doi.org/10.1016/j.neuron.2007.01.006>

Kim, J., Ghim, J. W., Lee, J. H., & Jung, M. W. (2013). Neural correlates of interval timing in rodent prefrontal cortex. *Journal of Neuroscience*, 33(34), 13834–13847. <https://doi.org/10.1523/JNEUROSCI.1443-13.2013>

Kraus, B. J., Robinson, R. J., White, J. A., Eichenbaum, H., & Hasselmo, M. E. (2013). Hippocampal “Time Cells”: Time versus Path Integration. *Neuron*, 78(6), 1090–1101. <https://doi.org/10.1016/j.neuron.2013.04.015>

Leon, M. I., & Shadlen, M. N. (2003). Representation of Time by Neurons in the Posterior Parietal Cortex of the Macaque. *Neuron*, 38, 317–327.

MacDonald, C. J., Lepage, K. Q., Eden, U. T., & Eichenbaum, H. (2011). Hippocampal “Time Cells” bridge the gap in memory for discontinuous events. *Neuron*, 71(4), 737–749. <https://doi.org/10.1016/j.neuron.2011.07.012>

Mau, W., Sullivan, D. W., Kinsky, N. R., Hasselmo, M. E., Howard, M. W., & Eichenbaum, H. (2018). The Same Hippocampal CA1 Population Simultaneously Codes Temporal Information over Multiple Timescales. *Current Biology*, 28(10), 1499-1508.e4. <https://doi.org/10.1016/j.cub.2018.03.051>

Mauk, M. D., & Buonomano, D. V. (2004). The neural basis of temporal processing. *Annual Review of Neuroscience*, 27, 307–340. <https://doi.org/10.1146/annurev.neuro.27.070203.144247>

Meirhaeghe, N., Sohn, H., & Jazayeri, M. (2021). A precise and adaptive neural mechanism for predictive temporal processing in the frontal cortex. *Neuron*, 109(18), 2995-3011.e5. <https://doi.org/10.1016/j.neuron.2021.08.025>

Mello, G. B. M., Soares, S., & Paton, J. J. (2015). A scalable population code for time in the striatum. *Current Biology*, 25(9), 1113–1122. <https://doi.org/10.1016/j.cub.2015.02.036>

Mendoza, G., Méndez, J. C., Pérez, O., Prado, L., & Merchant, H. (2018). Neural basis for categorical boundaries in the primate pre-SMA during relative categorization of time intervals. *Nature Communications*, 9(1). <https://doi.org/10.1038/s41467-018-03482-8>

Naya, Y., & Suzuki, W. A. (2011). Integrating what and when across the primate medial temporal lobe. *Science*, 333(6043), 773–776. <https://doi.org/10.1126/science.1206773>

Pastalkova, E., Itskov, V., Amarasingham, A., & Buzsáki, G. (2008). Internally Generated Cell Assembly Sequences in the Rat Hippocampus. *Science*, 321(5894), 1322–1327. <https://doi.org/10.1126/science.1159775>.Internally

Pilkiw, M., & Takehara-Nishiuchi, K. (2018). Neural representations of time-linked memory. *Neurobiology of Learning and Memory*, 153(October 2017), 57–70. <https://doi.org/10.1016/j.nlm.2018.03.024>

Plenz, D. (2003). When inhibition goes incognito: Feedback interaction between spiny projection neurons in striatal function. *Trends in Neurosciences*, 26(8), 436–443. [https://doi.org/10.1016/S0166-2236\(03\)00196-6](https://doi.org/10.1016/S0166-2236(03)00196-6)

Reddy, L., Zoefel, B., Possel, J. K., Peters, J., Dijksterhuis, D. E., Poncet, M., ... Self, M. W. (2021). Human hippocampal neurons track moments in a sequence of events. *Journal of Neuroscience*, 41(31), 674–6725. <https://doi.org/10.1523/JNEUROSCI.3157-20.2021>

Rescola, R. A., & Wagner, A. R. (1972). A theory of Pavlovian conditioning: The effectiveness of reinforcement and Nonreinforcement, (January 1972), 64–99.

Rolls, E. T. (2010). A computational theory of episodic memory formation in the hippocampus. *Behavioural Brain Research*, 215(2), 180–196. <https://doi.org/10.1016/j.bbr.2010.03.027>

Sabariego, M., Schönwald, A., Boubilil, B. L., Zimmerman, D. T., Ahmadi, S., Gonzalez, N., ... Leutgeb, S. (2019). Time Cells in the Hippocampus Are Neither Dependent on Medial Entorhinal Cortex Inputs nor Necessary for Spatial Working Memory. *Neuron*, 102(6), 1235-1248.e5. <https://doi.org/10.1016/j.neuron.2019.04.005>

Sakon, J. J., Naya, Y., Wirth, S., & Suzuki, W. A. (2014). Context-dependent incremental timing cells in the primate hippocampus. *Proceedings of the National Academy of Sciences of the United States of America*, 111(51), 18351–18356. <https://doi.org/10.1073/pnas.1417827111>

Sales-Carbonell, C., Taouali, W., Khalki, L., Pasquet, M. O., Petit, L. F., Moreau, T., ... Robbe, D. (2018). No Discrete Start/Stop Signals in the Dorsal Striatum of Mice Performing a Learned Action. *Current Biology*, 28(19), 3044-3055.e5. <https://doi.org/10.1016/j.cub.2018.07.038>

Schultz, W., Apicella, P., Scarnati, E., & Ljungberg, T. (1992). Neuronal Activity in Monkey Ventral Striatum Related to the Expectation of Reward. *Journal of Neuroscience*, 12(12), 4595–4610. <https://doi.org/10.1523/jneurosci.12-12-04595.1992>

Schultz, W., Dayan, P., & Montague, P. R. (1997). A neural substrate of prediction and reward. *Science*, 275(5306), 1593–1599. <https://doi.org/10.1126/science.275.5306.1593>

Schultz, Wolfram, Tremblay, L., & Hollerman, J. R. (2003). Changes in behavior-related neuronal activity in the striatum during learning. *Trends in Neurosciences*, 26(6), 321–328. [https://doi.org/10.1016/S0166-2236\(03\)00122-X](https://doi.org/10.1016/S0166-2236(03)00122-X)

Shikano, Y., Ikegaya, Y., & Sasaki, T. (2021). Minute-encoding neurons in hippocampal-striatal circuits. *Current Biology*, 31(7), 1438-1449.e6. <https://doi.org/10.1016/j.cub.2021.01.032>

Shimbo, A., Izawa, E. I., & Fujisawa, S. (2021). Scalable representation of time in the hippocampus. *Science Advances*, 7(6). <https://doi.org/10.1126/sciadv.abd7013>

Skaggs, W. E., McNaughton, B. L., & Gothard, K. M. (1992). An Information-Theoretic Approach to Deciphering the Hippocampal Code. *Advances in Neural Information Processing Systems* 5, 1030–1038.

Tallot, L., & Doyère, V. (2020). Neural encoding of time in the animal brain. *Neuroscience and Biobehavioral Reviews*, 115(June 2019), 146–163. <https://doi.org/10.1016/j.neubiorev.2019.12.033>

Tiganj, Z., Jung, M. W., Kim, J., & Howard, M. W. (2017). Sequential firing codes for time in rodent medial prefrontal cortex. *Cerebral Cortex*, 27(12), 5663–5671. <https://doi.org/10.1093/cercor/bhw336>

Tsao, A., Sugar, J., Lu, L., Wang, C., Knierim, J. J., Moser, M. B., & Moser, E. I. (2018). Integrating time from experience in the lateral entorhinal cortex. *Nature*, 561(7721), 57–62. <https://doi.org/10.1038/s41586-018-0459-6>

Tsao, A., Yousefzadeh, S. A., Meck, W. H., Moser, M. B., & Moser, E. I. (2022). The neural bases for timing of durations. *Nature Reviews Neuroscience*, 0123456789. <https://doi.org/10.1038/s41583-022-00623-3>

Umbach, G., Kantak, P., Jacobs, J., Kahana, M., Pfeiffer, B. E., Sperling, M., & Lega, B. (2020). Time cells in the human hippocampus and entorhinal cortex support episodic memory. *Proceedings of the National Academy of Sciences of the United States of America*, 117(45), 28463–28474. <https://doi.org/10.1073/pnas.2013250117>

Wang, J., Narain, D., Hosseini, E. A., & Jazayeri, M. (2018). Flexible timing by temporal scaling of cortical responses. *Nature Neuroscience*, 21(1), 102–112. <https://doi.org/10.1038/s41593-017-0028-6>

Wang, Y., Toyoshima, O., Kunimatsu, J., Yamada, H., & Matsumoto, M. (2021). Tonic firing mode of midbrain dopamine neurons continuously tracks reward values changing moment-by-moment. *ELife*, 10, 1–17. <https://doi.org/10.7554/eLife.63166>

Worbe, Y., Baup, N., Grabli, D., Chaigneau, M., Mounayar, S., McCairn, K., ... Tremblay, L. (2009). Behavioral and movement disorders induced by local inhibitory dysfunction in primate striatum. *Cerebral Cortex*, 19(8), 1844–1856. <https://doi.org/10.1093/cercor/bhn214>

Zhou, S., & Buonomano, D. V. (2022). Neural population clocks: Encoding time in dynamic patterns of neural activity. *Behavioral Neuroscience*. <https://doi.org/10.1037/bne0000515>

Zhou, S., Masmanidis, S. C., & Buonomano, D. V. (2020). Neural Sequences as an Optimal Dynamical Regime for the Readout of Time. *Neuron*, 108(4), 651-658.e5. <https://doi.org/10.1016/j.neuron.2020.08.020>

C.7. Figures and Legends

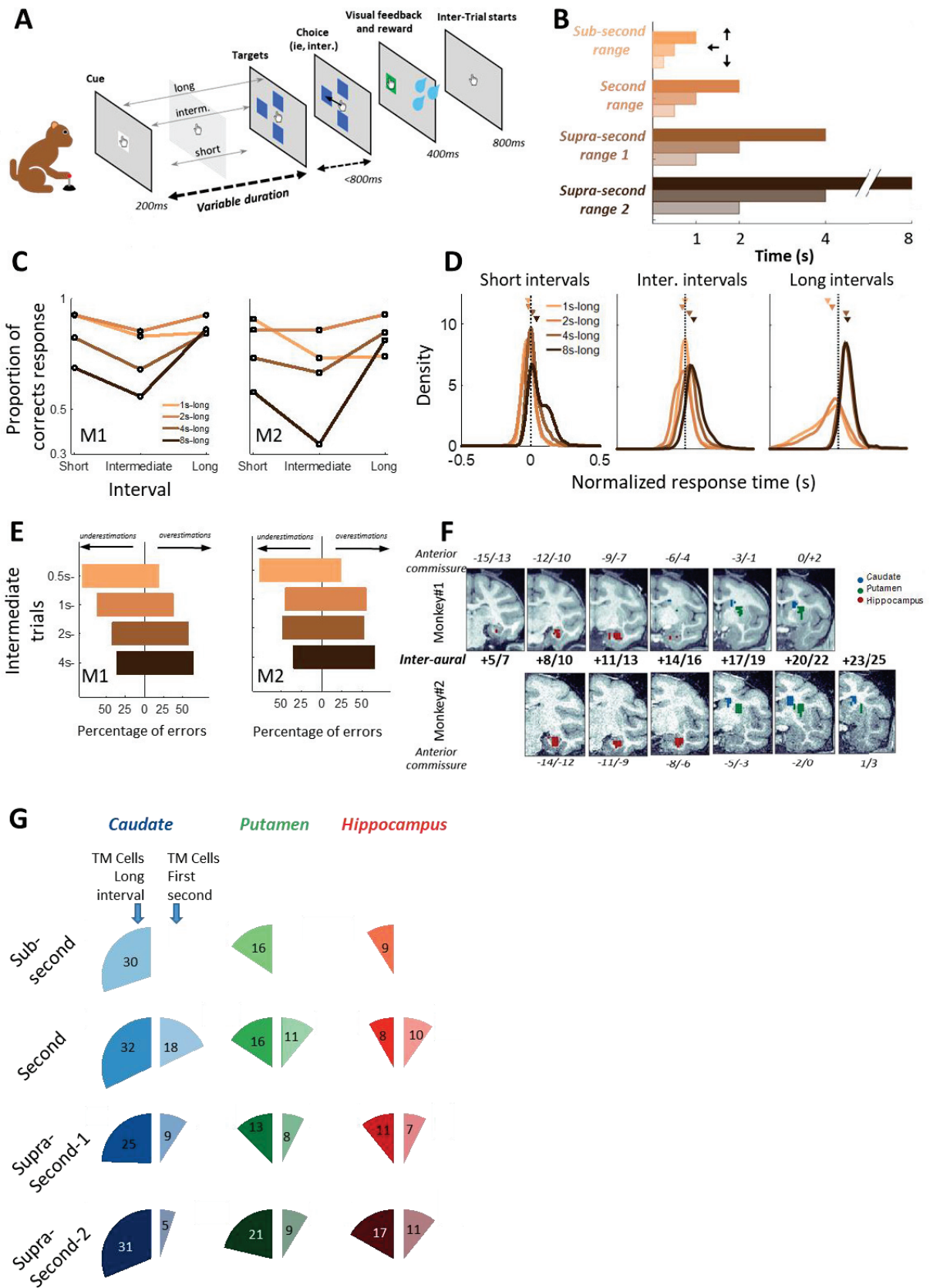


Figure 1. Ongoing time categorization task, and striatal and hippocampal neuronal population.

A. The ongoing time categorization task. A trial started with a cue presented briefly on the screen. Its offset indicated the beginning of the interval to be timed and categorized into short, intermediate or long duration. The end of the interval is indicated by the appearance of three targets, at the bottom, left and top of the screen. If the response is correct, *i.e.* bottom for short, left for intermediate (as illustrated), or top for long, the monkey is rewarded with a drop of juice. The inter-trial interval starts once the monkey moves back the joystick to the centre of the screen. **B. Sets of intervals tested across time-ranges.** Length of the durations at sub-second (0.25-0.5-1s), second (0.5-1-2s), supra-second-1 (1-2-4s) and supra-second-2 (2-4-8s) ranges. **C. Behavioural categorization of intervals across sets.** Proportion of correct responses for short, intermediate and long intervals across sets for monkey 1 (M1, left panel) and monkey 2 (M2, right panel). **D. Response time density for each interval across sets.** Normalized response time normalized to mean motor response (see Methods). The density of the distribution is represented for both monkeys together. **E. Nature of errors for intermediate trials.** Nature of errors for the intermediate trials across sets: shift to the left indicates underestimations and shift to the right overestimations. From top to bottom, intermediate trials at sub-second, second, supra-second-1, supra-second-2 ranges. **F. Recording sites.** Recording sites in both monkeys: blue dots for caudate, green dots for putamen and red dots for hippocampus. Hippocampus coordinates of both monkeys are aligned to the inter-aural, striatal coordinates are aligned to the anterior commissure. **G. Percentage of Time-Modulated cells.** Sets are displayed in rows, brain areas in columns. In each column, the left pie represents the percentage of TM cells obtained during the long interval of the set. The right pie represents the percentage of TM cells obtained once the first second of the long interval was truncated.

	CATEGORIZATION ACCURACY						
	Estimate	SE	tStat	DF	p-Value	Lower	Upper
Set 1s-long							
Short * 1s-long (Intercept)	2,47	0,09	26,80	74685	0,00	2,29	2,65
Intermediate	-1,11	0,06	-19,77	74685	0,00	-1,22	-1,00
Long	-1,05	0,06	-18,44	74685	0,00	-1,16	-0,94
2s-long	-0,25	0,06	-4,30	74685	0,00	-0,36	-0,14
4s-long	-1,15	0,06	-18,73	74685	0,00	-1,27	-1,03
8s-long	-1,86	0,06	-29,51	74685	0,00	-1,99	-1,74
Intermediate * 2s-long	0,70	0,07	9,85	74685	0,00	0,56	0,84
Long * 2s-long	1,40	0,08	18,40	74685	0,00	1,25	1,55
Intermediate * 4s-long	0,56	0,07	7,71	74685	0,00	0,41	0,70
Long * 4s-long	1,46	0,08	19,15	74685	0,00	1,31	1,61
Intermediate * 8s-long	0,40	0,07	5,43	74685	0,00	0,26	0,55
Long * 8s-long	2,13	0,08	26,31	74685	0,00	1,98	2,29
Intermediate * 1s-long (Intercept)	1,36	0,09	15,87	74685	0,00	1,19	1,52
Long	0,07	0,04	1,49	74685	0,14	-0,02	0,15
2s-long	0,45	0,04	10,64	74685	0,00	0,37	0,54
4s-long	-0,59	0,05	-12,53	74685	0,00	-0,69	-0,50
8s-long	-1,46	0,05	-28,46	74685	0,00	-1,56	-1,36
Short * 2s-long	-0,70	0,07	-9,85	74685	0,00	-0,84	-0,56
Long * 2s-long	0,70	0,07	10,74	74685	0,00	0,57	0,83
Short * 4s-long	-0,56	0,07	-7,71	74685	0,00	-0,70	-0,41
Long * 4s-long	0,91	0,07	13,81	74685	0,00	0,78	1,04
Short * 8s-long	-0,40	0,07	-5,43	74685	0,00	-0,55	-0,26
Long * 8s-long	1,73	0,07	23,96	74685	0,00	1,59	1,87
Long * 1s-long (Intercept)	1,42	0,09	16,67	74685	0,00	1,25	1,59
2s-long	1,15	0,05	22,85	74685	0,00	1,06	1,25
4s-long	0,31	0,05	5,80	74685	0,00	0,21	0,42
8s-long	0,27	0,06	4,46	74685	0,00	0,15	0,39
Short * 2s-long	-1,40	0,08	-18,40	74685	0,00	-1,55	-1,25
Intermediate * 2s-long	-0,70	0,07	-10,74	74685	0,00	-0,83	-0,57
Short * 4s-long	-1,46	0,08	-19,15	74685	0,00	-1,61	-1,31
Intermediate * 4s-long	-0,91	0,07	-13,81	74685	0,00	-1,04	-0,78
Short * 8s-long	-2,13	0,08	-26,31	74685	0,00	-2,29	-1,98
Intermediate * 8s-long	-1,73	0,07	-23,96	74685	0,00	-1,87	-1,59
Set 2s-long							
Short * 2s-long (Intercept)	2,22	0,08	27,85	74685	0,00	2,06	2,38
Intermediate	-0,41	0,04	-9,40	74685	0,00	-0,50	-0,33
Long	0,36	0,05	7,01	74685	0,00	0,26	0,46
4s-long	-0,90	0,05	-18,24	74685	0,00	-1,00	-0,80
8s-long	-1,61	0,05	-31,55	74685	0,00	-1,71	-1,51
Intermediate * 4s-long	-0,15	0,06	-2,33	74685	0,02	-0,27	-0,02
Long * 4s-long	0,06	0,07	0,81	74685	0,42	-0,08	0,20
Intermediate * 8s-long	-0,30	0,07	-4,57	74685	0,00	-0,43	-0,17
Long * 8s-long	0,73	0,08	9,47	74685	0,00	0,58	0,88
Intermediate * 2s-long (Intercept)	1,81	0,08	23,29	74685	0,00	1,66	1,96
Long	0,77	0,05	16,05	74685	0,00	0,67	0,86
4s-long	-1,05	0,04	-24,33	74685	0,00	-1,13	-0,96
8s-long	-1,91	0,05	-40,87	74685	0,00	-2,00	-1,82
Short * 4s-long	0,15	0,06	2,33	74685	0,02	0,02	0,27
Long * 4s-long	0,21	0,07	3,02	74685	0,00	0,07	0,34
Short * 8s-long	0,30	0,07	4,57	74685	0,00	0,17	0,43
Long * 8s-long	1,03	0,07	13,84	74685	0,00	0,88	1,17
Long * 2s-long (Intercept)	2,58	0,08	31,30	74685	0,00	2,42	2,74
4s-long	-0,84	0,06	-15,03	74685	0,00	-0,95	-0,73
8s-long	-0,88	0,06	-14,19	74685	0,00	-1,01	-0,76
Short * 4s-long	-0,06	0,07	-0,81	74685	0,42	-0,20	0,08
Intermediate * 4s-long	-0,21	0,07	-3,02	74685	0,00	-0,34	-0,07
Short * 8s-long	-0,73	0,08	-9,47	74685	0,00	-0,88	-0,58
Intermediate * 8s-long	-1,03	0,07	-13,84	74685	0,00	-1,17	-0,88

	Estimate	SE	tStat	DF	p-Value	Lower	Upper
Set 4s-long							
Short * 4s-long (Intercept)	1,32	0,07	19,28	74685	0,00	1,18	1,45
Intermediate	-0,56	0,04	-12,40	74685	0,00	-0,64	-0,47
Long	0,42	0,05	8,14	74685	0,00	0,32	0,52
8s-long	-0,71	0,05	-14,57	74685	0,00	-0,81	-0,62
Intermediate * 8s-long	-0,15	0,07	-2,30	74685	0,02	-0,28	-0,02
Long * 8s-long	0,67	0,08	8,69	74685	0,00	0,52	0,82
Intermediate * 4s-long (Interce	0,76	0,07	11,38	74685	0,00	0,63	0,89
Long	0,97	0,05	20,14	74685	0,00	0,88	1,07
8s-long	-0,87	0,04	-19,38	74685	0,00	-0,95	-0,78
Short * 8s-long	0,15	0,07	2,30	74685	0,02	0,02	0,28
Long * 8s-long	0,82	0,07	11,04	74685	0,00	0,68	0,97
Long * 4s-long (Intercept)	1,73	0,07	24,68	74685	0,00	1,60	1,87
8s-long	-0,04	0,06	-0,70	74685	0,49	-0,16	0,08
Short * 8s-long	-0,67	0,08	-8,69	74685	0,00	-0,82	-0,52
Intermediate * 8s-long	-0,82	0,07	-11,04	74685	0,00	-0,97	-0,68
Set 8s-long							
Short * 8s-long (Intercept)	0,60	0,07	9,15	74685	0,00	0,48	0,73
Intermediate	-0,71	0,05	-14,59	74685	0,00	-0,80	-0,61
Long	1,09	0,06	18,77	74685	0,00	0,97	1,20
Intermediate * 8s-long (Interce	-0,10	0,07	-1,59	74685	0,11	-0,23	0,02
Long	1,80	0,06	31,58	74685	0,00	1,69	1,91
Long * 8s-long (Intercept)	1,69	0,07	23,35	74685	0,00	1,55	1,83

Supplementary Table 1. Results of the GLME computed for the categorization performance.

Each pair comparison for each Set*Interval condition. Left columns indicate the paired comparisons: the “Set*Interval” condition referenced as intercept versus all the others “Set*Interval” condition. Results are divided by set (dark grey) and interval (light grey). When set (1s-long, 2s-long, 4s-long or 8s-long) is not indicated in the left column, comparison is from the same set as the intercept. When interval (Short, Intermediate or Long) is not indicated, comparison is done with the same interval from another set.

	RESPONSE TIMES						
	Estimate	SE	tStat	DF	p-Value	Lower	Upper
Set 1s-long							
Short * 1s-long (Intercept)	-0,03	0,00	-28,56	59896	0,00	-0,04	-0,03
Intermediate	0,02	0,00	11,60	59896	0,00	0,02	0,02
Long	-0,09	0,00	-52,96	59896	0,00	-0,09	-0,08
2s-long	-0,01	0,00	-8,92	59896	0,00	-0,02	-0,01
4s-long	0,00	0,00	0,89	59896	0,37	0,00	0,01
8s-long	0,03	0,00	13,24	59896	0,00	0,03	0,03
Intermediate * 2s-long	-0,02	0,00	-10,45	59896	0,00	-0,03	-0,02
Long * 2s-long	0,04	0,00	17,21	59896	0,00	0,03	0,04
Intermediate * 4s-long	-0,01	0,00	-2,77	59896	0,01	-0,01	0,00
Long * 4s-long	0,13	0,00	51,75	59896	0,00	0,12	0,13
Intermediate * 8s-long	-0,01	0,00	-1,59	59896	0,11	-0,01	0,00
Long * 8s-long	0,10	0,00	35,83	59896	0,00	0,10	0,11
Intermediate * 1s-long (Intercept)	-0,02	0,00	-12,14	59896	0,00	-0,02	-0,01
Long	-0,11	0,00	-62,94	59896	0,00	-0,11	-0,10
2s-long	-0,03	0,00	-22,97	59896	0,00	-0,04	-0,03
4s-long	-0,01	0,00	-2,72	59896	0,01	-0,01	0,00
8s-long	0,02	0,00	9,90	59896	0,00	0,02	0,03
Short * 2s-long	0,02	0,00	10,45	59896	0,00	0,02	0,03
Long * 2s-long	0,06	0,00	27,19	59896	0,00	0,05	0,06
Short * 4s-long	0,01	0,00	2,77	59896	0,01	0,00	0,01
Long * 4s-long	0,13	0,00	52,91	59896	0,00	0,13	0,14
Short * 8s-long	0,01	0,00	1,59	59896	0,11	0,00	0,01
Long * 8s-long	0,11	0,00	35,14	59896	0,00	0,10	0,11
Long * 1s-long (Intercept)	-0,12	0,00	-96,17	59896	0,00	-0,12	-0,12
2s-long	0,02	0,00	15,09	59896	0,00	0,02	0,03
4s-long	0,13	0,00	69,16	59896	0,00	0,13	0,13
8s-long	0,13	0,00	63,06	59896	0,00	0,13	0,14
Short * 2s-long	-0,04	0,00	-17,21	59896	0,00	-0,04	-0,03
Intermediate * 2s-long	-0,06	0,00	-27,19	59896	0,00	-0,06	-0,05
Short * 4s-long	-0,13	0,00	-51,75	59896	0,00	-0,13	-0,12
Intermediate * 4s-long	-0,13	0,00	-52,91	59896	0,00	-0,14	-0,13
Short * 8s-long	-0,10	0,00	-35,83	59896	0,00	-0,11	-0,10
Intermediate * 8s-long	-0,11	0,00	-35,14	59896	0,00	-0,11	-0,10
Set 2s-long							
Short * 2s-long (Intercept)	-0,05	0,00	-43,32	59896	0,00	-0,05	-0,05
Intermediate	-0,05	0,00	-41,94	59896	0,00	-0,05	-0,05
Long	0,00	0,00	-2,02	59896	0,04	-0,01	0,00
4s-long	0,01	0,00	8,92	59896	0,00	0,01	0,02
8s-long	0,04	0,00	20,86	59896	0,00	0,04	0,05
Intermediate * 4s-long	0,01	0,00	6,38	59896	0,00	0,01	0,02
Long * 4s-long	0,09	0,00	41,64	59896	0,00	0,09	0,04
Intermediate * 8s-long	0,02	0,00	5,61	59896	0,00	0,01	0,02
Long * 8s-long	0,07	0,00	25,33	59896	0,00	0,06	0,07
Intermediate * 2s-long (Intercept)	-0,05	0,00	-45,84	59896	0,00	-0,05	-0,05
Long	-0,05	0,00	-39,58	59896	0,00	-0,05	-0,05
4s-long	0,03	0,00	16,90	59896	0,00	0,03	0,03
8s-long	0,06	0,00	25,81	59896	0,00	0,05	0,06
Short * 4s-long	-0,01	0,00	-6,38	59896	0,00	-0,02	-0,01
Long * 4s-long	0,08	0,00	34,00	59896	0,00	0,07	0,08
Short * 8s-long	-0,02	0,00	-5,61	59896	0,00	-0,02	-0,01
Long * 8s-long	0,05	0,00	17,72	59896	0,00	0,04	0,06
Long * 2s-long (Intercept)	-0,10	0,00	-93,80	59896	0,00	-0,10	-0,10
4s-long	0,11	0,00	66,44	59896	0,00	0,10	0,11
8s-long	0,11	0,00	59,10	59896	0,00	0,11	0,11
Short * 4s-long	-0,09	0,00	-41,64	59896	0,00	-0,10	-0,09
Intermediate * 4s-long	-0,08	0,00	-34,00	59896	0,00	-0,08	-0,07
Short * 8s-long	-0,07	0,00	-25,33	59896	0,00	-0,07	-0,06
Intermediate * 8s-long	-0,05	0,00	-17,72	59896	0,00	-0,06	-0,04

	Estimate	SE	tStat	DF	p-Value	Lower	Upper
Set 4s-long							
Short * 4s-long (Intercept)	-0,03	0,00	-19,17	59896	0,00	-0,04	-0,03
Intermediate	0,01	0,00	6,30	59896	0,00	0,01	0,02
Long	0,04	0,00	21,79	59896	0,00	0,04	0,04
8s-long	0,03	0,00	12,73	59896	0,00	0,02	0,03
Intermediate * 8s-long	0,00	0,00	0,61	59896	0,54	0,00	0,01
Long * 8s-long	-0,02	0,00	-8,32	59896	0,00	-0,03	-0,02
Intermediate * 4s-long (Interce	-0,02	0,00	-11,59	59896	0,00	-0,02	-0,02
Long	0,03	0,00	14,57	59896	0,00	0,02	0,03
8s-long	0,03	0,00	12,11	59896	0,00	0,03	0,03
Short * 8s-long	0,00	0,00	-0,61	59896	0,54	-0,01	0,00
Long * 8s-long	-0,03	0,00	-8,40	59896	0,00	-0,03	-0,02
Long * 4s-long (Intercept)	0,01	0,00	4,07	59896	0,00	0,00	0,01
8s-long	0,00	0,00	1,72	59896	0,09	0,00	0,01
Short * 8s-long	0,02	0,00	8,32	59896	0,00	0,02	0,03
Intermediate * 8s-long	0,03	0,00	8,40	59896	0,00	0,02	0,03
Set 8s-long							
Short * 8s-long (Intercept)	0,00	0,00	-2,26	59896	0,02	-0,01	0,00
Intermediate	0,01	0,00	5,25	59896	0,00	0,01	0,02
Long	0,01	0,00	6,42	59896	0,00	0,01	0,02
Intermediate * 8s-long (Interce	0,01	0,00	3,94	59896	0,00	0,00	0,01
Long	0,00	0,00	0,33	59896	0,74	0,00	0,01
Long * 8s-long (Intercept)	0,01	0,00	5,24	59896	0,00	0,01	0,01

Supplementary Table 2. Results of the GLME computed on the response times.

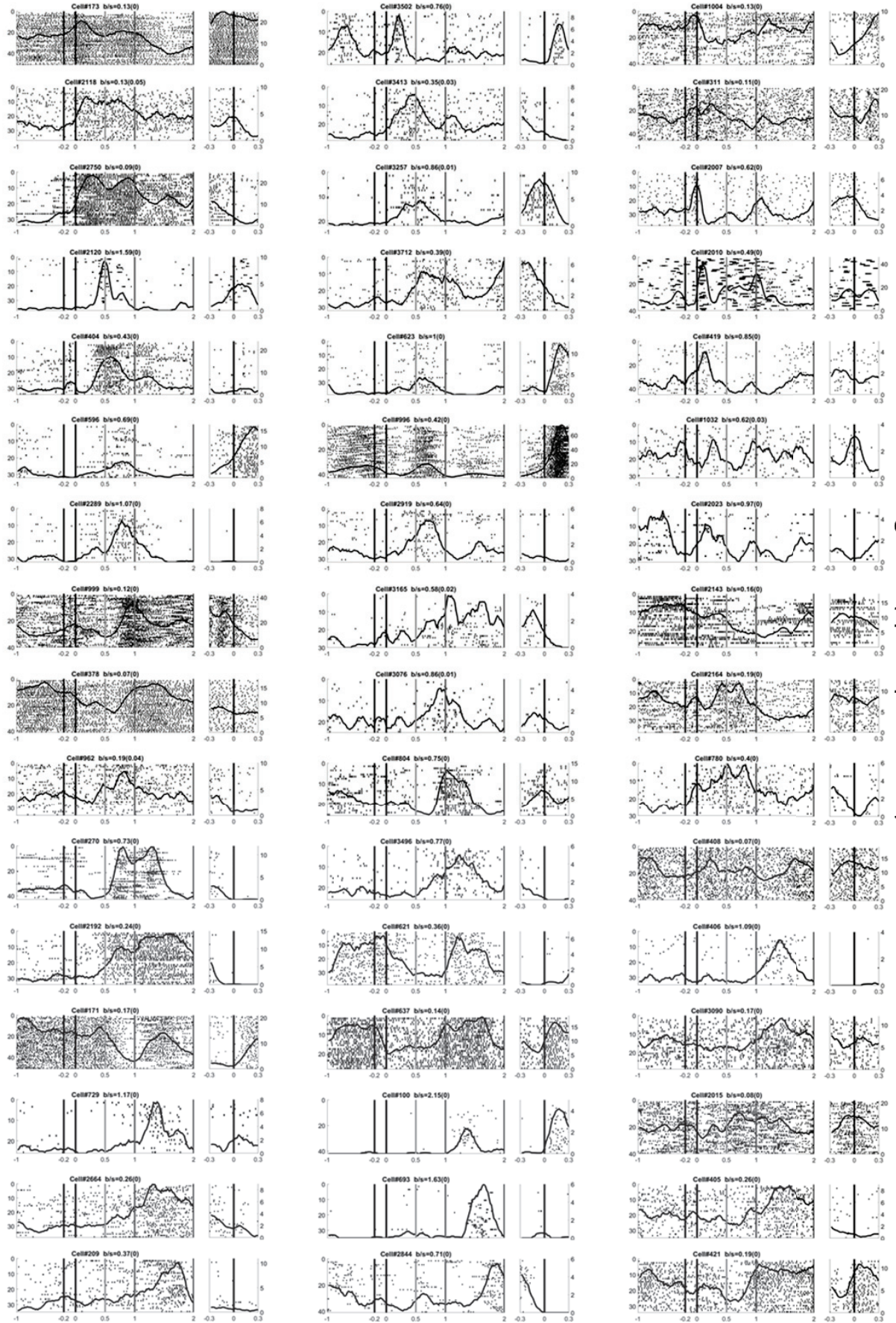
Table layout is the same as Supplementary Table 1.

Caudate

Putamen

Hippocampus

Trials



Firing rates (spikes per second)

Time (seconds)

Figure 2. Time-modulated single cell examples during the second range set.

From left to right columns, raster histograms of spikes recorded in the caudate, putamen and hippocampus with the superposed average activity (line). Left panels show the activity during baseline, the cue, and the long interval, aligned at 0 to the offset of the cue. The possible short and intermediate intervals are marked by light and dark grey lines, respectively. Right panels show the neural activity aligned to the reward delivery (black line), with -300ms corresponding to movement. Per each cell, we indicate its bit/spike score and its p -value.

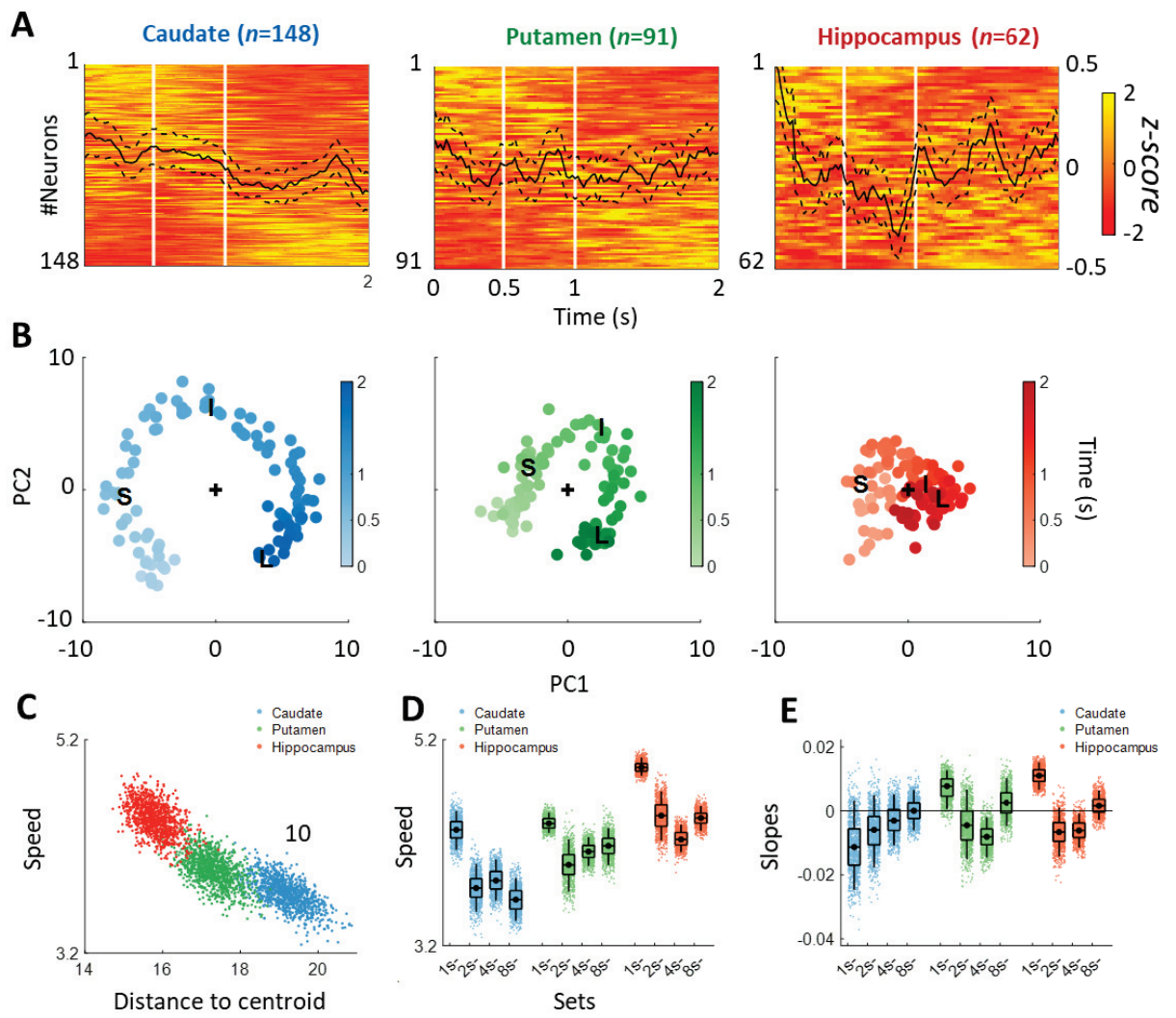


Figure 3. Population changes through time across regions at set 2s-long.

A. From left to right, neuronal population of TM cells recorded in the caudate (left), putamen (middle), and hippocampus (right). Activity is z-scored. Neurons are sorted as a function of their linear term computed during the stepwise regression analysis. Superposed on the population maps, solid line and dotted lines show average z-score and standard-deviation. Time of expected interval ends are indicated with white vertical lines. **B.** Population activity over time (2s-long) projected onto the first two Principal Components for caudate (left), putamen (middle), and hippocampus (right). The state of the population at time t was defined by 2 coordinates. Each coordinate is the score of each principal component at time t . The time of expected interval ends are indicated for short (S), intermediate (I) and long (L) intervals. The centroid of the distribution is represented with a cross. **C.** Average speed (y-axis) of the neural trajectories during the 2s-long interval, obtained with the first 9th PCs, from each iteration with the down sampling method ($i=1000$) plotted against the average distance to the centroid of the same trajectories (x-axis). **D.** Average speed (y-axis) of the neural trajectory obtained from each iteration ($i=1000$) for each brain region across sets. **E.** Slopes obtained on each neural trajectory obtained from each iteration for each brain region across sets.

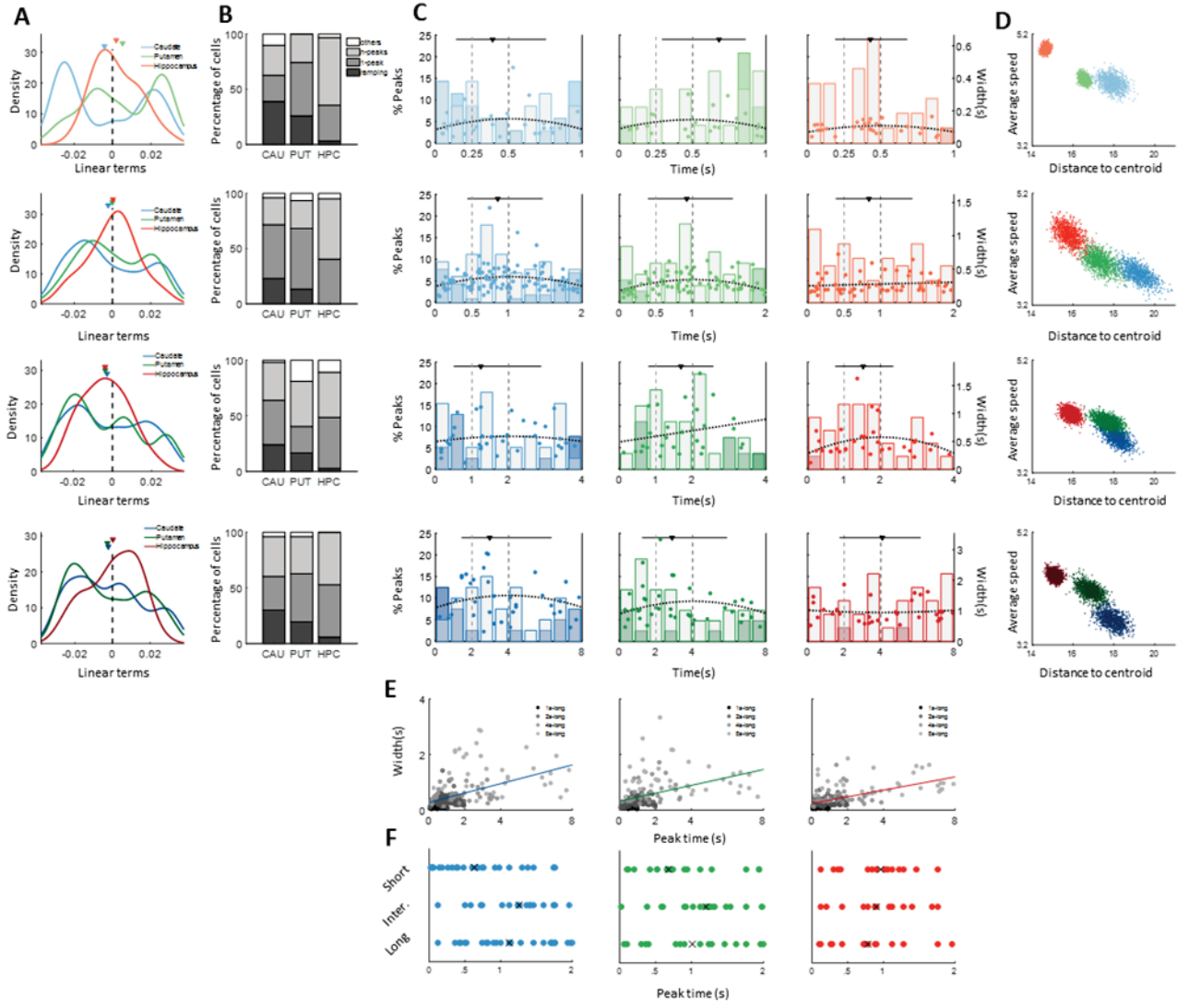


Figure Supplementary 3. Population measures across regions and sets.

A. Distribution of the linear terms obtained from the stepwise regression analysis, for each brain region across sets, from top to bottom, at sets 1s-long, 2s-long, 4s-long, 8s-long. **B.** Proportion of TM cells showing ramping, 1-peak, multi-peaks and other patterns per each brain region across sets, from top to bottom, at sets 1s-long, 2s-long, 4s-long, 8s-long. **C.** From top to bottom, peak times at set 1s-long, 2s-long, 4s-long and 8s-long. Columns from left to right: caudate, putamen, hippocampus. Left y-axis, distribution of peak times over the interval (white bars represent peak neurons, coloured bars ramping neurons). Median of the distribution (triangle) and interquartile range (horizontal line) summarize the peaks distribution. In the caudate, the peak times were mainly distributed within the first half of the interval (medians respectively at 39, 42.5, 31, and 37% of the interval duration at sets 1s-, 2s-, 4s- and 8s-long). In the putamen, the peaks were distributed in the second half of the interval at set 1s-long (median at 68%), and in the first half of the interval for the other sets (medians respectively 46, 42, and 36% of the interval duration for sets 2s-, 4s- and 8s-long). In the hippocampus, peak distributions were also mainly distributed within the first half of the interval duration (medians respectively at 43, 42, 38, and 51% of the interval). Right y-axis, width size of peaks. Dots represent width size as a function of peak times. Superposed dotted lines represent the linear fit for the hippocampus at set 2s-long and for the putamen at set 4s-long, and the quadratic fits for the other structures and sets. **D.** Average speed (y-axis) of the neural trajectories computed for each set and each brain region, obtained with the first 9th PCs plotted against the average distance to the centroid of the same trajectories (x-axis). Measures (N=1000) were obtained from each iteration with the down sampling method. **E.** Width size of the time “field” as a function of peak time for caudate (left), putamen (middle) and hippocampus (right) across all ranges. Solid lines represent the fit model of the linear regression. **F.** Distribution of peak times during the interval as a function of neurons selectivity to short, intermediate, and long trials during target task epoch in set 2s-long. From left to right: caudate, putamen and hippocampus.

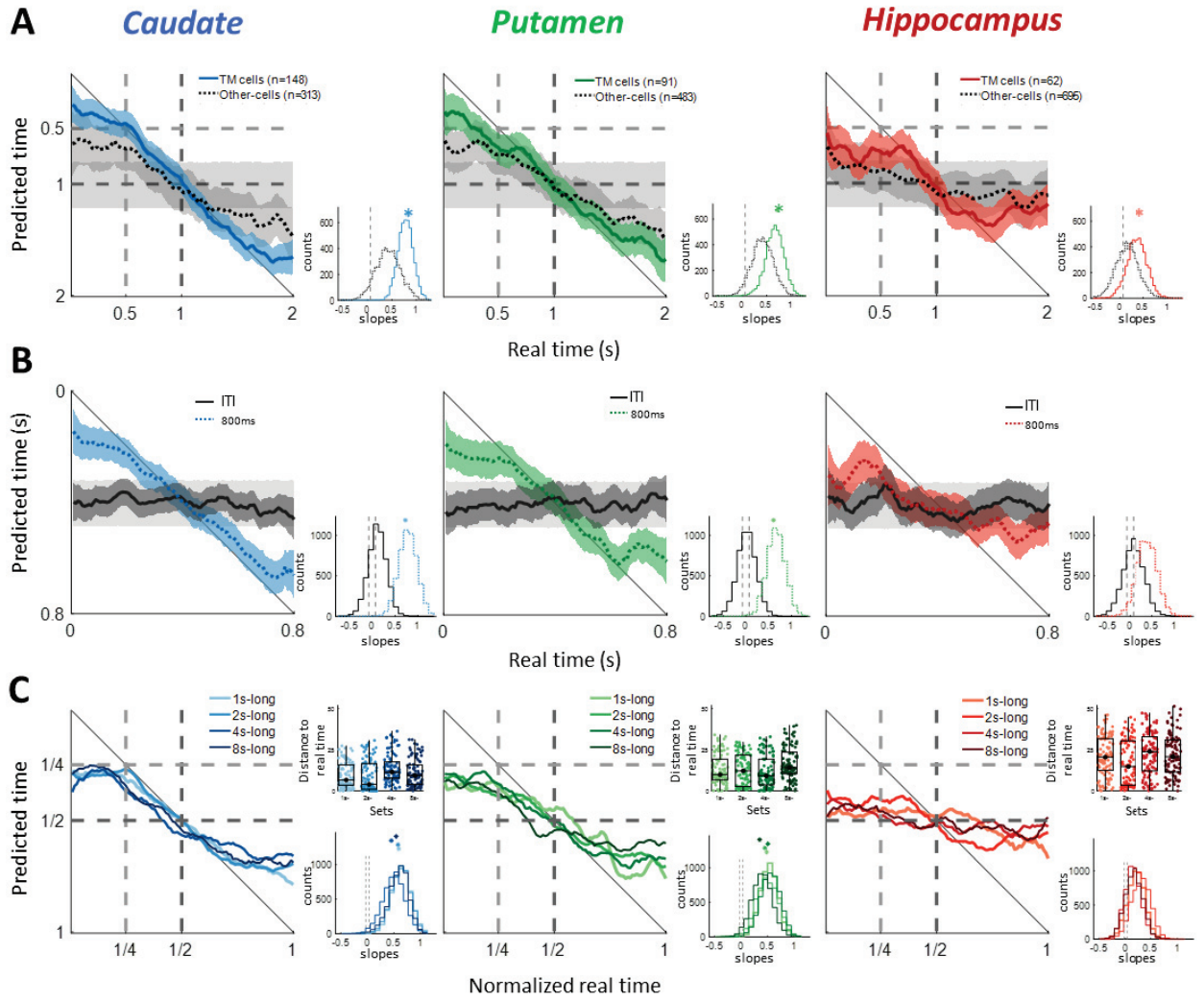
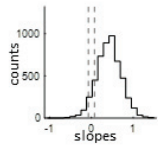
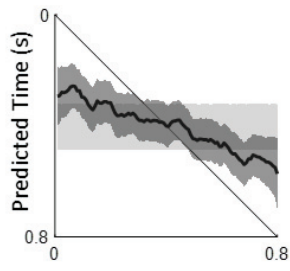


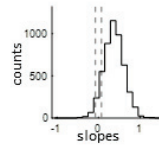
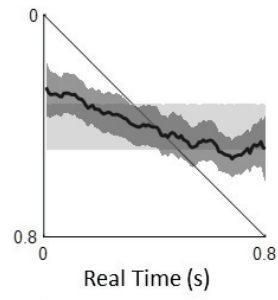
Figure 4. Population decoding as a function of time.

A. Multiclass decoding during 2s-long interval for caudate (left), putamen (middle) and hippocampus (right). Decoding of predicted time (y-axis) as a function of real time (x-axis). Decoding performance on TM cells is represented against decoding performance of other cells. Chance value is shown with light grey shade. Possible interval ends are indicated by light grey (short) and dark grey (long) dashed lines. Bottom right panel insets: Slopes distribution obtained from the 5000 decoding outputs for TM cells versus other cells. Vertical dashed line represents chance level (95th percentile). Distributions different from chance are indicated with an asterisk. **B.** Multiclass decoding tested on baseline activity (black line) after training on the first 800ms of the interval (coloured line) for caudate (left), putamen (middle) and hippocampus (right). Decoding of predicted time (y-axis) as a function of real time (x-axis). Bottom right panel: Slopes distribution obtained from the 5000 decoding outputs of first 800ms (coloured dotted line) and baseline activity (black line). Distributions different from chance are indicated with an asterisk. **C.** Decoding across sets after down-sampling the populations for caudate (left), putamen (middle) and hippocampus (right). Decoding of predicted time (y-axis) as a function of normalized time (x-axis). Possible ends of interval are indicated by light grey (short) and dark grey (long) on the normalized time axis. Top right panel. Distance from predicted time to real time for each time-point of the decoded interval. Bottom right panel insets: Slopes distribution obtained from the 5000 decoding outputs at each set. Chance level is represented in dashed lines. Distributions different from chance are indicated with an asterisk.

Caudate



Putamen



Hippocampus

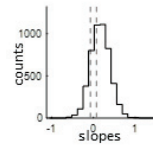
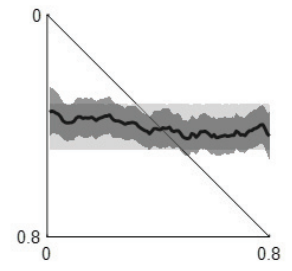
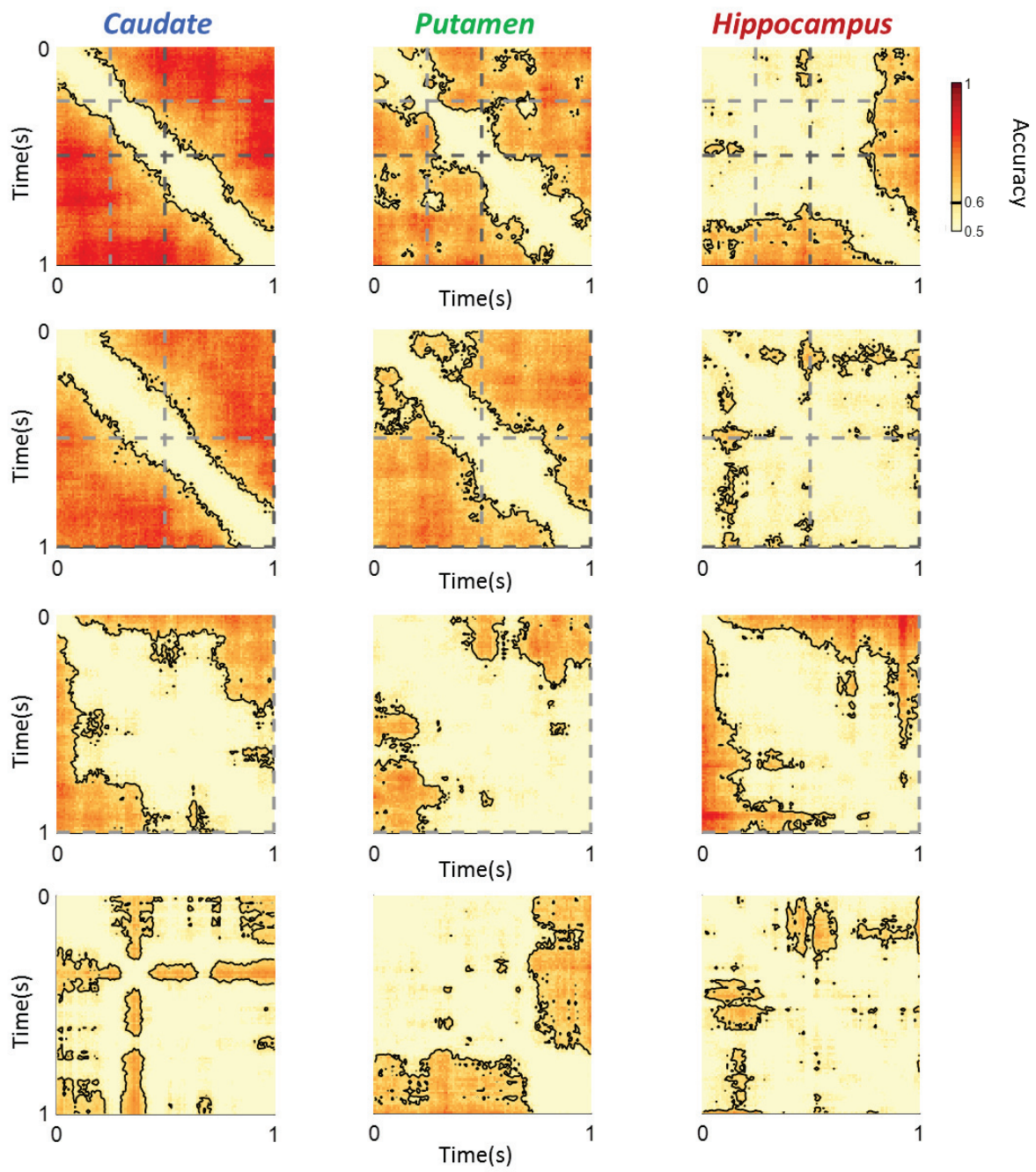


Figure Supplementary 4. Absence of time decoding from baseline activity.

Multiclass decoding trained and tested on baseline activity (black line). Decoding of predicted time (y-axis) as a function of real time (x-axis) for caudate (left), putamen (middle) and hippocampus (right). Chance value is shown with grey shade. Bottom panels: Slopes distribution obtained from the 5000 decoding outputs on baseline activity (black line) did not differ from chance.

Figure 5. Moment-to-moment time discrimination.

A. Pairwise decoding for caudate (left), putamen (middle) and hippocampus (right). Results for each set are presented in rows: from top to bottom are sets 1s-long, 2s-long, 4s-long and 8s-long and displayed in a time-by-time matrix in which each data-point is the discriminability accuracy between $t(x)$ and $t(y)$. Accuracy scores ranged from 0.5 to 1. Chance level is defined at 0.6. The temporal resolution is the window within the diagonal between black lines (chance level). Times for possible intervals to end are shown by light grey (short) and dark grey (intermediate) dashed vertical lines. **B.** Discriminability scores (dots) across sets for caudate (left), putamen (middle) and hippocampus (right). Each time on the x-axis (normalized time) is discriminated from n-points on the y-axis within the intervals. Coloured lines show the regressions of the accuracies scores by normalized time. Times for possible intervals to end are indicated by solid lines, light grey for short and dark grey for intermediate. **C.** Temporal resolution (dots) over time for caudate (left), putamen (middle) and hippocampus (right) across sets. Lines are the regressions of the temporal resolution over normalized time. Times for possible intervals to end are indicated by solid vertical lines, light grey for short and dark grey for intermediate.



Supplementary Figure 5. Moment-to-moment time discrimination within 1s.

Pairwise decoding computed on the neurons defined as TM cells within the first second of each interval, across different time ranges: from top to bottom are sets 1s-long, 2s-long, 4s-long and 8s-long. Brain regions are presented in columns: caudate (left), putamen (middle) and hippocampus (right). Possible times for the interval to end are represented by light grey (short) and dark grey (intermediate) dashed vertical lines. Results are displayed in a time-by-time matrix, each data-point is the discriminability accuracy between $t(x)$ and $t(y)$. Accuracy scores ranged from 0.5 to 1. Chance level is defined at 0.6. The temporal resolution is the window within the diagonal between black lines (chance level).

D. Chapter 2. Parallel absolute and relative codes in the striatum

Felipe Rolando¹, Tadeusz Kononowicz^{1,2}, Jean-René Duhamel¹, Valérie Doyère² and Sylvia Wirth¹

¹ Université de Lyon, CNRS, Institut des Sciences Cognitives Marc Jeannerod (UMR 5229), 69500, Bron, France.

² Université Paris-Saclay, CNRS, Institut des Neurosciences Paris-Saclay (NeuroPSI), 91190 Gif-sur-Yvette, France.

D.1. Abstract

Many of our behaviours in daily life follows temporal flexibility, allowing us to quickly adapt to the environment: this temporal scalability is related to the expectancy of an external event, or to an internal state to reach. It is triggered by a future event. The neural patterns allowing such scalability have been found in many brain regions, including the striatum and the hippocampus. On the contrary, absolute neural codes for time have been rarely reported. An absolute temporal code is a neural pattern that remains stable between different time-ranges. They may arise from a sensitive external cue, following feedforward process, and be triggered by a past event. We recorded single cells activity in the striatum and the hippocampus in two monkeys as they performed an ongoing time categorization task, across several time-ranges. We highlighted the fact that in the striatum (caudate and putamen), two sub-populations of neurons were well established: an absolute and a relative one. In the hippocampus, neurons remap in a way that did not follow these categories. Within the striatum, we showed that in caudate, both subpopulations adapted when durations were multiplied or halved, while putamen showed only partial adaptation. Finally, we showed when the entire caudate population is considered, the neural activity is maintained during first second between 2 time-ranges with a pattern consistent with a feedforward mechanism over time. This suggests, for the first time, the presence of a strong absolute code for time in the macaques caudate.

D.2. Introduction

The sensation that time passes slowly or faster depending on context is a feeling familiar to all of us. How do we measure time passing between two events? Do we use a universal clock fitting all events or do we rescale that clock depending on context? Whether there is a relative or an absolute code for time in the brain is therefore a legitimate question to ask. Many studies reported scalable patterns of neural activity between different temporal contexts in rodents (Shimbo et al., 2021; Zhou et al., 2020; Mello et al., 2015; Emmons et al., 2017) and monkeys (Meirhaeghe et al., 2021; Wang et al., 2018) in cortical regions, striatum and hippocampus. Relative codes are efficient because they allow quick adaptation and save energy by relying on pre-existing circuits. Such adaptive neural code could support behavioural scalability observed in animal timing intervals from second-to-minute scale (Gibbon et al., 1984; Gibbon, 1977). However, temporal absolute codes have also been reported in rodent's hippocampus timing tens of seconds (MacDonald, Lepage, Eden, & Eichenbaum, 2011), and lately, stable hippocampal activity was observed for two different 10s periods (Sabariego et al., 2019). Thus, absolute codes would allow a temporal representation that does not depend on the contexts nor tasks. For example, such a code may be suitable to recall events order or duration in retrospect. Here, asked how neural activity in the striatum and the hippocampus adapts to rescaling of intervals reduced from second to sub-second range, or increased from second to several seconds. We used a duration categorization task, which allows to compare the patterns of neuronal activity for the same duration shifting from intermediate to short or long.

D.3. Results

D.3.a. Behavioural results indicate a context dependant categorization of the durations

If a well-known duration is represented as an independent stimulus like an object, then it should be identified with the same accuracy regardless of its temporal context. We trained two rhesus macaques to perform a 3-intervals categorization task (Figure 1A) across multiple sets at different time ranges (Rolando et al., *submitted*). Durations varied across sets presented in block of 80 trials, thus, sets can be seen as temporal contexts. The sets varied from sub-second range (0.25-0.5-1s respectively for short, intermediate and long durations), second range (0.5-1-2s), supra-second-range-1 (1-2-4s) and surpa-second-range-2 (2-4-8s). Thus, some durations (*i.e.* 0.5, 1, 2 and 4s) were presented at multiple time ranges and had to be categorized either as short, intermediate or long in function of the set (Figure 1B). In other words, the same duration was the short one, the intermediate one, or the long one depending on the time range. Thus, if the categorization of duration T is context independent, it will be identified as T in any set without any difference in performance. Conversely, if the classification is context dependent, it will not be identified as T with the same accuracy as a function of the set (temporal context). To test if the temporal context influenced the categorization of the durations, we computed a General Linear Mixed-Effects (GLME) model (see Methods) testing for behavioural accuracy as a function of Interval identity. We found that 0.5, 2 and 4s were not identified with the same accuracy depending on time ranges (Figure 1C). The 0.5s duration was better discriminated when it was short than when it was intermediate ($t(16173)=-15.485$, $p<0.0001$), while 2 and 4 seconds were best identified when they were defined as long than intermediate ($t(18735)=28385$, $p<0.0001$ for 2s and $t(8844)=35.258$, $p<0.0001$ for 4s). The 2s duration was also best categorized as long than short ($t(18735)=27.09$, $p<0.0001$) and intermediate than short ($t(18735)=2.1395$, $p=0.0324$). On the other hand, the 1s duration was better discriminated when it was intermediate ($t(21400)=9.2981$, $p<0.0001$) compared with short, $t(21400)=9.0546$, $p<0.0001$ compared with long), with no difference between short and long labels ($t(21400)=1.01162$, $p=0.30957$). Overall, these results suggest that the categorization of a duration is dependent on the temporal context. As monkeys performed the task, we recorded neural activity in the striatum (caudate-putamen) and hippocampus.

D.3.b. Classification of absolute and relative neurons across different time-ranges

To examine neural activity, we recorded single-cells while animals classified intervals in multiple time ranges. Monkeys were tested separately in blocks of “retiming-to-short” condition and “retiming-to-long” conditions (Figure 1B). In retiming-to-short condition, they always first discriminated the durations at the second range (0.5-1-2s), and after n trials (around 100), the durations were halved with no external cue: monkeys started discriminating durations at the sub-

second range and adapted by trial-and-error. Days when monkeys were performing retiming-to-short condition, they were only tested on retiming-to-short condition. Then, on alternate days, monkeys were tested on retiming-to-long conditions. During these blocks, monkeys discriminated durations at the second range, then they were tested at the supra-second-1 range (durations were multiplied by 2, after n trials), and then at the supra-second-range-2 (durations were multiplied by 2 another time, after n trials). For some sets, monkeys were tested in the retiming-to-long but the recording session started from supra-second-range-2 (2-4-8s) and went to second range (0.5-1-2s) by halving the durations 2 times. This design allows us to characterize neural activity between different temporal context. Although, it restrained our analysis as no neurons were recorded from sub-second range to supra-second ranges: neurons in retiming conditions are always compared to the second range condition. First, we selected the neurons that kept a stable baseline between sets (see Methods) and asked which pattern they displayed when the durations to-be-timed changes: an absolute pattern, with no change of their discharge rate between sets, or a relative pattern, characterized by a modulation of their discharge rate relative to the long interval of each set.

Next, among neurons with stable baseline, we identified time-modulated (TM) cells as the ones displaying a pattern of activity modulated by the time within the interval during at least one of the two sets using the same method as described previously (Rolando et al., *submitted*, see Methods). During retiming-to-short condition, there was 87 neurons defined as TM cells in caudate, 48 in putamen and 32 in hippocampus. At the retiming-to-long-1 condition, 45, 47 and 35 neurons were defined as TM cells with stable baseline respectively in caudate, putamen and hippocampus, and 27, 40 and 23 in the retiming-to-long-2 condition (see Table 1). Then, to classify the neurons as relative or absolute, we followed two different methods: a method based on the centre of mass (CoM) of the neurons at different ranges, inspired from a previous study (Mello et al., 2015), and a method based on the correlation between activity at different ranges.

First, we computed three temporal CoM of the neurons (Figure 2A): 1) on the longest interval of the shortest range between the two ranges to compare (reference in red in Figure 2A); 2) on its twin duration during the longer range, *i.e.* the intermediate interval of the longest duration (light grey in Figure 2A); 3) on the long interval of the longest duration (black in Figure 2A). These measures were computed for all comparisons from second to sub-second and from second to supra-second ranges (Figure 1B), yielding a relative and an absolute comparison for each cell (Figure 2A, supplementary Figure 1 for retiming-to-long-2 condition). Then, for each cell, we computed two ratios using the CoM from each of these durations: the relative ratio (RR) and the absolute ratio (AR, Figure 2A, see Methods). We classified neurons as relative when the relative ratio was closer to 1 compared to the absolute ratio: it reflected a smaller change of the position of the CoM between the reference and the longer duration. Neurons were classified as absolute when the opposite was true (see Methods). Figure

3A-I, left panels, shows the distribution of a relative/absolute index computed on the ratios (see Methods). All the distributions of the relative/absolute indexes were centred on 0. Consistently, the proportions of relative and absolute neurons were equal in all structures at all ranges (Table 1), except in caudate at retiming-to-long-2 conditions where relative neurons were more abundant ($\chi^2(1,2)=8.33$, $p=0.0039$) and in hippocampus at retiming-to-short, where absolute neurons were more abundant ($\chi^2(1,2)=8$, $p=0.0047$).

As the classification using CoM is new, we validated it by comparing correlation computed on rate scaled in a relative or absolute way. Figure 3A-I, right panels, represent the two correlation coefficients for each cell, labelled with a symbol representing its previously identified classification obtained with the CoM method: relative (square) or absolute (diamond). Then, we computed the distances of each neuron to the diagonal. A measure of 0 represents the case in which there is no difference between relative and absolute coefficients. To validate classifications made earlier, we tested if the distances to the diagonal per each subpopulation previously identified were different from 0 (1-sample T-test, see Methods and supplementary results). If the mean distance of the subpopulation was shifted, the direction of the shift (positive or negative) indicated if the subpopulation has higher relative coefficients or higher absolute coefficients. Overall, caudate relatives' codes were consistent in all the retiming conditions, while absolute codes were confirmed by both methods in retiming-to-short and retiming-to-long-1 condition. For putamen, both methods indicate that relative codes in retiming-to-short condition are not strong, but absolute codes were. In the hippocampus, the classification of absolute and relative neurons was not confirmed by the correlations, in any retiming condition (Figure 3). Altogether, these results show strong absolute and relative codes in caudate at retiming-to-short and retiming-to-long-1 conditions. In putamen, absolute codes seem better established than relatives' ones at retiming-to-short and retiming-to-long-1 condition. In the hippocampus, remapping was not consistent with an absolute or a relative neural pattern. In sum, only caudate exhibited neurons that showed convincing patterns of relative or absolute code.

D.3.c. Caudate adaptation to contexts can be explained by a shift in the centre of masses

We used only striatal and putamen neurons identified with the CoM classifications, as these populations were cross-validated by the correlation methods. Therefore, we excluded the retiming-to-long-2 condition as the categorization to absolute or relative cells did not pass the cross-validation threshold. Next, we asked whether either class of absolute or relative neurons in the caudate or putamen scaled better. We fitted a linear model on each subpopulation of neurons in each brain area separately: explained variable was the centre of mass of the reference duration (CoM-R) on the y-axis and explanatory variables were either centre of mass on the intermediary duration of the longer set (CoM-A) or centre of mass in the longer duration (CoM-Long) on the x-axis (Figure 4A-D, see Methods

and supplementary results). Next, we tested differences in the absolute or relative fits across brain areas and sets by comparing the distances of the slopes obtained from each iteration from the leaving-one-out method in the relative subpopulations, to the hypothesized slope 1 or to the hypothesized slope 0.5 respectively for the absolute and the relative population. We tested the effect of brain region and retiming condition with a 2-way ANOVA. In the absolute condition, we found that caudate slopes were significantly closer to the theoretical model compared to the putamen ($F(1,101)=151.99$, $p<0.0001$) and closer to theoretical model for the retiming-to-short than the retiming-to-long-1 condition ($F(1,101)=600.55$, $p<0.0001$). The interaction revealed that there was no difference between conditions in caudate, but neurons in putamen were closer to theoretical model in retiming-to-short than retiming-to-long-1 condition ($F(1,101)=83.62$, $p<0.0001$). In the relative subpopulations, slopes in the caudate were closer to the theoretical model than putamen ($F(1,108)=28.87$, $p<0.0001$). Further, data was closer to the theoretical model in the retiming-to-long condition ($F(1,108)=513.05$, $p<0.0001$). Nonetheless, caudate fits to theoretical models did not differ between conditions (retiming-to-short or retiming-to-long-1), but putamen followed the theoretical model better for retiming-to-long-1 condition ($F(1,108)=5.62$, $p=0.0195$). Altogether, these results show that caudate slopes fitted the hypothetical model whether the monkey retimed to short or long for both absolute and relative slopes. This was not the case for putamen: absolute neurones adapted better when the monkey retimed to long, but relative neurones retimed better the monkey retimed to short. Therefore, this suggest that caudate adapt their rates when retiming to long or short, while putamen neurones adapted only partially.

D.3.d. Caudate population activity between sets correlates stronger with an absolute pattern when time is rescaled down

In this section, we tested population-based representation of time to examine adjustments at the global level between relative and absolute populations. We focused on neurons identified in the caudate, because we showed that this region rescaled better during retiming. We concentrated the analysis on the condition in which animals retimed to short because there was sufficient neurons to carry the analysis ($n=87$). To display the neural populations, we sorted the neurons by their maximal activity during the reference duration (1s-long at the sub-second range), and aligned the neurons following the same sequence, in 1s-intermediate and 2s-long at second range. We did this for each subpopulation separately, and then for all the neurons together (Figure 5A-C). Then, for each subpopulation, we correlated the neural activity between 1) the reference duration versus its twin duration for absolute comparison and 2) the reference duration and the long duration for relative comparison, after z-scoring the activity within each interval separately, and obtained the correlations

matrices (Figure 5D-E, top row). To test whether the correlations results matched our subpopulations classifications, we compared the correlations coefficients of the significant positive correlations between the two correlations matrices (Figure 5D-E, bottom left). We found that the activity at 1s-long was more correlated with the activity at 1s-intermediate than at the 2s-long for the absolute subpopulation (2-sample T-test, $t(10908)=-36.3098$, $p<0.0001$, Figure 5D bottom left). Conversely, we found that for relative population, the reference duration was more strongly correlated with the longer duration (2-sample T-test, $t(11212)=27.7316$, $p<0.0001$, Figure 5E, bottom left). Thus, taken separately, the subpopulations activity matched our single-cells' classification. Then, we asked where were the time-points strongly correlated with each other. To this end, we quantified the significant and positive correlations, over time (Figure 5D-E, bottom right). As one could imagine, most of the positive correlations from the absolute populations were distributed within the first second. The number of time-points correlated with each other increased as the time gets closer to the end of the 1s. For the relative sub-population, activity during the 1s-long (reference) was highly correlated with the first half and the end of the 2s-long (longer duration), but the middle of the interval between both durations was not. This shows that the relative patterns of the neurons were explained by a maintained activity at the beginning and the end of the intervals. Then, we asked which pattern was followed by the entire population, when all neurons were put together (Figures 5C and 5F, top row). When comparing the correlations coefficients, the 1s-long duration was more correlated with the 1s-intermediate duration (absolute) than with the 2s-long (relative) as shown in Figure 5F, bottom left (2-sample T-test, $t(10982)=-13.6449$, $p<0.0001$). This suggests an overall stability of the neural activity within the first second between sets. In addition, we observed that within the first second many time-points were correlated with each other, and this count decreased to zero after the end of the first second. Although, time-points were correlated with each other also at the end of the durations (Figure 5F, bottom right). Thus, caudal activity maps the first second, and the end of the intervals.

D.3.e. Caudal population activity is maintained between 1 and 2 seconds

Can the neural activity from one temporal context be decoded with a model based on the neural activity in the other temporal context? To answer this question, we used a multiclass decoder (see Methods) that we trained on neural activity when animals retimed from the sub-second range to the second range. As a control, we first trained the decoder on the reference duration, 1s-long, and cross-validated the decoding on the same trial types to control that there was no difference when training and testing from relative and absolute subpopulations (2-sample KS-test, $k=0.12$, $p=0.4431$). Then, we tested the decoder for absolute retiming on the 1s-intermediate of the longer duration and for relative retiming on the full 2s-long duration (following the scheme presented in Figure 6A). Each one of these durations was divided into 100 bins (see Methods). Thus, for 1s-intermediate, tested and

trained durations were equal in an absolute scale. On the other hand, for 2s-long, tested and trained durations were equal in a relative scale: one bin from 2s-long is twice the duration than a bin from 1s-long. We computed decoding in both subpopulations separately (Figure 6B-C, left panels). To test the acuity of the decoding, we compared the distances between predicted time in absolute and relative comparisons (blue and pink lines respectively) to predicted time from the reference (grey line) (Figure 6B-C, left panels). We tested the effect of population type (absolute or relative neurons) and retiming type (absolute or relative comparisons). Consistent with their classification, in absolute neurons, there was no difference in decoding 1s in the absolute comparison (2-sample KS test, $k=0.16$, $p=0.14$) but there was a difference in the relative comparison (2-sample KS test, $k=0.25$, $p=0.003$, with Bonferroni correction, Figure 6B, right panel). In relative neurons, there was a difference in the absolute comparison (2-sample KS test, $k=0.36$, $p<0.0001$, with Bonferroni correction) and in the relative comparison (2-sample KS test, $k=0.22$, $p=0.0131$, with Bonferroni correction). The results suggest that the absolute population is very stable in the first second whether across sets, while in the relative population, the adaptation of neural activity in a relative scale is less accurate.

Next, we focused on the results obtained from the entire populations. We selected the time-points decoded above chance (see Methods) when testing decoding for absolute code (training on the reference interval and testing on first half of the longer interval: 1s-intermediate (in blue in Figure 6E) and when testing for relative code when training on reference set and testing on the whole length of the longer interval (in pink in Figure 6F). Then, we plotted these points together with the decoding obtained when training and testing with the identical reference duration (in grey in Figures 6E-F). The performance above chance overlapped in absolute comparison (Figure 6E), but not in relative comparison (Figure 6F).

At each predicted time-point, we calculated the maximum value of the predictions obtained from real-time (see Methods), and compared it between absolute or relative predictions. We show that maximal predictions did not differ between absolute comparison (reference 1s-long vs 1s-intermediate, 2-sample KS-test, $KS=0.14$, $p=0.2606$, Bonferroni correction), but differed between relative comparisons (1s-long versus 2s-long, ($KS=0.22$, $p=0.0131$). Finally, we tested whether the maximal predictions were close to real time. We tested each distribution versus zero (black line in Figure 6G, 1-sample T-test). The distribution for the control decoding (1s long on 1s long), had a mean equal to 0: the maximal predictions were distributed around real time and decoding performance was convincing ($t(99)=-1.4632$, $p=0.1416$). For absolute comparisons (blue on Figure 6G), the maximal predictions were estimated above real-time, ($t(99)=7.3516$, $p<0.0001$) with a confidence intervals ($CI=[2.5626\ 4.4574]$) showing that during the first half of the longer interval, time was overestimated in average between 2 and 4 timepoints compared to 1s-long. On the contrary, in the relative comparison, time was underestimated when the decoding was tested on the whole 2s-long duration

(pink in Figure 6G, CI=[-12.1317 -7.8683], $t(99)=-9.3083$, $p<0.0001$). Overall, the decoding results show that subpopulations correctly decoded time in an absolute or a relative way respectively, which means that from a set to the other, the same pattern of neural activity was observed either by maintaining the neural activity or by downscaling it. Further, we showed that performance above chance computed on the entire population matched better an absolute rather than a relative decoding. When tested in a relative comparison, decoder tended to largely underestimate time, but on the contrary, it tended to overestimate time only slightly when tested in the absolute comparison. These results reveal underlying a dynamic that could reflect an absolute way to map time triggered by feedforward processing following the beginning of the trial (dotted line in Figure 6F).

D.4. Discussion

The first question we asked was whether monkey's time categorizations were contexts dependent or not. Our results show that temporal categorization is indeed context dependent: an interval is categorized with more or less difficulty as a function of its relative position in different time ranges. For example, the 2s interval is more easily categorized as the longest in a short time range than as the shortest in a long time range. Indeed, in line with this, we showed previously that the intermediate interval was increasingly less well discriminated with increasing time across sets (Rolando et al., *submitted*). These results suggest that monkeys map the individual intervals using short-intermediate-long mapping according to the temporal context, and that neural activity may follow a relative rather than an absolute rescaling as a function of time.

What then happens at the neural level? One possibility is that a neuron maintains the same discharge pattern between two temporal contexts, or that its discharge rate follows the structure of the task, and adapt its rate accordingly, as it has been shown in fixed-interval procedures (Zhou et al., 2020; Emmons et al., 2017 ; Mello et al., 2015), temporal discrimination tasks (Shimbo et al., 2021) and time-productions (Meirhaeghe et al., 2021). To test this, we used two different metrics in the caudate, putamen and hippocampus to compare absolute or relative adaptations. First, our results show that caudate displays relative temporal codes across all the time ranges. Previously, caudal activity was shown to scale durations in a temporal production task at the second range (Wang et al., 2018). Our results bring evidences that caudal activity may scale time during a categorization task at longer ranges too (Figure 4). In addition, we are also the first reporting absolute temporal codes in caudate, from 1s to 4s categorizations, during a timing task. In contrast, putamen neurons display absolute codes at all the retiming conditions, and relative codes at the retiming-to-long conditions. However, despite the presence of absolute or relative adaptations in the putamen, caudate adaptation was much stronger than putamen. In the hippocampus, the classification we performed were inconclusive, suggesting that neurones did not present neither patterns that were maintained across retiming, nor patterns that adapted across retiming.

Then, we focused on the striatal activity, and asked whether at the populational level, neurons from relative subpopulations scaled their activity by adjusting their center of masses, and whether the neurons from the absolute populations did not. We showed that neurons from caudate matched our expectations very closely, at both ranges, while putamen neurons did not. Although, even if both structures, caudate and putamen, showed absolute and relative patterns of activity at the single-cell level; at the populational level, the CoM is a relevant measure for caudate neurons only. This result indicate that caudate TM-cells can be divided into two different subpopulations: absolute ones and relative ones.

Finally, we examined further neural activity in the caudate, as it consisted of a sufficient number of neurones. We aimed to understand the dynamics of population activity when animal retimed from 2s to 1s and asked which one of absolute or relative pattern during remapping drives the neural code in the entire population. Using decoding methods, we have shown that a decoder trained on a reference duration can decode the corresponding duration taken from a longer set. This is in favour of an absolute code across sets. We showed that when we trained a decoder on a reference set, and tested it on a longer duration adapted to match relatively the reference duration, decoding was poor and underestimated time. This was also in favour of the absolute code driving the neural population and shows that caudal activity is captured within the first second in an absolute way. In addition, via the cross correlations and the decoding, we show that the end of the duration only is captured in a relative way. The results suggest a two steps recruitment within the interval: an absolute forward processing at the start of the interval maintained throughout different set durations, followed by a relative recruitment, which may correspond, to a temporal backwards discounting anticipating the end of the trial. Our results suggest that these two populations span the entire duration at short range, while they become gradually disconnected as duration increased.

In conclusion, we reported for the first-time evidence that absolute patterns of neurons drive the primates' caudate nucleus in a feedforward process.

D.5. Methods and supplementary results

D.5.a. Baseline comparison across sets

To compare the baseline between sets, we focused on the inter-trial-interval activity, which lasted 800ms. The neural activity during baseline was cut into 100 equal time-bins. First, we computed the standard deviation of the baseline activity during the reference set after convolution (sub-second range in retiming-to-short condition, second range in retiming-to-long conditions). Next, we tested at each time-point of the baseline, if inter-trial-activity during retiming condition at time t did not differ from activity at time $t \pm 2$ standard deviations from the reference set. A neuron with an equal activity during 66% of the inter-trial interval was defined as having a stable baseline.

D.5.b. Behavioural analysis

To test if durations categorization were influenced by temporal context, we tested a General Linear Mixed-Effect (GLME) model following the formula:

$$\text{Accuracy} \sim \text{Interval identity} + (1 | \text{Monkey}) + (\text{Monkey} | \text{Block})$$

where Accuracy follows a binomial distribution coding for correct categorization and errors, Label is a fixed categorical factor, and Monkey and Block are random factors respectively categorical and numerical. Note that for 0.5 and 4s, Interval had only two modalities, respectively “short” or “intermediate” (0.5s was never defined as long), and “intermediate” or “long” (4s was never defined as short). Interval had three modalities for 1 and 2s: “short”, “intermediate” or “long”. Thus, each duration, 0.5, 1, 2, and 4 seconds, was tested separately. 16175 trials were tested for 0.5 interval, 21403 for 1s interval, 18738 for 2s interval, 8846 for 4s interval.

D.5.c. Relative and absolute patterns defined by the centre of masses

To define if a neuron displayed an absolute or a relative pattern of discharge rate during retiming conditions, we computed the temporal centre of masses (CoM) according the formula:

$$\text{CoM} = \frac{\sum_{i=1}^{100} x_i \times t_i}{\sum_{i=1}^{100} x_i}$$

where x_i is the activity of the neuron at time t_i . We adapted this method from a previous study (Mello et al., 2015). This previous study computed the CoM on two different durations: a reference duration (CoM-R) and a longer duration (CoM-L). Although, by definition the CoM of a neuron will always be pulled towards the centre of an interval, thus the relation CoM-R/CoM-L will always tend to the ratio: reference duration by long duration. Thus, we added a condition in which we also computed the CoM-A, which is the CoM in the absolute comparison: CoM-A is the centre of mass calculated after cutting the long duration of the longer set to be the same size as the reference one. To summarize, for each neuron, we are interested in the activity during 1) the reference duration 2) the longer duration of the

condition, and 3) the duration of the reference obtained by cutting the longer duration in an equal length of the reference. For example, in retiming-to-short condition, the reference duration is 1s-long at the sub-second range, so the twin duration is 1s-intermediate at the second range. Long duration is 2s-long at the second range. In retiming-to-long condition, the reference duration is 2s-long of second-range discrimination. The twin durations are 2s-intermediate or 2s-short and the long durations are 4s-long and 8s-long respectively from supra-second-1 and supra-second-2 ranges. In conclusion, per each neuron we computed 3 CoM: the reference CoM-R, the twin CoM-A and the long CoM-L. The CoM were calculated on the post-stimuli time histogram (PSTH) of neural activity, obtained by cutting the duration into 100 time-bins (time-bins size was different between durations, 10ms for 1s, 20ms for 2s, 40ms for 4s, and 80ms for 8s), and smoothing it with +/- 4 bins. Then, the CoM are used to compute the absolute ratios (AR) and the (RR) relative ratios such that

$$AR = CoM-R / CoM-A$$

and

$$RR = CoM-R / CoM-L$$

Finally, the neuron was defined as relative if the RR was closer to 1 than the AR, as illustrated by

$$|1-RR| < |1-AR|$$

or as absolute if the absolute ratio was closer to 1 than the relative ratio, illustrated by

$$|1-RR| > |1-AR|$$

Then, we compared the distances, $|1-RR|$ and $|1-AR|$, for each subpopulation separately, and for all the structures at all ranges. These comparisons show that at the sub-second range, as expected, relative ratios were closer to one for caudate (1-sample T-test, $t(39)=-6.56$, $p<0.0001$) and hippocampus ($t(7)=-2.74$, $p=0.0288$); but not for putamen ($t(20)=-1.72$, $p=0.1012$). This means that using this classification, relative ratios (RR) from relative putamen neurons did not differ from their absolute ratios (AR) and thus, putamen relative neurons did not show strong relative codes at the retiming-to-short condition. For absolute neurons, as expected, absolute ratios were smaller than relative ones for all the structures (1-sample paired T-test, $t(46)=9.28$, $p<0.0001$ for caudate, $t(16)=4.37$, $p=0.0005$ for putamen, $t(23)=4.91$, $p=0.0001$). In both retiming-to-long conditions, the hypothesis that relative subpopulations had relative ratios closer to one than their absolute ratios, and the opposite assumption for the absolute neurons (absolute ratios closer to one than their relative ratios), was verified (1-sample paired T-test, at retiming-to-long-1: $t(27)=-6.61$, $p<0.0001$ for the relative subpopulation in caudate, $t(16)=4.32$, $p=0.0005$ for the absolute subpopulation in caudate, $t(22)=-2.6451$, $p=0.0148$ for the relative's neurons in putamen; $t(23)=6.22$, $p<0.0001$ for the absolute ones, and $t(17)=-3.45$, $p=0.0031$ for the hippocampal relative subpopulation; and $t(16)=5.86$, $p<0.0001$ for the absolute one; and at retiming-to-long-2, $t(20)=-5.06$, $p=0.0001$, for the caudate' relative subpopulation, $t(5)=3.83$, $p=0.0123$ for the absolute one, $t(22)=-5.67$, $p<0.0001$, for the relative

subpopulation of putamen and $t(16)=4.35$, $p=0.0005$ for the absolute one and $t(14)=-4.51$, $p=0.0005$ for the relative population in hippocampus and $t(7)=3.11$, $p=0.017$ for its absolute one.

Finally, we computed the relative/absolute ratio per each cell following the formula:

$$(AR-RR) / (AR+RR)$$

We displayed the distributions of the relative/absolute ratios in Figure 3, per each structure in each retiming condition.

D.5.d. Relative and absolute patterns defined by the correlations

Because our method to defined absolute and relative neurons is new, we tested a second method by correlating the neuron's activity between the different durations. A similar method has already been used previously (MacDonald et al., 2011). First, we correlated the neural activity between reference and twin durations using Spearman correlation (the absolute correlation), and obtained the absolute rho (r_{abs}). Then, we correlated the neural activity between reference and long duration to get the relative rho (r_{rel} , relative correlation). The two correlations were computed per each neuron. Then, we calculated the distance D of each data-point P, defined by two coordinates r_{abs} and r_{rel} , to the diagonal, representing the hypothesis $r_{abs}=r_{rel}$, following the formula

$$D = (r_{rel} - r_{abs}) / \sqrt{1^2+1}$$

Negative values indicated a higher shift to the left of the diagonal, positive values a shift to the right. Then we tested, for each subpopulation obtained from the CoM method, if the distances to the diagonal differed from 0 (1-sample T-test). If the distances were significantly negative, it meant that the subpopulation had, overall, higher relative coefficients. This pattern is expected for the relative subpopulations. Otherwise, if the distances were significantly positives, it meant that the subpopulation had, overall, higher absolute coefficients. This pattern is expected for the relative subpopulations. In caudate (Figure 3A, D, G), the classification of absolute and relative neurons hold at retiming-to-short and retiming-to-long-1 conditions ($t(39)=-4.3032$, $p=0.0001$; and $t(27)=-2.5012$, $p=0.0187$ for relative neurons respectively for each condition, and $t(46)=7.1538$, $p<0.0001$; and $t(16)=3.2866$, $p=0.0046$ for absolute ones). In retiming-to-long-2, only relative neurons were confirmed ($t(20)=-3.10$, $p=0.0056$, and $t(5)=-0.86$, $p=0.4310$ for absolute neurons. For putamen (Figure 3B, E, H), relative neurons were not correctly classified at the retiming-to-short condition ($t(20)=-0.2950$, $p=0.77106$), but absolute neurons were ($t(16)=5.17$, $p<0.0001$). At the longer retiming conditions, the classifications of the neurons was confirmed by the correlation method ($t(22)=-3.1231$, $p=0.0049$ and $t(22)=-2.752$, $p=0.0116$ for the relative populations at retiming-to-long-1 and -to-long-2 conditions; and $t(23)=4.2325$, $p=0.0003$ and $t(16)=2.207$, $p=0.0422$ for the absolute populations). In hippocampus (Figure 3D, F, I), none of the subpopulations was confirmed in any condition (at the retiming-to-short condition, $t(7)=0.4015$, $p=0.7$ for relative neurons, and $t(23)=1.641$, $p=0.1144$, for

absolute neurons; at retiming-to-long-1, $t(17)=-0.5910$, $p=0.5622$ for relative neurons and $t(16)=1.54$, $p=0.1426$ for absolute neurons, and at retiming-to-long-2, $t(14)=-1.048$, $p=0.3120$ for relative neurons and $t(7)=1.49$, $p=0.1887$ for absolute neurons).

D.5.e. Leaving-one-out method for linear regression

To test whether the CoM at the reference duration was linearly explained by the COM at the twin or long durations, we computed a linear regression on the different subpopulations of neurons testing two models. The relative model tested on relative neurons was defined by

$$\text{COM-R} \sim a \times \text{COM-L} + b$$

and the absolute model tested on absolute neurons was defined by

$$\text{COM-R} \sim a \times \text{COM-T} + b$$

For caudate neurons, regressions computed on each subpopulation at each retiming condition showed slopes close to the theoretical values ($a=0.9702$, $p<0.0001$, $a=1.0390$, $p=0.0013$ for absolute neurons in retiming-to-short and retiming-to-long-1 condition; and $a=0.4602$ and $a=0.4712$ respectively for retiming-to-short and retiming-to-long-1 in the relative subpopulation, $p<0.0001$ for both conditions). For putamen neurons, regressions were also significant but further away from theoretical model ($a=0.8677$, $p<0.0001$, and $a=1.2765$, $p=0.0011$ for absolute subpopulations respectively in retiming-to-short and retiming-to-long-1 condition; $a=0.6283$, $p=0.0001$, $a=0.3984$, $p=0.0002$, for relative neurons in the retiming-to-short and retiming-to-long-1 condition). Then, to test if within the same population there was a difference between relative and absolute model, we computed N-1 times the regression analysis on each subpopulation of N neurons. Each time, a different neuron was left out of the analysis. Then, we tested the N-1 slopes obtained from each model within the same subpopulation using 1-sample paired T-test.

D.5.f. Populational correlations

To test whether the neural activity between a temporal context to the other was correlated, we tested the correlation of the activity at the populational level. The population is ordered in an N-by-T matrix, where N are the neurons and T are the times. For correlations, durations were cut into 10ms bins and smoothed by +/- 4 bins. For example, a 1s- duration was displayed in a N-by-100 matrix and a 2s- duration was displayed in a N-by-200 matrix. Each neuron was z-scored in function of its activity during the interval of interest: either 1s-long, 1s-intermediate or 2s-long. Then, the vector from the reference matrix at t_1 was correlated with all the vectors of the other matrix, from t_1 to t_T . The reference duration was correlated versus the twin duration and the longer duration. Next, we extracted the correlations coefficients of the significant positive correlations from each matrix output,

and compared the distribution of these coefficients using 2-sample T-test in the aim to determine whether a matrix was more correlated with the reference duration than another. Finally, we represented for each time-point of the tested duration, either twin or long, the number of time-points from the reference duration that were positively correlated with. This indicates whether the correlations of the two matrices differed, and where they differed.

D.5.g. Temporal multiclass decoding

In addition of the correlations, we tested at the retiming-to-short condition, whether the activity from the 1s-long was similar enough of the 1s-intermediate or 2s-long durations. In other words, we asked whether 1s-intermediate or 2s-long could be decoded in function of the activity of 1s-long. We trained an Error-Coding Output Codes (ECOC) model on the z-scored post-stimuli time histogram of neural data following the same procedure as for the CoM computations in order to obtain, for each neuron, a 100 bins vector of its neural activity. The model was trained on 15 trials of the reference duration (1s-long), and tested on 5 different trials for 1000 iterations. Thus, after a decoding iteration, the output was a trial-by-time matrix, in our case is a 5-by-100 matrix. Once the 1000 iterations were completed, all decoding outputs were obtained on a 5-by-100-by-1000 array. Then, the same model was also tested on the 1s-intermediate and 2s-long durations. To compare the distances from predicted-time to real-time, the decoding output was averaged across trials. Next, to define the chance level by performing the same decoding analysis after shuffling the labels during training phase and decoding phase on the reference duration. From the 5-by-100-by-1000 matrix obtained by chance, we multiplied the 95th percentile of the distribution by 1.5 to define the chance-level. Chance-level value was 94.5. Shades in Figure 6C shows all the time-points decoded above chance. Next, we wanted to know for each time-point, what was its maximal prediction. For each predicted-time t_i , we identified the maximal prediction as the real-time value for which t_i was categorized as such out of the 5000 outputs. In case of multiple maximal predictions, the maximal prediction kept was the closer to predicted-time or the first one.

D.6. Bibliography of Chapter 2

Emmons, E. B., De Corte, B. J., Kim, Y., Parker, K. L., Matell, M. S., & Narayanan, N. S. (2017). Rodent medial frontal control of temporal processing in the dorsomedial striatum. *Journal of Neuroscience*, 37(36), 8718–8733. <https://doi.org/10.1523/JNEUROSCI.1376-17.2017>

Gibbon, J. (1977). Scalar expectancy theory and Weber's law in animal timing. *Psychological Review*, 84(3), 279–325. <https://doi.org/10.1037/0033-295X.84.3.279>

Gibbon, J., Church, R. M., & Meck, W. H. (1984). Scalar Timing in Memory. *Annals of the New York Academy of Sciences*, 423(1), 52–77. <https://doi.org/10.1111/j.1749-6632.1984.tb23417.x>

MacDonald, C. J., Lepage, K. Q., Eden, U. T., & Eichenbaum, H. (2011). Hippocampal “Time Cells” bridge the gap in memory for discontinuous events. *Neuron*, 71(4), 737–749. <https://doi.org/10.1016/j.neuron.2011.07.012>

Meirhaeghe, N., Sohn, H., & Jazayeri, M. (2021). A precise and adaptive neural mechanism for predictive temporal processing in the frontal cortex. *Neuron*, 109(18), 2995-3011.e5. <https://doi.org/10.1016/j.neuron.2021.08.025>

Mello, G. B. M., Soares, S., & Paton, J. J. (2015). A scalable population code for time in the striatum. *Current Biology*, 25(9), 1113–1122. <https://doi.org/10.1016/j.cub.2015.02.036>

Sabariego, M., Schönwald, A., Boublil, B. L., Zimmerman, D. T., Ahmadi, S., Gonzalez, N., ... Leutgeb, S. (2019). Time Cells in the Hippocampus Are Neither Dependent on Medial Entorhinal Cortex Inputs nor Necessary for Spatial Working Memory. *Neuron*, 102(6), 1235-1248.e5. <https://doi.org/10.1016/j.neuron.2019.04.005>

Shimbo, A., Izawa, E. I., & Fujisawa, S. (2021). Scalable representation of time in the hippocampus. *Science Advances*, 7(6). <https://doi.org/10.1126/sciadv.abd7013>

Wang, J., Narain, D., Hosseini, E. A., & Jazayeri, M. (2018). Flexible timing by temporal scaling of cortical responses. *Nature Neuroscience*, 21(1), 102–112. <https://doi.org/10.1038/s41593-017-0028-6>

Zhou, S., Masmanidis, S. C., & Buonomano, D. V. (2020). Neural Sequences as an Optimal Dynamical Regime for the Readout of Time. *Neuron*, 108(4), 651-658.e5. <https://doi.org/10.1016/j.neuron.2020.08.020>

D.7. Figures and Legends

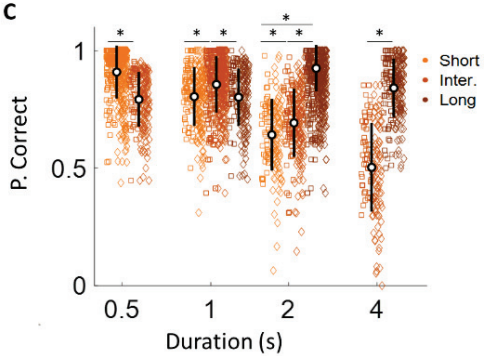
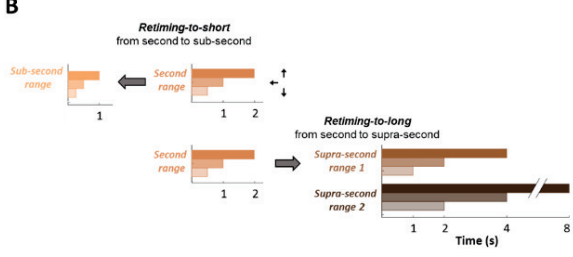
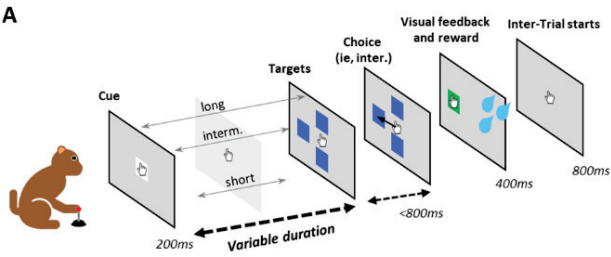


Figure 1. Behavioural task and categorization performance.

A. 3-ongoing categorization task design. Trial starts with a cue, then the screen remains dark for a short, intermediate or long interval. The end of the interval is indicated by the appearance of three targets at the bottom, left and top of the screen. Monkey moves a joystick in function of the elapsed time between cue and targets to categorize the interval: to the bottom if it is short, left if it is intermediate (example in the figure) and top if it is long. After a correct response, a reward is delivered. Inter-trial starts when the monkey returns the joystick to the centre of the screen. **B.** Time-ranges of the task. Monkeys were tested on different temporal contexts where the short, intermediate and long durations varied from a set to the other. Retiming-to-short defines the sessions where monkeys were tested on second to sub-second range. Retiming-to-long defines the sessions where monkeys were tested on second to supra-second ranges. There is two retiming-to-long-conditions: retiming-to-long-1 condition refers to the sets second and supra-second-range-1. Retiming-to-long-2 condition conditions refers to the sets second and supra-second-range-2. **C.** Probability to categorize correctly a duration in function of their relative position in the temporal context. Each duration is represented in function of its label “short”, “intermediate” or “long”. Note that there is no “long” label for 0.5s and no label “short” for 4s. Average performance for both monkeys and standard deviation are represented by the white dot and the black lines. Asterixis indicate significant differences.

	Caudate				Putamen				Hippocampus			
	Absolute	Relative	Total TM cells	<i>Total cells</i>	Absolute	Relative	Total TM cells	<i>Total cells</i>	Absolute	Relative	Total TM cells	<i>Total cells</i>
Retiming-to-short	47	40	87	153	17	21	38	152	24	8	32	261
Retiming-to-long-1	17	28	45	136	24	23	47	205	17	18	35	234
Retiming-to-short-2	6	21	27	76	17	23	40	120	17	23	40	121

Table 1.

Number of recorded time-modulated (TM) cells by-structures and sets and the number of neurons classify as absolute or relative per each retiming condition. Right column for each structure displays the total number of neurons with stable baseline for each retiming condition.

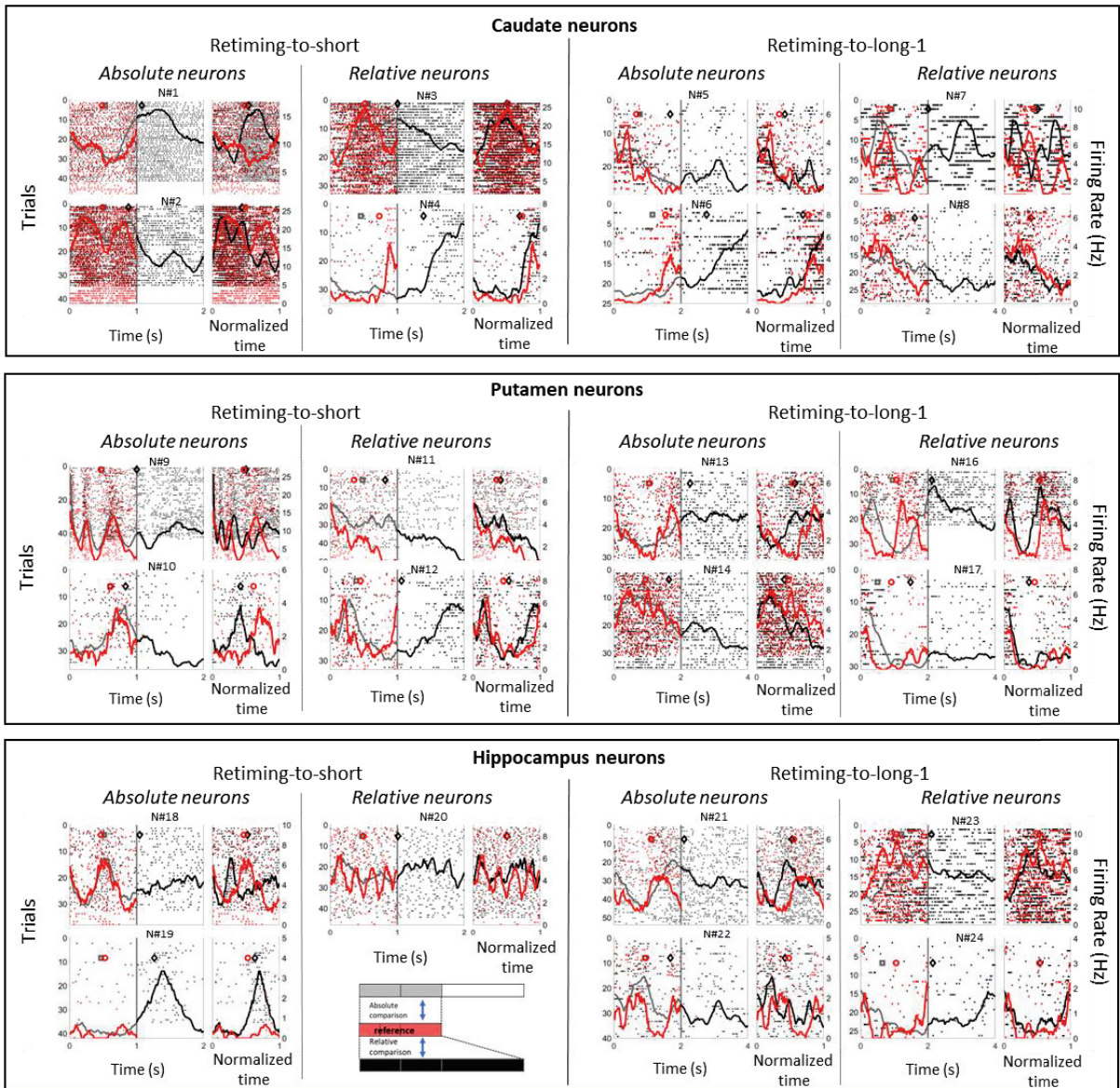


Figure 2. Single cells example for caudate (top) putamen (middle) and hippocampus (bottom).

Single cells example in the retiming-to-short condition (left) and retiming-to-long-1 condition (right). Neurons are classified as absolute or relative depending on the ratios computed on their centre of masses, indicated with red circle (reference from shorter set), grey square (intermediate duration of longer set) and black diamond (long duration of longer set). Each neuron is displayed twice. First, on an absolute scale, where all the durations are represented (grey is the first half of black and are from the same set, red is from the different set). Second, on a relative scale, where the black line is shrunk to match the red one. We show that for absolute neurons, grey and red activity are similar, and red circle and grey square are close in the absolute panel. For relative neurons, black diamond and red circle on the normalized panel are closer than red circle and grey square on the absolute panel. Bottom schemas show how the comparisons are computed.

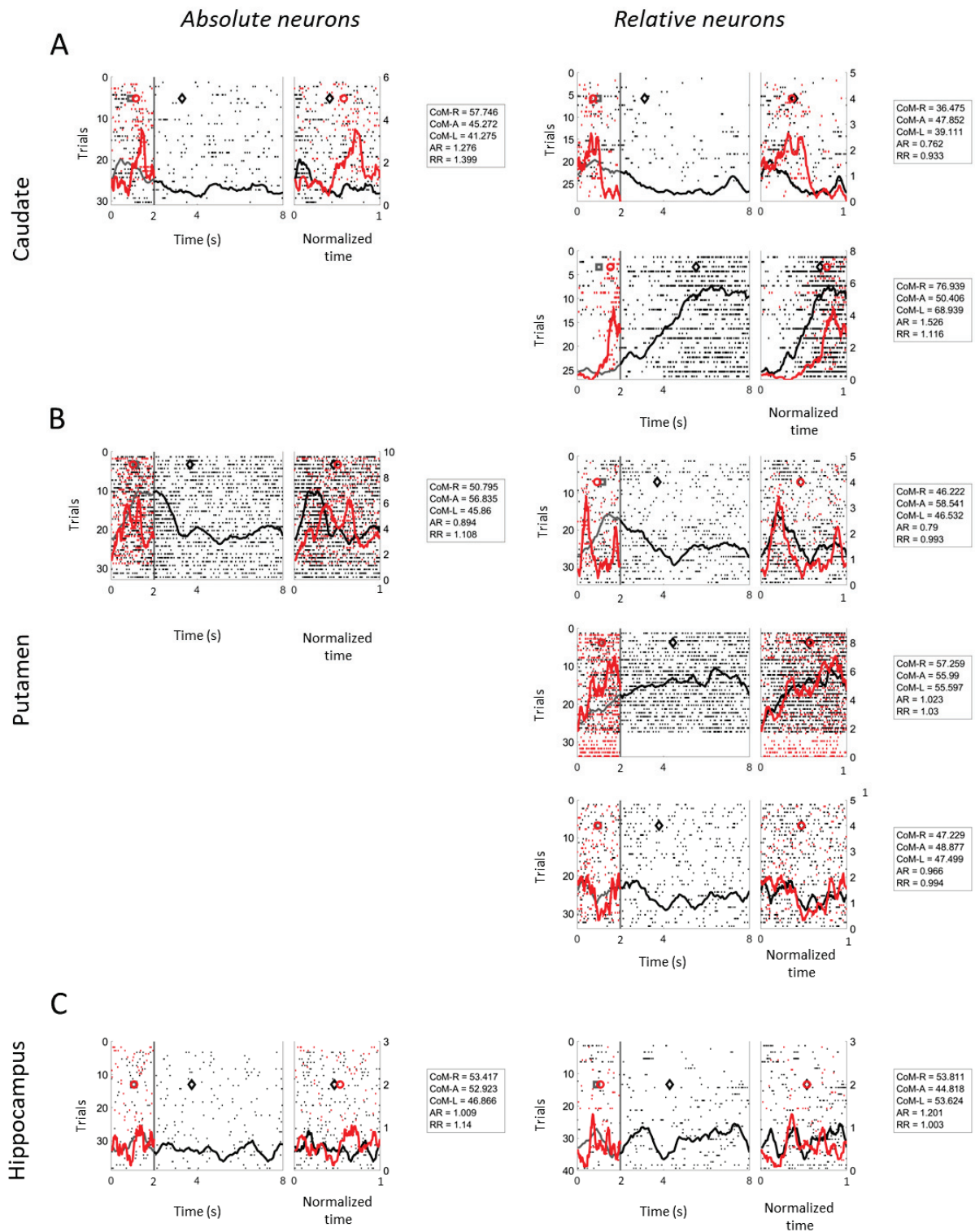


Figure Supplementary 1. Single cells example for caudate (A), putamen (B), and hippocampus (C) in the retiming-to-long-2 condition.

Legend is the same than in figure 2, except that reference duration is the short interval of the longer set (supra-second-range). Left column shows absolute neurons, right column shows relative neurons. Per each neuron, we show the value of CoM-R, CoM-A and CoM-L expressed in % of the interval (2 seconds for reference and short, red and grey line, 8 seconds for the long interval, black line) and the value of the absolute ratio AR (CoM-R/CoM-A) and relative ratio RR (CoM-R/CoM-L).

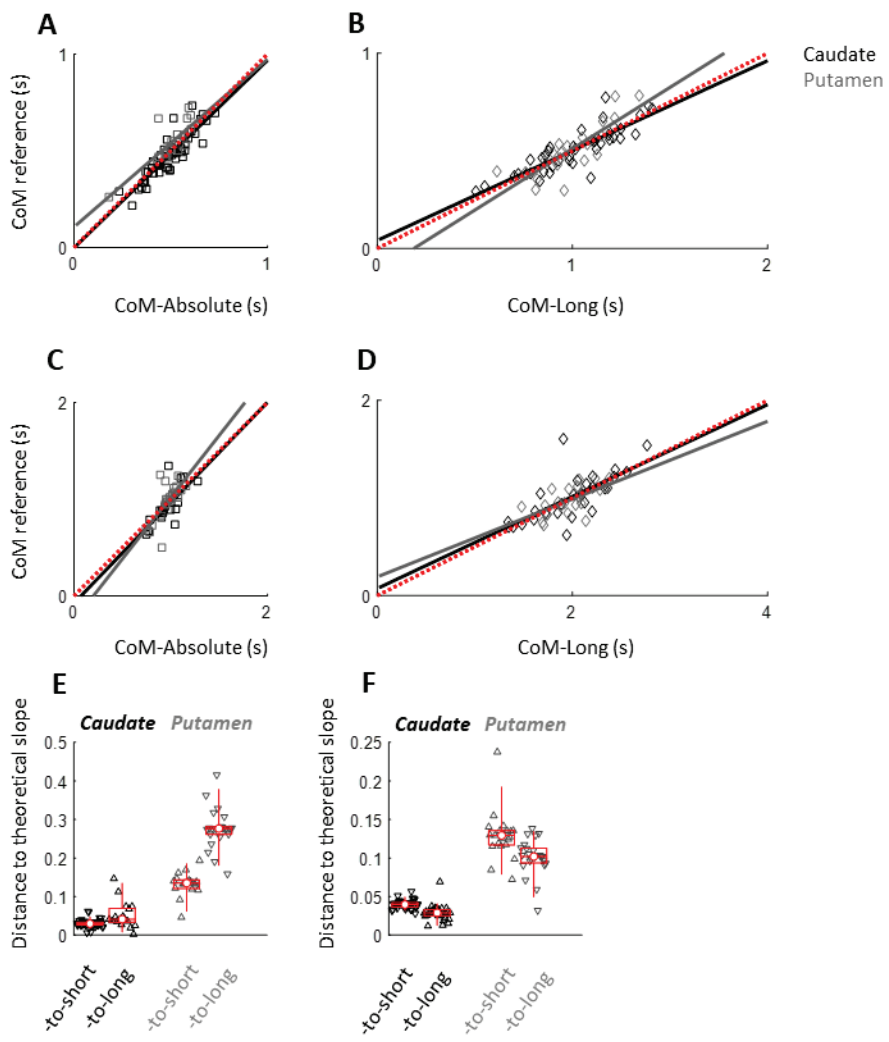


Figure 4. Linear regressions computed on the centre of masses.

A. Centre of masses of absolute neurons in caudate (black) and putamen (grey) in the retiming-to-short condition. CoM-R (y-axis, 1s-long) were regressed according the CoM-Absolute (x-axis, 1s-intermediate). Fit on population centre of masses are displayed in coloured lines (black for caudate, grey for putamen). Dotted red line is the theoretical fit ($Y = 1 \times X$). **B.** Centre of masses of relative neurons in caudate (black) and putamen (grey) in the retiming-to-short condition. CoM-R (y-axis, 1s-long) were regressed according the CoM-Long (x-axis, 2s-long). Fit on population centre of masses are displayed in coloured lines (black for caudate, grey for putamen). Dotted red line is the theoretical fit ($Y = 0.5 \times X$). **C.** Same as in A, but for retiming-to-long-1 condition. CoM-R (y-axis, 2s-long) regressed by CoM-A (x-axis, 2s-intermediate). **D.** Same as in B, but for retiming-to-long-1 condition. CoM-R (y-axis, 2s-long) regressed by CoM-L (x-axis, 4s-long). **E.** Distance to theoretical slope (=1) computed with the leaving-one-out method for absolute subpopulations in each structure and each set. **F.** Same as in E for relative subpopulations. Theoretical slope is equal to 0.5.

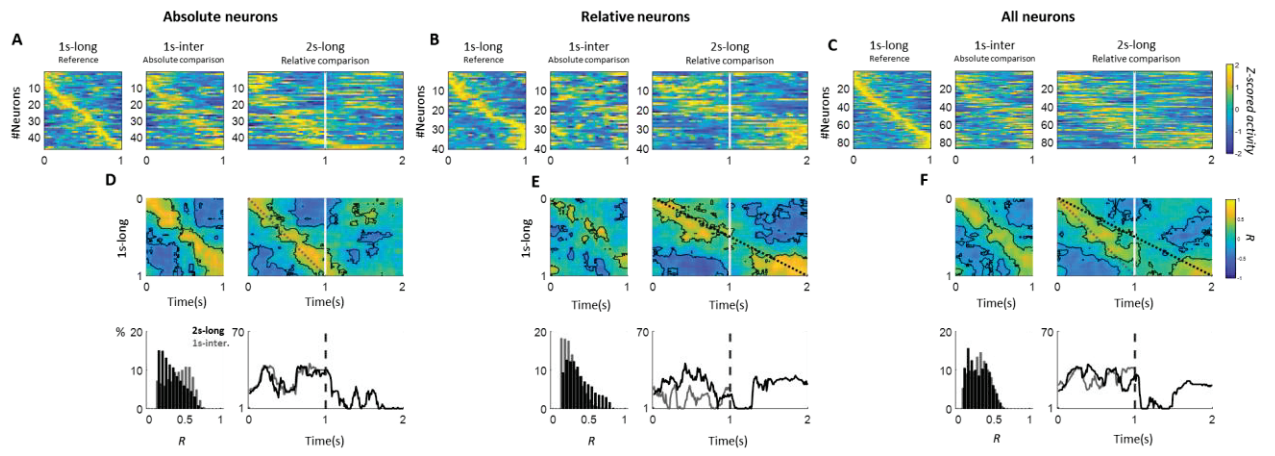


Figure 5. Neural activity strongly correlates within the 1s-duration between temporal contexts at the retiming-to-short condition.

A. Left panel. Activity of caudate absolute neurons during the reference duration (1s-long) of the retiming-to-short condition sorted by their peak. Central panel. Activity of the caudate absolute neurons during the twin duration (1s-intermediate) sorted in function of the peak during reference duration. Right panel. Activity of the caudate absolute neurons during the longer duration (2s-long) sorted in function of the peak during reference duration. **B.** Same as in A with absolute neurons. **D.** Same as in A with all the neurons. **D.** Top row. Matrix of correlation coefficients obtained from reference matrix and 1s-intermediate matrix (left panel) and reference matrix and 2s-long (right panel). Contours define the significant correlations. Dotted line in the right panel indicates the theoretical pattern of correlation for absolute neurons. Bottom left. Distribution of the correlation's coefficients of the significant positive correlations in grey for the reference and 1s-intermediate correlation, in black for the reference and 2s-long duration. Bottom right. Number of time-points from reference duration correlated significantly with each time-point from the 1s-intermediate matrix (grey) and 2s-long matrix (black). **E.** Same as in D for the relative neurons. Top right panel. Dotted lines represent the theoretical pattern for relative neurons. **F.** Same as in D and E for all the neurons.

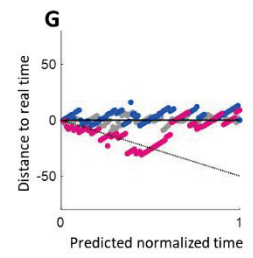
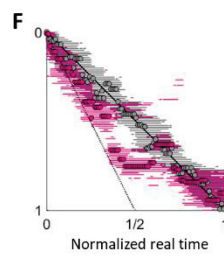
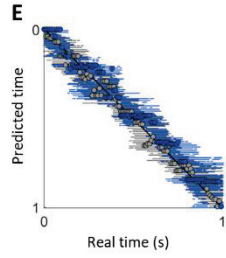
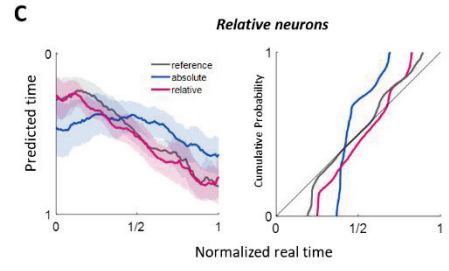
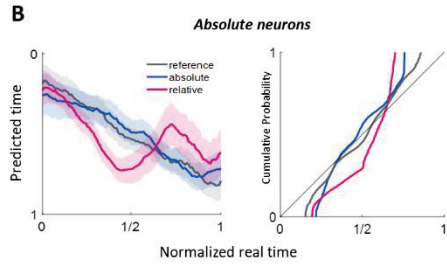
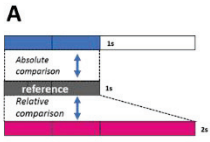


Figure 6. Decoding caudal activity in the retiming-to-short condition follows an absolute.

A. Schema showing the comparisons from decoding output. The model was trained on the grey duration (reference), and tested on the grey, blue (1s-intermediate) and pink (2s-long) durations. **B.** Left panel. Decoding results on the absolute subpopulation. We display for each time point (real time, x-axis), its predicted time (average and standard deviation, y-axis) when the model was tested on the reference (grey), 1s-intermediate (blue) and 2s-long (pink) durations. Right panel. Cumulative probability distribution computed with an empirical cumulative distribution function on the averaged decoding outputs tested on reference (grey), 1s-intermediate (blue) and 2s-long (pink). **C.** Same as in B for the relative neurons. **D.** Decoding results from the entire population when trained on reference and tested on reference (grey) or 1s-intermediate (blue). Shades represent the time-points decoded above chance (see methods). Dots show the maximal prediction per each real time point. **E.** Same as in D when model was trained on reference (grey) and tested on 2s-long (pink). **F.** Distance of maximal prediction to real time for each tested duration: reference, 1s-intermediate and 2s-long respectively in grey, blue and pink. Dotted line represents the absolute pattern of time in the long condition, it is equivalent to the diagonal in F.

E. General discussion

E.1. Time categorization differs across ranges

To address whether time-ranges influences temporal estimations, we designed a time-categorization task that could be tested at different time-ranges. We trained two rhesus macaques to perform the task. Monkeys are able to categorize temporal duration in a sequential order: short, intermediate or long. Previously, it has been shown that monkeys categorize durations into short and long at the second range (Mendoza, Méndez, Pérez, Prado, & Merchant, 2018; Leon & Shadlen, 2003). In an interval-generation task, monkeys are able to time their movements over 2, 4 or 8 seconds, and their temporal production follows a scalar rule (Mita et al., 2009). Scalability in their behaviour suggest that they are as good producing a 2s interval than an 8s interval, in a relative scale. Our task differs from that in the sense that durations must be categorized as they are intertwined in the longer one. In line with their results, 4s and 8s were categorized with the same accuracy when they were long. In our task, monkey's performance was influenced by training: they performed better at the range they were trained on (second range, 0.5-1-2s). Nonetheless, temporal categorization did not follow the same patterns whether durations were divided (retiming-to-short) or multiplied by two (retiming-to-long). Indeed, performance on retiming-to-short conditions were higher than retiming-to-long conditions. This can be due to a lack of motivation to time long durations. Indeed, long durations can be perceived as aversive before getting a reward, as it has been shown with delay-discounting tasks (Martinez, Pasquereau, Saga, Météreau, & Tremblay, 2020; Minamimoto, La Camera, & Richmond, 2009). Thus, a lack of motivation to perform the task could be illustrated by an increase of aborted trials and/or a tendency to respond randomly. First, the proportion of anticipated trials did not vary across ranges in the retiming conditions are were always below 5% for both monkeys. Second, even at longer ranges, up to 8s, categorization was above 0.5 correct for short and long trials for both monkeys, while chance level was at defined 0.33. In addition, the nature of the errors at intermediate trials was not randomly distributed (0.5-0.5 for both, underestimations and overestimations) but rather showed a shift in temporal perception. At the sub-second range, intermediate trials (0.5s) were classified more often as shorts (0.25s) than long (1s). As time-range increased, intermediate trials were gradually more often overestimated than underestimated, with the higher difference at the set 8s-long, where intermediate trials (4s) were more often categorized as long (8s) than short (2s). This can be interpreted as a slowdown in temporal perception. Thus, decreased performance in time categorization cannot be linked with a decreased motivation when time-ranges increased.

E.2. Is there a shift of timing strategies?

In addition, we showed that response times were shorter and illustrated anticipation of the end of the long intervals at shorter ranges. On the other hand, at longer ranges, the end of longer durations was not anticipated. We hypothesise that this could illustrate a change in the timing strategy of the monkeys. Congruently, the anticipation patterns were different between shorter time ranges (sub-second and second) and supra-second ranges. Indeed, at shorter ranges, the anticipation of the end of intervals (anticipated trials) increased gradually during the second half of the long interval (when there was only one possible response left, *i.e.* the long one). Monkeys anticipated the end of the intervals by moving the joystick before its end. On the contrary, at supra-second ranges, the anticipation of the end of the intervals was higher at the beginning of the durations: monkeys do not anticipate the end of the longer intervals anymore. One possibility to explain this differential behaviour is that at shorter ranges, monkeys explicitly time the interval, and at longer ranges, monkeys time the longer interval in an implicit manner: they respond long when the target appear after 4 or 8s without “actively” expecting its end. In this case, increasing responses times could reflect a lack of motor preparation. On the other hand, it is also possible that responses times increasing reflect uncertainty: in this case, the response time pattern matches the fact that temporal discrimination is more difficult at longer ranges. Even if some observations could suggest a shift in timing strategies, we cannot make any statement because we cannot reject any alternative hypothesis.

E.3. Time categorization follows a sequential rule

If we take our results altogether, we show that durations categorizations were context dependent and that intermediate duration was always the most difficult to categorize. This is in contrast with temporal production task, where time productions followed a regression to the mean pattern: short durations are overproduced and longer durations are underproduced (Meirhaeghe, Sohn, & Jazayeri, 2021; Jazayeri & Shadlen, 2015). We suggest that in our task, a regression to the mean would be illustrated by a better categorization of intermediate trials, as time categorization would be biased to the intermediate duration. On the contrary, the results show that monkeys categorized better longer durations from second to supra-second ranges and shorter durations in sub-second range. At the exception of this shorter range, time categorization followed a sequential rule where long was better discriminated than short, and short was better discriminated than intermediate. This result shows that monkeys perform the task similarly as how they perform the temporal bisection task: the extreme durations are easier to identify (Mendoza et al., 2018; Leon & Shadlen, 2003).

Now we can move to the next level and ask: what are the neural correlates of these behavioural observations?

E.4 TM-cells are not directly recruited as a function of movement

Many of the proposed neural correlates for time have been linked with motor responses. This is the case in macaques pre-supplementary motor area (pre-SMA), lateral intra-parietal (LIP), orbitofrontal (OFC) and prefrontal cortices (PFC) and caudate nucleus (Meirhaeghe et al., 2021; Wang, Narain, Hosseini, & Jazayeri, 2018; Jazayeri & Shadlen, 2015; Tsujimoto, Genovesio, & Wise, 2009; Mita et al., 2009; Quintana & Fuster, 1999) and in rodents orbitofrontal cortex (OFC), motor (M2), prefrontal cortex (PFC), and striatum for example (Zhou, Masmanidis, & Buonomano, 2020; Bakhurin et al., 2017; Emmons et al., 2017; Mello, Soares, & Paton, 2015). Even rodents time-cells in the hippocampus are recruited during running episodes (Shimbo, Izawa, & Fujisawa, 2021; Mau et al., 2018; Robinson et al., 2017; Kraus, Robinson, White, Eichenbaum, & Hasselmo, 2013; Pastalkova, Itskov, Amarasingham, & Buzsáki, 2008) or modulated by spatial position (MacDonald et al., 2011). This suggest that time can be decoded from these regions because movement take place in time, and these activities are part of the execution of movement in time. Nevertheless, not all the temporal signatures are related to movement in macaques pre-SMA, but they rather target a temporal boundary (Mendoza et al., 2018); while in orbitofrontal, caudate nucleus and ventral striatum, neural activity can be modulated over time by reward expectancy (Hori et al., 2021; Cai, Kim, & Lee, 2011; Tremblay & Schultz, 1999). In striatum rodents, temporal decision threshold coded in the striatum can also be unrelated to movement (Gouvêa et al., 2015). In addition, in the medial temporal lobe, human time-cells differed from the ones observed in rodents as they are recruited during episodic memory tasks without involving any movement (Reddy et al., 2021; Umbach et al., 2020). Our results correspond to these latest observations, as our set up allowed to probe time cells while animals waited for an interval to end, rather than prepare an action in time. Therefore, we did not find strong evidences to link time-modulated (TM) cells activity to motor movement per se. First, time cells distribution in the interval did not take place only during movement times, but rather were distributed during the whole interval. We found that time changes of neural states were almost continuous through time. Some of the TM cells were indeed responsive to movement, and were also responsive to the target's appearance, which can be linked to movement preparation. However, for TM cells selective to one type of motor response (top, left, down of the joystick movement) peak distribution of these cells did not differ between groups in any structure. This supports the idea that the activity of these cells during the interval is unrelated with the execution of the motor response. In addition, in the second chapter, we showed that caudate dynamics during 1s where highly similar between sets at sub-second and second ranges, even if the motor responses associated within this second differed between sets. So, rather than a specific movement related task, it may be more accurate to describe the activity of the cells as

a temporally organized sequence recruited continuously but with a density adjusted to the rate of expected events.

E.5. Can we decode time from neural activity?

When neural activity carries information about time, one could be able to predict time by looking at the state of the population. Indeed, we followed the statement that to decode time from neural activity, changes in the neural states of the population must be detectable from a moment to the other (Buonomano & Maass, 2009; Karmarkar & Buonomano, 2007). It has been shown that neural population does not carry temporal information with the same strength as a function of the timing task: indeed, in explicit timing tasks, temporal predictability is more accurate than in implicit timing tasks (Cueva et al., 2020). Here, we want to highlight the fact that the “code” for a duration depends on the cognitive demand by addressing the question differently. First, we used TM cells from the 2s-long set as we had more cells in all structures, and we showed that TM cells activity outside the baseline could not be decoded based on the activity during the interval -explicit timing task- nor decoded as a function of baseline activity neither. Then, we also showed that across sets, the consistency of the time codes during the first second (cropping the rest of the interval) decreased as intervals increased. The first evidence comes from the proportion of TM cells defined on the entire duration or on the first second of the same duration. On the striatal territories, TM cells were more abundant when they were defined on the longer interval of the sets (2, 4 and 8 seconds) than when they were defined on the first second of the same duration. On the hippocampus, such a difference was not observed. Then, we decoded activity moment-to-moment, and showed that the first second of the intervals was differently decoded as a function of the timing demand on the duration. Indeed, we showed that at shorter ranges (sub-second and second ranges), time was better decoded than at longer ranges. Thus, our result reported evidences that within the first second, the amount of change in the neural population depends on the probability that an event can occur within this second or not. So, what does this mean if we confront to our starting question? Decoding time is a tool to probe whether neural activity has a structure that changes as a function of time, and that this structure is repeated over and over across different trials. It would of course be possible to decode time from temporal cortex if we showed a movie on each trial, and the time selective activity would support time decoding because neural activity is different as a function of the stimuli of the frames. Would this mean that the activity encodes time? The main point from our results is that we show that the structure of the activity as a function of time in the trial, following a simple stimulus, supports the decoding of time and adapts to the expectations within the trial. As such, the neural activity encodes expectancies in time sustained by a modification of the neural circuit.

E.6. Are all neural structures equally recruited?

The main idea of the first manuscript is to compare the neural dynamics between striatum and hippocampus. Both structures have been mainly studied separately. In rodents, time can be decoded from hippocampal activity at the tens of seconds range (Mau et al., 2018) and from striatal activity, at the second, and tens of seconds-to-minute range (Mello et al., 2015; Gouvêa et al., 2015). In addition, when striatal neurons are compared with cortical regions, it was demonstrated that temporal decoding is better in the striatum than in motor and orbitofrontal cortex at the supra-second range (Zhou et al., 2020; Bakhurin et al., 2017). A striking observation is that in these studies, striatal and cortical neurons display similar activity, but decoding is still better in the striatum. Recently, it was shown that in rodents, both structures, striatum and hippocampus, sustained temporal codes in a foraging task over a 5-minute delay (Shikano et al., 2021). In both structures, the sequentiality of time-cells peaks emerged with learning, and allow proper decoding but without direct comparisons between structures. The authors also show that inactivating the hippocampus disrupted the peaks' sequentiality in the striatum, highlighting a network for time code between both regions, and suggesting a directionality: time information is conveyed from the hippocampus to the striatum. Altogether, these results convey the hypothesis that time is encoded across multiple brain regions, but that the striatum act as a time reader (Matell & Meck, 2004; Matell & Meck, 2000). We are the first ones comparing directly the neurophysiological activity of these two brain regions during a timing task in primates. Our results fit the previous reports as time is better decoded in the striatum than in another structure, in this case the hippocampus. Thus, to the fact that striatum is a better temporal reader than the cortex, we can add the fact that it is a best temporal reader than the hippocampus when considering single-unit activity, during an interval categorization task. Nevertheless, time codes are presented in both areas even if they are weaker in the hippocampus. Thus, we suggest that in our task, temporal information does not convey from the hippocampus as previously reported in rodents (Shikano et al., 2021), but rather from cortical areas.

E.7. Striatum scales duration better

It has been demonstrated that caudate, as prefrontal cortex, adapt the amount of changes between two consecutive time-points over an interval to be produced (Wang et al., 2018). This kind of temporal code allows rapid adaptability to produce movements over different durations. Our results fit this hypothesis, and extend these findings to categorization tasks. Indeed, between two time-points, the changes in caudate population gradually decreased over time within an interval, and between ranges. In addition, we showed, even if the amount of change between two consecutive timepoints were higher in hippocampus and in putamen (higher speed), the trajectories of the neural populations

were more “disorganised” than in caudate. On the contrary, in caudate, the amount of change of the neural states were smaller between two time points, but the overall changes in population activity over time were larger and its intrinsic organization allows a better temporal decoding. The neurons we recorded from are inhibitory spiny neurons which can be excited by cortical input, or dopamine and cholinergic input, and they can be inhibited/disinhibited by other spiny neurones (Burke et al., 2017). Their activation results in facilitation or inhibition of various actions. In the task we use, the activations we measured are the start of an inhibitory/disinhibitory circuit that results in a final action. We show that this circuit is best organized in time in the caudate, and this can be the result of local or global circuit recruitment, for which caudate prevails in our task.

E.8. Striatum predictability decreases over ranges

Temporal decoding in the striatum can be explained by the striatal anatomy. With collateral inhibition in the striatum (Plenz, 2003), neurons in the striatum present the characteristics to compute time in a discretised way. Indeed, when neuron A is stimulated by a cortical input, neuron A can inhibit neuron B with collaterals. Once neuron A is not stimulated anymore, it releases its inhibition to neuron B, that can in turn inhibits its neighbours. This can be described as a pull-push mechanism: when neuron A is activated, neuron B is not, and when neuron B is activated, neuron A is not. Such a mechanism conveys into a peak sequentially informative about time. Our results challenged the temporal maintenance of such a mechanism over longer ranges. Indeed, such a mechanism may not be maintained over long periods in macaques’ striatum, involving a loss of time tracking over long durations reflected by our decoding results in chapter 1. Our analysis in chapter 2 convey this hypothesis in caudate. Indeed, the timing track of 1s is maintained between sub- and supra-second ranges in an absolute way. Thus, the activity modulation is not set dependent between sub-second and second ranges, and can result on a basic chain reaction at the neural level triggered by the sensory cue. The lack of decoding accuracy moment-by-moment in the longer sets can illustrate that at longer ranges, this feedforward process does not hold.

An overall mechanism may involve at a short time-range, a feedforward activation of a sequence of cells, until reward following the appropriate action. This reward acts as a feedback which modifies feedforward in retrospect. This may explain the differential recruitment following the start of a trial (extinction of white square) at short time-range. At a longer time-range, the temporal distance between the cells activated in feedforward and the feedback from midbrain dopamine or cholinergic tonically active neurons (TANs) at the time of reward (Martel & Apicella, 2021), may be too large to support plasticity maintaining this predictive sequence. To test this, it would be interesting in the

future to study changes as a function of learning, and to test the effects of blocking dopaminergic and cholinergic feedback by pharmacological manipulations.

E.9. Linking ramping activity to reward anticipation

Within a duration, moments of interest can be overrepresented via dopaminergic stimulations with transient -phasic- activity that encode rewards and reinforces moments of reward (Schultz, 2016). The major outputs of the midbrain neurons are the striatum (Haber, 2014), thus striatal role in timing can be directly linked with its dopaminergic inputs. In addition to its phasic dopaminergic stimulation, it has been demonstrated that dopaminergic neurons may provide the striatum with tonic inputs (Howe & Dombeck, 2016). Tonic dopaminergic modulation is sensitive to ongoing expectations about reward (Wang, Toyoshima, Kunitatsu, Yamada, & Matsumoto, 2021), and thus can also provide temporal information to the striatum in a constant way. In the second chapter, we showed that the middle of the longer duration does not correlate with any other state of the reference duration. Right after the middle of the longer duration, reinforcements never occur. On the contrary, the end of the longer durations for each set are highly correlated with each other. This can be explained by a consequent number of ramping neurons, ramping to the end of the interval in both sets and in consequence triggering the end of the duration in any set (1s-long or 2s-long). These neurons ramping to the end of the intervals could be triggered by tonic dopaminergic inputs in the striatum.

E.10. Can be time decoding linked with ramping activity?

If we consider that dopaminergic inputs to the striatum could initiate temporal codes in the striatum. Another mechanism between structures was proposed to account for temporal codes between entorhinal cortex and hippocampus (Rolls & Mills, 2019) where hippocampal time-cells are provided with temporal information from ramping neurons of the entorhinal cortex (Bright et al., 2020; Umbach et al., 2020; Tsao et al., 2018). One of the differences we found between striatum and hippocampus is that the latter has a very low proportion of ramping neurons. This raises an important question: which one of the phasic (time cells) and tonic (ramping cells) is better to predict time? Previously, some studies supported the idea that monotonic changes in neural activity over time allows better temporal prediction (Cueva et al., 2020), while others sustained the idea that a well-organized sequence of peaks allows a better readout of time (Zhou et al., 2020; Pilkiw & Takehara-Nishiuchi, 2018). This is an ongoing debate (Zhou & Buonomano, 2022). Our results suggest that ramping activity allows better temporal prediction but not necessarily moment-to-moment decoding. Indeed, the striatum is the structure with the higher proportion of ramping neurons and the higher monotonic changes occurring at the single-cell level, without any difference between sets. Striatum is also the

best temporal predictor, for all ranges. Thus, it can be suggested that striatum is a better temporal predictor because it has higher ramping activity. But on the contrary, temporal prediction computed on a population of relaxation cells (displaying a pattern similar to ramping down activity), reflects higher decoding accuracies at the beginning of the interval than at the end (Bright et al., 2020) but not a maintained performance over time. On the other hand, we showed that moment-to-moment decoding does decrease as the length of the ranges increased. In this case, the maintained proportion of ramping activity is not consistent with the lack of decoding accuracy over time. Here, we conclude that ramping cells are needed for temporal prediction but not for moment-to-moment classification.

E.11. Is time processed in sequence or in a parallel way?

The cognitive models of temporal processing attempted to create a universal framework in which a duration is processed in a sequential way and reaches a final stage in which time is encoded in the striatum. However, if we consider the well-studied reward circuitry, it has been proposed that reward information is processed by multiple areas in a parallel way and not necessary in a sequential network (Phillips, 1984). We can make the same hypothesis for time processing. Multiple areas integrate time information, from sensory inputs and reward values from the external world, but also for motor coordination, needing a time processing from the inner world: temporal codes emerge from multiple brain areas. Do they all convey to the same “clock”, *i.e.* the striatum? In the striatal beat frequency (SBF) model, all the temporal information conveys to the striatum before reaching the cortex back for response (Kononowicz & van Wassenhove, 2016; Matell & Meck, 2004). The temporal processing follows the sequential model: pacemaker, integrator and decision process. One example of a parallelization of temporal processing would be reflected by the fact that multiple brain areas process temporal information, but on the contrary to SBF model, not all the temporal information conveys to striatum. Another example of parallelization of temporal processing, would be that, if we accept the striatum as a “central clock” and all the temporal information conveys to there, time could still be process in parallel via its parallel cortico-striato-pallidal loops (Jahanshahi et al., 2015; Alexander et al., 1986). The first hypothesis is innovative and has to be asked at some point. Nevertheless, many studies show or strongly suggest that the temporal code they observe in cortical areas convey to the striatum but that the temporal code is refined by striatal circuits (Zhou et al., 2020; Wang et al., 2018; Mendoza et al., 2018; Emmons et al., 2017; Bakhurin et al., 2017).

The second question is whether all the temporal information conveyed to the striatum via a unique time network? It has been shown that in a 5-minutes foraging task, hippocampal inactivation’s disrupt temporal patterns in the rodent’s striatum, highlighting an hippocampal-striatal neural network for temporal processing (Shikano et al., 2021). These authors posit the hippocampus is the

source of temporal code in the striatum. However, the hippocampal-striatum network could also be activated during associative learning via the ventral tegmental area (Lisman & Grace, 2005). Even if we did not manipulate neural activity as monkeys performed the task, our data suggest that the hippocampus is not involved in the task. We make the prediction that inactivating the hippocampus in our task will not disrupt the temporal patterns observed in striatal populations. Indeed, in our task, it is unlikely that temporal information emerge from the hippocampus, but rather from the cortex: probably pre-SMA (Lehéricy et al., 2004) or OFC (Ferry et al., 2000). Our study combined with the previous results points out at least two different time networks going through the striatum. In addition, a purely speculative assumption is that, for example, during social interactions, temporal information could convey from the amygdala, as it has been shown that neurons in the amygdala triggered time in a social interaction (Gilardeau et al., 2021). Parallelization of the neural networks in time processing explained why we do not have strong temporal activity in the hippocampus.

E.12. Future perspectives

We have shown that neural changes in caudate, putamen and hippocampus are different during a timing task. Hippocampal activity was barely modulated by ongoing time, while striatum showed strong time processing. We highlighted what happens at the neural level during the temporal intervals, but how the temporal modulations are integrated by the striatum remains unclear. The next step is to identify more clearly the role of the dopaminergic and cholinergic inputs of the striatum in temporal processing. Recently, it has been shown that dopaminergic modulation influences choices in a temporal bisection tasks (Soares et al., 2016), so does striatum (Gouvêa et al., 2015). To further explicit the differential roles of these structures in temporal processing, we suggest that double dissociations inactivating these structures is needed. Further, the manipulation of the different neurons in the striatum (*i.e.* medium spiny-neurons, tonically active neurons, fast-spiking neurons) during a timing task would allow to distinguish time linked with the reward responses (TANs) and time linked with action selection (fast-spiking neurons) for example (Kreitzer, 2009). In addition, whether the striatum act as a time-keeper, a comparator (Gouvêa et al., 2015) or a memory component (Coull et al., 2008) in a timing-task remains unclear. To address this, inactivation's of the striatal territories during a temporal task that would distinguish an encoding, storage, comparison and response phase (Chiba et al., 2015) would allow to clarify at what moment of the temporal processing the striatum is involved. The final question is: are the monkeys able to perform a temporal categorization task if we remove the caudate and/or the putamen (assuming that they would be still able to produce a response)? The SBF model would predict that it would be impossible, nonetheless, one could assume that some kind of categorization computed by the cortex would be possible.

F. General bibliography

- Abela, A. R., Duan, Y., & Chudasama, Y. (2015). Hippocampal interplay with the nucleus accumbens is critical for decisions about time. *European Journal of Neuroscience*, *42*(5), 2224–2233. <https://doi.org/10.1111/ejn.13009>
- Adler, A., Katabi, S., Finkes, I., Israel, Z., Prut, Y., & Bergman, H. (2012). Temporal convergence of dynamic cell assemblies in the striato-pallidal network. *Journal of Neuroscience*, *32*(7), 2473–2484. <https://doi.org/10.1523/JNEUROSCI.4830-11.2012>
- Ager, A. L., Borms, D., Deschepper, L., Dhooghe, R., Dijkhuis, J., Roy, J. S., & Cools, A. (2020). Proprioception: How is it affected by shoulder pain? A systematic review. *Journal of Hand Therapy*, *33*(4), 507–516. <https://doi.org/10.1016/j.jht.2019.06.002>
- Albouy, G., Fogel, S., King, B. R., Laventure, S., Benali, H., Karni, A., Carrier, J., Robertson, E. M., & Doyon, J. (2015). Maintaining vs. enhancing motor sequence memories: Respective roles of striatal and hippocampal systems. *NeuroImage*, *108*, 423–434. <https://doi.org/10.1016/j.neuroimage.2014.12.049>
- Alexander, G. E., & DeLong, M. R. (1985). Microstimulation of the primate neostriatum. II. Somatotopic organization of striatal microexcitable zones and their relation to neuronal response properties. *Journal of Neurophysiology*, *53*(6), 1417–1430. <https://doi.org/10.1152/jn.1985.53.6.1417>
- Alexander, G. E., DeLong, M. R., & Strick, P. L. (1986). Parallel organization of functionally segregated circuits linking basal ganglia and cortex. *Annual Review of Neuroscience*, *VOL. 9*, 357–381. <https://doi.org/10.1146/annurev.ne.09.030186.002041>
- Amaral, D. G., Scharfman, H. E., & Lavenex, P. (2007). The dentate gyrus: fundamental neuroanatomical organization (dentate gyrus for dummies). *Progress in Brain Research*, *163*(6), 3–22. <https://doi.org/10.15407/fz67.06.074>
- Antzoulatos, E. G., & Miller, E. K. (2014). Increases in Functional Connectivity between Prefrontal Cortex and Striatum during Category Learning. *Neuron*, *83*(1), 216–225. <https://doi.org/10.1016/j.neuron.2014.05.005>
- Aosaki, T., Graybiel, A. M., & Kimura, M. (1994). Effect of the Nigrostriatal Dopamine System on Acquired Neural Responses in the Striatum of Behaving Monkeys. *Science*, *265*(July), 412–415.
- Apicella, P., Scarnati, E., & Schultz, W. (1991). Tonicly discharging neurons of monkey striatum respond to preparatory and rewarding stimuli. *Experimental Brain Research*, *84*(3), 672–675. <https://doi.org/10.1007/BF00230981>
- Apicella, Paul. (2007). Leading tonically active neurons of the striatum from reward detection to context recognition. *Trends in Neurosciences*, *30*(6), 299–306. <https://doi.org/10.1016/j.tins.2007.03.011>

- Baddeley, A. D., Allen, R. J., & Hitch, G. J. (2011). Binding in visual working memory: The role of the episodic buffer. *Neuropsychologia*, *49*(6), 1393–1400. <https://doi.org/10.1016/j.neuropsychologia.2010.12.042>
- Bakhurin, K. I., Goudar, V., Shobe, J. L., Claar, L. D., Buonomano, D. V., & Masmanidis, S. C. (2017). Differential encoding of time by prefrontal and striatal network dynamics. *Journal of Neuroscience*, *37*(4), 854–870. <https://doi.org/10.1523/JNEUROSCI.1789-16.2016>
- Balasubramaniam, R., Haegens, S., Jazayeri, M., Merchant, H., Sternad, D., & Song, J. H. (2021). Neural encoding and representation of time for sensorimotor control and learning. *Journal of Neuroscience*, *41*(5), 866–872. <https://doi.org/10.1523/JNEUROSCI.1652-20.2020>
- Balsam, P. D., & Gallistel, C. R. (2009). Temporal maps and informativeness in associative learning. *Trends in Neurosciences*, *32*(2), 73–78. <https://doi.org/10.1016/j.tins.2008.10.004>
- Baraduc, P., Duhamel, J. R., & Wirth, S. (2019). Schema cells in the macaque hippocampus. *Science*, *363*(6427), 635–639. <https://doi.org/10.1126/science.aav5404>
- Barbeau, E. J., Pariente, J., Felician, O., & Puel, M. (2011). Visual recognition memory: A double anatomo-functional dissociation. *Hippocampus*, *21*(9), 929–934. <https://doi.org/10.1002/hipo.20848>
- Barker, G. R. I., & Warburton, E. C. (2011). When is the hippocampus involved in recognition memory? *Journal of Neuroscience*, *31*(29), 10721–10731. <https://doi.org/10.1523/JNEUROSCI.6413-10.2011>
- Besson, G., Ceccaldi, M., Didic, M., & Barbeau, E. J. (2012). The speed of visual recognition memory. *Visual Cognition*, *20*(10), 1131–1152. <https://doi.org/10.1080/13506285.2012.724034>
- Bjerknes, T. L., Moser, E. I., & Moser, M. B. (2014). Representation of geometric borders in the developing rat. *Neuron*, *82*(1), 71–78. <https://doi.org/10.1016/j.neuron.2014.02.014>
- Blazquez, P. M., Fujii, N., Kojima, J., & Graybiel, A. M. (2002). A Network representation of response probability in the striatum. *Neuron*, *33*(6), 973–982. [https://doi.org/10.1016/S0896-6273\(02\)00627-X](https://doi.org/10.1016/S0896-6273(02)00627-X)
- Boccarda, C. N., Sargolini, F., Thoresen, V. H., Solstad, T., Witter, M. P., Moser, E. I., & Moser, M. B. (2010). Grid cells in pre-and parasubiculum. *Nature Neuroscience*, *13*(8), 987–994. <https://doi.org/10.1038/nn.2602>
- Bowman, E. M., Aigner, T. G., & Richmond, B. J. (1996). Neural signals in the monkey ventral striatum related to motivation for juice and cocaine rewards. *Journal of Neurophysiology*, *75*(3), 1061–1073. <https://doi.org/10.1152/jn.1996.75.3.1061>

- Bright, I. M., Meister, M. L. R., Cruzado, N. A., Tiganj, Z., Buffalo, E. A., & Howard, M. W. (2020). A temporal record of the past with a spectrum of time constants in the monkey entorhinal cortex. *Proceedings of the National Academy of Sciences of the United States of America*, *117*(33), 20274–20283. <https://doi.org/10.1073/PNAS.1917197117>
- Buffalo, E. A., Reber, P. J., & Squire, L. R. (1998). The human perirhinal cortex and recognition memory. *Hippocampus*, *8*, 330–339. <https://doi.org/10.1111/j.1460-9568.2004.03710.x>
- Buhusi, C. V., & Meck, W. H. (2002). Differential effects of methamphetamine and haloperidol on the control of an internal clock. *Behavioral Neuroscience*, *116*(2), 291–297. <https://doi.org/10.1037/0735-7044.116.2.291>
- Buhusi, C. V., & Meck, W. H. (2005). Delay-period activities in two subdivisions of monkey inferotemporal cortex during pair association memory task. *Nature Reviews*, *6*, 755–765. <https://doi.org/10.1007/s10674-005-5184-z>
- Buonomano, D. V., & Maass, W. (2009). State-dependent computations: Spatiotemporal processing in cortical networks. *Nature Reviews Neuroscience*, *10*(2), 113–125. <https://doi.org/10.1038/nrn2558>
- Burke, D. A., Rotstein, H. G., & Alvarez, V. A. (2017). Striatal Local Circuitry: A New Framework for Lateral Inhibition. *Neuron*, *96*(2), 267–284. <https://doi.org/10.1016/j.neuron.2017.09.019>
- Buzsáki, G. (2020). The brain–cognitive behavior problem: A retrospective. *ENeuro*, *7*(4), 1–8. <https://doi.org/10.1523/ENEURO.0069-20.2020>
- Buzsáki, G., & Tingley, D. (2018). Space and Time: The Hippocampus as a Sequence Generator. *Trends in Cognitive Sciences*, *22*(10), 853–869. <https://doi.org/10.1016/j.tics.2018.07.006>
- Cai, X., Kim, S., & Lee, D. (2011). Heterogeneous Coding of Temporally Discounted Values in the Dorsal and Ventral Striatum during Intertemporal Choice. *Neuron*, *69*(1), 170–182. <https://doi.org/10.1016/j.neuron.2010.11.041>
- Chaudhuri, R., Knoblauch, K., Gariel, M. A., Kennedy, H., & Wang, X. J. (2015). A Large-Scale Circuit Mechanism for Hierarchical Dynamical Processing in the Primate Cortex. *Neuron*, *88*(2), 419–431. <https://doi.org/10.1016/j.neuron.2015.09.008>
- Cheng, R. K., Tipples, J., Narayanan, N. S., & Meck, W. H. (2016). Clock Speed as a Window into Dopaminergic Control of Emotion and Time Perception. *Timing and Time Perception*, *4*(1), 99–122. <https://doi.org/10.1163/22134468-00002064>
- Chevaleyre, V., & Piskorowski, R. A. (2016). Hippocampal Area CA2: An Overlooked but Promising Therapeutic Target. *Trends in Molecular Medicine*, *22*(8), 645–655. <https://doi.org/10.1016/j.molmed.2016.06.007>

- Chevaleyre, V., & Siegelbaum, S. A. (2010). Strong CA2 pyramidal neuron synapses define a powerful disinaptic cortico-hippocampal loop. *Neuron*, *66*(4), 560–572. <https://doi.org/10.1016/j.neuron.2010.04.013>
- Chiba, A., Oshio, K. I., & Inase, M. (2015). Neuronal representation of duration discrimination in the monkey striatum. *Physiological Reports*, *3*(2), 1–17. <https://doi.org/10.14814/phy2.12283>
- Cisek, P. (2019). Resynthesizing behavior through phylogenetic refinement. *Attention, Perception, and Psychophysics*, *81*(7), 2265–2287. <https://doi.org/10.3758/s13414-019-01760-1>
- Clayton, N. S., & Dickinson, A. (1998). Episodic-like memory during cache recovery by scrub jays. *Nature*, *395*(September), 765–768.
- Cole, S., Stone, A. D., & Petrovich, G. D. (2017). The dorsomedial striatum mediates pavlovian appetitive conditioning and food consumption. *Behavioral Neuroscience*, *131*(6), 447–453. <https://doi.org/10.1037/bne0000216>
- Corbit, L. H., & Janak, P. H. (2010). Posterior dorsomedial striatum is critical for both selective instrumental and Pavlovian reward learning. *European Journal of Neuroscience*, *31*(7), 1312–1321. <https://doi.org/10.1111/j.1460-9568.2010.07153.x>
- Coull, J. T., Cheng, R. K., & Meck, W. H. (2011). Neuroanatomical and neurochemical substrates of timing. *Neuropsychopharmacology*, *36*(1), 3–25. <https://doi.org/10.1038/npp.2010.113>
- Coull, J. T., Nazarian, B., & Vidal, F. (2008). Timing, storage, and comparison of stimulus duration engage discrete anatomical components of a perceptual timing network. *Journal of Cognitive Neuroscience*, *20*(12), 2185–2197. <https://doi.org/10.1162/jocn.2008.20153>
- Coull, J. T., & Nobre, A. C. (1998). Where and when to pay attention: The neural systems for directing attention to spatial locations and to time intervals as revealed by both PET and fMRI. *Journal of Neuroscience*, *18*(18), 7426–7435. <https://doi.org/10.1523/jneurosci.18-18-07426.1998>
- Coull, J. T., Vidal, F., Nazarian, B., & Macar, F. (2004). Functional Anatomy of the Attentional Modulation of Time Estimation. *Science*, *303*(5663), 1506–1508. <https://doi.org/10.1126/science.1091573>
- Cowan, N. (2008). Chapter 20 What are the differences between long-term, short-term, and working memory? In *Progress in Brain Research* (Vol. 169, Issue 07). Elsevier. [https://doi.org/10.1016/S0079-6123\(07\)00020-9](https://doi.org/10.1016/S0079-6123(07)00020-9)
- Cromwell, H. C., Tremblay, L., & Schultz, W. (2018). Neural encoding of choice during a delayed response task in primate striatum and orbitofrontal cortex. *Experimental Brain Research*, *236*(6), 1679–1688. <https://doi.org/10.1007/s00221-018-5253-z>
- Csicsvari, J., Hirase, H., Czurkó, A., Mamiya, A., & Buzsáki, G. (1999). Oscillatory coupling of hippocampal pyramidal cells and interneurons in the behaving rat. *Journal of Neuroscience*, *19*(1), 274–287. <https://doi.org/10.1523/jneurosci.19-01-00274.1999>

- Cueva, C. J., Saez, A., Marcos, E., Genovesio, A., Jazayeri, M., Romo, R., Salzman, C. D., Shadlen, M. N., & Fusi, S. (2020). Low-dimensional dynamics for working memory and time encoding. *Proceedings of the National Academy of Sciences of the United States of America*, *117*(37), 23021–23032. <https://doi.org/10.1073/pnas.1915984117>
- D'Argembeau, A., Jeunehomme, O., Majerus, S., Bastin, C., & Salmon, E. (2015). The Neural Basis of Temporal Order Processing in Past and Future Thought. *Journal of Cognitive Neuroscience*, *27*(1), 185–197. <https://doi.org/10.1162/jocn>
- Dalley, J. W., & Robbins, T. W. (2017). Fractionating impulsivity: Neuropsychiatric implications. *Nature Reviews Neuroscience*, *18*(3), 158–171. <https://doi.org/10.1038/nrn.2017.8>
- De Corte, B. J., Wagner, L. M., Matell, M. S., & Narayanan, N. S. (2019). Striatal dopamine and the temporal control of behavior. *Behavioral Brain Research*, *356*(23), 375–379. <https://doi.org/10.1016/j.bbr.2018.08.030>.Striatal
- De Kock, R., Zhou, W., Joiner, W. M., & Wiener, M. (2021). Slowing the body slows down time perception. *ELife*, *10*, 1–23. <https://doi.org/10.7554/ELIFE.63607>
- Delgado, M. R. (2007). Reward-related responses in the human striatum. *Annals of the New York Academy of Sciences*, *1104*, 70–88. <https://doi.org/10.1196/annals.1390.002>
- DeLong, M. R. (1990). Primate models of movement disorders of basal ganglia origin. *Trends in Neurosciences*, *13*(7), 281–285. [https://doi.org/10.1016/0166-2236\(90\)90110-V](https://doi.org/10.1016/0166-2236(90)90110-V)
- Ding, L., & Gold, J. I. (2010). Caudate encodes multiple computations for perceptual decisions. *Journal of Neuroscience*, *30*(47), 15747–15759. <https://doi.org/10.1523/JNEUROSCI.2894-10.2010>
- Donnelly, N. A., Paulsen, O., Robbins, T. W., & Dalley, J. W. (2015). Ramping single unit activity in the medial prefrontal cortex and ventral striatum reflects the onset of waiting but not imminent impulsive actions. *European Journal of Neuroscience*, *41*(12), 1524–1537. <https://doi.org/10.1111/ejn.12895>
- Draganski, B., Kherif, F., Klöppel, S., Cook, P. A., Alexander, D. C., Parker, G. J. M., Deichmann, R., Ashburner, J., & Frackowiak, R. S. J. (2008). Evidence for segregated and integrative connectivity patterns in the human basal ganglia. *Journal of Neuroscience*, *28*(28), 7143–7152. <https://doi.org/10.1523/JNEUROSCI.1486-08.2008>
- Effron, D. A., Niedenthal, P. M., Gil, S., & Droit-Volet, S. (2006). Embodied temporal perception of emotion. *Emotion*, *6*(1), 1–9. <https://doi.org/10.1037/1528-3542.6.1.1>
- Emmons, E. B., De Corte, B. J., Kim, Y., Parker, K. L., Matell, M. S., & Narayanan, N. S. (2017). Rodent medial frontal control of temporal processing in the dorsomedial striatum. *Journal of Neuroscience*, *37*(36), 8718–8733. <https://doi.org/10.1523/JNEUROSCI.1376-17.2017>

- Ergorul, C., & Eichenbaum, H. (2004). The hippocampus and memory for “what”, “where”, and “when.” *Learning & Memory (Cold Spring Harbor, N.Y.)*, 11(4), 397–405. <https://doi.org/10.1101/lm.73304.mals>
- Falcone, R., Weintraub, D. B., Setogawa, T., Wittig, J. H., Chen, G., & Richmond, B. J. (2019). Temporal coding of reward value in monkey ventral striatal tonically active neurons. *Journal of Neuroscience*, 39(38), 7539–7550. <https://doi.org/10.1523/JNEUROSCI.0869-19.2019>
- Farovik, A., Dupont, L. M., & Eichenbaum, H. (2010). Distinct roles for dorsal CA3 and CA1 in memory for sequential nonspatial events. *Learning and Memory*, 17(1), 801–806. <https://doi.org/10.1101/lm.1616209>
- Feigenbaum, J. D., & Rolls, E. T. (1991). Allocentric and egocentric spatial information processing in the hippocampal formation of the behaving primate. *Psychobiology*, 19(1), 21–40. <https://doi.org/10.1007/BF03337953>
- Ferry, A. T., Öngür, D., An, X., & Price, J. L. (2000). Prefrontal cortical projections to the striatum in macaque monkeys: Evidence for an organization related to prefrontal networks. *Journal of Comparative Neurology*, 425(3), 447–470. [https://doi.org/10.1002/1096-9861\(20000925\)425:3<447::AID-CNE9>3.0.CO;2-V](https://doi.org/10.1002/1096-9861(20000925)425:3<447::AID-CNE9>3.0.CO;2-V)
- Fortin, N. J., Agster, K. L., & Eichenbaum, H. B. (2002). Critical role of the hippocampus in memory for sequences of events. *Nature Neuroscience*, 5(5), 458–462. <https://doi.org/10.1038/nn834>
- Foster, D. J., & Wilson, M. A. (2006). Reverse replay of behavioural sequences in hippocampal place cells during the awake state. *Nature*, 440(7084), 680–683. <https://doi.org/10.1038/nature04587>
- Frost, R., & McNaughton, N. (2017). The neural basis of delay discounting: A review and preliminary model. *Neuroscience and Biobehavioral Reviews*, 79(April), 48–65. <https://doi.org/10.1016/j.neubiorev.2017.04.022>
- Gaffield, M. A., Sauerbrei, B. A., & Christie, J. M. (2022). Cerebellum encodes and influences the initiation, performance, and termination of discontinuous movements in mice. *ELife*, 11, 1–24. <https://doi.org/10.7554/eLife.71464>
- Gallistel, C. R. (1989). Animal cognition: the representation of space, time and number. *Annual Review of Psychology*, 40, 155–189. <https://doi.org/10.1146/annurev.ps.40.020189.001103>
- Gallistel, C. R., & Gelman, R. (2000). Non-verbal numerical cognition: From reals to integers. *Trends in Cognitive Sciences*, 4(2), 59–65. [https://doi.org/10.1016/S1364-6613\(99\)01424-2](https://doi.org/10.1016/S1364-6613(99)01424-2)
- Gann, M. A., King, B. R., Dolfen, N., Veldman, M. P., Chan, K. L., Puts, N. A. J., Edden, R. A. E., Davare, M., Swinnen, S. P., Mantini, D., Robertson, E. M., & Albouy, G. (2021). Hippocampal and striatal responses during motor learning are modulated by prefrontal cortex stimulation. *NeuroImage*, 237(December 2020), 118158. <https://doi.org/10.1016/j.neuroimage.2021.118158>

- Gauthier, B., Prabhu, P., Kotegar, K. A., & van Wassenhove, V. (2020). Hippocampal contribution to ordinal psychological time in the human brain. *Journal of Cognitive Neuroscience*, *32*(11), 2071–2086. https://doi.org/10.1162/jocn_a_01586
- Gauthier, J. L., & Tank, D. W. (2018). A Dedicated Population for Reward Coding in the Hippocampus. *Neuron*, *99*(1), 179-193.e7. <https://doi.org/10.1016/j.neuron.2018.06.008>
- Geddes, C. E., Li, H., & Jin, X. (2018). Optogenetic Editing Reveals the Hierarchical Organization of Learned Action Sequences. *Cell*, *174*(1), 32-43.e15. <https://doi.org/10.1016/j.cell.2018.06.012>
- Genovesio, A., Tsujimoto, S., & Wise, S. P. (2009). Feature- and Order-Based Timing Representations in the Frontal Cortex. *Neuron*, *63*(2), 254–266. <https://doi.org/10.1016/j.neuron.2009.06.018>
- Gerardin, E., Lehericy, S., Pochon, J. B., Du Montcel, S. T., Mangin, J. F., Poupon, F., Agid, Y., Le Bihan, D., & Marsault, C. (2003). Foot, hand, face and eye representation in the human striatum. *Cerebral Cortex*, *13*(2), 162–169. <https://doi.org/10.1093/cercor/13.2.162>
- Gerardin, E., Pochon, J. B., Poline, J. B., Tremblay, L., Van De Moortele, P. F., Levy, R., Dubois, B., Le Bihan, D., & Lehericy, S. (2004). Distinct striatal regions support movement selection, preparation and execution. *NeuroReport*, *15*(15), 2327–2331. <https://doi.org/10.1097/00001756-200410250-00005>
- Gibbon, J. (1977). Scalar expectancy theory and Weber's law in animal timing. *Psychological Review*, *84*(3), 279–325. <https://doi.org/10.1037/0033-295X.84.3.279>
- Gibbon, J., & Church, R. M. (1990). Representation of time. *Cognition*, *37*(1–2), 23–54. [https://doi.org/10.1016/0010-0277\(90\)90017-E](https://doi.org/10.1016/0010-0277(90)90017-E)
- Gibbon, J., Church, R. M., & Meck, W. H. (1984). Scalar Timing in Memory. *Annals of the New York Academy of Sciences*, *423*(1), 52–77. <https://doi.org/10.1111/j.1749-6632.1984.tb23417.x>
- Gilardeau, S., Cirillo, R., Jazayeri, M., Dupuis, C., Wirth, S., & Duhamel, J. R. (2021). Two functions of the primate amygdala in social gaze. *Neuropsychologia*, *157*(May). <https://doi.org/10.1016/j.neuropsychologia.2021.107881>
- Gill, P. R., Mizumori, S. J. Y., & Smith, D. M. (2011). Hippocampal episode fields develop with learning. *Hippocampus*, *21*(11), 1240–1249. <https://doi.org/10.1002/hipo.20832>
- Girardeau, G., & Lopes-Dos-Santos, V. (2021). Brain neural patterns and the memory function of sleep. *Science*, *374*(6567), 560–564. <https://doi.org/10.1126/SCIENCE.ABI8370>
- Gobin, C., Wu, L., & Schwendt, M. (2020). Using rat operant delayed match-to-sample task to identify neural substrates recruited with increased working memory load. *Learning and Memory*, *27*(11), 467–476. <https://doi.org/10.1101/LM.052134.120>
- Gouvêa, T. S., Monteiro, T., Motiwala, A., Soares, S., Machens, C., & Paton, J. J. (2015). Striatal dynamics explain duration judgments. *eLife*, *4*(December2015), 1–14. <https://doi.org/10.7554/eLife.11386>

- Gouvêa, T. S., Monteiro, T., Soares, S., Atallah, B. V., & Paton, J. J. (2014). Ongoing behavior predicts perceptual report of interval duration. *Frontiers in Neurobotics*, *8*(MAR), 1–9. <https://doi.org/10.3389/fnbot.2014.00010>
- Grabot, L., Kononowicz, T. W., La Tour, T. D., Gramfort, A., Doyère, V., & Van Wassenhove, V. (2019). The strength of alpha-beta oscillatory coupling predicts motor timing precision. *Journal of Neuroscience*, *39*(17), 3277–3291. <https://doi.org/10.1523/JNEUROSCI.2473-18.2018>
- Grace, A. A., Floresco, S. B., Goto, Y., & Lodge, D. J. (2007). Regulation of firing of dopaminergic neurons and control of goal-directed behaviors. *Trends in Neurosciences*, *30*(5), 220–227. <https://doi.org/10.1016/j.tins.2007.03.003>
- Grahn, J. A., Parkinson, J. A., & Owen, A. M. (2008). The cognitive functions of the caudate nucleus. *Progress in Neurobiology*, *86*(3), 141–155. <https://doi.org/10.1016/j.pneurobio.2008.09.004>
- Green, L., Myerson, J., Holt, D. D., Slevin, J. R., & Estle, S. J. (2004). Discounting of Delayed Food Rewards in Pigeons and Rats: Is There a Magnitude Effect? *Journal of the Experimental Analysis of Behavior*, *81*(1), 39–50. <https://doi.org/10.1901/jeab.2004.81-39>
- Griggs, W. S., Kim, H. F., Ghazizadeh, A., Costello, M. G., Wall, K. M., & Hikosaka, O. (2017). Flexible and stable value coding areas in caudate head and tail receive anatomically distinct cortical and subcortical inputs. *Frontiers in Neuroanatomy*, *11*(November), 1–19. <https://doi.org/10.3389/fnana.2017.00106>
- Grondin, S., Meilleur-Wells, G., & Lachance, R. (1999). When to start explicit counting in a time-intervals discrimination task: A critical point in the timing process of humans. *Journal of Experimental Psychology: Human Perception and Performance*, *25*(4), 993–1004. <https://doi.org/10.1037//0096-1523.25.4.993>
- Guo, J., Zhang, Z., Sternad, D., & Song, J.-H. (2019). Improved motor timing enhances time perception. *Journal of Vision*, *19*(10), 2018b.
- Haber, S. N. (2014). The place of dopamine in the cortico-basal ganglia circuit. *Neuroscience*, *282*, 248–257. <https://doi.org/10.1016/j.neuroscience.2014.10.008>
- Haber, S. N. (2016). Corticostriatal circuitry. *Dialogues in Clinical Neuroscience*, *18*(1), 7–21. https://doi.org/10.1007/978-1-4614-6434-1_135-1
- Haber, S. N., Kim, K. S., Maily, P., & Calzavara, R. (2006). Reward-related cortical inputs define a large striatal region in primates that interface with associative cortical connections, providing a substrate for incentive-based learning. *Journal of Neuroscience*, *26*(32), 8368–8376. <https://doi.org/10.1523/JNEUROSCI.0271-06.2006>
- Hafele, J. C., & Keating, R. E. (1972). Around-the-World Atomic Clocks: Observed Relativistic Time Gains. *Science*, *177*.

- Hamamouche, K., & Cordes, S. (2019). A divergence of sub- and supra-second timing abilities in childhood and its relation to academic achievement. *Journal of Experimental Child Psychology*, *178*, 137–154. <https://doi.org/10.1016/j.jecp.2018.09.010>
- Hampson, R. E., Heyser, C. J., & Deadwyler, S. A. (1993). Hippocampal Cell Firing Correlates of Delayed-Match-to-Sample Performance in the Rat. *Behavioral Neuroscience*, *107*(5), 715–739. <https://doi.org/10.1037/0735-7044.107.5.715>
- Harrington, D. L., Castillo, G. N., Greenberg, P. A., Song, D. D., Lessig, S., Lee, R. R., & Rao, S. M. (2011). Neurobehavioral mechanisms of temporal processing deficits in Parkinson's disease. *PLoS ONE*, *6*(2). <https://doi.org/10.1371/journal.pone.0017461>
- Harrington, D. L., Zimbelman, J. L., Hinton, S. C., & Rao, S. M. (2010). Neural modulation of temporal encoding, maintenance, and decision processes. *Cerebral Cortex*, *20*(6), 1274–1285. <https://doi.org/10.1093/cercor/bhp194>
- Hastings, M. H., Maywood, E. S., & Brancaccio, M. (2018). Generation of circadian rhythms in the suprachiasmatic nucleus. *Nature Reviews Neuroscience*, *19*, 453–469. <https://doi.org/10.1038/s41583-018-0026-z>
- Hikosaka, O., Sakamoto, M., & Usui, S. (1989). Functional properties of monkey caudate neurons. I. Activities related to saccadic eye movements. *Journal of Neurophysiology*, *61*(4), 780–798. <https://doi.org/10.1152/jn.1989.61.4.780>
- Hikosaka, Okihide, Kim, H. F., Amita, H., Yasuda, M., Isoda, M., Tachibana, Y., & Yoshida, A. (2019). Direct and indirect pathways for choosing objects and actions. *European Journal of Neuroscience*, *49*(5), 637–645. <https://doi.org/10.1111/ejn.13876>.Direct
- Hitti, F. L., & Siegelbaum, S. A. (2014). The hippocampal CA2 region is essential for social memory. *Nature*, *508*(7494), 88–92. <https://doi.org/10.1038/nature13028>.The
- Holland, P. C., & Bouton, M. E. (1999). Hippocampus and context in classical conditioning. *Current Opinion in Neurobiology*, *9*(2), 195–202. [https://doi.org/10.1016/S0959-4388\(99\)80027-0](https://doi.org/10.1016/S0959-4388(99)80027-0)
- Hollerman, J. R., & Schultz, W. (1998). Dopamine neurons report an error in the temporal prediction of reward during learning. *Nature Neuroscience*, *1*(4), 304–309. <https://doi.org/10.1038/1124>
- Hori, Y., Mimura, K., Nagai, Y., Fujimoto, A., Oyama, K., Kikuchi, E., Inoue, K. I., Takada, M., Suhara, T., Richmond, B. J., & Minamimoto, T. (2021). Single caudate neurons encode temporally discounted value for formulating motivation for action. *ELife*, *10*(Cd), 1–23. <https://doi.org/10.7554/eLife.61248>
- Hoscheidt, S. M., Nadel, L., Payne, J., & Ryan, L. (2010). Hippocampal activation during retrieval of spatial context from episodic and semantic memory. *Behavioural Brain Research*, *212*(2), 121–132. <https://doi.org/10.1016/j.bbr.2010.04.010>

- Howard, E. (2001). The hippocampus and declarative memory: cognitive mechanisms and neural codes. *Behavioural Brain Research*, *127*(1–2), 199–207. <http://www.sciencedirect.com/science/article/pii/S0166432801003655>
- Howe, M. W., & Dombeck, D. D. (2016). Rapid signaling in distinct dopaminergic axons during locomotion and reward. *Nature*, *535*(7613), 505–510. <https://doi.org/10.1038/nature18942>.Rapid
- Howe, M. W., Tierney, P. L., Sandberg, S. G., Phillips, P. E. M., & Graybiel, A. M. (2013). Prolonged dopamine signalling in striatum signals proximity and value of distant rewards. *Nature*, *500*(7464), 575–579. <https://doi.org/10.1038/nature12475>
- Humphries, M. D., & Prescott, T. J. (2010). The ventral basal ganglia, a selection mechanism at the crossroads of space, strategy, and reward. *Progress in Neurobiology*, *90*(4), 385–417. <https://doi.org/10.1016/j.pneurobio.2009.11.003>
- Hunnicutt, B. J., Jongbloets, B. C., Birdsong, W. T., Gertz, K. J., Zhong, H., & Mao, T. (2016). A comprehensive excitatory input map of the striatum reveals novel functional organization. *ELife*, *5*(November2016), 1–32. <https://doi.org/10.7554/eLife.19103>
- Insausti, R., & Muñoz, M. (2001). Cortical projections of the non-entorhinal hippocampal formation in the cynomolgus monkey (*Macaca fascicularis*). *European Journal of Neuroscience*, *14*(3), 435–451. <https://doi.org/10.1046/j.0953-816X.2001.01662.x>
- Jacobs, N. S., Allen, T. A., Nguyen, N., & Fortin, N. J. (2013). Critical role of the hippocampus in memory for elapsed time. *Journal of Neuroscience*, *33*(34), 13888–13893. <https://doi.org/10.1523/JNEUROSCI.1733-13.2013>
- Jacobsen, C. . F., & Nissen, H. W. (1937). Studies of cerebral function in primates. IV. The effects of frontal lobe lesions on the delayed alternation habit in monkeys. *Journal of Comparative Psychology*, *23*(1), 55–135. <https://doi.org/10.1037/h0071866>
- Jagiello, J. A., Nonneman, A. J., Isaac, W. L., & Jackson-Smith, P. A. (1990). Hippocampal lesions impair rats' performance of a nonspatial matching-to-sample task. *Psychobiology*, *18*(1), 55–62. <https://doi.org/10.3758/BF03327215>
- Jahanshahi, M., Obeso, I., Rothwell, J. C., & Obeso, J. A. (2015). A fronto-striato-subthalamic-pallidal network for goal-directed and habitual inhibition. *Nature Reviews Neuroscience*, *16*(12), 719–732. <https://doi.org/10.1038/nrn4038>
- Janssen, P., & Shadlen, M. N. (2005). A representation of the hazard rate of elapsed time in macaque area LIP. *Nature Neuroscience*, *8*(2), 234–241. <https://doi.org/10.1038/nn1386>
- Jazayeri, M., & Shadlen, M. N. (2015). A Neural Mechanism for Sensing and Reproducing a Time Interval. *Current Biology*, *25*(20), 2599–2609. <https://doi.org/10.1016/j.cub.2015.08.038>

- Jellinger, K. A. (2015). Neuropathobiology of non-motor symptoms in Parkinson disease. *Journal of Neural Transmission*, 122(10), 1429–1440. <https://doi.org/10.1007/s00702-015-1405-5>
- Kamada, T., & Hata, T. (2021). Striatal dopamine D1 receptors control motivation to respond, but not interval timing, during the timing task. *Learning and Memory*, 28(1), 24–29. <https://doi.org/10.1101/LM.052266.120>
- Karlin, L. (1959). Reaction time as a function of foreperiod duration and variability. *Journal of Experimental Psychology*, 58(2), 185–191.
- Karmarkar, U. R., & Buonomano, D. V. (2003). Temporal specificity of perceptual learning in an auditory discrimination task. *Learning and Memory*, 10(2), 141–147. <https://doi.org/10.1101/lm.55503>
- Karmarkar, U. R., & Buonomano, D. V. (2007). Timing in the Absence of Clocks: Encoding Time in Neural Network States. *Neuron*, 53(3), 427–438. <https://doi.org/10.1016/j.neuron.2007.01.006>
- Kawagoe, R., Takikawa, Y., & Hikosaka, O. (1998). Expectation of reward modulates cognitive signals in the basal ganglia. *Nature Neuroscience*, 1(5), 411–416. <https://doi.org/10.1038/1625>
- Kesner, R. P., & Hunsaker, M. R. (2010). The temporal attributes of episodic memory. *Behavioural Brain Research*, 215(2), 299–309. <https://doi.org/10.1016/j.bbr.2009.12.029>
- Kesner, R. P., Hunsaker, M. R., & Gilbert, P. E. (2005). The role of CA1 in the acquisition of an object-trace-odor paired associate task. *Behavioral Neuroscience*, 119(3), 781–786. <https://doi.org/10.1037/0735-7044.119.3.781>
- Kim, H. F., & Hikosaka, O. (2015). Parallel basal ganglia circuits for voluntary and automatic behaviour to reach rewards. *Brain*, 138(7), 1776–1800. <https://doi.org/10.1093/brain/awv134>
- Kim, J., Ghim, J. W., Lee, J. H., & Jung, M. W. (2013). Neural correlates of interval timing in rodent prefrontal cortex. *Journal of Neuroscience*, 33(34), 13834–13847. <https://doi.org/10.1523/JNEUROSCI.1443-13.2013>
- Kim, S., Hwang, J., & Lee, D. (2008). Prefrontal Coding of Temporally Discounted Values during Intertemporal Choice. *Neuron*, 59(1), 161–172. <https://doi.org/10.1016/j.neuron.2008.05.010>
- Kimchi, E. Y., & Laubach, M. (2009). Dynamic encoding of action selection by the medial striatum. *Journal of Neuroscience*, 29(10), 3148–3159. <https://doi.org/10.1523/JNEUROSCI.5206-08.2009>
- Kimura, M., Kato, M., & Shimazaki, H. (1990). Physiological properties of projection neurons in the monkey striatum to the globus pallidus. *Experimental Brain Research*, 82, 672–676.
- Klein, É. (2007). About the confusion between the course of time and the arrow of time. *Foundations of Science*, 12(3), 203–221. <https://doi.org/10.1007/s10699-006-9103-2>
- Klein, S. B., Loftus, J., & Kihlstrom, J. F. (2002). Memory and temporal experience: The effects of episodic memory loss on an amnesic patient's ability to remember the past and imagine the future. *Social Cognition*, 20(5), 353–379. <https://doi.org/10.1521/soco.20.5.353.21125>

- Kononowicz, T. W., & van Wassenhove, V. (2016). In Search of Oscillatory Traces of the Internal Clock. *Frontiers in Psychology, 7*(February), 1–5. <https://doi.org/10.3389/fpsyg.2016.00224>
- Kraus, B. J., Robinson, R. J., White, J. A., Eichenbaum, H., & Hasselmo, M. E. (2013). Hippocampal “Time Cells”: Time versus Path Integration. *Neuron, 78*(6), 1090–1101. <https://doi.org/10.1016/j.neuron.2013.04.015>
- Kravitz, A. V., Freeze, B. S., Parker, P. R. L., Kay, K., Thwin, M. T., Deisseroth, K., & Kreitzer, A. C. (2010). Regulation of parkinsonian motor behaviours by optogenetic control of basal ganglia circuitry. *Nature, 466*(7306), 622–626. <https://doi.org/10.1038/nature09159>
- Kreitzer, A. C. (2009). Physiology and pharmacology of striatal neurons. *Annual Review of Neuroscience, 32*, 127–147. <https://doi.org/10.1146/annurev.neuro.051508.135422>
- Künzle, H. (1975). Bilateral projections from precentral motor cortex to the putamen and other parts of the basal ganglia. An autoradiographic study in *Macaca fascicularis*. *Brain Research, 88*(2), 195–209. [https://doi.org/10.1016/0006-8993\(75\)90384-4](https://doi.org/10.1016/0006-8993(75)90384-4)
- Laroche, S., Davis, S., & Jay, T. M. (2000). Plasticity at hippocampal to prefrontal cortex synapses: Dual roles in working memory and consolidation. *Hippocampus, 10*(4), 438–446. [https://doi.org/10.1002/1098-1063\(2000\)10:4<438::AID-HIPO10>3.0.CO;2-3](https://doi.org/10.1002/1098-1063(2000)10:4<438::AID-HIPO10>3.0.CO;2-3)
- Lavenex, P. B., Amaral, D. G., & Lavenex, P. (2006). Hippocampal lesion prevents spatial relational learning in adult macaque monkeys. *Journal of Neuroscience, 26*(17), 4546–4558. <https://doi.org/10.1523/JNEUROSCI.5412-05.2006>
- Lee, A. K., & Wilson, M. A. (2002). Memory of sequential experience in the hippocampus during slow wave sleep. *Neuron, 36*(6), 1183–1194. [https://doi.org/10.1016/S0896-6273\(02\)01096-6](https://doi.org/10.1016/S0896-6273(02)01096-6)
- Lehéricy, S., Ducros, M., Krainik, A., Francois, C., Van De Moortele, P. F., Ugurbil, K., & Kim, D. S. (2004). 3-D diffusion tensor axonal tracking shows distinct SMA and pre-SMA projections to the human striatum. *Cerebral Cortex, 14*(12), 1302–1309. <https://doi.org/10.1093/cercor/bhh091>
- Leon, M. I., & Shadlen, M. N. (2003). Representation of Time by Neurons in the Posterior Parietal Cortex of the Macaque. *Neuron, 38*, 317–327.
- Lever, C., Burton, S., Jeewajee, A., O’Keefe, J., & Burgess, N. (2009). Boundary vector cells in the subiculum of the hippocampal formation. *Journal of Neuroscience, 29*(31), 9771–9777. <https://doi.org/10.1523/JNEUROSCI.1319-09.2009>
- Lewis, P. A., & Miall, R. C. (2003). Distinct systems for automatic and cognitively controlled time measurement: Evidence from neuroimaging. *Current Opinion in Neurobiology, 13*(2), 250–255. [https://doi.org/10.1016/S0959-4388\(03\)00036-9](https://doi.org/10.1016/S0959-4388(03)00036-9)
- Lind, J., Enquist, M., & Ghirlanda, S. (2015). Animal memory: A review of delayed matching-to-sample data. *Behavioural Processes, 117*, 52–58. <https://doi.org/10.1016/j.beproc.2014.11.019>

- Lisman, J. E., & Grace, A. A. (2005). The hippocampal-VTA loop: Controlling the entry of information into long-term memory. *Neuron*, *46*(5), 703–713. <https://doi.org/10.1016/j.neuron.2005.05.002>
- Lopez-Rojas, J., de Solis, C. A., Leroy, F., Kandel, E. R., & Siegelbaum, S. A. (2022). A direct lateral entorhinal cortex to hippocampal CA2 circuit conveys social information required for social memory. *Neuron*, *110*(9), 1559-1572.e4. <https://doi.org/10.1016/j.neuron.2022.01.028>
- Lopez-Rojas, J., & Kreutz, M. R. (2016). Mature granule cells of the dentate gyrus—Passive bystanders or principal performers in hippocampal function? *Neuroscience and Biobehavioral Reviews*, *64*, 167–174. <https://doi.org/10.1016/j.neubiorev.2016.02.021>
- Louie, K., & Wilson, M. A. (2001). Temporally structured replay of awake hippocampal ensemble activity during rapid eye movement sleep. *Neuron*, *29*(1), 145–156. [https://doi.org/10.1016/S0896-6273\(01\)00186-6](https://doi.org/10.1016/S0896-6273(01)00186-6)
- Macar, F., Lejeune, H., Bonnet, M., Ferrara, A., Pouthas, V., Vidal, F., & Maquet, P. (2002). Activation of the supplementary motor area and of attentional networks during temporal processing. *Experimental Brain Research*, *142*(4), 475–485. <https://doi.org/10.1007/s00221-001-0953-0>
- MacDonald, C. J. (2014). Prospective and retrospective duration memory in the hippocampus: Is time in the foreground or background? *Philosophical Transactions of the Royal Society B: Biological Sciences*, *369*(1637). <https://doi.org/10.1098/rstb.2012.0463>
- MacDonald, C. J., Carrow, S., Place, R., & Eichenbaum, H. (2013). Distinct hippocampal time cell sequences represent odor memories in immobilized rats. *Journal of Neuroscience*, *33*(36), 14607–14616. <https://doi.org/10.1523/JNEUROSCI.1537-13.2013>
- MacDonald, C. J., Lepage, K. Q., Eden, U. T., & Eichenbaum, H. (2011). Hippocampal “Time Cells” bridge the gap in memory for discontinuous events. *Neuron*, *71*(4), 737–749. <https://doi.org/10.1016/j.neuron.2011.07.012>
- Macpherson, T., Morita, M., & Hikida, T. (2014). Striatal direct and indirect pathways control decision-making behavior. *Frontiers in Psychology*, *5*(NOV), 1–7. <https://doi.org/10.3389/fpsyg.2014.01301>
- Maimon, G., & Assad, J. A. (2006). A cognitive signal for the proactive timing of action in macaque LIP. *Nature Neuroscience*, *9*(7), 948–955. <https://doi.org/10.1038/nn1716>
- Mankin, E. A., Sparks, F. T., Slayyeh, B., Sutherland, R. J., Leutgeb, S., & Leutgeb, J. K. (2012). Neuronal code for extended time in the hippocampus. *Proceedings of the National Academy of Sciences of the United States of America*, *109*(47), 19462–19467. <https://doi.org/10.1073/pnas.1214107109>
- Manns, J. R., Howard, M. W., & Eichenbaum, H. (2007). Gradual Changes in Hippocampal Activity Support Remembering the Order of Events. *Neuron*, *56*(3), 530–540. <https://doi.org/10.1016/j.neuron.2007.08.017>

- Marche, K., Martel, A. C., & Apicella, P. (2017). Differences between dorsal and ventral striatum in the sensitivity of tonically active neurons to rewarding events. *Frontiers in Systems Neuroscience*, *11*(July), 1–12. <https://doi.org/10.3389/fnsys.2017.00052>
- Marcos, E., Tsujimoto, S., & Genovesio, A. (2016). Event- and time-dependent decline of outcome information in the primate prefrontal cortex. *Scientific Reports*, *6*(November 2015), 1–9. <https://doi.org/10.1038/srep25622>
- Maricq, A. V., & Church, R. M. (1983). The differential effects of haloperidol and methamphetamine on time estimation in the rat. *Psychopharmacology*, *79*(1), 10–15. <https://doi.org/10.1007/BF00433008>
- Martel, A. C., & Apicella, P. (2021). Temporal processing in the striatum: Interplay between midbrain dopamine neurons and striatal cholinergic interneurons. *European Journal of Neuroscience*, *53*(7), 2090–2099. <https://doi.org/10.1111/ejn.14741>
- Martinez, E., Pasquereau, B., Saga, Y., Météreau, É., & Tremblay, L. (2020). The anterior caudate nucleus supports impulsive choices triggered by pramipexole. *Movement Disorders*, *35*(2), 296–305. <https://doi.org/10.1002/mds.27898>
- Matell, M. S., & Meck, W. H. (2000). Neuropsychological mechanisms of interval timing behavior. *BioEssays*, *22*(1), 94–103. [https://doi.org/10.1002/\(SICI\)1521-1878\(200001\)22:1<94::AID-BIES14>3.0.CO;2-E](https://doi.org/10.1002/(SICI)1521-1878(200001)22:1<94::AID-BIES14>3.0.CO;2-E)
- Matell, M. S., & Meck, W. H. (2004). Cortico-striatal circuits and interval timing: Coincidence detection of oscillatory processes. *Cognitive Brain Research*, *21*(2), 139–170. <https://doi.org/10.1016/j.cogbrainres.2004.06.012>
- Matell, M. S., Meck, W. H., & Nicolelis, M. A. L. (2003). Interval timing and the encoding of signal duration by ensembles of cortical and striatal neurons. *Behavioral Neuroscience*, *117*(4), 760–773. <https://doi.org/10.1037/0735-7044.117.4.760>
- Mau, W., Sullivan, D. W., Kinsky, N. R., Hasselmo, M. E., Howard, M. W., & Eichenbaum, H. (2018). The Same Hippocampal CA1 Population Simultaneously Codes Temporal Information over Multiple Timescales. *Current Biology*, *28*(10), 1499–1508.e4. <https://doi.org/10.1016/j.cub.2018.03.051>
- Mauk, M. D., & Buonomano, D. V. (2004). The neural basis of temporal processing. *Annual Review of Neuroscience*, *27*, 307–340. <https://doi.org/10.1146/annurev.neuro.27.070203.144247>
- Meck, W. H. (1996). Neuropharmacology of timing and time perception. *Cognitive Brain Research*, *3*(3–4), 227–242. [https://doi.org/10.1016/0926-6410\(96\)00009-2](https://doi.org/10.1016/0926-6410(96)00009-2)
- Meck, W. H. (2005). Neuropsychology of timing and time perception. *Brain and Cognition*, *58*(1), 1–8. <https://doi.org/10.1016/j.bandc.2004.09.004>
- Meck, W. H., & Church, R. M. (1984). Simultaneous Temporal Processing. *Journal of Experimental Psychology: Animal Behavior Processes*, *10*(1), 1–29. <https://doi.org/10.1037/0097-7403.29.1.c2>

- Meirhaeghe, N., Sohn, H., & Jazayeri, M. (2021). A precise and adaptive neural mechanism for predictive temporal processing in the frontal cortex. *Neuron*, *109*(18), 2995-3011.e5. <https://doi.org/10.1016/j.neuron.2021.08.025>
- Melissa Flesher, M., Butt, A. E., & Kinney-Hurd, B. L. (2011). Differential acetylcholine release in the prefrontal cortex and hippocampus during pavlovian trace and delay conditioning. *Neurobiology of Learning and Memory*, *96*(2), 181–191. <https://doi.org/10.1016/j.nlm.2011.04.008>
- Mello, G. B. M., Soares, S., & Paton, J. J. (2015). A scalable population code for time in the striatum. *Current Biology*, *25*(9), 1113–1122. <https://doi.org/10.1016/j.cub.2015.02.036>
- Mendez, J. C., Prado, L., Mendoza, G., & Merchant, H. (2011). Temporal and spatial categorization in human and non-human primates. *Frontiers in Integrative Neuroscience*, *5*(September), 1–10. <https://doi.org/10.3389/fnint.2011.00050>
- Mendoza, G., Méndez, J. C., Pérez, O., Prado, L., & Merchant, H. (2018). Neural basis for categorical boundaries in the primate pre-SMA during relative categorization of time intervals. *Nature Communications*, *9*(1). <https://doi.org/10.1038/s41467-018-03482-8>
- Merritt, D. J., Casasanto, D., & Brannon, E. M. (2010). Do monkeys think in metaphors? Representations of space and time in monkeys and humans. *Cognition*, *117*(2), 191–202. <https://doi.org/10.1016/j.cognition.2010.08.011>
- Messinger, A., Squire, L. R., Zola, S. M., & Albright, T. D. (2001). Neuronal representations of stimulus associations develop in the temporal lobe during learning. *Proceedings of the National Academy of Sciences of the United States of America*, *98*(21), 12239–12244. <https://doi.org/10.1073/pnas.211431098>
- Miall, C. (1989). The Storage of Time Intervals Using Oscillating Neurons. *Neural Computation*, *3*71(Jeffress 1948), 359–371.
- Milivojevic, B., & Doeller, C. F. (2013). Mnemonic networks in the hippocampal formation: From spatial maps to temporal and conceptual codes. *Journal of Experimental Psychology: General*, *142*(4), 1231–1241. <https://doi.org/10.1037/a0033746>
- Minamimoto, T., La Camera, G., & Richmond, B. J. (2009). Measuring and modeling the interaction among reward size, delay to reward, and satiation level on motivation in monkeys. *Journal of Neurophysiology*, *101*(1), 437–447. <https://doi.org/10.1152/jn.90959.2008>
- Mita, A., Mushiake, H., Shima, K., Matsuzaka, Y., & Tanji, J. (2009). Interval time coding by neurons in the presupplementary and supplementary motor areas. *Nature Neuroscience*, *12*(4), 502–507. <https://doi.org/10.1038/nn.2272>
- Miyachi, S., Hikosaka, O., & Lu, X. (2002). Differential activation of monkey striatal neurons in the early and late stages of procedural learning. *Experimental Brain Research*, *146*(1), 122–126. <https://doi.org/10.1007/s00221-002-1213-7>

- Miyachi, S., Hikosaka, O., Miyashita, K., Kárádi, Z., & Rand, M. K. (1997). Differential roles of monkey striatum in learning of sequential hand movement. *Experimental Brain Research*, *115*(1), 1–5. <https://doi.org/10.1007/PL00005669>
- Montague, P. R., & Sejnowski, T. J. (1994). The predictive brain: Temporal coincidence and temporal order in synaptic learning mechanisms. *Learning Memory*, *1*(1), 1–33. <https://doi.org/10.1101/lm.1.1.1>
- Moscovitch, M., Rosenbaum, R. S., Gilboa, A., Addis, D. R., Westmacott, R., Grady, C., McAndrews, M. P., Levine, B., Black, S., Winocur, G., & Nadel, L. (2005). Functional neuroanatomy of remote episodic, semantic and spatial memory: A unified account based on multiple trace theory. *Journal of Anatomy*, *207*(1), 35–66. <https://doi.org/10.1111/j.1469-7580.2005.00421.x>
- Murray, J. D., Bernacchia, A., Freedman, D. J., Romo, R., Wallis, J. D., Cai, X., Padoa-Schioppa, C., Pasternak, T., Seo, H., Lee, D., & Wang, X. J. (2014). A hierarchy of intrinsic timescales across primate cortex. *Nature Neuroscience*, *17*(12), 1661–1663. <https://doi.org/10.1038/nn.3862>
- Nakazawa, K., McHugh, T. J., Wilson, M. A., & Tonegawa, S. (2004). NMDA receptors, place cells and hippocampal spatial memory. *Nature Reviews Neuroscience*, *5*(5), 361–372. <https://doi.org/10.1038/nrn1385>
- Narayanan, N. S., & Laubach, M. (2009). Delay activity in rodent frontal cortex during a simple reaction time task. *Journal of Neurophysiology*, *101*(6), 2859–2871. <https://doi.org/10.1152/jn.90615.2008>
- Naya, Y., Yoshida, M., & Miyashita, Y. (2001). Backward spreading of memory-retrieval signal in the primate temporal cortex. *Science*, *291*(5504), 661–664. <https://doi.org/10.1126/science.291.5504.661>
- Naya, Yuji, Chen, H., Yang, C., & Suzuki, W. A. (2017). Contributions of primate prefrontal cortex and medial temporal lobe to temporal-order memory. *Proceedings of the National Academy of Sciences of the United States of America*, *114*(51), 13555–13560. <https://doi.org/10.1073/pnas.1712711114>
- Naya, Yuji, & Suzuki, W. A. (2011). Integrating what and when across the primate medial temporal lobe. *Science*, *333*(6043), 773–776. <https://doi.org/10.1126/science.1206773>
- Naya, Yuji, Yoshida, M., Takeda, M., Fujimichi, R., & Miyashita, Y. (2003). Delay-period activities in two subdivisions of monkey inferotemporal cortex during pair association memory task. *European Journal of Neuroscience*, *18*(10), 2915–2918. <https://doi.org/10.1111/j.1460-9568.2003.03020.x>
- Nicoll, R. A., Kauer, J. A., & Malenka, R. C. (1988). The current excitement in long term potentiation. *Neuron*, *1*(2), 97–103. [https://doi.org/10.1016/0896-6273\(88\)90193-6](https://doi.org/10.1016/0896-6273(88)90193-6)

- O'Connor, D. H., Krubitzer, L., & Bensmaia, S. (2021). Of mice and monkeys: Somatosensory processing in two prominent animal models. *Progress in Neurobiology*, 201, 102008. <https://doi.org/10.1016/j.pneurobio.2021.102008>
- O'Doherty, J. P., Cockburn, J., & Pauli, Wolfgang, M. (2017). Learning, Reward, and Decision Making. *Annual Review of Psychology*, 68, 73–100. <https://doi.org/10.1146/annurev-psych-010416-044216>.Learning
- O'Keefe, J., & Conway, D. H. (1978). Hippocampal place units in the freely moving rat: Why they fire where they fire. *Experimental Brain Research*, 31(4), 573–590. <https://doi.org/10.1007/BF00239813>
- O'Keefe, J., & Dostrovsky, J. (1971). The hippocampus as a spatial map. Preliminary evidence from unit activity in the freely-moving rat. *Brain Research*, 34(1), 171–175. <http://www.ncbi.nlm.nih.gov/pubmed/5124915>
- O'Keefe, John. (1990). A computational theory of the hippocampal cognitive map. *Progress in Brain Research*, 83, 301–312. [https://doi.org/10.1016/S0079-6123\(08\)61258-3](https://doi.org/10.1016/S0079-6123(08)61258-3)
- Ohmae, S., Kunimatsu, J., & Tanaka, M. (2017). Cerebellar roles in self-timing for sub- and supra-second intervals. *Journal of Neuroscience*, 37(13), 3511–3522. <https://doi.org/10.1523/JNEUROSCI.2221-16.2017>
- Okuda, J., Fujii, T., Ohtake, H., Tsukiura, T., Tanji, K., Suzuki, K., Kawashima, R., Fukuda, H., Itoh, M., & Yamadori, A. (2003). Thinking of the future and past: The roles of the frontal pole and the medial temporal lobes. *NeuroImage*, 19(4), 1369–1380. [https://doi.org/10.1016/S1053-8119\(03\)00179-4](https://doi.org/10.1016/S1053-8119(03)00179-4)
- Oprisan, S. A., Aft, T., Buhusi, M., & Buhusi, C. V. (2018). Scalar timing in memory: A temporal map in the hippocampus. *Journal of Theoretical Biology*, 438, 133–142. <https://doi.org/10.1016/j.jtbi.2017.11.012>
- Oprisan, S. A., & Buhusi, C. V. (2014). What is all the noise about in interval timing? *Philosophical Transactions of the Royal Society B: Biological Sciences*, 369(1637). <https://doi.org/10.1098/rstb.2012.0459>
- Oprisan, S. A., Dix, S., & Buhusi, C. V. (2014). Phase resetting and its implications for interval timing with intruders. *Behavioural Processes*, 101, 146–153. <https://doi.org/10.1016/j.beproc.2013.09.005>
- Otto, T., & Eichenbaum, H. (1992). Neuronal activity in the hippocampus during delayed non-match to sample performance in rats: Evidence for hippocampal processing in recognition memory. *Hippocampus*, 2(3), 323–334. <https://doi.org/10.1002/hipo.450020310>

- Parker, K. L., Lamichhane, D., Caetano, M. S., & Narayanan, N. S. (2013). Executive dysfunction in Parkinson's disease and timing deficits. *Frontiers in Integrative Neuroscience*, 7(OCT), 1–9. <https://doi.org/10.3389/fnint.2013.00075>
- Pastalkova, E., Itskov, V., Amarasingham, A., & Buzsáki, G. (2008). Internally generated cell assembly sequences in the rat hippocampus. *Science*, 321(5894), 1322–1327. <https://doi.org/10.1126/science.1159775>
- Paton, J. J., & Buonomano, D. V. (2018). The Neural Basis of Timing: Distributed Mechanisms for Diverse Functions. *Neuron*, 98(4), 687–705. <https://doi.org/10.1016/j.neuron.2018.03.045>
- Pernía-Andrade, A. J., Wenger, N., Esposito, M. S., & Tovote, P. (2021). Circuits for State-Dependent Modulation of Locomotion. *Frontiers in Human Neuroscience*, 15(November), 1–20. <https://doi.org/10.3389/fnhum.2021.745689>
- Pezzulo, G., van der Meer, M. A. A., Lansink, C. S., & Pennartz, C. M. A. (2014). Internally generated sequences in learning and executing goal-directed behavior. *Trends in Cognitive Sciences*, 18(12), 647–657. <https://doi.org/10.1016/j.tics.2014.06.011>
- Phillips, A. G. (1984). Brain reward circuitry: A case for separate systems. *Brain Research Bulletin*, 12(2), 195–201. [https://doi.org/10.1016/0361-9230\(84\)90189-8](https://doi.org/10.1016/0361-9230(84)90189-8)
- Pilkiw, M., & Takehara-Nishiuchi, K. (2018). Neural representations of time-linked memory. *Neurobiology of Learning and Memory*, 153(October 2017), 57–70. <https://doi.org/10.1016/j.nlm.2018.03.024>
- Plenz, D. (2003). When inhibition goes incognito: Feedback interaction between spiny projection neurons in striatal function. *Trends in Neurosciences*, 26(8), 436–443. [https://doi.org/10.1016/S0166-2236\(03\)00196-6](https://doi.org/10.1016/S0166-2236(03)00196-6)
- Polti, I., Martin, B., & Van Wassenhove, V. (2018). The effect of attention and working memory on the estimation of elapsed time. *Scientific Reports*, 8(1), 1–11. <https://doi.org/10.1038/s41598-018-25119-y>
- Pöppel, E. (2009). Pre-semantically defined temporal windows for cognitive processing. *Philosophical Transactions of the Royal Society B: Biological Sciences*, 364(1525), 1887–1896. <https://doi.org/10.1098/rstb.2009.0015>
- Poucet, B., Sargolini, F., Song, E. Y., Hangya, B., Fox, S., & Muller, R. U. (2014). Independence of landmark and selfmotion-guided navigation: A different role for grid cells. *Philosophical Transactions of the Royal Society B: Biological Sciences*, 369(1635). <https://doi.org/10.1098/rstb.2013.0370>
- Quintana, J., & Fuster, J. M. (1999). From perception to action: Temporal integrative functions of prefrontal and parietal neurons. *Cerebral Cortex*, 9(3), 213–221. <https://doi.org/10.1093/cercor/9.3.213>

- Quiroga, Quian R. (2020). No Pattern Separation in the Human Hippocampus. *Trends in Cognitive Sciences*, 24(12), 994–1007. <https://doi.org/10.1016/j.tics.2020.09.012>
- Quiroga, R. Q., Reddy, L., Kreiman, G., Koch, C., & Fried, I. (2005). Invariant visual representation by single neurons in the human brain. *Nature*, 435(7045), 1102–1107. <https://doi.org/10.1038/nature03687>
- Rakitin, B. C., Penney, T. B., Gibbon, J., Malapani, C., Hinton, S. C., & Meck, W. H. (1998). Scalar expectancy theory and peak-interval timing in humans. *Journal of Experimental Psychology: Animal Behavior Processes*, 24(1), 15–33. <https://doi.org/10.1037/0097-7403.24.1.15>
- Ranganath, C., & Hsieh, L. T. (2016). The hippocampus: A special place for time. *Annals of the New York Academy of Sciences*, 1369(1), 93–110. <https://doi.org/10.1111/nyas.13043>
- Rao, S. M., Mayer, A. R., & Harrington, D. L. (2001). The evolution of brain activation during temporal processing. *Nature Neuroscience*, 4(3), 317–323.
- Reddy, L., Poncet, M., Self, M. W., Peters, J. C., Douw, L., Van Dellen, E., Claus, S., Reijneveld, J. C., Baayen, J. C., & Roelfsema, P. R. (2015). Learning of anticipatory responses in single neurons of the human medial temporal lobe. *Nature Communications*, 6. <https://doi.org/10.1038/ncomms9556>
- Reddy, L., Zoefel, B., Possel, J. K., Peters, J., Dijksterhuis, D. E., Poncet, M., van Straaten, E. C. W., Baayen, J. C., Idema, S., & Self, M. W. (2021). Human hippocampal neurons track moments in a sequence of events. *Journal of Neuroscience*, 41(31), 674–6725. <https://doi.org/10.1523/JNEUROSCI.3157-20.2021>
- Rescola, R. A., & Wagner, A. R. (1972). *A theory of Pavlovian conditioning: The effectiveness of reinforcement and Nonreinforcement*. January 1972, 64–99.
- Reutimann, J., Yakovlev, V., Fusi, S., & Senn, W. (2004). Climbing Neuronal Activity as an Event-Based Cortical Representation of Time. *Journal of Neuroscience*, 24(13), 3295–3303. <https://doi.org/10.1523/JNEUROSCI.4098-03.2004>
- Riesen, J. M., & Schnider, A. (2001). Time estimation in Parkinson's disease: normal long duration estimation despite impaired short duration discrimination. *Journal of Neurology*, 248, 27–35.
- Riley, M. R., & Constantinidis, C. (2016). Role of prefrontal persistent activity in working memory. *Frontiers in Systems Neuroscience*, 9(JAN2016), 1–14. <https://doi.org/10.3389/fnsys.2015.00181>
- Robinson, N. T. M., Priestley, J. B., Rueckemann, J. W., Garcia, A. D., Smeglin, V. A., Marino, F. A., & Eichenbaum, H. (2017). Medial Entorhinal Cortex Selectively Supports Temporal Coding by Hippocampal Neurons. *Neuron*, 94(3), 677–688.e6. <https://doi.org/10.1016/j.neuron.2017.04.003>

- Rockland, K. S., & Van Hoesen, G. W. (1999). Some temporal and parietal cortical connections converge in CA1 of the primate hippocampus. *Cerebral Cortex*, 9(3), 232–237. <https://doi.org/10.1093/cercor/9.3.232>
- Rolls, E. T. (1991). Functions of the primate hippocampus in spatial and nonspatial memory. *Hippocampus*, 1(3), 258–261. <https://doi.org/10.1002/hipo.450010310>
- Rolls, E. T. (1999). Spatial view cells and the representation of place in the primate hippocampus. *Hippocampus*, 9(4), 467–480. [https://doi.org/10.1002/\(SICI\)1098-1063\(1999\)9:4<467::AID-HIPO13>3.0.CO;2-F](https://doi.org/10.1002/(SICI)1098-1063(1999)9:4<467::AID-HIPO13>3.0.CO;2-F)
- Rolls, E. T. (2010). A computational theory of episodic memory formation in the hippocampus. *Behavioural Brain Research*, 215(2), 180–196. <https://doi.org/10.1016/j.bbr.2010.03.027>
- Rolls, E. T. (2021). On pattern separation in the primate, including human, hippocampus. *Trends in Cognitive Sciences*, 25(11), 920–922. <https://doi.org/10.1016/j.tics.2021.07.004>
- Rolls, E. T., & Mills, P. (2019). The Generation of Time in the Hippocampal Memory System. *Cell Reports*, 28(7), 1649-1658.e6. <https://doi.org/10.1016/j.celrep.2019.07.042>
- Rolls, E. T., & Wirth, S. (2018). Spatial representations in the primate hippocampus, and their functions in memory and navigation. *Progress in Neurobiology*, 171, 90–113. <https://doi.org/10.1016/j.pneurobio.2018.09.004>
- Roux, S., Coulmance, M., & Riehle, A. (2003). Context-related representation of timing processes in monkey motor cortex. *European Journal of Neuroscience*, 18(4), 1011–1016. <https://doi.org/10.1046/j.1460-9568.2003.02792.x>
- Rovelli, C. (2017). *L'ordine del tempo* (Piccola Biblioteca Adelphi (ed.); 15th ed.).
- Sabariego, M., Schönwald, A., Boublil, B. L., Zimmerman, D. T., Ahmadi, S., Gonzalez, N., Leibold, C., Clark, R. E., Leutgeb, J. K., & Leutgeb, S. (2019). Time Cells in the Hippocampus Are Neither Dependent on Medial Entorhinal Cortex Inputs nor Necessary for Spatial Working Memory. *Neuron*, 102(6), 1235-1248.e5. <https://doi.org/10.1016/j.neuron.2019.04.005>
- Safaie, M., Jurado-Parras, M. T., Sarno, S., Louis, J., Karoutchi, C., Petit, L. F., Pasquet, M. O., Eloy, C., & Robbe, D. (2020). Turning the body into a clock: Accurate timing is facilitated by simple stereotyped interactions with the environment. *Proceedings of the National Academy of Sciences of the United States of America*, 117(23), 13084–13093. <https://doi.org/10.1073/pnas.1921226117>
- Sakon, J. J., Naya, Y., Wirth, S., & Suzuki, W. A. (2014). Context-dependent incremental timing cells in the primate hippocampus. *Proceedings of the National Academy of Sciences of the United States of America*, 111(51), 18351–18356. <https://doi.org/10.1073/pnas.1417827111>

- Sales-Carbonell, C., Taouali, W., Khalki, L., Pasquet, M. O., Petit, L. F., Moreau, T., Rueda-Orozco, P. E., & Robbe, D. (2018). No Discrete Start/Stop Signals in the Dorsal Striatum of Mice Performing a Learned Action. *Current Biology*, 28(19), 3044–3055.e5. <https://doi.org/10.1016/j.cub.2018.07.038>
- Salz, D. M., Tiganj, Z., Khasnabish, S., Kohley, A., Sheehan, D., Howard, M. W., & Eichenbaum, H. (2016). Time cells in hippocampal area CA3. *Journal of Neuroscience*, 36(28), 7476–7484. <https://doi.org/10.1523/JNEUROSCI.0087-16.2016>
- Samejima, K., Ueda, Y., Doya, K., & Kimura, M. (2005). Representation of action-specific reward values in the striatum. *Science*, 310(5752), 1337–1340. <https://doi.org/10.1126/science.1115270>
- Sarno, S., De Lafuente, V., Romo, R., & Parga, N. (2017). Dopamine reward prediction error signal codes the temporal evaluation of a perceptual decision report. *Proceedings of the National Academy of Sciences of the United States of America*, 114(48), E10494–E10503. <https://doi.org/10.1073/pnas.1712479114>
- Saund, J., Dautan, D., Rostron, C., Urcelay, G. P., & Gerdjikov, T. V. (2017). Thalamic inputs to dorsomedial striatum are involved in inhibitory control: evidence from the five-choice serial reaction time task in rats. *Psychopharmacology*, 234(16), 2399–2407. <https://doi.org/10.1007/s00213-017-4627-4>
- Schiller, D., Eichenbaum, H., Buffalo, E. A., Davachi, L., Foster, D. J., Leutgeb, S., & Ranganath, C. (2015). Memory and space: Towards an understanding of the cognitive map. *Journal of Neuroscience*, 35(41), 13904–13911. <https://doi.org/10.1523/JNEUROSCI.2618-15.2015>
- Schmidt, B., Marrone, D. F., & Markus, E. J. (2012). Disambiguating the similar: The dentate gyrus and pattern separation. *Behavioural Brain Research*, 226(1), 56–65. <https://doi.org/10.1016/j.bbr.2011.08.039>
- Schultz, W., Apicella, P., & Ljungberg, T. (1993). Responses of monkey dopamine neurons to reward and conditioned stimuli during successive steps of learning a delayed response task. *Journal of Neuroscience*, 13(3), 900–913. <https://doi.org/10.1523/jneurosci.13-03-00900.1993>
- Schultz, W., Apicella, P., Scarnati, E., & Ljungberg, T. (1992). Neuronal Activity in Monkey Ventral Striatum Related to the Expectation of Reward. *Journal of Neuroscience*, 12(12), 4595–4610. <https://doi.org/10.1523/jneurosci.12-12-04595.1992>
- Schultz, W., Dayan, P., & Montague, P. R. (1997). A neural substrate of prediction and reward. *Science*, 275(5306), 1593–1599. <https://doi.org/10.1126/science.275.5306.1593>
- Schultz, Wolfram. (2007). Behavioral dopamine signals. *Trends in Neurosciences*, 30(5), 203–210. <https://doi.org/10.1016/j.tins.2007.03.007>
- Schultz, Wolfram. (2016). Reward functions of the basal ganglia. *Journal of Neural Transmission*, 123(7), 679–693. <https://doi.org/10.1007/s00702-016-1510-0>

- Schultz, Wolfram, Tremblay, L., & Hollerman, J. R. (2003). Changes in behavior-related neuronal activity in the striatum during learning. *Trends in Neurosciences*, 26(6), 321–328. [https://doi.org/10.1016/S0166-2236\(03\)00122-X](https://doi.org/10.1016/S0166-2236(03)00122-X)
- Scoville, W. B., & Milner, B. (1957). Loss of recent memory after bilateral hippocampal lesions. *The Journal of Neurology, Neurosurgery, and Psychiatry*, 20(11), 11–21. <https://doi.org/10.1176/jnp.12.1.103-a>
- Seger, C. A., & Spiering, B. J. (2011). A critical review of habit learning and the basal ganglia. *Frontiers in Systems Neuroscience*, 5(AUGUST 2011), 1–9. <https://doi.org/10.3389/fnsys.2011.00066>
- Selemon, L., & Goldman-Rakic, P. (1985). Longitudinal Topography and Interdigitation Projections in the Rhesus Monkey. *The Journal of Neuroscience*, 5(3), 776–794. <http://www.jneurosci.org/content/jneuro/5/3/776.full.pdf>
- Setogawa, T., Mizuhiki, T., Matsumoto, N., Akizawa, F., Kuboki, R., Richmond, B. J., & Shidara, M. (2019). Neurons in the monkey orbitofrontal cortex mediate reward value computation and decision-making. *Communications Biology*, 2(1), 1–9. <https://doi.org/10.1038/s42003-019-0363-0>
- Shahbaba, B., Li, L., Agostinelli, F., Saraf, M., Cooper, K. W., Haghverdian, D., Elias, G. A., Baldi, P., & Fortin, N. J. (2022). Hippocampal ensembles represent sequential relationships among an extended sequence of nonspatial events. *Nature Communications*, 13(1), 1–17. <https://doi.org/10.1038/s41467-022-28057-6>
- Shankar, K. H., & Howard, M. W. (2012). A scale-invariant internal representation of time. *Neural Computation*, 24(1), 134–193. https://doi.org/10.1162/NECO_a_00212
- Shidara, M., & Richmond, B. J. (2002). Anterior cingulate: Single neuronal signals related to degree of reward expectancy. *Science*, 296(5573), 1709–1711. <https://doi.org/10.1126/science.1069504>
- Shikano, Y., Ikegaya, Y., & Sasaki, T. (2021). Minute-encoding neurons in hippocampal-striatal circuits. *Current Biology*, 31(7), 1438-1449.e6. <https://doi.org/10.1016/j.cub.2021.01.032>
- Shimbo, A., Izawa, E. I., & Fujisawa, S. (2021). Scalable representation of time in the hippocampus. *Science Advances*, 7(6). <https://doi.org/10.1126/sciadv.abd7013>
- Skaggs, W. E., McNaughton, B. L., & Gothard, K. M. (1992). An Information-Theoretic Approach to Deciphering the Hippocampal Code. *Advances in Neural Information Processing Systems* 5, 1030–1038.
- Sliwa, J., Plante, A., Duhamel, J. R., & Wirth, S. (2016). Independent Neuronal Representation of Facial and Vocal Identity in the Monkey Hippocampus and Inferotemporal Cortex. *Cerebral Cortex*, 26(3), 950–966. <https://doi.org/10.1093/cercor/bhu257>

- Sloan, H. L., Döbrössy, M., & Dunnett, S. B. (2006). Hippocampal lesions impair performance on a conditional delayed matching and non-matching to position task in the rat. *Behavioural Brain Research*, *171*(2), 240–250. <https://doi.org/10.1016/j.bbr.2006.03.042>
- Soares, S., Atallah, B. V., & Paton, J. J. (2016). Midbrain dopamine neurons control judgment of time. *Science*, *354*(6317), 1273–1277. <https://doi.org/10.1126/science.aah5234>
- Sørensen, K. E., & Witter, M. P. (1983). Entorhinal efferents reach the caudato-putamen. *Neuroscience Letters*, *35*, 259–264.
- Staddon, J. E. R. (2005). Interval timing: Memory, not a clock. *Trends in Cognitive Sciences*, *9*(7), 312–314. <https://doi.org/10.1016/j.tics.2005.05.013>
- Staddon, J. E. R., & Higa, J. J. (1999). Time and Memory: Towards a Pacemaker-Free Theory of Interval Timing. *Journal of the Experimental Analysis of Behavior*, *71*(2), 215–251. <https://doi.org/10.1901/jeab.1999.71-215>
- Stern, E. A., Jaeger, D., & Wilson, C. J. (1998). Membrane potential synchrony of simultaneously recorded striatal spiny neurons in vivo. *Nature*, *394*(6692), 475–478. <https://doi.org/10.1038/28848>
- Suzuki, W. A., & Amaral, D. G. (2003). Perirhinal and parahippocampal cortices of the Macaque monkey: Cytoarchitectonic and chemoarchitectonic organization. *Journal of Comparative Neurology*, *463*(1), 67–91. <https://doi.org/10.1002/cne.10744>
- Tallot, L., Capela, D., Brown, B. L., & Doyère, V. (2016). Individual trial analysis evidences clock and non-clock based conditioned suppression behaviors in rats. *Behavioural Processes*, *124*, 97–107. <https://doi.org/10.1016/j.beproc.2016.01.003>
- Tallot, L., & Doyère, V. (2020). Neural encoding of time in the animal brain. *Neuroscience and Biobehavioral Reviews*, *115*(June 2019), 146–163. <https://doi.org/10.1016/j.neubiorev.2019.12.033>
- Tallot, L., Graupner, M., Diaz-Mataix, L., & Doyère, V. (2020). Beyond freezing: Temporal expectancy of an aversive event engages the amygdalo-prefronto-dorsostriatal network. *Cerebral Cortex*, *30*(10), 5257–5269. <https://doi.org/10.1093/cercor/bhaa100>
- Tam, S. K. E., & Bonardi, C. (2012). Dorsal hippocampal lesions disrupt Pavlovian delay conditioning and conditioned-response timing. *Behavioural Brain Research*, *230*(1), 259–267. <https://doi.org/10.1016/j.bbr.2012.02.016>
- Tecuapetla, F., Jin, X., Lima, S. Q., & Costa, R. M. (2016). Complementary Contributions of Striatal Projection Pathways to Action Initiation and Execution. *Cell*, *166*(3), 703–715. <https://doi.org/10.1016/j.cell.2016.06.032>

- Theves, S., Fernández, G., & Doeller, C. F. (2020). The hippocampus maps concept space, not feature space. *Journal of Neuroscience*, *40*(38), 7318–7325. <https://doi.org/10.1523/JNEUROSCI.0494-20.2020>
- Tiganj, Z., Jung, M. W., Kim, J., & Howard, M. W. (2017). Sequential firing codes for time in rodent medial prefrontal cortex. *Cerebral Cortex*, *27*(12), 5663–5671. <https://doi.org/10.1093/cercor/bhw336>
- Treisman, M. (1963). Temporal discrimination and the indifference interval. *Psychological Monographs: General and Applied*, *77*(13), 1–31.
- Tremblay, L., & Schultz, W. (1999). Relative reward preference in primate orbitofrontal cortex. *Nature*, *398*(6729), 704–708. <https://doi.org/10.1038/19525>
- Treves, A., & Rolls, E. T. (1994). Computational analysis of the role of the hippocampus in memory. *Hippocampus*, *4*(3), 374–391. <https://doi.org/10.1002/hipo.450040319>
- Tsao, A., Sugar, J., Lu, L., Wang, C., Knierim, J. J., Moser, M. B., & Moser, E. I. (2018). Integrating time from experience in the lateral entorhinal cortex. *Nature*, *561*(7721), 57–62. <https://doi.org/10.1038/s41586-018-0459-6>
- Tsao, A., Yousefzadeh, S. A., Meck, W. H., Moser, M. B., & Moser, E. I. (2022). The neural bases for timing of durations. *Nature Reviews Neuroscience*, *0123456789*. <https://doi.org/10.1038/s41583-022-00623-3>
- Tse, D., Langston, R. F., Kakeyama, M., Bethus, I., Spooner, P. A., Wood, E. R., Witter, M. P., & Morris, R. G. M. (2007). Schemas and memory consolidation. *Science*, *316*(5821), 76–82. <https://doi.org/10.1126/science.1135935>
- Tsujimoto, S., Genovesio, A., & Wise, S. P. (2009). Monkey orbitofrontal cortex encodes response choices near feedback time. *Journal of Neuroscience*, *29*(8), 2569–2574. <https://doi.org/10.1523/JNEUROSCI.5777-08.2009>
- Tulving, E. (2001). Episodic memory and common sense: How far apart? *Philosophical Transactions of the Royal Society B: Biological Sciences*, *356*(1413), 1505–1515. <https://doi.org/10.1098/rstb.2001.0937>
- Tulving, Endel. (1993). What is episodic memory? *Current Directions in Psychological Science*, *2*(3), 67–70.
- Umbach, G., Kantak, P., Jacobs, J., Kahana, M., Pfeiffer, B. E., Sperling, M., & Lega, B. (2020). Time cells in the human hippocampus and entorhinal cortex support episodic memory. *Proceedings of the National Academy of Sciences of the United States of America*, *117*(45), 28463–28474. <https://doi.org/10.1073/pnas.2013250117>
- Van Hoesen, G. W., & Pandya, D. N. (1975). Some connections of the entorhinal (area 28) and perirhinal (area 35) cortices of the rhesus monkey: I. Temporal lobe afferents. *Brain Research*, *95*, 1–24.

- Van Hoesen, G. W., Pandya, D. N., & Butters, N. (1975). Some connections of the entorhinal (area 28) and perirhinal (area 35) cortices of the rhesus monkey. II. Frontal lobe afferents. *Brain Research*, *95*(1), 25–38. [https://doi.org/10.1016/0006-8993\(75\)90205-X](https://doi.org/10.1016/0006-8993(75)90205-X)
- van Zomeren, A. H., & Brouwer, W. H. (1994). *Clinical neuropsychology of attention*. Oxford University Press.
- Viskontas, I., Ekstrom, A., Wilson, C., & Fried, I. (2007). Characterizing Interneuron and Pyramidal Cells in the Human Medial Temporal Lobe In Vivo Using Extracellular Recordings. *Hippocampus*, *17*, 49–57. <https://doi.org/10.1002/hipo>
- Vo, A., Tabrizi, N. S., Hunt, T., Cayanan, K., Chitale, S., Anderson, L. G., Tenney, S., White, A. O., Sabariego, M., & Hales, J. B. (2021). Medial entorhinal cortex lesions produce delay-dependent disruptions in memory for elapsed time. *Neurobiology of Learning and Memory*, *185*(July). <https://doi.org/10.1016/j.nlm.2021.107507>
- Wackermann, J., & Ehm, W. (2006). The dual klepsydra model of internal time representation and time reproduction. *Journal of Theoretical Biology*, *239*(4), 482–493. <https://doi.org/10.1016/j.jtbi.2005.08.024>
- Walsh, V. (2003). A theory of magnitude: Common cortical metrics of time, space and quantity. *Trends in Cognitive Sciences*, *7*(11), 483–488. <https://doi.org/10.1016/j.tics.2003.09.002>
- Wang, J., Narain, D., Hosseini, E. A., & Jazayeri, M. (2018). Flexible timing by temporal scaling of cortical responses. *Nature Neuroscience*, *21*(1), 102–112. <https://doi.org/10.1038/s41593-017-0028-6>
- Wang, Y., Toyoshima, O., Kunitatsu, J., Yamada, H., & Matsumoto, M. (2021). Tonic firing mode of midbrain dopamine neurons continuously tracks reward values changing moment-by-moment. *eLife*, *10*, 1–17. <https://doi.org/10.7554/eLife.63166>
- Wearden, J. H., & Lejeune, H. (2007). Scalar properties in human timing: Conformity and violations. *Quarterly Journal of Experimental Psychology*, *61*(4), 569–587. <https://doi.org/10.1080/17470210701282576>
- Wilson, C. J., Chang, H. T., & Kitai, S. T. (1990). Firing patterns and synaptic potentials of identified giant aspiny interneurons in the rat neostriatum. *Journal of Neuroscience*, *10*(2), 508–519. <https://doi.org/10.1523/jneurosci.10-02-00508.1990>
- Wilson, M. A., & McNaughton, B. L. (1994). Reactivation of Hippocampal Ensemble Memories During Sleep. *Science*, *265*, 676–679.
- Wirth, S., Avsar, E., Chiu, C. C., Sharma, V., Smith, A. C., Brown, E., & Suzuki, W. A. (2009). Trial Outcome and Associative Learning Signals in the Monkey Hippocampus. *Neuron*, *61*(6), 930–940. <https://doi.org/10.1016/j.neuron.2009.01.012>

- Wirth, S., Yanike, M., Frank, L. M., Smith, A. C., Brown, E. N., & Suzuki, W. A. (2003). Single neurons in the monkey hippocampus and learning of new associations. *Science*, *300*(5625), 1578–1581. <https://doi.org/10.1126/science.1084324>
- Wittmann, M. (2013). The inner sense of time: how the brain creates a representation of duration. *Nature Reviews Neuroscience*, *14*(March), 217–223. <http://dx.doi.org/10.1038/nrn3452>
- Worbe, Y., Baup, N., Grabli, D., Chaigneau, M., Mounayar, S., McCairn, K., Féger, J., & Tremblay, L. (2009). Behavioral and movement disorders induced by local inhibitory dysfunction in primate striatum. *Cerebral Cortex*, *19*(8), 1844–1856. <https://doi.org/10.1093/cercor/bhn214>
- Xiao, X., Deng, H., Wei, L., Huang, Y., & Wang, Z. (2016). Neural activity of orbitofrontal cortex contributes to control of waiting. *European Journal of Neuroscience*, *44*(6), 2300–2313. <https://doi.org/10.1111/ejn.13320>
- Yelnik, J., Francis, C., Percheron, G., & Tandéa, D. (1991). Morphological taxonomy of the neurons of the primate striatum. *Journal of Comparative Neurology*, *313*(2), 273–294. <https://doi.org/10.1002/cne.903130207>
- Zhang, X., & Naya, Y. (2022). Retrospective memory trace sustained by the human hippocampus during working memory task. *European Journal of Neuroscience*, *55*(1), 107–120. <https://doi.org/10.1111/ejn.15549>
- Zhou, S., & Buonomano, D. V. (2022). Neural population clocks: Encoding time in dynamic patterns of neural activity. *Behavioral Neuroscience*. <https://doi.org/10.1037/bne0000515>
- Zhou, S., Masmanidis, S. C., & Buonomano, D. V. (2020). Neural Sequences as an Optimal Dynamical Regime for the Readout of Time. *Neuron*, *108*(4), 651–658.e5. <https://doi.org/10.1016/j.neuron.2020.08.020>
- Zhou, W., & Crystal, J. D. (2009). Evidence for remembering when events occurred in a rodent model of episodic memory. *Proceedings of the National Academy of Sciences of the United States of America*, *106*(23), 9525–9529.
- Zola-Morgan, S., Squire, L. R., Rempel, N. L., Clower, R. P., & Amaral, D. G. (1992). Enduring memory impairment in monkeys after ischemic damage to the hippocampus. *Journal of Neuroscience*, *12*(7), 2582–2596. <https://doi.org/10.1523/jneurosci.12-07-02582.1992>
- Zola, S. M., Squire, L. R., Teng, E., Stefanacci, L., Buffalo, E. A., & Clark, R. E. (2000). Impaired recognition memory in monkeys after damage limited to the hippocampal region. *Journal of Neuroscience*, *20*(1), 451–463. <https://doi.org/10.1523/jneurosci.20-01-00451.2000>